The Role of the Prostaglandin E_2 EP3 Receptor in Obesity, Insulin Resistance, and Glycemic Control

By

Ryan Patrick Ceddia

Dissertation

Submitted to the Faculty of the

Graduate School of Vanderbilt University

in partial fulfillment of the requirements

for the degree of

DOCTOR OF PHILOSOPHY

in

Pharmacology

December, 2015

Nashville, Tennessee

Approved:

Richard M. Breyer, Ph.D.

Kevin P. Currie, Ph.D.

Maureen A. Gannon, Ph.D.

James M. Luther, M.D.

Owen P. McGuinness, Ph.D.

To my parents, Joe and Susan Ceddia. Thank you for your love and inspiration.

ACKNOWLEDGMENTS

I would like to thank all of the people who have made this work possible. Many thanks are extended to Dr. Rich Breyer for his guidance and support throughout my Ph.D. project. I would also like to thank all the members of the Breyer lab, Rich Breyer, Sarah Davis, Maria Kraemer, Kelli Simpson, Jason Downey, Christie Bartlett, Evan Lund, and Nathan Gilbert. I thank the members of my committee, Dr. Rich Breyer, Dr. Kevin Currie, Dr. Maureen Gannon, Dr. J. Matt Luther, and Dr. Owen McGuinness for their direction throughout my project.

I would like to express my gratitude towards everyone and all of the wonderful cores at Vanderbilt who have provided me technical assistance on the project. I would like to thank Anastasia Coldren and Marcela Brissova at the Vanderbilt Islet Procurement & Analysis Core for all of their excellent help with all of the islet experiments, which could not have been done without them. I would also thank the Vanderbilt Translational Pathology Shared Resource for performing histology and especially Kelli Boyd for helping us interpret the histology and scoring necrosis in the adipose tissue. I would like to thank Joe Roland at the Vanderbilt University Institute of Imaging Science for his help with the slide image analysis. I would also like to thank the Mouse Metabolic Phenotyping Center Lipid Lab for measuring the triglycerides and free fatty acids, which were essential to this project. I would like to thank Ginger Milne and the Vanderbilt Eicosanoid Core Laboratory for measuring the prostaglandins in these studies. I would also like to acknowledge the Vanderbilt University Hormone Assay & Analytical Services Core for the numerous hormone analyses. I would also like to thank the Vanderbilt Mouse Metabolic Phenotyping Center for performing the energy balance studies. I would also like to thank Maureen Gannon and Ambra Pozzi for providing antibodies used in these studies. I would

also like to thank the American Society for Pharmacology and Experimental Therapeutics (ASPET) for providing funding through the Integrative Research in Pharmacology fellowship.

Finally, I would like to thank my parents for all of their love and support. Without their support, this would not have been possible.

TABLE OF CONTENTS

Page

LIST OF TABLES

LIST OF FIGURES

LIST OF ABBREVIATIONS

15Δ-PGJ_2	15-Deoxy-$\Delta^{12,14}$-Prostaglandin J_2
AA	Arachidonic Acid
Adipoq	Adiponectin
AdPLA	Adipose-Specific PLA
AIS	Adipocyte Incubation Solution
ALT	Alanine Aminotransferase
ApoB	Apolipoprotein B
ATGL	Adipose Triglyceride Lipase
ΔAUC	Difference from Baseline of the Area Under the Curve
BAT	Brown Adipose Tissue
BMI	Body Mass Index
cAMP	Cyclic Adenosine Monophosphate
C/EBP	CCAAT/Enhancer-Binding Protein
CGI-58	Comparative Gene Identification-58
COX	Cyclooxygenase
CRP	C-Reactive Protein
CRTH2	Chemoattractant Receptor-Homologous Molecule Expressed on Th2 Cells
cPGES	Cytosolic PGES
$cPLA_2$	Calcium-Dependent Cytosolic PLA_2
Cpt1a	Carnitine Palmitoyltransferase 1A (liver)
DP	PGD_2 Receptor

EET	Epoxyeicosatrienoic Acids
Emr1	EGF-Like Module-Containing Mucin-Like Hormone Receptor-Like 1 (a.k.a. F4/80)
EP	PGE_2 Receptor
F1	First Filial Generation Hybrid
Fasn	Fatty Acid Synthase
FFA	Free Fatty Acid
FP	$PGF_{2\alpha}$ Receptor
Gα	G-Protein Alpha Subunit
Gβγ	G-Protein Beta and Gamma Subunits
Gapdh	Glyceraldehyde 3-Phosphate Dehydrogenase
GEF	Guanine Nucleotide Exchange Factor
GLP-1	Glucagon-Like Peptide-1
GPCR	G-Protein Coupled Receptor
GRK	GPCR Kinase
GSIS	Glucose Stimulated Insulin Secretion
HbA1c	Glycated Hemoglobin
H&E	Hematoxylin and Eosin
HFD	High Fat Diet
HOMA-IR	Homeostatic Model Assessment of Insulin Resistance
HPA	Hypothalamic-Pituitary-Adrenal
HPETE	Hydroperoxyeicosatetraenoic Acids
IBMX	3-Isobutyl-1-Methylxanthine
IκB	NFκB inhibitor

IKK-β	IκB Kinase-β
IL	Interleukin
iNOS	Inducible Nitric Oxide Synthase
IP	PGI_2 Receptor
IP-GTT	Intraperitoneal Glucose Tolerance Tests
$iPLA_2$	Calcium-Independent Cytosolic
ITT	Insulin Tolerance Tests
K_d	Dissociation Constant
K_i	Inhibition Constant
Lep	Leptin
L-PGDS	Lipocalin-Type PGDS
LPS	Lipopolysaccharide
MAPK	Mitogen-Activated Protein Kinase
MCP-1	Monocyte Chemotactic Protein 1
MEF	Mouse Embryonic Fibroblasts
MGL	Monoacylglycerol Lipase
mPGES	Membrane Bound PGES
Mttp	Microsomal Triglyceride Transfer Protein
NFκB	Nuclear Factor Kappa-Light-Chain-Enhancer of Activated B Cells
NSAID	Non-Steroidal Anti-Inflammatory Drug
ORO	Oil Red O
PAF-AH	Platelet-Activating Factor Acetylhydrolase
PBS	Phosphate Buffered Saline

Pecam1	Platelet Endothelial Cell Adhesion Molecule-1 (a.k.a. CD31)
PG	Prostaglandin
PGC-1α	PPARγ Coactivator-1α
PGDS	PGD_2 Synthase
PGES	PGE Synthase
PGIS	PGI_2 Synthase
PGI_2	Prostacyclin
PKA	Protein Kinase A
PKC	Protein Kinase C
PLA_2	Phospholipase A_2
PLIN	Perilipin
PPAR	Peroxisome Proliferator-Activated Receptors
Ptger3	Prostaglandin E Receptor 3 (subtype EP3)
PTGS	Prostaglandin-Endoperoxide Synthase
qPCR	Quantitative Real-Rime RT-PCR
SEM	Standard Error of the Mean
SNAP-25	Synaptosomal-Associated Protein-25
SNARE	Soluble NSF Attachment Protein Receptor
$sPLA_2$	Secreted PLA_2
StDev	Standard Deviation
STZ	Streptozotocin
TNF	Tumor Necrosis Factor
TP	TXA_2 Receptor

TXA_2	Thromboxane
TXA2S	TXA_2 Synthase
Ucp1	Uncoupling Protein 1
VAMP-2	Vesicle-Associated Membrane Protein 2
Vegfa	Vascular Endothelial Growth Factor A
VHFD	Very High Fat Diet
VLDL	Very-Low-Density Lipoproteins
WAT	White Adipose Tissue

CHAPTER I

INTRODUCTION

Obesity – Why is it a problem?

Obesity is rapidly becoming a major problem for both adults and children in the United States and throughout the world. This condition can be caused by many factors, including genetic, metabolic, behavioral, and environmental influences (1). In fact, obesity has reached epidemic proportions in many countries, including the U.S. Obesity is defined as having a body mass index (BMI) that is greater than 30 kg/m^2 and as of 2012, 35.04% of men and 36.84% of women in the US were considered obese (2). Between 1950 and 2000, the proportion of overweight men and women rose from 21.8% to 35.2% and from 15.0% to 33.1.9%, respectively (3). Even more striking has been the approximately three fold rise in BMI between 1950 and 2000, with men seeing a change from 5.8% to 14.8% for a BMI of $\geq$ 30 kg/m^2, and from 0.2% to 5.4% for a BMI $\geq$ 35 kg/m^2 (3). Women also saw a rise in the prevalence of obesity with a change from 3.9% to 14% for a BMI of $\geq$ 30 kg/m^2, and 1.7% to 4.4% for a BMI $\geq$ 35 kg/m^2 (3). Obesity has been estimated to have caused between 95,000 and 163,000 excess deaths in 2004 (4) and it has been estimated to cost the US over $147 billion per year (5).

Diabetes – Why is it a problem?

Increased body mass correlates with and increased risk for type 2 diabetes (6-8). Diabetes had a total cost of $218 billion to the United States in 2007 (9). It is the seventh leading cause of death and affects an estimated 25.8 million people in the U.S. or 8.3% of the population (10). Diabetes is a group of metabolic diseases characterized by elevated blood glucose levels caused by a failure to produce enough insulin and/or a reduced response to the insulin produced. Type 1 diabetes results from an autoimmune destruction of insulin producing pancreatic β-cells. Type 2

diabetes results from a reduction in both insulin sensitivity and β-cell function. Type 2 diabetes is a comorbidity of obesity, occurring when the body is unable to produce enough insulin to maintain glycemic control. As fat mass increases, the amount of insulin needed to maintain glycemic control increases due to both the increasing body mass as well as declining insulin sensitivity. β-cell mass and insulin production are initially increased to compensate for the increasing insulin need (11). As the disease progresses, β-cell function begins to decline and a disparity arises between the insulin produced and the insulin needed to maintain glycemic control, which is Type 2 diabetes (12). Type 2 diabetes is the most prevalent form of diabetes and has the highest economic burden of $159.5 billion per year (9). Complications from diabetes can result in kidney damage, vision loss, loss of limbs, and death.

Initial therapies for diabetes primarily focus on either providing more insulin to the patient, by increasing endogenous production or exogenous administration, or improving the function of insulin. Insulin was first administered to a patient with type 1 diabetes in 1922 by Frederick Banting (13). Administration exogenous insulin is still standard for persons with type 1 and advanced Type 2 diabetes. More recently, insulin secretagogues have come onto the market that attempt to reduce the need for regular insulin administration for patients with type 2 diabetes. The first class of drugs to become available in the 1950's were sulfonylureas which act by increasing insulin release from the pancreatic β-cells (14). Agonists for the glucagon-like peptide-1 (GLP-1) receptor also increase glucose stimulated insulin secretion (GSIS) from pancreatic β-cells. The first commercial GLP-1 receptor agonists to be used in the clinic were liraglutide and exenatide; these are mimetics of human GLP-1 and exendin-4, a peptide found in the venom of the Gila Monster, respectively (15). Exenatide was the first of this class of drug to come onto the market, approved in 2005, and was marketed as Byetta. Aside from insulin and

drugs to improve insulin secretion, some therapies attempt to improve insulin sensitivity, such as metformin, which improves glucose tolerance and reduces hepatic gluconeogenesis (16). Metformin, which was first approve in Canada in 1972 (17), is the first-line drug of choice for patients with type 2 diabetes and may be used as a therapy for prevention in those at risk for diabetes (18). Similar to metformin, thiazolidinediones are insulin-sensitizing drugs, which act through the peroxisome proliferator-activated receptors (PPAR), first saw clinical use in 1997 (19). In addition to improving insulin resistance, thiazolidinediones reduce systemic inflammation (20). Inflammation plays an important role in diabetes and targeting inflammation may become an important mechanism to treat diabetes (21).

Diabetes as an inflammatory disease

Inflammation has long been known to be a complicating factor worsening diabetes mellitus. An early review on the subject by Valy Menkin in 1941, discussed the observation that diabetes complications worsen during inflammation or infection (22). Little did Menkin know, the interaction of diabetes and inflammation would become a subject of intense scientific investigation for the rest of the twentieth century and beyond (23-25).

The pathological involvement of the immune system in type 2 diabetes has been well established. During obesity macrophage infiltrate metabolically important tissues, such as adipose tissue, liver, muscle and pancreas (26-31). These proinflammatory macrophages produce cytokines, which are pro-inflammatory signaling molecules. Pro-inflammatory cytokines such as interleukin (IL)-1β, IL-6, C-reactive protein (CRP), and tumor necrosis factor (TNF)-α are elevated in obese and diabetic subjects (32-34). These cytokines activate signaling pathways which contribute to insulin resistance (35). Notably, activation of IKK-β (IκB kinase-β) and its downstream target NFκB (nuclear factor κ-light-chain-enhancer of activated B cells), a

transcription factor that regulates genes responsible for the innate and adaptive immune response, leads to insulin resistance (36-38). In addition to causing insulin resistance, IL-1β signaling in islets leads to activation of cyclooxygenase (COX) and inducible nitric oxide synthase (iNOS), which reduces GSIS from pancreatic islets (39,40). COX enzymes generate prostaglandins (PGs), which are themselves important mediators of inflammation (41-45). PGE_2 is one of the most prevalent PGs produced and it plays important roles in inflammation and other biological processes (41,44).

The importance of inflammation in the pathogenesis of obesity and diabetes has culminated in numerous clinical trials targeting inflammation as an approach to treat type 2 diabetes (23). Many of these trials utilize mechanisms to block IL-1 or IKK-β/NFκB. Several of these studies resulted in a prolong lowering of blood glucose following the treatment (23). Modulation of PGs has also been investigated as a potential therapy for improving the diabetic phenotype. Aspirin was found to decrease the risk of developing type 2 diabetes, though this was not found with other non-steroidal anti-inflammatory drugs (NSAIDs) (46). NSAIDs act by inhibiting COX mediated PG production (47), though it should be appreciated that some NSAIDS, such as salicylate and aspirin, also block the activity of the pro-inflammatory transcription factor NFκB (48). Recently, much interest has focused on the use of salicylate and related drugs to improve the diabetic phenotype because it has the ability to inhibit both NFκB signaling and COX mediated PG production (23,49,50)

Historical Overview of Prostaglandins and Metabolism

Salicylic acid received its name from salicin, from which it was first synthesized in 1838 (51). Salicin, is named after *salix*, which is Latin for willow, because it was first isolated from the bark of the white willow (*Salix alba*) in 1828 (52). Willow bark and leaves have been used as

a treatment for headaches and inflammation since ancient times. One of the earliest references for using willow leaves to treat inflammatory rheumatic diseases comes from Assyrian tablets from the Sumerian period (53). The Ebers papyrus, from ancient Egypt circa 1550 B.C., suggests using leaves of the willow to treat an inflamed wound (53). Hippocrates of Kos, circa 460-370 B.C., also recommended an extract of willow bark to treat inflammation (53). The Reverend Edmund Stone gave the first scientific description of the beneficial effects of willow bark in 1763, describing the ability of willow bark to treat agues (a febrile illness involving successive cold, hot, and sweating fits) (54).

There is a long history of salicylate, NSAIDs, and PGs being investigated for their potential therapeutic benefits in the treatment of diabetes and other metabolic complications (Figure 1). The first recorded use of salicylate to treat diabetes was by Wilhelm Ebstein in 1876 who found that it decreased urinary glucose in diabetic patients indicating that the diabetic condition was improved (55). The beneficial effects of salicylate on glucosuria were replicated by other physicians; however, it appears that treatment of diabetes with salicylates never became common (56). In 1957, acetylsalicylic acid, also known as aspirin, was shown to lower blood glucose in diabetic patients (57,58). In 1967 it was shown that salicylate increased plasma insulin explaining the reduction in blood glucose during aspirin treatment that had been previously reported (59). Sodium salicylate and other aspirin-like drugs were shown to block the synthesis of PGs in 1971 (47) which was later shown to be due to inhibition of COX enzymes. PGs had been known for some time prior, with their effect of causing uterine contractions being first described in 1930 (60) and the term “prostaglandin” being first used in 1935 (61). The first prostaglandin isolated was isolated in 1957 and termed “prostaglandin factor (PGF)” (62). At the time of the isolation of PGF, it was noted that at least one other factor was present in the sheep

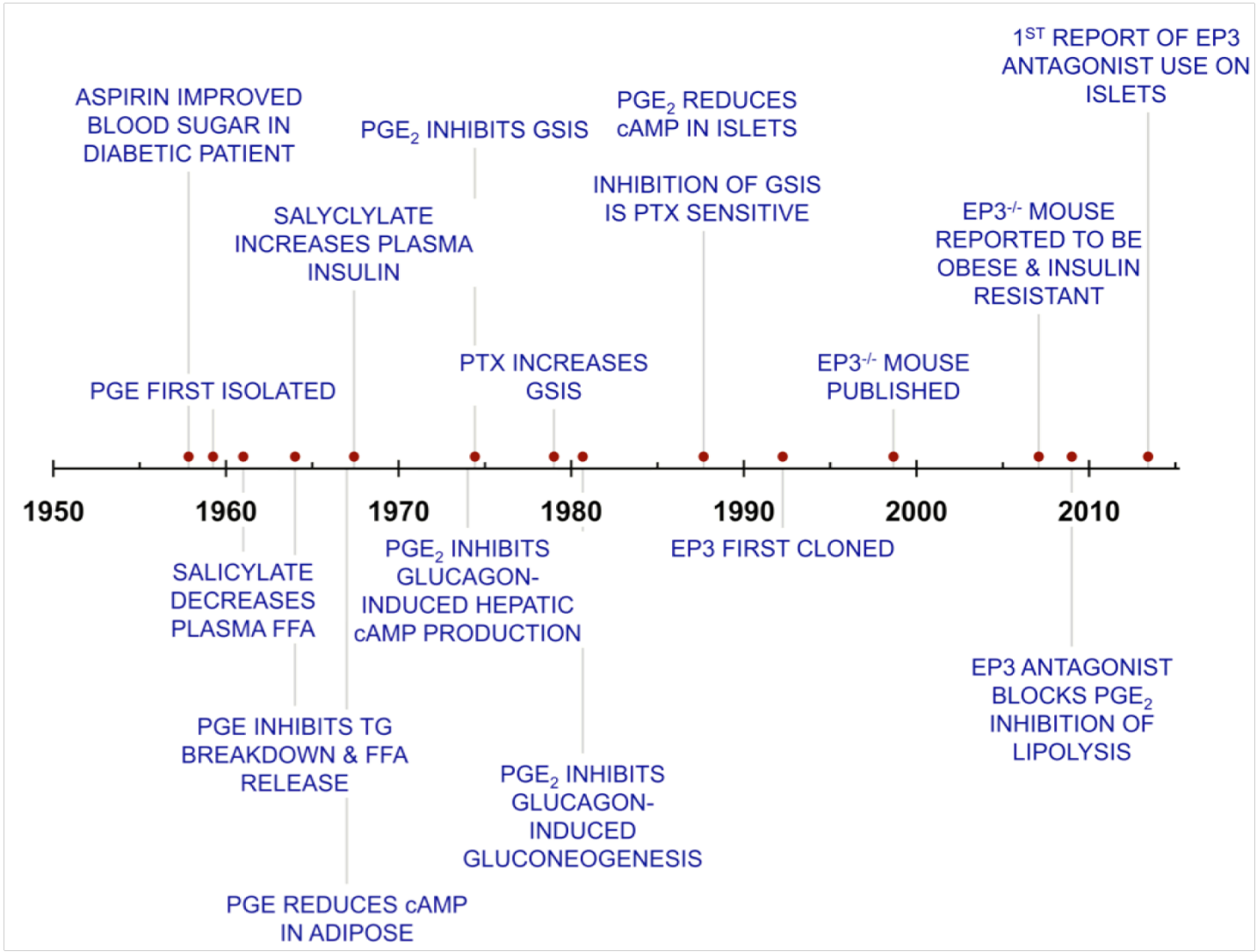
1ST REPORT OF EP3 ANTAGONIST USE ON ISLETS
ASPIRIN IMPROVED BLOOD SUGAR IN DIABETIC PATIENT
PGE2 INHIBITS GSIS
PGE2 REDUCES cAMP IN ISLETS
INHIBITION OF GSIS IS PTX SENSITIVE
SALYCLYLATE INCREASES PLASMA INSULIN
EP3-/- MOUSE REPORTED TO BE OBESE & INSULIN RESISTANT
PTX INCREASES GSIS
EP3-/- MOUSE PUBLISHED
PGE FIRST ISOLATED
1950
1960
1970
1980
1990
2000
2010
SALICYLATE DECREASES PLASMA FFA
PGE2 INHIBITS GLUCAGON-INDUCED HEPATIC cAMP PRODUCTION
EP3 FIRST CLONED
EP3 ANTAGONIST BLOCKS PGE2 INHIBITION OF LIPOLYSIS
PGE INHIBITS TG BREAKDOWN & FFA RELEASE
PGE2 INHIBITS GLUCAGON-INDUCED GLUCONEOGENESIS
PGE REDUCES cAMP IN ADIPOSE

Figure 1. History of prostaglandins and metabolism
Early studies show that salicylate and other NSAIDs decrease plasma free fatty acids and improve glucose homeostasis. These effects were later shown to be due to blockade of prostaglandin synthesis, namely PGE_2. PGE_2 inhibits GSIS, lipolysis, and glucagon-induced gluconeogenesis. GSIS and lipolysis inhibition by PGE_2 have been shown to occur via the EP3 receptor.

prostate glands. This factor was found in the more lipid soluble ether fractions, whereas PGF was found in the buffer fractions, and was termed PGE (63). In 1959 the biological effects of PGE and PGF were characterized with these PGs being found to affect smooth muscle and have cardiovascular effects (64). The structures of PGE and PGF were determined in 1960 (63,65) and those of other PGs were found about 10-15 years later (66-68). Much later, in 2002, the COX2 selective inhibitor SC58236 was shown to improve GSIS from Ins-1 cells suggesting that salicylate and aspirin's effect of raising plasma insulin is due to inhibition of the COX2 enzyme (69). Three years after salicylate was shown to block PG synthesis, PGE_2 was shown to inhibit GSIS (70). In 1987 PGE_2 was shown to reduce cyclic adenosine monophosphate (cAMP) in islets and to inhibit GSIS in a pertussis toxin sensitive manner indicating that PGE_2 signaling in islets is mediated through the inhibitory PGE_2 receptor (71). This inhibitory, Gi alpha ($G\alpha_i$) coupled PGE_2 receptor was named prostaglandin E receptor 3 (EP3) and was first cloned in 1992 (72). In 2008 a U.S. patent application suggested that EP3 antagonist GW67021B may be used to lower blood glucose (73). It was not until 2013 that the use of an EP3 antagonist, L-798,106, on islets was first published, confirming that PGE_2 inhibits GSIS by signaling through EP3 (74). These landmark studies indicate that salicylate and other aspirin-like drugs block PGE_2 production via COX2, which leads to reduced PGE_2 evoked EP3 signaling in islets, resulting in enhanced GSIS lowering blood glucose and improving glucosuria.

PGE_2 also reduces hepatic glucose production in addition to improving GSIS; in 1974 PGE_2 was shown to inhibit glucagon-induced production of hepatic cAMP (75) and in 1980 inhibition of glucagon-induced gluconeogenesis was demonstrated (76). An alternative mechanism of improving diabetic phenotype by saliclyate and aspirin was found in 1994 when it was shown that these drugs block the activity of the pro-inflammatory transcription factor NFκB

(48) by inhibiting the activity of IKK-β (77). In 2001 inhibition of IKK-β by salicylates was shown to reverse hyperglycemia by improving insulin sensitivity (78,79). Hence, salicylates may lower blood glucose by both improving insulin sensitivity and increasing GSIS. Unfortunately, the doses of NSAIDs required to have a clinical impact on diabetes by improving GSIS caused negative side effects so their therapeutic use for diabetes was abandoned (80). However, recent studies with salsalate in humans have been promising showing reduced inflammation and increased insulin levels (81-87).

In addition to improving GSIS, salicylate and PGE_2 also have a profound effect on adiposity. An effect was first noted in 1961 when salicylate was shown to decrease plasma free fatty acid (FFA) (88), though this result is controversial as it was later shown that salicylate increased FFA (89). Two years later PGE_2 was shown to inhibit lipolysis, the breakdown of triglycerides into FFA (90-92). PGE_2 was shown to reduce cAMP in adipose tissue, similar to its effect in pancreatic islets; however, the effect in adipose tissue was first reported in 1967, preceding the first report in islets by twenty years (93,94). Despite these early observations that PGE_2 inhibits lipolysis, it was not until 1968 that PG release from adipose tissue was first demonstrated (95). The effects of PGE_2 in obesity and adiposity received much attention early on. In 1975 Curtis-Prior proposed that metabolic obesity is caused by the over production of PGs (96). He reasoned that because PGs prevented lipolysis, the over production of PGs would cause lipids to be unable to leave the adipose tissue and travel to other tissues to be metabolized. He therefore proposed that NSAIDs would treat obesity by promoting lipolysis and causing lipid redistribution to ectopic tissues where the lipid could be metabolized. Aspirin was not shown to reduce body-weight in people (97), but $COX2^{-/-}$ mice have reduced adiposity (98,99) and the NSAID indomethacin has been shown to prevent high fat diet (HFD) induced obesity in mice

(100). In 2009 the EP3 antagonist L-826,266 was shown to block PGE_2's inhibition of lipolysis (101). Hence, the mechanism of PGE_2 action on adipocytes appears similar to its mechanism of action in pancreatic islets. NSAIDs block PGE_2 synthesis, which signals through the EP3 receptor to decrease cAMP, and thereby reduces conversion of triglycerides into FFA. In 2007 it was noted that $EP3^{-/-}$ mice become obese and insulin resistant when fed a breeder chow diet; this was attributed to hyperphagia and increased feeding during the day (102). More recent understanding of lipid signaling indicates that lipid accumulation in ectopic tissues causes insulin resistance as opposed to simply reducing obesity as Curtis-Prior proposed in 1975 (35). It is possible that these $EP3^{-/-}$ mice had enhanced lipolysis, which culminated in increased insulin resistance. Curtis-Prior's proposal for using NSAIDs to promote lipolysis may work to decrease lipid storage in adipose tissue; however, subsequent accumulation of lipid in ectopic tissues will likely not be metabolized as he proposed, but rather stored in those tissues contributing to insulin resistance and thereby promoting the diabetic phenotype.

The drug salsalate has recently been of interest as a possible anti-inflammatory drug that may be beneficial for improving diabetes (50,103,104). Salsalate is a prodrug that is converted into salicylate (salicylic acid). Salicylate has been long known to increase plasma insulin (59) and this effect is shared among most NSAIDs except indomethacin (50,105,106). It is thought that this occurs by inhibiting COX enzymes, which synthesize PGs, and which would normally act to inhibit GSIS. Salicylate also improves insulin sensitivity by inhibition of IKK-β (78,79). Hence, salicylate appears to have a beneficial effect on both reducing insulin resistance and improving insulin secretion.

Thus PGs, though perhaps best known for their role in pain and inflammation, have a long history of modulating metabolism. PGE_2 and EP3 in particular play an important role in

regulating GSIS from pancreatic islets and lipolysis from adipose tissue. With the recent understanding of the role inflammation plays in obesity and diabetes, PGs present an attractive therapeutic target because they modulate insulin secretion, adiposity, and inflammatory processes.

Prostaglandin Signaling

PGs are oxidative metabolites of arachidonic acid (AA) that are produced by COX enzymes (COX1 and COX2). They are lipid-signaling molecules that are named for the prostate because they were first detected in seminal fluid and that comes from the prostate (61). AA is liberated from the plasma membrane by phospholipase A_2 (PLA_2). COX converts AA into PGH_2 which is converted into five primary bio-active prostanoids: PGE_2, $PGF_{2\alpha}$, PGD_2, prostacyclin (PGI_2, and its degradation product 6-keto-$PGF_{1\alpha}$), and thromboxane (TXA_2, and its more stable metabolite TXB_2). These prostanoids act locally in an autocrine or paracrine manner. The local action of PGs depends on activation of a family of specific G-protein coupled receptors (GPCRs) designated EP for E-prostanoid receptors, FP, DP, IP and TP receptors, for the other PGs, respectively.

(Reviewed in (43,107-109))

Phospholipase A_2

PLA_2s are enzymes which catalyze the release of a fatty acid from the second carbon group (*sn*-2 position) of membrane glycerophospholipids. PLA_2s can be divided into six families: low-molecular weight secreted PLA_2s ($sPLA_2$), calcium-dependent cytosolic ($cPLA_2$), calcium-independent cytosolic ($iPLA_2$), platelet-activating factor acetylhydrolase (PAF-AH), lysosomal PLA_2s, and adipose-specific PLA (AdPLA). Of these, $cPLA_2$s have specificity for AA in the *sn*-2 position hence they are associated with the production of eicosanoids, which include

leukotrienes and PGs. In addition, $cPLA_2$s are important because they are hormonally regulated and are therefore the source of hormonally regulated AA release (110,111). The other PLA_2 family members can liberate a wide variety of fatty acids.

(Reviewed in (112-117))

Arachidonic Acid

AA is a polyunsatataturated omega-6 fatty acid, 20:4(ω-6) which was first isolated from liver lipids (118). AA can function as a signaling molecule itself or it can be metabolized into a variety of potent signaling molecules. The enzymes 5-lipoxygenase, 8-lipoxygenase, 12-lipoxygenase, and 15-lipoxygenase convert AA into the hydroperoxyeicosatetraenoic acids (HPETE): 5-HPETE, 8-HPETE, 12-HPETE, and 15-HPETE, respectively. 5-lipoxyenase is notable because leukotrienes, a family of eicosanoid inflammatory mediators, are derived from 5-HPETE. Alternatively, COX metabolism of AA into PGH_2 is the first committed step towards PG synthesis. In addition, AA can be metabolized into epoxyeicosatrienoic acids (EET) by cytochrome P450 enzymes.

(Reviewed in (119,120))

Cyclooxygenase

The COX1 and COX2 enzymes are encoded by the genes prostaglandin-endoperoxide synthase 1 (*Ptgs1*) and 2 (*Ptgs2*), respectively. Both COX enzymes carry out an identical chemical reaction. The COX enzymes are the key enzymes for catalyzing the conversion of AA into PGG_2. PGG_2 is an intermediate PG that is quickly converted into PGH_2 by COX. PGH_2 is converted into the five primary prostanoids by enzymatic conversion or spontaneous rearrangement.

Both COX enzymes are the targets for NSAIDs, such as aspirin, which inhibit the conversion of AA into PGG_2. Selective COX inhibitors have recently been developed which allow specific inhibition of COX1 or COX2. Although there are exceptions, expression of *Ptgs1* is generally considered to be constitutive expressed whereas *Ptgs2* expression is generally thought of as being inducible. For this reason it has been classically thought that COX2 mediates inflammatory reactions whereas COX1 mediates many of the "housekeeping" effects.

(Reviewed in (121-123))

Prostaglandins

PGH_2 is converted into the five primary prostanoids by their respective synthases or by spontaneous rearrangement. The five primary bioactive prostanoids are PGE_2, $PGF_{2\alpha}$, PGD_2, PGI_2, and TXA_2. Conversion of PGH_2 to PGE_2 is performed by one of three PGE synthases (PGES): cytosolic PGE synthase (cPGES) and two membrane bound PGE synthases (mPGES-1 and mPGES-2). There are two types of PGD_2 synthases (PGDS): the lipocalin-type PGDS (glutathione (GSH)-independent) (L-PGDS) and the hematopoietic PGDS (GSH-dependent). Three different enzymes, PGE 9-ketoreductase, PGD 11-ketoreductase, and PGH 9-, 11-endoperoxide reductase, make PGF from PGE_2, PGD_2, or PGH_2, respectively. PGI_2 is synthesized from PGH_2 by a single enzyme, PGI_2 synthase (PGIS). TXA_2 is also synthesized from PGH_2 by a single enzyme, TXA_2 synthase (TXA2S).

(Reviewed in (124-129))

Prostaglandin Receptors

PGs signal through GPCRs which are receptors containing seven-transmembrane spanning domains that couple to heterotrimeric G-proteins that consist of α and βγ subunits. Most Gα subunits can be broadly classified into four main types: $G\alpha_s$, $G\alpha_i$, $G\alpha_q$, and $G\alpha_{12/13}$. $G\alpha_s$

stimulates adenylyl cyclases which increases the second messenger cAMP, while $G\alpha_i$ inhibits adenylyl cyclase thereby decreasing cAMP. $G\alpha_q$ activates phospholipase C which increases the second messengers diacyl-glycerol (DAG) and inositol trisphosphate (IP_3) which in turn activates calcium release from the endoplasmic reticulum. $G\alpha_{12/13}$ activate RhoGEFs that activate Rho GTPases.

PGE_2 signals through four GPCRs termed EP1-EP4. EP3 has three splice variants in mice (α, β, γ); the number of splice variants varies between species with at least ten in human (130) that differ in their carboxy-terminal tails. The different carboxy-terminal tails affects the subcellular localization of the EP3 receptor splice variants and signal transduction pathways by coupling to different G proteins (131,132). Pharmacological studies have defined EP2 and EP4 as $G\alpha_s$ coupled, EP1 as $G\alpha_q$ coupled, and EP3 as $G\alpha_i$ and $G\alpha_{12/13}$ coupled. Recent studies indicate that in pancreatic islets EP3 is also coupled to $G\alpha_z$, which is a pertussis toxin insensitive inhibitory G-protein (133,134). Agonist activation of EP2 can cause β-arrestin binding and a subsequent β-arrestin-Src complex, which can activate downstream signaling pathways (135,136). EP3 can be internalized in response to PGE_2; however, the degree and the mechanism of internalization vary between the isoforms (137). EP4 can be phosphorylated and desensitized by G protein–coupled receptor kinases (GRKs) (138). In addition, EP4 can bind β-arrestin (139), which can activate Src and its downstream signaling pathways (140,141). The receptors have varying affinities for PGE_2, and EP3 and EP4 have the highest affinity with K_d's of 0.8-5 and 2-3.2 nM, respectively. EP1 and EP2 have lower affinity with K_d's of about 20 and 13-40 nM, respectively.

$PGF_{2\alpha}$ signals through a single GPCR, FP. FP has two splice variants and is primarily coupled to $G\alpha_q$ though it also signals through $G\alpha_i$. FP has been reported to lack associatiation

with β-arrestin (142). FP is very similar in sequence to the EP3 receptor and is located on opposite strands of chromosome 1 in the human or chromosome 3 in the mouse. It is thought that FP arose as a gene duplication of EP3.

PGD_2 signals through two GPCRs: DP1 and DP2 (previously called CRTH2 {chemoattractant receptor-homologous molecule expressed on Th2 cells}, PTGDR2, GPR44, or CD294). DP1 is $G\alpha_s$ coupled while DP2 is coupled to $G\alpha_i$. PGD_2 can signal through DP2 to induce β-arrestin phosphorylation and activation of its downstream signaling pathways (143). DP1 is closely related to the other members of the prostanoid GPCR family in sequence. DP2 does not share homology with other prostanoid GPCRs, being more closely related to chemoattractant receptors, though its affinity for PGD_2 is similar to that of DP1.

PGI_2 signals through a single GPCR, IP. IP is primarily $G\alpha_s$ coupled, but has been shown to couple to $G\alpha_i$ and $G\alpha_q$. Agonist-induced desensitization of IP occurs through PKC phosphorylation of IP and does not involve GRKs or β-arrestins but instead is mediated at least partially through clathrin-coated vesicles (144,145).

TXA_2 signals through a single GPCR, TP. The TP receptor has two splice variants. Though initially described as being $G\alpha_q$ coupled, TP has been shown to couple to $G\alpha_s$, $G\alpha_i$, and $G\alpha_{12/13}$ also. Both splice variants of TP are desensitized by GRKs and are internalized by arrestins (146,147), but the signaling mechanisms leading to desensitization differ between the two splice variants (148). (Reviewed in (43,44,107,109,149-151))

The Role of Prostaglandins in Metabolism

Eicosanoids play an important role in metabolism (152). PGs have been implicated in roles as diverse as pancreatic insulin secretion and energy homeostasis. They are also important modulators of the immune system which itself plays a critical role in obesity and diabetes.

Regulation of Insulin Secretion

Insulin is an important regulator of metabolic homeostasis. Insulin acts on tissues to cause uptake of glucose from the blood. It also has a variety of tissue specific effects. In the liver, insulin inhibits gluconeogenesis, the production of glucose from glycogen stores, while stimulating glycogen synthesis. It also fosters energy storage by increasing *de novo* lipogenesis. Similarly, in skeletal muscle, insulin also promotes glycogen synthesis. In adipose tissue, insulin inhibits lipolysis, which is the conversion of stored triglycerides into FFA and the release of the FFA into the bloodstream.

Insulin is secreted from β-cells, which reside in the islets of Langerhans in the pancreas. In addition to β-cells, islets also contain α-, δ-, PP-, and ε-cells, which secrete glucagon, somatostatin, pancreatic polypeptide, and ghrelin, respectively (153). Glucose is the primary regulator of insulin secretion. Glucose metabolism increases intracellular ATP, raising the ATP-ADP ratio, which closes the ATP-sensitive potassium channels. The resulting membrane depolarization allows voltage-operated calcium channels to open, resulting in a rise in intracellular calcium, the main trigger for insulin exocytosis. Exocytosis occurs when an insulin-containing secretory granule fuses to the plasma membrane. This process is catalyzed by the formation of a SNARE (Soluble NSF Attachment Protein Receptor) complex, which is formed by vesicle-associated membrane protein 2 (VAMP-2)/synaptobrevin2 from the vesicle interacting with syntaxin-1 and synaptosomal-associated protein-25 (SNAP-25) on the plasma membrane (154). Vesicle fusion and insulin release occur when calcium binds synaptotagmin activating the SNARE complex (154,155).

In addition to the canonical glucose mediated pathway, there are multiple alternative mechanisms that serve to modulate GSIS or can even alter insulin release in the absence of

changes in glucose concentration. For example, cytokines and nitric oxide both decrease GSIS (156), GSIS can be enhanced by estrogen signaling through its cognate nuclear hormone receptors (157), and signaling through the insulin receptors promote β-cell proliferation and insulin synthesis (158). One of the most prevalent class of GSIS modulators are GPCRs (159,160). GPCRs modulate GSIS through their heterotrimeric G-proteins. $G\alpha_q$ mobilizes internal calcium stores to promote insulin secretion via activation of protein kinase C (PKC), a serine and threonine kinase, and calcium responsive calcium channels, such as ryanodine receptors. cAMP increases insulin release via multiple pathways, hence $G\alpha_s$ activation usually increases insulin release while $G\alpha_i$ signaling has an opposing effect. cAMP directly activates Epac, which is a guanine nucleotide exchange factor (GEF) for Rap, a Ras-related GTPase. Rap activates phospholipase C-ε resulting in the production of IP_3 and thereby calcium. Epac also directly interacts with SNAP-25 (161) and indirectly with other secretory granule-associated proteins and SNARE proteins that control exocytosis (162). cAMP also activates protein kinase A (PKA), which is a serine/threonine kinase. PKA phosphorylates SNAP-25 increasing secretory capacity (163). PKA sensitizes intracellular calcium release channels to stimulatory second messengers such as IP_3 and calcium which also increases insulin secretion (162). In addition to Gα, GPCRs affect insulin release through Gβγ (164-167) and β-arrestin (168) mediated signaling.

PGs play an important role in regulating GSIS. Glucose stimulation rapidly increases AA concentration in islets (169,170), which appears to be caused by decreasing intracellular calcium concentrations, following the glucose stimulated rise in intracellular calcium, activating $iPLA_2$ (171). Both COX1 and COX2 are expressed in pancreatic islets; however, it is COX2 that mediates the classical inhibition of GSIS by PGs (69,172). Expression of COX2 has been

reported to be higher in β-cells than α-cells indicating that β-cells may produce the PGs that regulate GSIS (173). PGD_2, PGE_2, $PGF_{2\alpha}$, PGI_2 and TXB_2 are produced in pancreatic islets in response to glucose and may function as a way to fine-tune GSIS (74,169,172,174-182). PGD_2 and $PGF_{2\alpha}$ are typically associated with increasing insulin release while PGE_2 inhibits insulin release (71,74,177,183-197).

Prostaglandin E_2

PGE_2 is typically thought to inhibit GSIS (198-200). Glucose stimulates PGE_2 release from islets (169,174,178,180,182). During islet perifusion, the peak release of PGE_2 occurs about 4 minutes after the peak release of insulin (169). This suggests that PGE_2 may function to prevent the overproduction of insulin during GSIS. Though many studies indicate that PGE inhibits GSIS, the results remain controversial as some studies find that PGE_2 has no effect or even increases GSIS while others report specific culture conditions or phenotypes of the islet source being necessary to observe PGE_2's effects (Table 1).

The effects of PGE on insulin secretion in a whole animal were the first studies to establish a link between PGE_2 and GSIS. Multiple researchers have utilized continuous infusion of PGE_2 into different model organisms to determine the effect of PGE_2 on plasma insulin. In a whole animal setting, continuous infusion of PGE is used because over 90% of PGs are metabolized by a single pass through the lungs that removes 97% of intravenously administered PGE_2 after 1.5 minutes (201,202). Most of these studies indicate that *in vivo* PGE_2 decreases GSIS. These studies lack target organ specificity; hence, PGE_2 could be affecting plasma insulin levels through mechanisms other than inhibiting GSIS in pancreatic islets. For example, PGE_2 injected into the third cerebral ventricle causes hyperglycemia (203). In addition to affecting

Method	Species	Ligand	Concentration	Change in GSIS	Reference
in vivo Bolus Injection					
	mouse (white)	PGE_1	2.5 µg 5.0 µg	↑	(204)
	sheep (Merino)	PGE_1	20 µg/kg	No Change	(205)
	human	15(S)-15-methyl PGE_2 methyl ester	1.0 µg/kg	↓	(206)
in vivo Continuous Infusion					
	rat (albino)	PGE_2	2 µg/min	↓	(193)
	human	PGE_2	10 µg/min	↓	(185)
	human	PGE_2	10 µg/min	↓	(192)
	human	PGE_2	10 µg/min	↓	(191)
	human (diabetic)	PGE_2	10 µg/min	↓ (response to arginine)	(207)
	human	PGE_1	0.2 µg/kg/min	↓	(185)
	human	PGE_1	0.2 µg/kg/min	↓	(208)
	human	PGE_1	0.2 µg/kg/min	No Change	(209)
	human	PGE_1	0.2 µg/kg/min	No Change	(210)
	human	PGE_1	0.2 µg/kg/min 0.5 µg/kg/min	No Change ↓	(211)
	human	PGE_1	0.5 µg/kg/min	↓	(212)
	rat (Sprague-Dawley)	PGE_1	0.5 µg/kg/min 1.0 µg/kg/min	No Change	(213)
	dog (mongrel)	PGE_1	0.5 µg/kg/min 1.0 µg/kg/min	No Change	(214)
	rat (albino)	PGE_1	2 µg/min	↓	(193)
	dog (mongrel)	PGE_1	10 µg/min	↓	(190)
	dog (mongrel)	PGE_1	10 µg/min	↓	(70)
	dog (mongrel)	PGE_1	10 µg/min	↓	(215)
	human	15(S)-15-methyl PGE_2	0.5 g/kg-hr	↓	(206)
	rat (Sprague-Dawley)	PGA_1	0.5 µg/min	No Change	(213)
	rat (albino)	PGA_1	2 µg/min	↓	(193)
	dog (mongrel)	PGB_1	10 µg/min	No Change	(216)

Method	Species	Ligand	Concentration	Change in GSIS	Reference
Perfused Pancreas					
	rat (Sprague-Dawley)	PGE_2	≥ 0.14 μM	↑	(217)
	rat (albino)	PGE_2	0.1 μM 1.0 μM 10 μM	↑	(183)
	rat (Sprague-Dawley)	PGE_2	0.28 μM 1.4 μM	↑	(189)
	rat (Wistar)	PGE_2	3 μM	↑	(218)
	rat (Sprague-Dawley)	PGE_2	1 μM 10 μM	No Change	(219)
	rat (Sprague-Dawley)	PGE_2	14 μM	↑	(187)
	rat (Sprague-Dawley)	PGE_1	0.28 μM	↑	(189)
	rat (Wistar)	PGE_1	3 μM	↑	(218)
	rat (Lewis)	16,16-dimethyl PGE_2-methyl-ester	10 μg/kg 100 μg/kg	↓	(220)
Isolated Islet -Perifusion					
	human	PGE_2	1 μM	NS (↑)	(221)
	rat (Sprague-Dawley)	PGE_2	1 μM 10 μM	No Change	(222)
	hamster (Syrian Golden)	PGE_2	10 μM	↑	(223)
	rat (Wistar)	PGE_1	0.85 μM	↑ 50 mg/dl glucose ↓ 300 mg/dl glucose	(224)
Isolated Islet - Static Incubation Insulin Secretion					
	mouse ($BTBR^{ob/ob}$)	PGE_2	0.05 μM	↓	(74)
	rat (Wistar)	PGE_2	0.1 μM	↓	(196)
	human	PGE_2	0.1 μM	No Change	(225)
	rat	PGE_2	1 μM	↓	(226)
	rat (Sprague-Dawley)	PGE_2	1 μM	↓	(227)
	mouse (ICR)	PGE_2	1 μM	↓	(228)
	mouse (C57B6/J)	PGE_2	1 μM	↓	(177)
	mouse (C57B6/J PGES-$1^{-/-}$)	PGE_2	1 μM	↓	(177)
	rat (Sprague-Dawley)	PGE_2	10 μM	↓	(184)
	rat (Wistar)	PGE_2	100 μM	↓	(197)
	rat (Wistar)	PGE_2	100 μM	↑	(229)
	rat (Sprague-Dawley)	PGE_2 (40 hours)	1 μM	No Change	(225)
	rat (Wistar)	PGE_1	0.01 - 10 μM	↑	(229)
	rat (Wistar)	PGE_1	2.8 μM	NS (↑)	(230)

Method	Species	Ligand	Concentration	Change in GSIS	Reference
Isolated Islet - Static Incubation Insulin Secretion - continued					
	mouse (BTBR) mouse (BTBR$^{ob/ob}$)	PGE_1	10 μM	No Change ↓	(74)
	mouse (BTBR$^{ob/ob}$)	Sulprostone	0.001 μM	↓	(74)
	rat (Wistar)	Sulprostone	0.1 μM	↓	(197)
	Mouse (C57BL/6$^{ob/ob}$)	Sulprostone	10 μM	↓	(134)
	rat (Wistar)	Misoprostol	0.3 μM 0.6 μM	↓	(197)
	rat (Wistar)	PGA_1	100 μM	No Change	(229)
Cell Line					
	guinea pig, HIT	PGE_2	EC_{50} = 1 nM	↓	(71)
	rat, Ins-1 (832/3)	PGE_2	EC_{50} ~50 nM	↓	(74)
	mouse, βHC13	PGE_2	0.1 μM	↓	(196)
	guinea pig, HIT-T15	PGE_2	0.1 μM	↓	(196)
	guinea pig, HIT-T15	PGE_2	1 μM	↓	(227)
	guinea pig, HIT-T15	PGE_2	1 μM	↓	(228)
	guinea pig, HIT	PGE_2	1 μM	↓	(194)
	rat (Sprague-Dawley), fetal pancreas cells	PGE_2	10 μM	↓	(195)
	rat, Ins-1 (832/13)	PGE_1	10 μM	↓	(133)
	rat (Sprague-Dawley), neonatal pancreas cells	PGE_1	10 μM	↓	(231)
	rat (Sprague-Dawley), fetal pancreas cells	PGE_1	10 μM	↓	(195)
	rat (Sprague-Dawley), neonatal pancreas cells	PGE_1 PGE_1 + sodium salicylate	10 μM	↑ ↓	(232)
	rat, Ins-1 (832/3)	Sulprostone	EC_{50} ~10 nM	↓	(74)

Table 1. Summary of the effects of E prostanoid receptor agonists on glucose stimulated insulin secretion

The effects of PGE_2 and PGE_2 analogs on insulin secretion have been extensively studied. The majority of studies have found that PGE_2 and PGE_2 analogs decrease GSIS, being frequently seen in studies utilizing whole animals and cell lines. Studies utilizing isolated islets have produced discordant results, but decreased GSIS in response to PGE_2 is frequently observed. Contradicting these results, studies utilizing pancreas perfusion often show that PGE_2 increases GSIS.

NS = not significant, parenthesis indicates direction of change

Method	Species	Ligand	Receptor	Concentration	Change in GSIS	Reference
Isolated Islet - Static Incubation Insulin Secretion						
	rat (Wistar)	AH-6809	EP1	0.1 – 10 μM	No Change	(197)
	mouse (C57BL/6)	L-798,106	EP3	10 μM	↑	(233)
	mouse (BTBR) mouse ($BTBR^{ob/ob}$)	L-798,106	EP3	20 μM 10 – 20 μM	No Change ↑	(74)
	human human (type 2 diabetic)	L-798,106	EP3	20 μM	No Change ↑	(74)
Cell Line						
	rat, Ins-1 (832/3)	L-798,106	EP3	> 100 nM	↑	(74)

Table 2. Summary of the effects of E prostanoid receptor antagonists on glucose stimulated insulin secretion
Selective EP receptor agonists suggest that EP3 is a negative regulation of GSIS.

GSIS, PGE_2 has also been shown to increase glucagon secretion in whole animal and perfused pancreas models, this may alter in insulin or glucose utilization (183,189,208-210,217,218,234).

The effects of PGE_2 in perfused pancreata have also been examined. This method keeps the entire pancreas with islets and exocrine tissue intact, but still removes it from the effect of other organs and innervation. The majority of studies show that PGE_2 increases GSIS during pancreas perfusion. These results are contrary to what has been observed in β-cell lines and some islet studies where PGE_2 decreased GSIS. It is possible that PGE_2 acts upon non-β-cell cell types in the intact pancreas, which in turn, raises GSIS.

Isolated islets, which contain a mixture of all islet cell types but lack innervation and pancreatic exocrine tissue, give more varied results, though the majority of studies still found that PGE_2 decreased GSIS. β-cell line models give consistent results with PGE reducing GSIS in all published reports that were reviewed, which clearly indicates that PGE decreases GSIS in β-cells.

Several groups have speculated upon the reason for the varied results in isolated islets. One group has reported that islets must be taken from obese or diabetic subjects in order to observe the PGE-mediated inhibition of GSIS (74,134). This suggests that PGE can only inhibit GSIS in islets from obese animals; however, most other studies used islets derived from normal animals (184,196,197,224). Robertson and colleagues emphasized that in order to see the inhibitory effects of PGE_2, islets must be cultured in the presence a phosphodiesterase inhibitor, such as IBMX (177) or theophylline (229). It is thought that in the presence of active phosphodiesterases, cAMP is quickly degraded mitigating the effect of $G\alpha_i$ signaling. Similarly, Sharp and colleagues used forskolin and 12-*O*-tetradecanoylphorbol 13-acetate (184) while Kimple and colleagues used GLP-1 (74) to keep cAMP at super maximal concentrations in order

to maximize insulin release allowing the detection of inhibitory $G\alpha_i$ signaling by PGE_2 or sulprostone, respectively. The contradictory nature of these data makes it difficult to definitively determine the effect of PGE_2 on GSIS from isolated islets. From the experiments discussed, it is clear that the islet source and culture conditions can have a profound effect on the results.

These studies indicate that PGE_2 is most likely inhibits GSIS by causing a reduction in intracellular cAMP in the pancreatic β-cell. The $G\alpha_i$ coupled EP3 receptor is a good candidate for the PGE_2 evoked inhibition of GSIS in islets. Gene expression of EP receptors has been shown in the mouse (181,235) and human pancreas (236), in human pancreatic stellate cells (237), in human (221), mouse (74,181), rat (196,197,238), and guinea pig islets (71), mouse β-cells (239), HIT and Min6 β-cell lines (71,74,227,240), 832/13 rat insulinoma cell line (238), and in the α-cell line, αTC1 (74). These data suggest that EP3, the $G\alpha_i$ coupled receptor, has the highest expression of the four EP receptors in islets. EP3 is not highly expressed in embryonic β-cells; but in adult β-cells, it is the sixth highest expressed $G\alpha_{i/o}$ coupled GPCR (239). The diabetic phenotype increases the expression of all three mouse EP3 splice variants and PGE_2 production in islets (74).

Selective agonists were first used to identify the EP receptors mediating PGE_2's inhibition of GSIS. Several studies have shown that PGE_2 inhibition of GSIS is pertussis toxin sensitive, indicating that PGE_2 inhibition of GSIS occurs through a $G\alpha_i$ coupled receptor (71,197,226). Sulprostone, an EP1/EP3 selective agonist, and misoprostol, an EP2, EP3, and EP4 selective agonist, inhibit GSIS in a pertussis toxin-sensitive manner in rat islets which implicates the $G\alpha_i$ coupled EP3 receptor as the primary mediator of PGE_2 signaling (197). Selective antagonists have also been used to elucidate PGE_2's signaling mechanisms in islets (Table 2). The involvement of EP3 was further confirmed by the use of EP3 antagonist L-798,106 which

blocked PGE_2 inhibition of GSIS and cAMP production in diabetic mouse islets (74). L-798,106 was shown to increase GSIS in Min6 cells, mouse islets, and diabetic human islets (74,233). In summary, PGE_2 appears to signal through the EP3 receptor on β-cells to cause a decrease in intracellular cAMP reducing GSIS (Figure 2). These results indicate that EP3 blockade may be a therapeutically useful mechanism to increase GSIS.

Few studies that examine the effects of PGE_2 and EP receptors on β-cell function, *in vivo*. Transgenic mice that have increased β-cell PGE_2 production by expressing COX2 and mPGES-1 in their β-cells using the rat insulin-2 gene promoter had reduced plasma insulin and displayed a poorer glucose tolerance (188). This effect was confounded by the observation that these transgenic mice had reduced β-cell proliferation and fewer β-cells. Other studies have shown that PGE_2 inhibits β-cell proliferation (195) and that salicylate prevents β-cell death (241). PGE_2 has also been shown to decrease cell viability in HIT cells, but it has no significant effect on cell cycle phase or apoptosis (227). However, a study using Min6 cell showed that PGE_2 reduces apoptosis (240). In a setting of streptozotocin (STZ)-induced diabetes, $COX2^{-/-}$ mice and $EP2^{-/-}$ mice treated with an EP4 antagonist have decreased survival; while mice treated with EP2 and EP4 agonists concurrently have increased survival (181). The EP4-selective agonist, ONO-AE1-329 improves glucose homeostasis and insulin resistance in $Lepr^{db/db}$ (leptin receptor diabetes mutation) mice (242). These studies indicate that PGE_2 signaling through an EP2/EP4 mediated pathway is protective for β-cells. It could be hypothesized that $EP3^{-/-}$ mice would have increased survival because the signaling pathway of EP3 classically opposes that of EP2/EP4. Furthermore, signaling through $G\alpha_{i/z}$ coupled GPCRs restrict β-cell expansion (134,239). Though this study did not report survival of STZ treated $EP3^{-/-}$ mice, STZ treated $EP3^{-/-}$ mice were reported to have no difference in blood glucose indicating that β-cell function was not improved

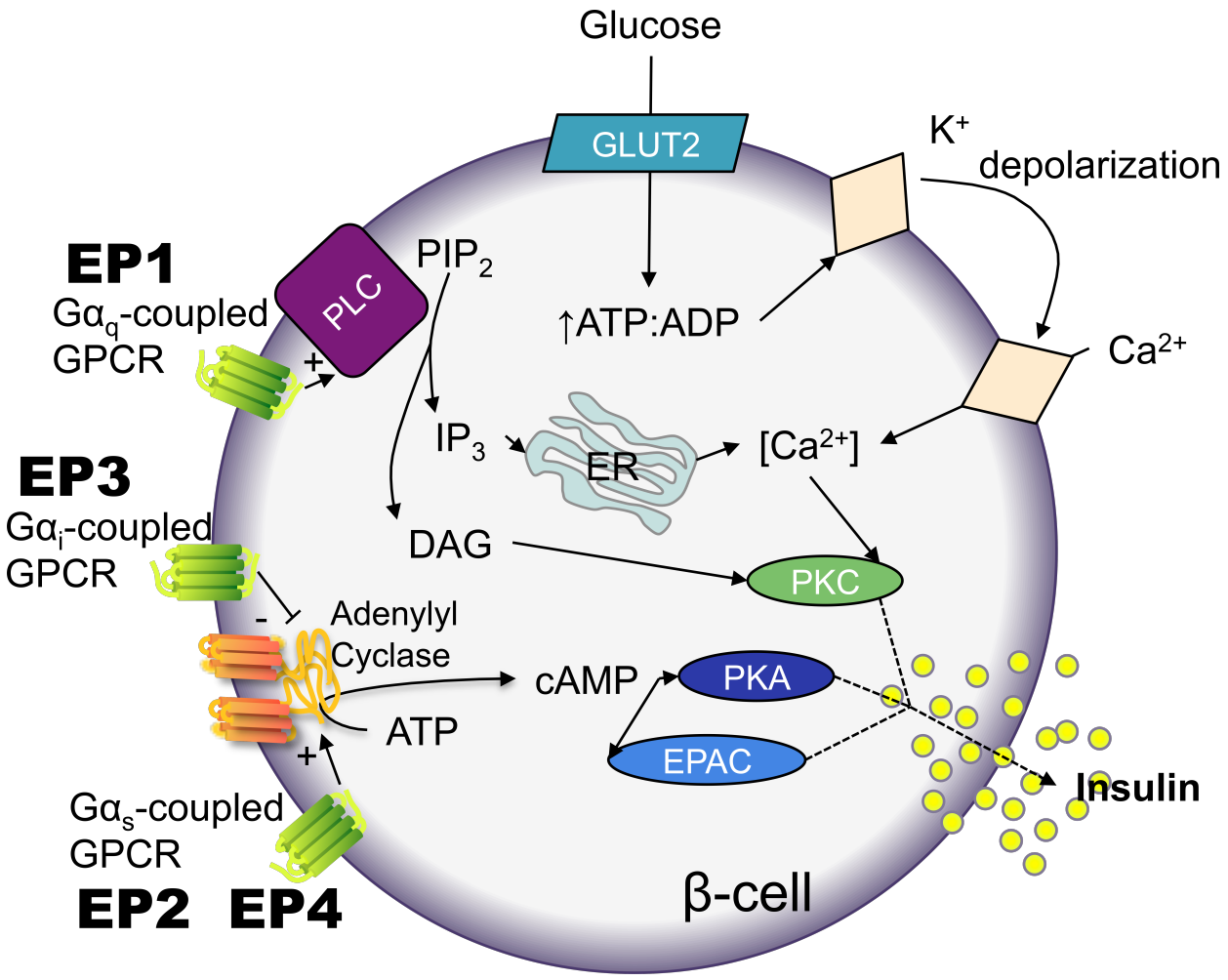

Figure 2. Prostaglandin signaling in the β-cell
Glucose import into the β-cell is the main trigger of insulin secretion. Glucose triggers insulin release by opening voltage dependent calcium channels thereby increasing the concentration of free cytoplasmic calcium. PKA and PKC phosphorylate proteins required for exocytosis. PGE_2 signals through its four cognate G-protein coupled receptors to modulate the activity of regulators of exocytosis, such as PKA, PKC, and Epac. EP3 is one of the most prominently expressed prostaglandin receptors on the β-cell and mediates the inhibition of insulin secretion by PGE_2.

(181). Contradicting this lack of change in $EP3^{-/-}$ STZ treated mice, an U.S. patent application demonstrated that EP3 antagonist GW671021B ameliorated hyperglycemia in mice when diabetes was induced with diet induced obesity in combination with STZ treatment (73). It is possible that the beneficial effects of EP3 inhibition can only be seen in a setting of obesity. The EP3 antagonist L-798,106 has been reported to only have beneficial effects in islets from diabetic patients or *Leptin*$^{ob/ob}$ mice (74). This may be because the EP3 receptor functions to decrease intracellular cAMP; hence, the lack of EP3 signaling has no effect in physiological states when cAMP is already low. In another study, $EP3^{-/-}$ mice have been reported to have elevated plasma insulin; however, these results are confounded by the fact that this study also reported that their $EP3^{-/-}$ mice were obese and insulin resistant (102). In a setting of insulin resistance, higher plasma insulin is necessary to compensate for the declining efficacy and therefore does not indicate differences in GSIS. These data indicate that PGE_2 has both beneficial and deleterious effects on the pancreatic β-cell *in vivo*. PGE_2 signaling through EP2 and EP4 promote β-cell survival whereas signaling through EP3 appears to reduce β-cell proliferation and function.

Prostaglandin D_2

The effects of other PGs in the islet have received little attention. PGD_2 is found in the pancreatic islet (186) and its production is increased in the presence of high glucose (174). Unlike PGE_2, PGD_2 has no or a very minimal effect on insulin release but is a potent stimulator of glucagon secretion (183,186,187,218). The PGD_2 receptor, DP1, does not appear to be expressed in islets, so PGD_2 signaling in islets may occur through DP2 which exhibits somewhat ubiquitous expression including the pancreas and islets of Langerhans (235). However, it has been reported that within the islet, DP2 is primarily expressed on β-cells and not on α-cells

(243). *In vivo* the contradictory effects of PGD_2 have been reported. One study reported L-PGDS$^{-/-}$ mice to have worse glycemic control due to impaired insulin sensitivity on both control and HFD (244). Another group reported no differences in L-PGDS$^{-/-}$ mice fed control diet, but glucose utilization being improved in L-PGDS$^{-/-}$ mice when fed HFD (245,246). Two independent groups found no differences in insulin sensitivity in L-PGDS$^{-/-}$ mice (245-247). These conflicting results give no clear answer as to the effect of PGD_2 on glucose homeostasis necessitating further studies.

Prostaglandin $F_{2\alpha}$

$PGF_{2\alpha}$ is found in the pancreatic islet (176,186) and its production is increased in the presence of high glucose (174). $PGF_{2\alpha}$ increases GSIS in isolated rat islets and NIT-1β cells (229,248). In perfused pancreata, $PGF_{2\alpha}$ increases GSIS at a concentration of 1 μM, but the effect is diminished at 10 μM (183,219). In contrast, $PGF_{2\alpha}$ infused into humans at 0.2 and 0.5 μg/kg/min had no effect on plasma glucose or insulin (208). $PGF_{2\alpha}$ has also been reported to increase glucagon levels (183,189). FP has low expression in islets (235), and 1 μM $PGF_{2\alpha}$ is a sufficient concentration to activate other PG receptors indicating that any effect of $PGF_{2\alpha}$ on GSIS may not be through FP but rather is an off target effect.

Prostacyclin

Production of PGI_2 is mediated by PGIS which is expressed in islets in response to glucose (249). The IP receptor is expressed in islets, but the level of expression is not high (235). The effects of PGI_2 on insulin secretion vary with both PGI_2 and glucose concentration. At low glucose, PGI_2 stimulates cAMP in rat islets in a dose dependent manner but increases insulin secretion following a bell shaped curve, with maximal stimulation occurring at 1 μM PGI_2 (250). At high glucose concentrations, high levels of PGI_2 still increase cAMP, but have an inhibitory

effect on insulin release (250,251). PGI_2 leads to varying responses in GSIS (251). Perfusion of the rat pancreas with 100 nM – 10 μM PGI_2 also had no effect on insulin or glucagon secretion (183). PGIS over-expression promotes GSIS by increasing intracellular cAMP and signaling through the Epac2 pathway (249). Consistent with PGI_2 improving GSIS during periods of low glucose, IP knockout mice have decreased blood insulin and increased blood glucose during the fasting state (252). Exogenous administrations of PGI_2 or the PGI_2 analog, Beraprost, have been reported to reduced blood insulin (253-255), though this has not been noted every study (256). Most studies noticed a concomitant increase in blood glucose following PGI_2 administration (255,257); however, Beraprost treatment tended to lower blood glucose (253,254). It should also be noted that PGI_2 has significant effect on gluconeogenesis which impacts blood glucose levels *in vivo* (252). PGI_2 agonists Beraprost and Iloprost both improve islet viability (258,259), which may explain in part why long-term Beraprost treatment lowers blood glucose and improves glycated hemoglobin (HbA1c) (253,254). It should also be noted that Beraprost might improve HbA1c due to increasing circulation, which is known to improve insulin sensitivity (254,260).

Thromboxane

TXA_2 does not appear to have an effect on islet insulin production. The TP receptor has low expression in islets (235) and TXA_2 is produced by islets as evidenced by low levels of TXB_2 found in islet arachidonic acid metabolites (179). With these low levels of expression, it is not surprising that TXA_2 has no effect on insulin secretion in the perfused rat pancreas (183).

(Reviewed in (39,40,50,105,108,119,198-200,261-274))

Obesity and Adiposity

Obesity and adiposity are greatly influenced by insulin. Insulin is an anabolic hormone and hence acts to increase body mass (275,276). In addition, insulin activates phosphodiesterase

3B in adipocytes to reduce cAMP levels and lipolysis (277,278). Insulin sensitivity declines during obesity and the concomitant decline of β-cell function ultimately leads to reduced insulin production in obese individuals (11,279). In addition to regulating insulin secretion, PGs have also been found to be involved with the development and progression of obesity. There are several reports of PLA enzyme and PG signaling disruption that cause a reduction in obesity. Knockout mouse models of a $cPLA_2$ (*pla2g4a*) (280,281), AdPLA (101), COX2 (98,99,282), and IP (283) all show resistance to obesity. In addition to knockout models, obesity can also be reduced pharmacologically with indomethacin, an NSAID (100), and 5-(4-benzyloxyphenyl)-(4S)-(phenyl-heptanoylamino)-pentanoic acid [KH064], a selective $sPLA_2$ (pla2g2a) inhibitor (284). In contrast, group X $sPLA2^{-/-}$ (285), $LPGDS^{-/-}$ (247), $EP3^{-/-}$ (102), and mice treated with indomethacin (286) have been reported to be more prone to obesity. Obesity is a complex disease that is mediated by numerous physiological processes. PGs play a role in regulating some of these processes, such as energy homeostasis, adipocyte proliferation, and lipolysis, all of which may be involved in contributing to the role of PGs in obesity.

Energy Homeostasis

Feeding Behavior

PGE_2 is involved in stress responses which signal through hypothalamic-pituitary-adrenal (HPA) axis which affects a variety of behaviors including feeding and social behavior (287). PGE_2 and $PGF_{2\alpha}$ are known to inhibit food intake in rats (288-291). Anorexia can also be promoted by arachidonic acid and this is reversible by NSAID administration implicating PG action in this effect (292,293). Experiments in sheep reveal a more complex role of hypothalmic PGs and feeding behavior. PGE_1 decreases feeding when injected into the medial and anterior loci of the hypothalmus but increases feeding when injected into the lateral loci (294). This

indicates that PGE_2 may elicit different feeding responses depending on the area of the brain in which it is produced. The anorexic actions of PGE_2 may be mediated through the EP4 receptor in mice; EP4 agonist ONO-AE1-329 mimicks the anorexic action of PGE_2 while EP4 antagonist ONO-AE3-208 blocks PGE_2's effect (295). However, a different study has reported no effect of the ONO-AE1-329 on food intake or body weight in $Lepr^{db/db}$ mice (242). PGE_2 also stimulates leptin release from adipocytes (296,297). Leptin acts mainly on the central nervous system to reduce food intake and energy expenditure (298); therefore, systemic PGE_2 may also have anorexic effects via leptin. Conversely, PGD_2 stimulates feeding behavior through the DP1 receptor in mice, but it does so indirectly requiring the neuropeptide Y1 receptor, which is a $G\alpha_{i/o}$ coupled GPCR (299). In human cerebral spinal fluid, the L-PGDS protein levels correlates with neuropeptide Y levels and visceral adiposity (300).

The $EP3^{-/-}$ mouse has been reported to be obese due to hyperphagia, which was attributed to disrupted sleep patterns and increased "night eating" (daytime feeding for these nocturnal animals) (102). Numerous studies have shown that PGD_2 promotes sleep (301-303), while PGE_2 has been shown to promote wakefulness (304-307). $EP3^{-/-}$ mice demonstrated continuous feeding during the dark period which is in contrast to $EP3^{+/+}$ which had periods of increased feeding at the beginning and end of the dark cycle. Conversely, another study found that EP3 knockout in neuronal and glial cells had no effect of on sleep-wake rhythm (308). These data indicate that EP3 may be responsible for some of PGE_2's anorexic effects (102), despite the reported lack of effect of EP3 agonists on feeding behavior (295). It is possible that EP3 and EP4 mediate feeding behavior in different parts of the brain. Alternatively, it is possible that the effects of EP3 loss primarily affect circadian rhythms, which in turn result in hyperphagia.

Thermoregulation

PGE has been long known to induce fever (309). In the first study examining the effect of PGE_2 infusion in humans, a "feeling of warmth" was among the first symptoms reported (64). This pyretic response of PGE_2 is mediated through EP3 (310). PGE_2 activates hypothalamic neurons in the preoptic nucleus in order to increase thermogenic activity of brown adipose tissue (BAT) and thereby raise the body temperature (311,312). Though PGE_2 plays an important role in acute thermoregulation during fever, it does not appear to play a similar role in normal temperature regulation, and body temperature change does not alter PG levels in the cerebrospinal fluid (313,314). PGI_2 also appears plays a role in thermoregulation; PGI_2 analog Beraprost increases temperature two hours after injection (254). When $PGF_{2\alpha}$ is injected into the preoptic area of the anterior hypothalamus, it also causes a rise in temperature and this rise is curare sensitive indicating that the rise in temperature is due to shivering (203,315). The effect of intracerebroventricular PGD_2 on thermogenesis is variable; high doses produce mild hyperthermia whereas low doses reduce body temperature (203,316,317). Injections of PGE_2, PGD_2, and $PGF_{2\alpha}$ into the third cerebral ventricle also increase hepatic glucose production, with the effect of $PGF_{2\alpha}$ being especially pronounced, providing fuel for the increased thermogenesis (203).

PGs also influence energy utilization by playing an important role in BAT recruitment and development (Figure 3). BAT is adipose tissue that contains a large amount of mitochondria, which imparts its characteristic brown color, and functions primarily to burn energy and generate heat as opposed to white adipose tissue (WAT) which functions primarily to store energy. Cold exposure causes sympathetic nerves to release norepinephrine activating β_3-adrenergic receptors thereby inducing COX2 expression and activity (282,318). COX2 derived PGE_2 signals through

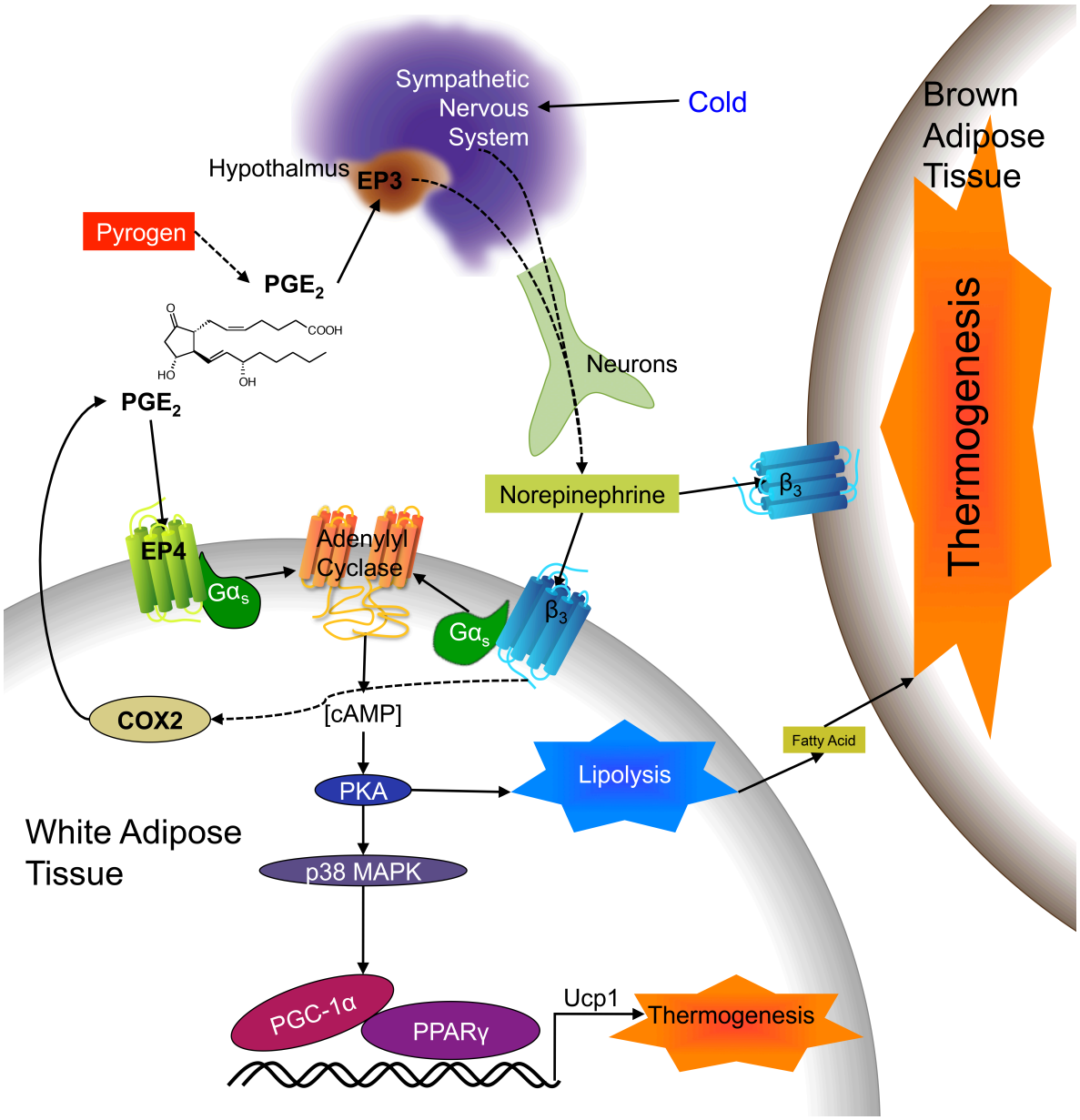

Figure 3. PGE_2 regulation of thermogenesis
The sympathetic nervous system is stimulated by cold exposure to release norepinephrine which binds to the β_3 adrenergic receptors to stimulate thermogenesis in adipose tissue. Stimulation of the β_3 receptor up regulates COX2 in white adipose tissue leading to increased PGE_2 production. PGE_2 signals in an autocrine or paracrine manner through the EP4 receptor to further promote *Ucp1* expression and thermogenesis.
In response to inflammatory stimuli, PGE_2 in the brain vasculature binds to EP3 receptors in the preoptic area to inhibit warm-sensitive, GABAergic inhibition of sympathoexcitatory neurons thereby promoting pro-thermogenic signaling of the sympathetic nervous system leading to fever.

EP4 to induce uncoupling protein 1 (UCP1) in adipose tissue (282,286). UCP1, a protein found exclusively in mitochondria of adipose tissue, uncouples respiration from ATP synthesis by causing the electron gradient to dissipate without the generation of ATP resulting in a loss of energy (318). Transcription of *Ucp1* is promoted by activation of PKA by $G\alpha_s$ coupled receptors, such as β_3-adrenergic receptor and EP4, resulting in the activation of p38α mitogen-activated protein kinase (MAPK) which in turn phosphorylates regulators of *Ucp1* transcription, such as PPARγ coactivator-1α (PGC-1α) (319). This "browning" of adipose tissue by PGE_2 induction of UCP1 would be expected to increase thermogenesis and energy expenditure. Indeed, mice over-expressing COX2 have increased oxygen consumption, increased energy expenditure, and reduced body fat due to increased BAT (282). $COX2^{-/-}$ mice have reduced body temperature and indomethacin treatment of mice reduces energy intake leading to increased adiposity (286).

BAT also expresses L-PGDS and this expression is positively correlated with thermogenesis (245). L-$PGDS^{-/-}$ mice preferentially utilize glucose for thermogenesis indicating that PGD_2 plays an important role in fat metabolism (245). The regulation of BAT recruitment indicates an important role of PGs in thermoregulation and energy expenditure. Though acute effects of PGs on body temperature appear to be primarily related to fever, PGs also have a chronic role in thermoregulation increasing BAT recruitment and long-term energy expenditure.

Adipose Tissue

Lipid signaling molecules, including PGs and other inflammatory mediators, play an important role in adipose tissue physiology (320). Altering PG signaling has been reported to either prevent or predispose animals to obesity depending on which part of the pathway is disrupted. As discussed above, PGs clearly affect energy homeostasis through their roles in feeding behavior and BAT mediated thermogenesis. These effects on global metabolic profiles

affect the amount of energy stored contributing to or reducing obesity. Changes in obesity are reflected by changes in adipocyte cell size or numbers. PGs play a crucial role regulating many of these changes.

Adipose tissue is an important site of PG action in obesity. Adipose tissue has been shown to express constitutively express COX1 while COX2 is inducible (282,286,321-336). Expression of all three PGES isoforms (324,327,334,335,337,338), L-PGDS (326,327,332,334,339-343), PGIS (327), and PGF synthase (335) has been reported in adipose tissue. Aldo-keto reductases have also been reported to function as PGF synthases in adipocytes (328,330,332,344,345). PGE_2, PGD_2, $PGF_{2\alpha}$, and PGI_2 are all produced by adipocytes, pre-adipocytes, or have been found in adipose tissue.

Adipocyte Differentiation and Proliferation

Transcriptional regulation of PG biosynthesis and adipogenesis are regulated by a common transcription factor; CCAAT/enhancer-binding protein (C/EBP) β promotes the transcription of both COX2 (346-348) and the critical transcription factors for adipogenesis, PPARγ and C/EBPα (349,350). PGs are generally thought to play an inhibitory role in WAT adipogenesis. Inhibition of COX1, COX2, and PGES activity increases adipogenesis and triglyceride accumulation (321,324,331,333,336,351). Consistent with this, expression of both COX enzymes and PGES are decreased during adipogenesis (323,327,330,331,336). Other studies suggest that only COX2 inhibition increases adipogenesis with no effect of COX1 inhibition being observed (323,352). In contrast, aspirin and indomethacin have been reported to reduce the formation of adipose cells (326,341,353,354). Analysis of PG receptor expression shows prominent expression of EP1-4, DP2, FP, and IP, but low expression of TP in WAT, BAT, and adipocytes (197,235,327,330,338). EP3 has the highest expression of the four EP

receptors in mouse epididymal fat pads, and EP2, EP3, and EP4 expression are all increased by high fat diet feeding (338). PGES expression has been reported to be both decreased during obesity (337) and unchanged by high fat diet feeding (338). Radioligand binding studies confirm that EP (355,356) and FP (357) proteins are present on adipocytes. WAT, BAT, and adipocytes are some of the highest EP3 expressing tissues in the body (235); however, all three splice variants of EP3 are expressed more in mature adipocytes suggesting that EP3 is more important for mature adipocyte function than for differentiation (327,352,358). EP1 and EP4 are expressed on pre-adipocytes implicating their involvement in adipogenesis (352,358). FP and aldo-keto reductase 1B expression are transiently increased during the early stages of adipogenesis but their expression is significantly lower in differentiated adipocytes compared to undifferentiated cells (327,330,352,358). IP is not expressed in pre-adipocytes, but is expressed shortly after cells begin to differentiate and in fully mature adipocytes (358,359).

Some studies have shown that PGE_2 inhibits adipocyte differentiation (324,335), though this has not been shown in every study (351,360,361). This may be due to PGE_2 only exerting its inhibitory effects during the later stages of differentiation (362). Alternatively, the effect may be concentration dependent as 280 nM PGE_1 was unable to affect differentiation, but 28 μM stimulated differentiation (363). cAMP analog, dibutyryl cyclic AMP, similarly promotes adipogenesis during early stages, but inhibits at later time points (362). PGE_2 signals through the EP4 receptor to inhibit adipogenesis of WAT (352,364) and to promote *Ucp1* expression, which is indicative of beige adipose tissue (286,324). Further evidence that PGE_2-EP4-cAMP signaling is anti-adipogenic comes from studies that found that PGE_2, EP4 agonist AE1-392, and dibutyryl cyclic AMP, all suppress the expression of the key adipogenic genes *Pparg* and *Cepba* during 3T3-L1 adipocyte differentiation (365). This suppression of differentiation is dependent upon

PKA activity (331). Conflictingly, $EP4^{-/-}$ mice have reduced fat mass without differences in adipocyte size (338).

PGI_2 is well known to promote adipogenesis (366). PGI_2 and its stable analog carbacyclin are both known to stimulate differentiation of adipocytes (283,353,354,367-369). PGI_2 promotes differentiation in adipocytes by raising intracellular cAMP (283,353,370-372). However, there is at least one report that PGI_2 inhibits adipogenesis by raising cAMP (373). This increase in cAMP mediated by PGI_2 and other IP agonists increases the expression of adipogenic transcription factors PPARγ, C/EBPβ, and C/EBPδ (253,370). Consistent with these findings, $IP^{-/-}$ mice are resistant to diet induced obesity and have reduced fat mass (283).

$PGF_{2\alpha}$ is another potent inhibitor of adipose tissue differentiation (351,357,360-362,374-381), although at least one study has found that $PGF_{2\alpha}$ stimulates differentiation (363). $PGF_{2\alpha}$ analogs fluprostenol, cloprostenol, latanoprost, and travoprost likewise inhibit differentiation (357,375,380,382,383). However, there is a report of fluprostenol having no effect on differentiation in mouse embryonic fibroblasts (MEF) (352). Furthermore, at sub-maximal concentrations of PGI_2, $PGF_{2\alpha}$ potentiates PGI_2 induced adipocyte differentiation (366). $PGF_{2\alpha}$ inhibits adipogenesis via a $G\alpha_q$-Calcium-Calcineurin dependent signaling pathway that inhibits the expression of PPARγ and C/EBPα (379). In addition, activation of MAPK and subsequent PPARγ phosphorylation by $PGF_{2\alpha}$ signaling also reduces adipogenesis (380). More evidence supporting $PGF_{2\alpha}$'s role in inhibiting adipogenesis comes from mice lacking aldo-keto reductase 1B which are more obese because they have reduced $PGF_{2\alpha}$ production (345).

There are conflicting reports on the role of PGD_2 in adipogenesis. Knockdown of L-PGDS has been shown to either promote (339) or to inhibit adipogenesis (340). Over expression of L-PGDS in cell culture inhibits adipogenesis (341). However, transgenic mice over

expressing L-PGDS have increased adipogenesis (384). PGD_2 has also been reported to inhibit adipocyte differentiation, as evidenced by stimulation of Stearoyl-CoA desaturase-1 (SCD1) mRNA in 3T3-L1 preadipocytes (375). PGD_2 metabolite, 15-deoxy-$\Delta^{12,14}$-prostaglandin J_2 (15Δ-PGJ_2), is an agonist for PPARγ that stimulates adipogenesis (326,341,380,385-387). While it is unclear whether PGD_2 itself has an effect on adipogenesis, PGD_2 production promotes adipogeneisis via its metabolite 15Δ-PGJ_2.

In summary, COX metabolites negatively influenced differentiation of adipocytes (321,331,336,352). The PGs, PGE_2 and $PGF_{2\alpha}$, that play an important role in inhibiting WAT adipogenesis. PGE_2 and promotes the inhibition of WAT adipogenesis in part by promoting the "browning" of WAT and recruiting brown adipocytes. $PGF_{2\alpha}$ also inhibits adipose tissue development. 15Δ-PGJ_2 opposes the role of the aforementioned primary eicosanoids, promoting adipogenesis via PPARγ activation.

(Reviewed in (388-390))

Adipocyte Morphology

Several models of *in vivo* PG inhibition have reported differences in adipocyte cell size. $COX2^{-/-}$, $cPLA_2^{-/-}$, and $AdPLA^{-/-}$ mice have reduced adipocyte cell sizes (101,280,281,391) whereas L-$PGDS^{-/-}$ and group X $sPLA2^{-/-}$ mice have larger adipocytes (244,285). Treatment of mice with EP4 agonist CAY10580 decreases adipocyte size, but adipocyte size is unchanged in $EP4^{-/-}$ mice (338). Indomethacin treatment of mice fed a high fat and high salt diet also reduces adipocyte cell size (100); however, when fed a high fat diet, indomethacin caused a small increase in adipoctye cell size (286). $AdPLA^{-/-}$ mice have increased ectopic lipid accumulation accounting for the triglyceride, consistent with redistribution from the adipose tissue (101). However, $COX2^{-/-}$, $cPLA_2^{-/-}$, and mice treated with indomethacin have reduced ectopic lipid

accumulation (100,280,281,391). These changes in adipocyte size may be indicative of changes in energy homeostasis or adipocyte function.

Several studies have investigated the effects of PGE_2 signaling on adipose tissue inflammation. Signaling through the EP4 receptor has been shown to reduce crown-like structure formation, macrophage infilatration, and chemokine production in adipose tissue (242,338). Reduced prostaglandin production in $AdPLA^{-/-}$ mice had no effect on the expression of inflammatory markers (101).

Adipocyte Function

Production of PGE_2, PGD_2, $PGF_{2\alpha}$, and PGI_2 by adipocytes has been well characterized. Numerous studies have reported that PGE_2 inhibits lipolysis (90-92,101,296,297,321,392-400). Lipolysis is the generation of FFA from triglycerides (401-405). Triglycerides are first converted into diacylglycerol by adipose triglyceride lipase (ATGL). Hormone-sensitive lipase (HSL) converts diacylglycerol into monoacylglycerol. Monoacylglyerol is then converted into glycerol and three FFA by monoacylglycerol lipase (MGL). Prior to lipolysis, non-activated Perilipin (PLIN) and CGI-58 (comparative gene identification-58) binds to a triglyceride while unstimulated HSL is in the cytoplasm. External stimuli increase cAMP, which activates PKA that phosphorylates HSL and PLIN. Phosphorylation of PLIN causes CGI-58 to be released from the triglycyeride droplet, which then activates ATGL initiating lipolysis. Phosphorylated HSL translocates from the cytosol to the lipid droplet and interacts with PLIN. HSL's role as a diacylglyceride hydrolase is the rate-limiting step in lipolysis. MGL completes the final hydrolysis reaction producing the third FFA and glycerol. It should be noted that ATGL, HSL, and MGL will hydrolize all three acylglycerols, but not with equal activity.

Insulin is a major inhibitor of lipolytic activity. This serves to reduce the amount to FFA available to cells during periods of elevated insulin, which normally occurs when blood glucose is elevated. Insulin reduces lipolytic activity by reducing intracellular cAMP in adipocytes (406). Insulin causes the degradation of intracellular cAMP by activating phosphodiesterase 3B via PI3K-AKT signaling (277,278). In addition to inhibiting lipolytic activity, insulin is a driver of glucose uptake and fatty acid synthesis in adipocytes. PGE_2 has an additive effect with insulin on increasing glucose uptake and metabolism opposing the actions of adrenergic agonists (407-409), though PGE_1 was not found to have this effect in at least one study (377).

Many early studies of PG signaling in adipoctyes compared the effect of PGE_2 to that of catecholamines. Isoproterenol and the endogenous catecholamines, epinephrine and norepinepherine, stimulate lipolysis; this stimulation of lipolysis is inhibited by PGE_2 (91,92,393-399,410-419). Isoproterenol, epinephrine, and norepinephrine are all agonists for the β-3 adrenergic receptor, which is highly expressed in adipose tissue, is $G\alpha_s$ coupled, and promotes cAMP production. PGE_2 has been repeatedly shown to cause a marked reduction in cAMP in adipocytes (93,94,284,393,395,396,400,413,415,420-425). PGE_2 directly opposes the actions of β-adrenergic agonists on lipolysis and cAMP accumulation. PGE_2 also opposes the actions of other drugs which raise cAMP, such as forskolin (284,421), which activates adenylyl cyclase, and phosphodiesterase inhibitors such as theophylline (393,398,412,417-419,426) and IBMX (416). The pronounced effect of PGE_2 reducing cAMP levels and opposing the action of agonists for $G\alpha_s$ coupled receptors, suggests that PGE_2 signals through the $G\alpha_i$ coupled EP3 receptor in adipocytes. Sulprostone, an EP1 and EP3 selective agonist, has also been shown to reduce cAMP in adipocytes and to exhibit anti-lipolytic effects similar to PGE_2 (396,421,427). EP3 antagonist L-798,106 has been shown to block PGE_2 mediated reduction in cAMP in

adipocytes (284) and EP3 antagonist L-826,266 has been shown to block PGE_2's inhibition of lipolysis (101). These data clearly indicate that PGE_2 signals through the EP3 receptor to reduce cAMP in adipocytes and thereby inhibit lipolysis (Figure 4).

Administration of PGE *in vivo* produces mixed results on FFA levels; with reports of plasma FFA being decrease (410,428) or increased (209,210). Epinephrine causes an increase in FFA release *in vivo*, which is blocked by PGE_1 administration though PGE_1 administration alone showed only a minimal effect (92). This indicates that PGE does inhibit lipolysis *in vivo*, but other stimuli also heavily influence lipolysis and could potentially overwhelm the effects of PGE.

Opposing the action of PGE_2 on lipolysis is PGI_2, which is a stimulator of lipolysis (392). This is not surprising because PGI_2 increases intracellular cAMP in adipocytes (283,366,370-372). However, some pre-adipocyte cell lines lose the ability to respond to PGI_2 after differentiation and hence do not have a lipolytic response to PGI_2 (372). Some studies have reported that PGE_2 has biphasic effects on adipocyte adenylyl cyclase activity, inhibiting adenylyl cyclase at low concentrations but stimulating adenylyl cyclase and increasing cAMP levels at concentrations greater than 1 μM (413,421). PGE_2 has an affinity for the IP receptor of ~4 μM (429), hence PGE_2 is possibly stimulating IP, in addition to EP2 and EP4 which have Kd's ~1-5 nM, when used at 10 μM and greater. PGI_2analog Beraprost decreases adipocyte cell size, possibly due to increased lipolysis and increased thermogenesis, improving insulin sensitivity and other symptoms of metabolic syndrome (253,254).

$PGF_{2\alpha}$ signaling in adipocytes primarily raises intracellular calcium (357,430-433), though there is at least one report of $PGF_{1\alpha}$ inhibiting cAMP production in adipose tissue (94). $PGF_{2\alpha}$ causes adipose tissue to increase basal glucose uptake in a PKC dependent manner which

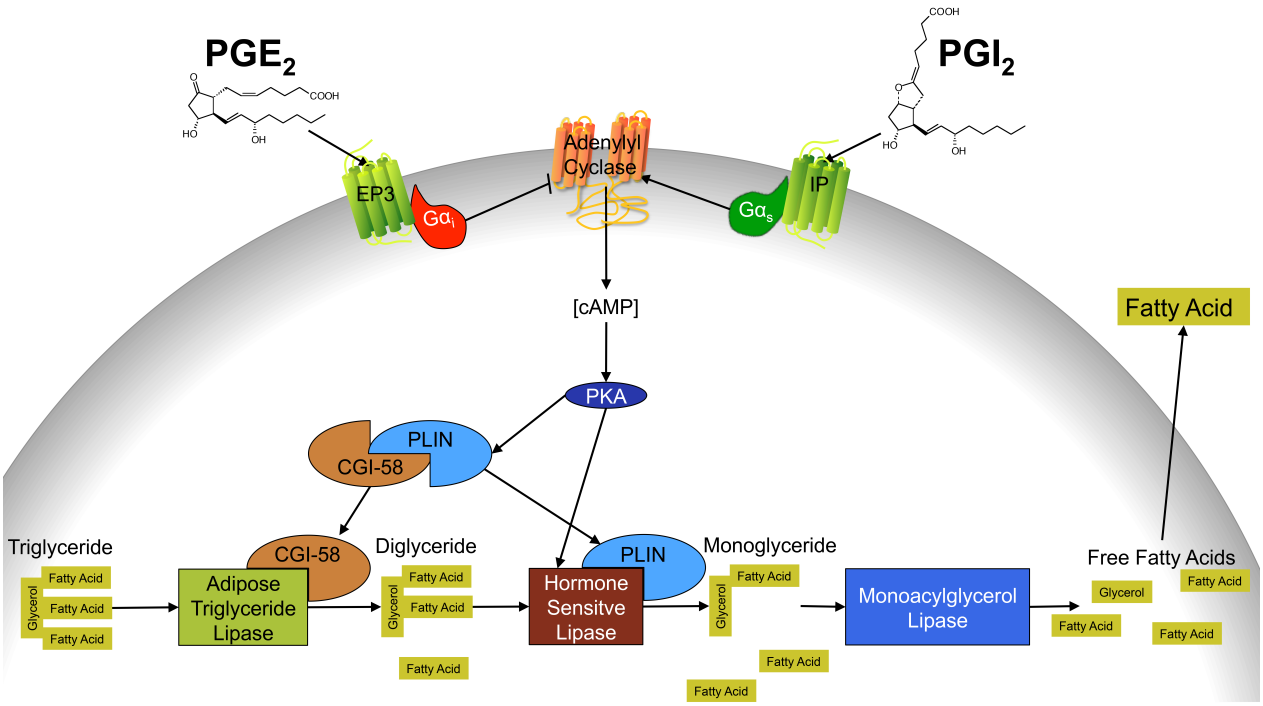

Figure 4. Prostaglandin regulation of lipolysis in adipocytes
Prostaglandins primarily regulate lipolysis in adipocytes by signaling through the EP3 and IP receptors. PGI_2 signals through the $G\alpha_s$ coupled IP receptor to increase lipolysis. PGE_2 signals through the $G\alpha_i$ coupled EP3 receptor to reduce adenylyl cyclase activity that is augmented by the pro-lipolytic signaling of catecholamines, PGI_2, and other $G\alpha_s$ dependent signaling pathways in adipose tissue.

was synergistic with increasing cAMP (377,434,435). Due to the general lack of effect of $PGF_{2\alpha}$ on cAMP levels, it is not surprising that $PGF_{2\alpha}$ has no effect on lipolysis (376).

Inhibition of PG synthesis *in vivo* has mixed effects on lipolysis. These conflicting results during global PG inhibition may be due, in part, to increased insulin which inhibits lipolysis. Knockout models of $cPLA_2$ (*pla2g4a*) (280,281), AdPLA (101), and COX2 (98,99) or treatment of mice with the NSAID indomethacin for seven weeks (100) causes an increase in plasma FFAs. Administration of aspirin for four days to humans or eight days to rats decreases plasma FFA in diabetic subjects (436,437). However; in normal subjects aspirin decreased FFA in non-diabetic humans (436) but increased FFA in control rats (437). Most studies indicate that salicylate decreases FFA release (83,88,438-443), but it has also been reported to have no effect (59,444,445) or to cause an increase (89).

(Reviewed in (390,401,446))

Liver

The liver is a key regulator of energy homeostasis. The liver regulates glucose homeostasis, being the site of glycogen synthesis, the conversion of excess glucose into glycogen for storage during times of hyperglycemia, glycogenolysis, the conversion of glycogen into glucose into for immediate use during times of hypoglycemia, and gluconeogenesis, the conversion of non-carbohydrate carbon substrates into glucose (447). These processes are primarily regulated by the opposing actions of the hormones insulin, promoting glycogenolysis and glycogen synthesis, and glucagon, promoting gluconeogenesis. In addition to being the site of carbohydrate storage, the liver also plays a role in storing excess triglycerides (448). The liver is the secondary site of lipid storage in the body, being the preferential place to store excess lipid that is unable to be stored in adipose tissue. Excess lipid storage in the liver can lead to insulin

resistance and fatty liver disease. Fatty liver disease can progress into steatohepatitis and eventually lead to cirrhosis. Lipids are capable of altering hepatic gene expression and lipid content (449). Among the many factors that affect the liver, PGs play an important role regulating hepatic function and disease (450-452).

Hepatic tissue expresses COX and PGES genes that are necessary for production of PGs (252,391,453-459). Kupffer cells, which are hepatic macrophages, have been reported to be the primary source of hepatic PGs (460). Kupffer cells can be induced to produce excess PGE_2 by stressors such as lipopolysaccharide (LPS) (460-464), alcohol (456,464,465), carbon tetrachloride (466), anaphylatoxin (467-470), or liver resection (471-473). Hepatic endothelial and Kupffer cells produces multiple PGs: $PGD_2 >> TxB_2 > PGF_{2\alpha} > PGE_2 >$ 6-Keto-$PGF_{1\alpha}$, with PGD_2 being the primary eicosanoid produced by both (474,475). Parenchymal cells primarily generate PGD_2 and $PGF_{2\alpha}$ with lesser quantities of TxB_2, PGE_2, and 6-Keto-$PGF_{1\alpha}$ being made (474,476). Providing free arachidonic acid to liver tissue changes the relative ratios of PGs produced with $PGE_2 >> PGF_{2\alpha} > PGD_2$ (477). Obesity and other models of liver damage, such as alcohol and inflammation, also increase hepatic PGE_2 production and expression of PGE_2 generating enzymes (252,454,462,465,478).

Radioligand binding studies show that PG receptors are expressed in the liver (479-488). Studies present conflicting reports on the relative expression of PG receptors in the liver. Most studies agree that EP1 is highly expressed, relative to the other PG receptors, with all other PG receptors being detected in liver (197,235,236,489-495). Hepatocytes are known to express EP3β and a splice variant of FP containing a unique 5' untranslated region, because both have been cloned from rat hepatocytes (496,497). Expression of hepatic PG receptors is not constitutive; the inflammatory cytokine, IL-6, can induce the expression of EP2, EP4, and DP (491,495).

Kupffer cells express EP1-4 and TP (490,498). Sinusoidal endothelial cells have high expression of EP1-4, IP, and TP (490). Hepatic stellate cells have high expression of EP1, EP3, and IP (490). Diabetic stress can increase the expression of the IP receptor (252).

Glycogen Synthesis, Glycogenolysis, & Gluconeogenesis

PGs play an important role in regulating hepatic glycogen stores and glucose production (Figure 5). Gluconeogenesis is classically promoted by glucagon which signals through a $G\alpha_s$ coupled GPCR; promoting glucose production by raising cAMP (499). The glycogen phosphorlase enzyme catalyzes the rate-limiting step in gluconeogensis; this enzyme is activated by phosphorylase kinase, which in turn is activated by increases in intracellular cAMP/PKA or an increase in intracellular calcium/calmodulin (500-504). Glucagon has been shown to induce PG formation (505). PGE_2 inhibits the glucagon mediated rise in cAMP and thereby reduces hepatic glycogenolysis and gluconeogenesis (75,76,482,494,505-513). This inhibition of hepatic glucose production by PGE_2 during periods of elevated cAMP is pertussis toxin sensitive (514-516). Sulprostone, an EP1/EP3 selective agonist, and misoprostol, an EP2, EP3, and EP4 selective agonist, inhibit glucagon stimulated cAMP formation in primary culture rat hepatocytes with a similar potency (494,516). These results are consistent with EP3 mediating a reduction in cAMP. In the absence of glucagon, PGE_2 increases intracellular IP_3, calcium, and cAMP in hepatocytes and thereby increases glucose output (75,479,517-522). Sulprostone also increases IP_3, but misoprostol only produces a minimal response (494). Sulprostone is more potent than misoprostol at increasing glycogen phosphorylase activity (516). These results are consistent with PGE_2 signaling through EP1 to activate PLC and thereby raise intracellular calcium. Together these studies indicate that EP1 and EP3 have opposing roles in hepatic glucose production. EP1 causes a rise in intracellular calcium, which promotes glycogen breakdown and

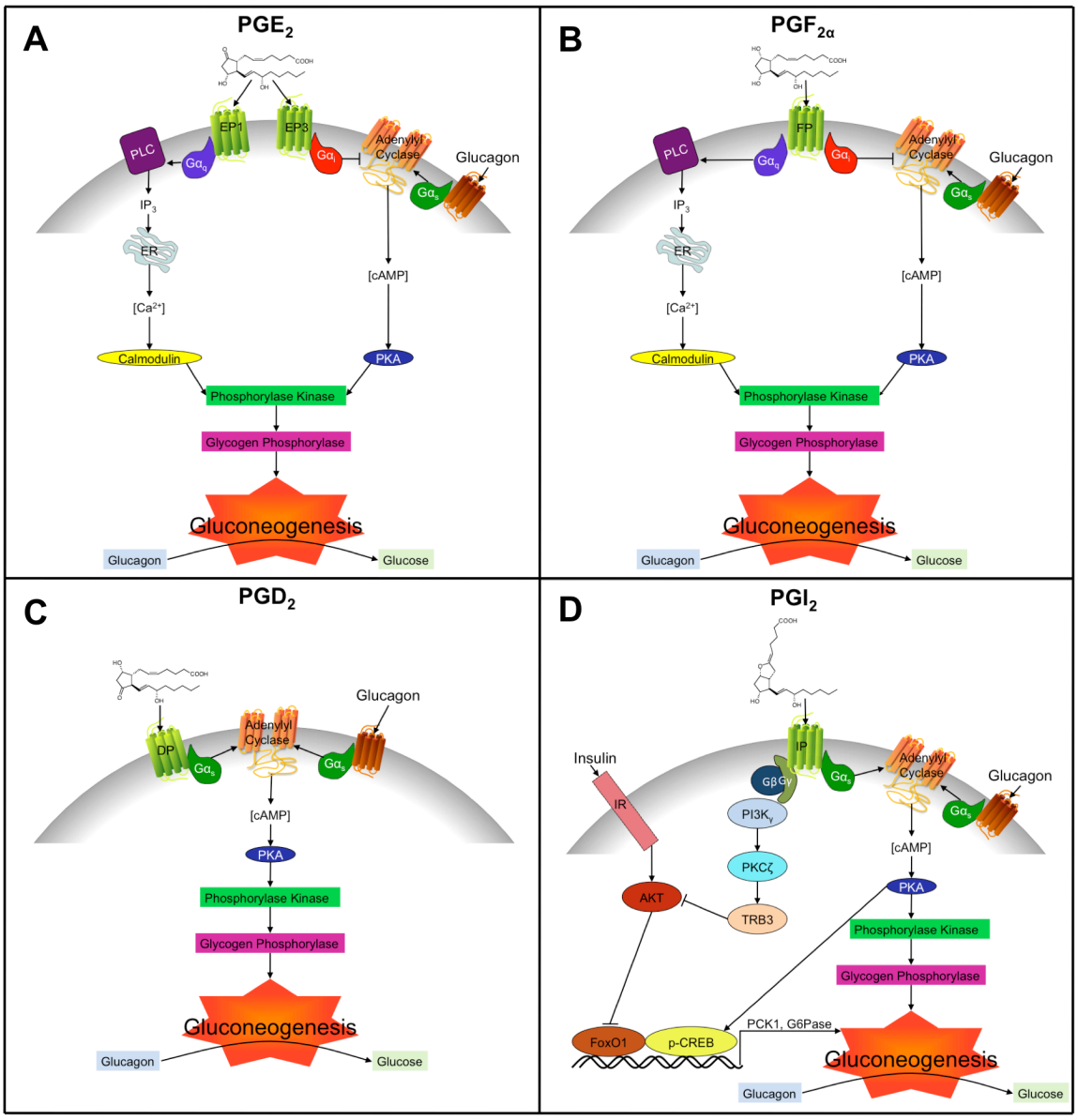

Figure 5. Prostaglandin regulation of hepatic glucose output

A. PGE_2 affects gluconeogenesis predominately through the EP1 and EP3 receptors. EP1 promotes gluconeogenesis in an IP_3- and calcium-dependent manner. EP3 inhibits glucagon-induced gluconeogenesis by reducing intracellular cAMP accumulation. **B.** $PGF_{2\alpha}$ signals through both $G\alpha_q$ and $G\alpha_i$ to promote and inhibit gluconeogenesis, respectively. **C.** PGD_2 signals through a $G\alpha_s$ coupled receptor, presumably DP, to promote gluconeogenesis. **D.** PGI_2 promotes gluconeogenesis through $G\alpha_s$ and $G\beta\gamma$ mediated signaling pathways. Figure D modified from (252).

gluconeogenesis. Signaling through EP3 reduces cAMP accumulation and thereby inhibits gluconeogenesis. Similar to what has been seen in pancreatic islets and adipose tissue, the inhibitory effect of PGE_2 on cAMP and gluconeogenesis cannot be seen in the absence of stimuli such as glucagon or β-adrenergic stimulation which raise cAMP above basal levels.

$PGF_{2\alpha}$ signals through the FP receptor to regulate hepatic gluconeogenesis. $PGF_{2\alpha}$ causes a reduction in glucagon stimulated cAMP and glucose production in a pertussis toxin sensitive manner, implicating a $G\alpha_i$ coupled signaling pathway (494,508,509,514). $PGF_{2\alpha}$ also signals through a $G\alpha_q$ dependent signaling pathway to increase IP_3 and intracellular calcium, and thereby promote glycogen phosphorylase activity and hepatic gluconeogensis (485,494,517,519,521,523). Similar to what was observed with PGE_2, the inhibitory; action of $PGF_{2\alpha}$ is only noticed during periods of elevated cAMP, such as during glucagon stimulation. Another similarity to hepatic PGE_2 signaling is that $PGF_{2\alpha}$ also increases glycogenesis (524).

PGD_2, which is the primary PG produced by the liver, functions to oppose the actions of PGE_2 and $PGF_{2\alpha}$. PGD_2 enhances hepatic glucose production (474,525). Furthermore, it does not play a role in promoting glycogen production (524).

PGI_2 also acts to promote gluconeogenesis. IP activation stimulates cAMP accumulation, thereby activating PKA, which phosphorylates CREB to promote the expression of gluconeogenic genes (252,479). In addition, IP signals through Gβγ subunits to block activation of AKT, an inhibitor of gluconeogenic gene expression (252).

Hepatic Lipolysis

In addition to regulating circulating glucose levels, the liver also plays an important role in regulating the extracellular transport of lipids in the form of lipoproteins. The liver packages triglycerides and cholesterol into very-low-density lipoproteins (VLDL) for transport to other

tissues via the circulatory system (526). PGE_2 and PGD_2 both suppress VLDL secretion from hepatocytes (506,527). Apolipoprotein B (ApoB) and microsomal triglyceride transfer protein (MTTP) are involved in packaging lipoproteins. PGE_2 acts synergistically with insulin to decrease the expression of *Apob* and *Mttp* (454,478). PGD_2 and $PGF_{2\alpha}$ also decrease expression *Apob* only, but do not affect *Mttp* (527). PGE_2, PGD_2 and $PGF_{2\alpha}$ reduce the lipid to ApoB ratio in VLDL resulting in smaller particles with less lipid content (527). The reduced lipids in VLDL particles may be due to reduced lipogenesis because fatty acid synthase gene expression is reduced by PGE_2 (454,455,506,527). Cholesterol biosynthesis has been reported to be reduced by PGE_2, PGD_2 and $PGF_{2\alpha}$ (527) or unaffected by PGE_2 and PGD_2 (506). The reduced secretion of lipoprotein in hepatocytes treated with PGE_2, PGD_2 or $PGF_{2\alpha}$ leads to an increase in cellular triglcyeride content (506).

Fatty Liver Disease

Hepatic lipid accumulation is well known to be a major contributing factor to nonalcoholic fatty liver disease and hepatosteatosis, which can lead to insulin resistance (448,528-531). PGE_2 promotes hepatic lipid accumulation in an EP2/4 dependent mechanism (465). Consistent with this, $EP3^{-/-}$ mice were observed to have increased liver weight when fed a breeder chow diet; however, progression of hepatic lipid contents were not evaluated (102). Beraprost, an IP agonist, reduces hepatic steatosis (253,254), whereas $IP^{-/-}$ mice were reported to have reduced hepatic triglycerides and steatosis (252), presenting conflicting conclusions on the role of IP in the development of fatty liver disease. Mice treated with the NSAID indomethacin, COX2 inhibitors, or lacking a $cPLA_2$ (*pla2g4a*) have decreased hepatic triglycerides providing further evidence that PGE_2 promotes hepatic lipid accumulation (100,280,281,391,459).

The major source of hepatic triglycerides is derived from adipose tissue lipolysis (528). The liver is also an important source of *de novo* lipogenesis, which also accounts for a significant portion of hepatic lipids (532). A large portion of hepatic triglycerides are packaged into VLDL and secreted; inhibition of this process can increase hepatic triglycerides content (533). Reduced mitorchondrial β-oxidation due to mitochondrial dysfunction can also lead to lipid accumulation in the liver (534). As has already been discussed, PGs play an important role in adipose tissue and hepatic lipolysis, which affects the amount of lipids in the liver. PGE_2 has been reported to decrease *de novo* lipogenesis in the liver (454,455,506,527). PGE_2 also decreases triglyceride breakdown and reduce β-oxidation of fatty acids (454). Taken together, these data indicate that PGE_2 increase hepatic triglyceride accumulation by increasing lipolyis in adipose tissue, increasing *de novo* hepatic lipogenesis, reducing lipid secretion, and reducing β-oxidation.

A progressive deterioration of the liver characterizes nonalcoholic fatty liver disease (NAFLD) (448,535). The liver begins to become diseased when it accumulates lipid and develops simple steatosis, which is frequently associated with insulin resistance. This disease state progresses into non-alcoholic steatohepatitis, which is characterized by inflammation. Advanced stages progress to cirrhosis, which is characterized by fibrosis, i.e. the replacement of liver tissue with scar tissue. Hepatocellular carcinoma may develop as the final stage of the disease. COX2 is expressed primarily in earlier stages of chronic liver disease and in hepatocellular carcinoma its expression is inversely correlated with tumor grade (453).

PGs play a protective role in the liver. PGs are well known to be cytoprotective and to promote regeneration in the liver (536-540). Metabolites of COX2 are proliferative and anti-apoptotic in hepatic tissues (492,494,541-544). These protective effects of PGE_2 are mediated through the EP4 receptor (492,493,545-549). IP agonists also decrease markers of liver injury

and fibrogenic gene expression (550,551). PGE_2 has anti-inflammatory effects in the liver that leads to immunosuppression (466). PGE_2 reduces TNF-α and other pro-inflammatory cytokines in an EP2 and EP4 dependent manner (498,552,553). TXA_2 synthetase inhibitors and receptor antagonists decrease markers of liver injury indicating that TXA_2 causes adverse effects in the liver (550).

Summary

Obesity and diabetes are a major health concern. Inflammatory signaling pathways represent an attractive therapeutic target for both diabetes and obesity. PGs are one of the many signaling molecules that play a role in inflammation and immune response and as have been noted play many diverse roles in obesity, diabetes, and metabolism. The roles these PGs play in metabolism are complex as the same molecules are oftentimes critical mediators of GSIS, feeding behavior, adipogenesis, adipocyte function, and hepatic function. The overlapping nature of the PGs and their receptors, with multiple PGs/receptors controlling the same physiological process and multiple physiological processes being modulated by the same PG/receptor, oftentimes necessitates investigation of the PG receptors individually. Due to the fact that the EP3 receptor has been shown to play an important role in the pancreatic islet, adipose tissue, and liver, I chose to investigate the physiological role of the EP3 receptor in a mouse model of diet induced obesity and diabetes. To accomplish this, I proposed the following aims: 1. Evaluate the physiological effects of EP receptor inhibition on diabetes *in vivo*, 2. Compare EP receptor expression in the pancreas and 3. Elucidate the signaling pathway by which PGE_2 inhibits insulin release *ex vivo*.

CHAPTER II

THE ROLE OF THE PROSTAGLANDIN E_2 EP3 RECEPTOR IN INSULIN ACTION

Introduction

Type 2 diabetes has recently been recognized as a disease of low-grade chronic inflammation (reviewed in (24,25)). This state of chronic inflammation contributes to the development of insulin resistance seen in type 2 diabetes and prediabetes. Antidiabetic drugs such as thiazolidinediones reduce systemic inflammation and improve insulin resistance (20), while inflammatory cytokines such as interleukin 1-β (IL1-β) have deleterious effects on pancreatic islet β-cell function and proliferation (40,177,196,197). Circulating inflammatory cytokines increase in obesity and type 2 diabetes. It is now appreciated that pancreatic islets respond to inflammatory signals, and inflammatory ligands likely contribute to the etiology of β-cell dysfunction in type 2 diabetes. Thus, inflammatory mediators negatively affect both insulin production as well as insulin action.

PGs are important mediators of inflammation (reviewed in (41-45)). These oxidative metabolites of arachidonic acid (AA), are produced by cyclooxygenases (COX1 and COX2), and act locally in an autocrine or paracrine manner (reviewed in (43)). Inhibition of COX activity and PG production by nonsteroidal anti-inflammatory drugs (NSAIDs) has long been appreciated to have beneficial effects on glucose homeostasis, consistent with inhibition of insulin secretion by PGs (105).

PGE_2 mediates its effects by activation of four GPCRs, designated E-Prostanoid (EP)1 through EP4 (43). EP1 elevates intracellular calcium, while EP2 activates adenylyl cyclase. The EP4 receptor was initially identified as activating adenylyl cyclase, but has been demonstrated to signal through a number of other pathways as well (151). Similarly, although EP3 activation was

first described to inhibit adenylyl cyclase, leading to decreased intracellular cyclic adenosine monophosphate (cAMP) levels by a $G\alpha_i$ coupled mechanism, it has also been appreciated to couple to multiple signal transduction pathways (see (43)). Pancreatic tissue expresses mRNA encoding each of the four EP GPCR types (181,196). Thus, PGE_2 is hypothesized to act in an autocrine or paracrine fashion in pancreatic islets through endogenous EP receptors. A more thorough analysis of GPCR expression across a panel of mouse tissues revealed that the EP3 receptor was most highly expressed in the pancreas, kidney and white adipose tissue, an expression pattern consistent with regulation of metabolic homeostasis (235). Recent studies have shown that EP3 is expressed in pancreatic β-cells and that signaling through inhibitory G proteins, $G\alpha_i/G\alpha_o/G\alpha_z$, within pancreatic β-cells negatively regulates glucose stimulated insulin secretion (GSIS) and β-cell proliferation (134,239,554).

Based upon its signal transduction properties, pharmacological blockade or genetic deletion of the EP3 receptor might be expected to increase GSIS, perhaps improving glycemic control. However, studies by Bartfai and co-workers utilizing global $EP3^{-/-}$ mice maintained on breeder chow were remarkable in that they observed an increase in insulin resistance and body weight, which was ascribed to altered circadian activity patterns and an increase in feeding during the normal daytime sleeping period (102). This phenotype had not been noted in previous descriptions of the EP3 null animals (310,555). These studies also demonstrated an increase in serum insulin levels that may have been a consequence of increased body weight and adiposity in the $EP3^{-/-}$ mice.

We have not previously observed obesity in our $EP3^{-/-}$ mice when maintained on a standard rodent chow diet. We predicted that $EP3^{-/-}$ mice would have enhanced GSIS resulting

from the loss of the EP3-evoked inhibition of insulin secretion. We hypothesized that $EP3^{-/-}$ mice would have improved glucose handling when fed a normal chow diet.

Materials and Methods

Materials

PGE_2 was obtained from Cayman Chemical Company (Ann Arbor, MI) and [^{3}H] PGE_2 was obtained from PerkinElmer (Boston, MA). DG-041, an EP3 antagonist (556), was provided by the Vanderbilt Institute of Chemical Biology Synthesis Core. Recombinant human IL-1β was obtained from R&D Systems (Mineapolis, MN, Cat. No. 201-LB). Formaldehyde 10% (v/v), buffered at pH 7.0 was obtained from Ricca Chemical Company (Arlington, TX). OCT was obtained from Tissue-Tek (Sakura Finetek U.S.A., Torrance, CA).

Animal procedures

Mice utilized for these experiments were generated from homozygous breeding of $EP3^{+/+}$ or $EP3^{-/-}$ mice on a C57BL/6 background at Vanderbilt University unless otherwise stated. Mice were maintained *ad libitum* on chow, Laboratory Rodent Diet 5001 (LabDiet, Richmond, IN). Mice were maintained on a 12-hour light/dark cycle and housed with three to five animals per cage on corncob bedding except during fasting when placed on Pure-o'Cel™ bedding (The Andersons, Maumee, OH). Body composition of live mice was measured by pulsed NMR with Minispec Model mq7.5 (Bruker Instruments, The Woodlands, TX). Mice were euthanized by isoflurane (Baxter Healthcare Corporation, Deerfield, IL) overdose for collection of tissues. All procedures were approved by the Institutional Animal Care and Use Committee at Vanderbilt University.

Radioligand binding

Pancreata for radioligand binding were obtained from 11.5 to 18.5 week old chow fed male mice. Prior to pancreas dissection, mice were perfused with 0.9% saline to remove blood from the pancreas. Pancreata were flash frozen in liquid nitrogen and ground with a mortar and pestle and stored at -80°C. Ground pancreata were further lysed with an electric homogenizer in a buffer containing the following: HEPES 15 mM, EDTA 5 mM, EGTA 5 mM, indomethacin 40 μM, PMSF 2 mM at pH 7.6. Pancreata lysates were placed on top of a 60% sucrose gradient and centrifuged at 32,000 RCF for 1.5 hours at 4°C. The layer of pancreas membranes was removed and further homogenized with an 18-26 gauge needle. Binding was performed on 250 μg pancreas membranes pooled from five $EP3^{+/+}$ or five $EP3^{-/-}$ mice. All dilutions and washes were performed using a chilled buffer containing the following substances: K_2HPO_4 15.8 mM, KH_2PO_4 6.14 mM, EDTA 1 mM, $MgCl_2$ 10 mM. Radioligand binding was performed using 5 nM [^{3}H] PGE_2 with nonspecific binding determined in the presence of 1 μM unlabeled PGE_2. Membranes were incubated with PGE_2 ligands for 1 hour at 30°C while shaking. Bound ligand was separated from free by vacuum filtration onto 24 mm GF/F Whatman filters and placed in scintillation vials with Ultima Gold scintillation cocktail (PerkinElmer, Boston, MA). Analysis [^{3}H] PGE_2 binging was measured, following overnight incubation at room temperature, by counting each sample for 10 minutes with a Beckman LS 6500 multi-purpose scintillation counter.

Autoradiography

The radiohistochemical technique was originally described by Eriksen, *et al.* (557). Briefly, 9 to 11 week old male mice were euthanized and subsequently perfused with 0.9% saline followed by 10% formaldehyde to fix the tissue. Pancreata were dissected and embedded in

OCT. Sections were cut 10 microns thick on a cryostat and thaw-mounted onto gelatinize slides (Lab Scientific, Livingston, NJ). Tissue sections were washed in 0.9% saline to remove OCT. The sections were then incubated for one hour at room temperature in a humidified chamber with 5 nM [^{3}H] PGE_2 ± 1 μM PGE_2 in buffer containing the following substances: HEPES 10 mM, NaCl 135 mM, KCl 4.8 mM, $MgSO_4$ 1.7 mM, $CaCl_2$ 0.5 mM, NaH_2PO_4 1.0 mM, and BSA 0.5% at pH 7.4. Free PGE_2 was separated from tissue-bound PGE_2 by three consecutive five-minute washes in ice-cold 0.9% saline. Sections were vacuum dried overnight at 4°C. Sections were imaged for 6-hours on a Micro Imager™ (Biospace Lab, Nesles-la-Vallée, France) at Vanderbilt University Institute of Imaging Science.

Mouse islet perifusion

Pancreatic islets were isolated from male C57BL/6 $EP3^{+/+}$ or $EP3^{-/-}$ mice and perifusion assays were performed at the Vanderbilt Islet Procurement & Analysis Core as previously described (558). Studies comparing $EP3^{+/+}$ or $EP3^{-/-}$ islets utilized fresh islets. For studies employing the EP3 antagonist DG-041, islets isolated from 9 week old mice were cultured for 24 hours following isolation in RPMI-1640 containing 10% fetal bovine serum and 5.6 mM glucose at 37°C. Islet preparations were equilibrated and stable baseline response established at 5.6 mM glucose, and insulin secretion was stimulated with 16.7 mmol/l glucose. For some studies, 1 μM DG-041 was added to the islets at the indicated times. The studies utilizing DG-041 contained 100 μM 3-Isobutyl-1-methylxanthine (IBMX) and 0.01% DMSO throughout the perifusion. Statistical analyses for differences in insulin secretion were performed on the difference of the area under the curve.

Mouse static incubation insulin secretion

Pancreatic islets were isolated from 8.5 to 9.5 week old male C57BL/6 $EP3^{+/+}$ or $EP3^{-/-}$ mice and static incubation insulin secretion assays were performed at the Vanderbilt Islet Procurement & Analysis Core as previously described (558). Briefly, isolated islets were cultured overnight in RPMI with 5.6 mM glucose. The following day islets were incubated in DMEM media with the indicated glucose and drug concentrations for one hour. For studies utilizing DG-041, islets were cultured for one hour in 5.6 mM glucose ± DG-041 prior to indicated conditions. 200 µl of acid ethanol was used to disrupt islets for total insulin content. Mice used for experiments containing IL-1β were purchased from The Jackson Laboratory (Bar Harbor, ME).

Intraperitoneal glucose tolerance tests (IP-GTT)

Male C57BL/6 $EP3^{+/+}$ or $EP3^{-/-}$ mice were fasted overnight for 16 hours and fasting blood glucose was measured from a drop of tail vein blood with an Accu-Check Aviva glucometer and glucose test strips (Roche Diagnostics, Indianapolis, IN). Fasting insulin was measured from plasma collected by saphenous vein blood draw. Animals received an intraperitoneal injection of filter-sterilized glucose in PBS (2 mg dextrose/g body weight) and blood glucose was measured at 15, 30, 60, 90, and 120 minutes while plasma for insulin analysis was collected at 15 and 30 minutes after injection. Statistical analyses for differences in glucose handling were performed on the difference from baseline of the area under the curve (ΔAUC). Insulin content was analyzed in duplicate by RIA by Vanderbilt University Hormone Assay & Analytical Services Core.

Intraperitoneal insulin tolerance tests (ITT)

Male $EP3^{+/+}$ or $EP3^{-/-}$ mice were fasted for 6 hours during the light cycle and fasting blood glucose level were measured with the Accu-Check Aviva blood glucose meter using blood obtained from the tail. Following intraperitoneal injection of 34.1 μg/kg insulin (human recombinant insulin, Sigma, St. Louis, MO, Cat. No. I9278) in 0.9% normal saline, blood glucose levels were measured at 15, 30, 60, 90, and 120 minutes post-injection.

Statistics

Data are means ± SEM, using GraphPad Prism version 6.0e for Mac OS X (GraphPad Software, La Jolla, CA). All analyses were performed with an unpaired t-test unless otherwise stated.

Results

Prostaglandin E_2 receptors are expressed in the mouse pancreas

Ligand binding studies were performed on pancreata from $EP3^{+/+}$ and $EP3^{-/-}$ mice to determine if EP receptors are expressed in the mouse pancreas. Total cell membranes prepared from pancreata of $EP3^{-/-}$ mice showed a decrease, but not a total elimination, of [^{3}H] PGE_2 binding (Figure 6A). This finding suggests EP3 constitutes a large proportion of PGE_2 receptors in the pancreas and that other EP receptors, in addition to EP3, are expressed in the pancreas.

In order to examine the location of EP3 protein expression in the mouse pancreas, autoradiography was performed on mouse pancreatic tissue sections (Figure 6B). Specific [^{3}H] PGE_2 binding was found throughout the $EP3^{+/+}$ pancreatic tissue section. Because specific [^{3}H] PGE_2 binding was global and not restricted to punctae, as islets constitute only 1-2% of pancreatic mass (559), it can be assumed that EP receptors are expressed in the exocrine tissue in the pancreas. The presence, or lack of, EP expression in islets cannot be determined because of

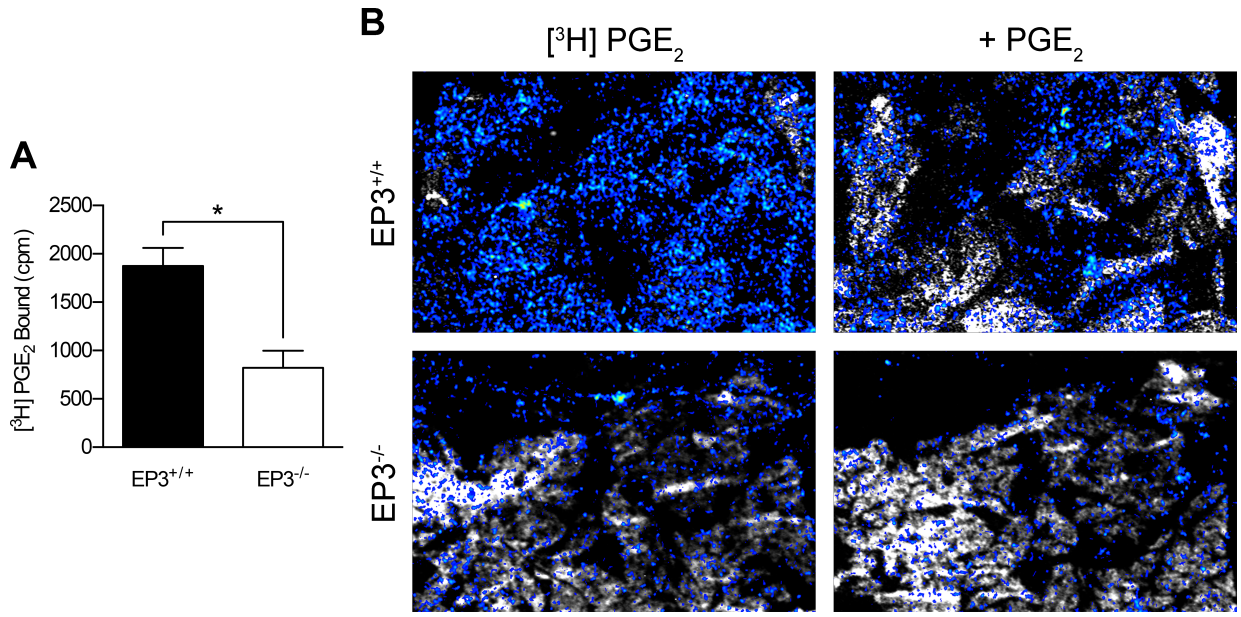

Figure 6. [^{3}H] PGE_2 binds to EP3 receptors in the mouse pancreas
A. Specific [^{3}H] PGE_2 binding to pancreata membranes pooled from five $EP3^{+/+}$ and five $EP3^{-/-}$ mice with each sample assayed in triplicate. Membranes from $EP3^{-/-}$ pancreata had less specific [^{3}H] PGE_2 binding ($P = 0.015$). **B.** PGE_2 receptor localization was performed using autoradiography. [^{3}H] PGE_2 had specific binding to wild-type pancreas that was greatly reduced in $EP3^{-/-}$ tissue. White is tissue, color is [^{3}H] counts with blue being lowest and red being highest. Binding data are representative samples of three independent experiments. Values are expressed as mean ± SEM.

the overwhelming nature of [^{3}H] PGE_2 binding to the surrounding tissue. Tissue sections from $EP3^{-/-}$ mice showed less [^{3}H] PGE_2 binding suggesting that the majority of [^{3}H] PGE_2 binding seen in $EP3^{+/+}$ sections is due to the EP3 receptor.

PGE_2-EP3 signaling does not affect glucose stimulated insulin secretion

Pancreatic islets isolated from $EP3^{+/+}$ and $EP3^{-/-}$ mice were assessed for alterations in GSIS by islet perifusion and static culture. EP3 genotype did not affect GSIS (Figure 7A,B). Furthermore, neither first nor second phase insulin secretion was altered by disruption of EP3 (Figure 7A). 1 μM PGE_2 failed to suppress GSIS in both $EP3^{+/+}$ and $EP3^{-/-}$ islets (Figure 7A,C). Moreover, treatment of islets with the EP3 antagonist DG-041 had no effect on GSIS (Figure 7D,E). In addition, IL-1β, which has previously been shown to suppress GSIS in a PGE_2 dependent manner (177,196,560), also had no significant effect on GSIS (Figure 7E).

$EP3^{-/-}$ mice do not have altered body or tissue mass

Male $EP3^{+/+}$ and $EP3^{-/-}$ mice fed a chow diet did not differ in body weight over the period observed, from four weeks of age to 38 weeks of age (Figure 8A). Post-mortem analysis found no difference in epididymal fat pad or liver weight (Figure 8B,C). *In vivo* body composition analysis at 40 weeks of age also found no difference in fat mass or lean body mass (Figure 8D,E). Similar results were found in female mice, which also exhibited no difference in body mass during the observed period (Figure 8F). Similarly, post-mortem analysis found no difference in gonadal fat pad or liver weight (Figure 8G,H).

$EP3^{-/-}$ mice are not glucose intolerant

$EP3^{+/+}$ and $EP3^{-/-}$ male mice fed chow had no difference in glucose tolerance at 20 weeks of age (Figure 9A), though a modest improvement was observed in $EP3^{-/-}$ mice at 40 weeks of age (Figure 9B). This difference in glucose tolerance could not be attributed to increased plasma

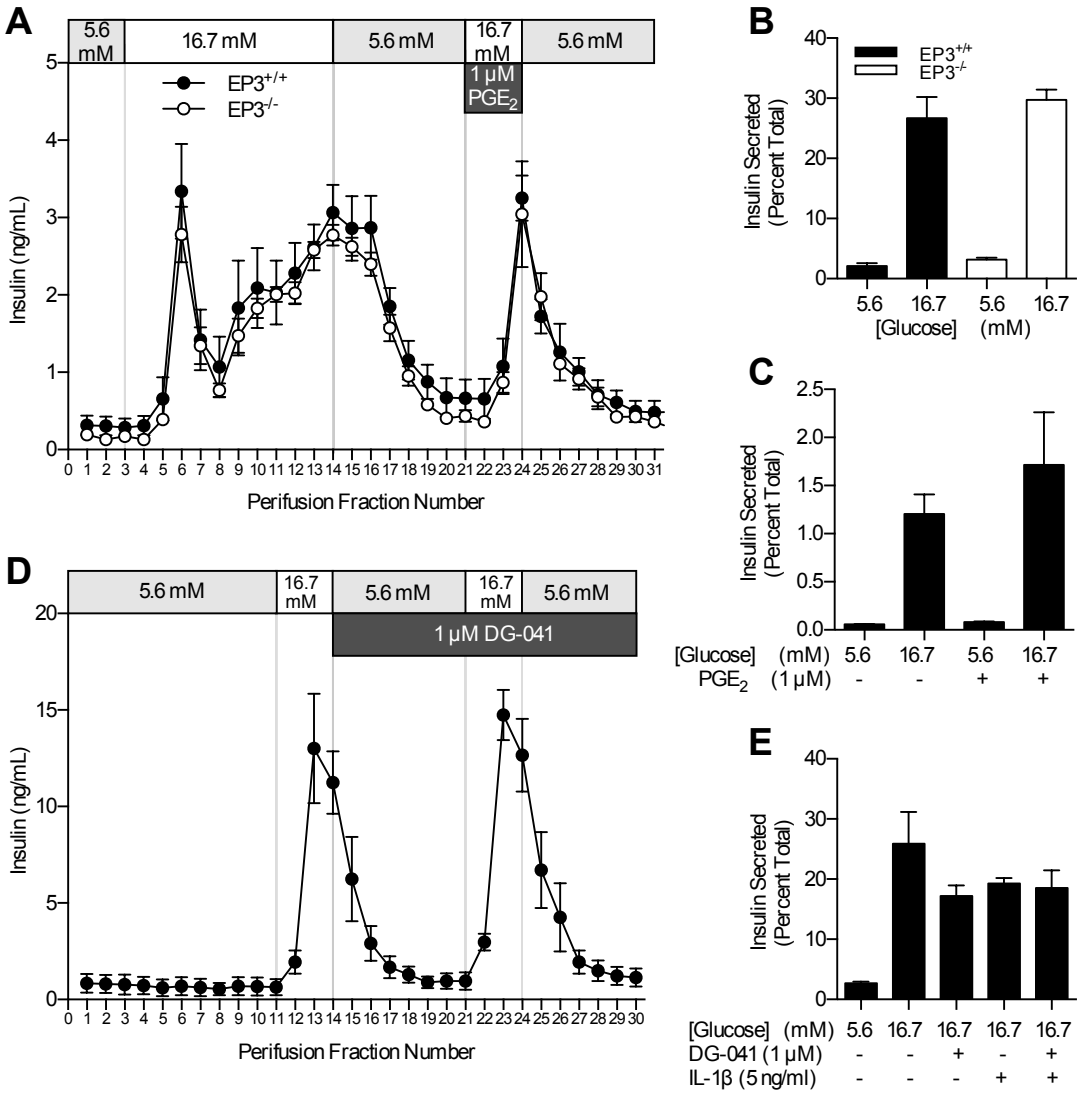
A
5.6 mM
16.7 mM
5.6 mM
16.7 mM
5.6 mM
1 μM PGE2
EP3+/+
EP3-/-
Insulin (ng/mL)
Perifusion Fraction Number
B
EP3+/+
EP3-/-
Insulin Secreted (Percent Total)
5.6
16.7
5.6
16.7
[Glucose] (mM)
C
Insulin Secreted (Percent Total)
[Glucose] (mM) 5.6 16.7 5.6 16.7
PGE2 (1 μM) - - + +
D
5.6 mM
16.7 mM
5.6 mM
16.7 mM
5.6 mM
1 μM DG-041
Insulin (ng/mL)
Perifusion Fraction Number
E
Insulin Secreted (Percent Total)
[Glucose] (mM) 5.6 16.7 16.7 16.7 16.7
DG-041 (1 μM) - - + - +
IL-1β (5 ng/ml) - - - + +

Figure 7. Glucose-stimulated insulin secretion is not affected by PGE_2-EP3 signaling
A. Perifusion of islets from $EP3^{+/+}$ and $EP3^{-/-}$ mice showed no effect of EP3 genotype on glucose-stimulated insulin secretion (GSIS). Both first phase (P = 0.741) and second phase (P = 0.945) insulin secretion were unchanged. PGE_2 administration during perifusion did not affect GSIS. N = 4 mice for each genotype. Values are expressed as mean ± SEM. **B.** Static incubation insulin secretion in the presence of 100 μM IBMX found no difference in GSIS from $EP3^{+/+}$ and $EP3^{-/-}$ islets (P = 0.592). N=5 mice per genotype, each sample assayed in duplicate. Values are expressed as mean ± SEM. **C.** Static incubation insulin secretion found no differences in GSIS when $EP3^{+/+}$ islets were treated with PGE_2. (P = 0.309). N = 2 mice. Values are expressed as mean ± StDev. **D.** Perifusion of islets from $EP3^{+/+}$ mice in the presence of 100 μM IBMX demonstrated that addition of the EP3 antagonist DG-041 does not alter GSIS. N = 4 mice. Values are expressed as mean ± SEM. **E.** Static incubation insulin secretion in the presence of 100 μM IBMX found no difference in GSIS when $EP3^{+/+}$ islets were treated with EP3 antagonist, DG-041, IL-1β, or DG-041 + IL-1β (P = 0.212). Statistical significance was determined by one-way ANOVA. N = 5 mice. Values are expressed as mean ± SEM. Within each panel, islets from each mouse were utilized for every condition.

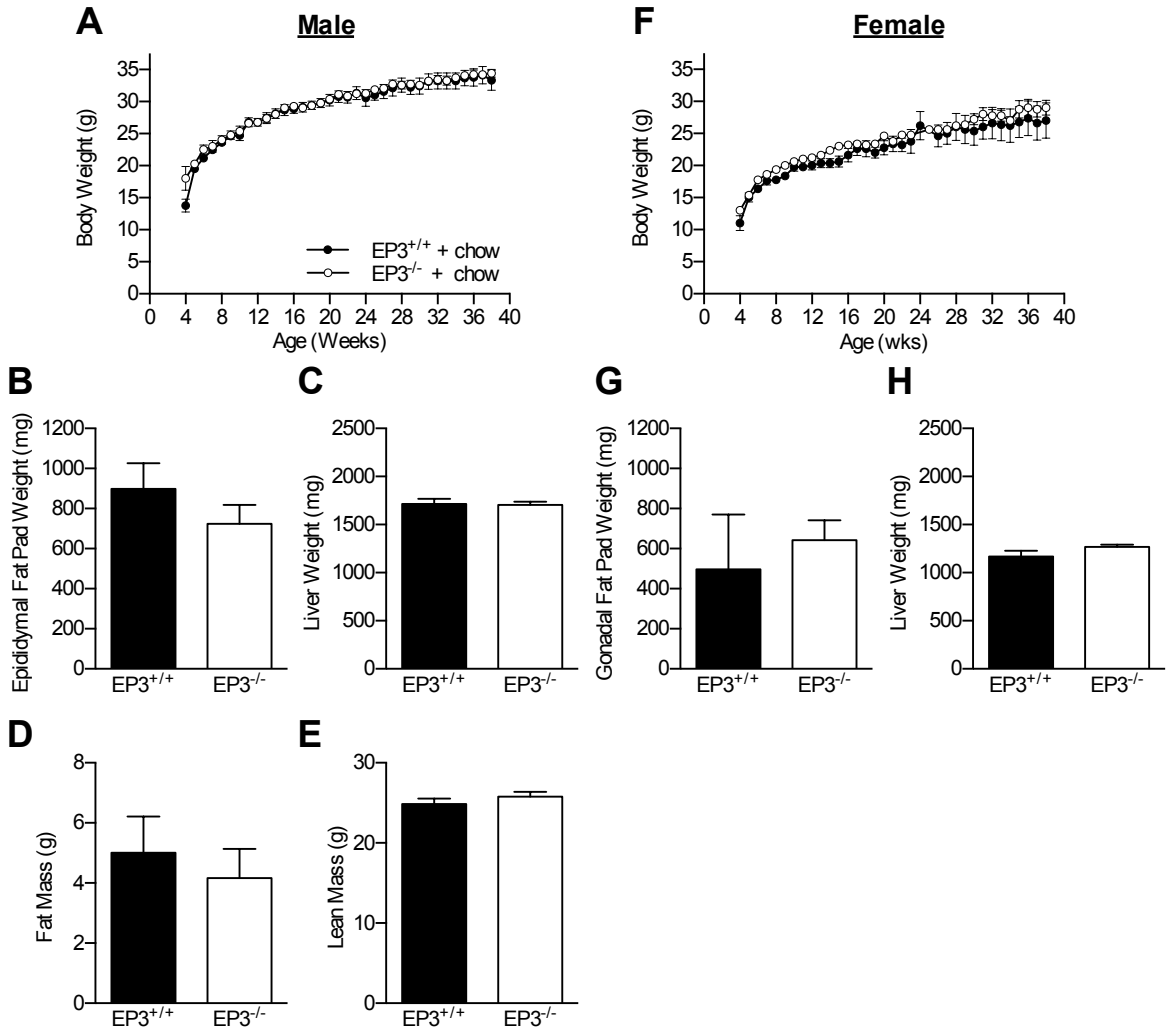

Figure 8. Chow fed EP3$^{-/-}$ mice have no overt morphological phenotype
A. Male EP3$^{+/+}$ and EP3$^{-/-}$ mice fed standard chow were weighed weekly from age 4 weeks to age 38 weeks. No difference in body weight was observed. N = 11 EP3$^{+/+}$ and 10 EP3$^{-/-}$. **B.** Epididymal fat pads weighed post mortem at ~40 weeks of age showed no difference between genotypes (P = 0.282). N = 9 EP3$^{+/+}$ and 10 EP3$^{-/-}$. **C.** Male livers weighed post mortem at ~40 weeks of age showed no difference between genotypes (P = 0.886). N = 9 EP3$^{+/+}$ and 10 EP3$^{-/-}$. Body composition was assessed around 40 weeks of age by pulsed NMR. **D.** No difference in body fat in males was observed (P = 0.619). N = 5 EP3$^{+/+}$ and 4 EP3$^{-/-}$. **E.** No difference in lean mass in males was observed (P = 0.367). N = 5 EP3$^{+/+}$ and 4 EP3$^{-/-}$. **F**. Female EP3$^{+/+}$ and EP3$^{-/-}$ mice fed standard chow were weighed weekly from age 4 weeks to age 38 weeks. No difference in body weight was observed. N = 5 for each genotype. **G.** Gonadal fat pads weighed post mortem at ~40 weeks of age showed no difference between genotypes (P = 0.637). N = 5 for each genotype. **H.** Female livers weighed post mortem at ~40 weeks of age showed no difference between genotypes (P = 0.203). N = 5 for each genotype. Values are expressed as mean ± SEM.

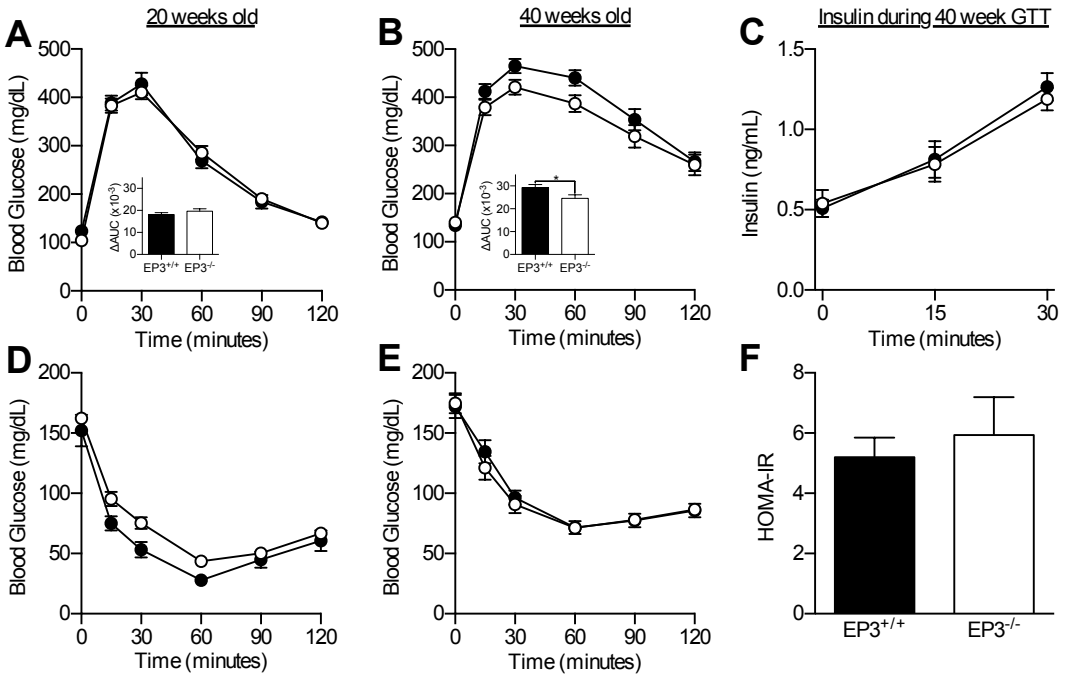

Figure 9. Chow fed EP3$^{-/-}$ male mice have no overt metabolic phenotype

A. Glucose tolerance was not different between 20 week old EP3$^{+/+}$ and EP3$^{-/-}$ male mice (P = 0.362). N = 10 EP3$^{+/+}$ and 18 EP3$^{-/-}$. **B.** Assessment of glucose tolerance in 40 week old EP3$^{+/+}$ and EP3$^{-/-}$ mice showed a modest improvement in the change in the area under the curve (29300 vs. 24600 min.×mg/ml; P = 0.0244). N = 24 each group. **C.** Measurement of plasma insulin levels during the first 30 minutes of the GTT of 40 week old chow fed mice showed no difference in insulin secretion between EP3$^{+/+}$ and EP3$^{-/-}$ mice (P = 0.759). N = 13 each group. **D.** Insulin tolerance was not different between EP3$^{+/+}$ and EP3$^{-/-}$ mice at 20 weeks of age. N = 10 EP3$^{+/+}$ and 19 EP3$^{-/-}$. **E.** Assessment of insulin tolerance in 40 week old EP3$^{+/+}$ and EP3$^{-/-}$ was also unchanged. N = 18 EP3$^{+/+}$ and 19 EP3$^{-/-}$. **F.** The homeostatic model assessment of insulin resistance (HOMA-IR), a function of fasting blood glucose (from B) and plasma insulin (from C), showed no difference between 40 week old chow fed EP3$^{+/+}$ and EP3$^{-/-}$ mice (P = 0.609). N = 13 each group. Values are expressed as mean ± SEM.

insulin levels (Figure 9C). Insulin sensitivity was also not altered in male $EP3^{-/-}$ mice at either 20 (Figure 9D) or 40 weeks of age (Figure 9E,F). Female $EP3^{-/-}$ mice also showed no difference in glucose or insulin tolerance at 40 weeks of age (Figure 10).

Discussion

Blockade of PGE_2 action at the inhibitory EP3 receptor has been hypothesized to be a therapeutic target to improve GSIS, which would be beneficial for the treatment of type 2 diabetes. Studies have shown that *ptger3* mRNA is highly expressed in the pancreas (181,235), pancreatic islets (74,181), and β-cells (239) of mice. The present studies suggest that EP3 protein is highly expressed in mouse pancreata. Prior studies have implicated EP3 function in β-cells of pancreatic islets (71,74,194,197,233). Autoradiography was performed to visualize EP3 expression predominantly in pancreatic islets; however, EP3 was globally expressed in the pancreas indicating that is also expressed in exocrine tissue, which makes up 98-99% of the pancreas (559).

There are conflicting data in the literature regarding the effects of EP3 receptor activation on GSIS. Some studies have suggested an improvement in GSIS upon EP3 receptor blockade or inhibition of PG production (74,233), while others have not found any effect of PGE_2 signaling on GSIS in isolated islets (222). Data from rat pancreatic islets showed that GSIS was inhibited by EP3 receptor agonists in a pertussis toxin sensitive manner (197). *Ex vivo* studies using human islets from individuals with or without diabetes found that in islets derived from non-diabetic humans no effect in GSIS was observed in agreement with data shown here (74). It is of interest that in these studies, the effect of EP3 receptor blockade on islets became apparent only when the subjects were obese and/or diabetic. Our studies using an EP3 antagonist in mouse islet perifusion studies, as well as perifusion of $EP3^{-/-}$ islets, did not find any effect on GSIS. The

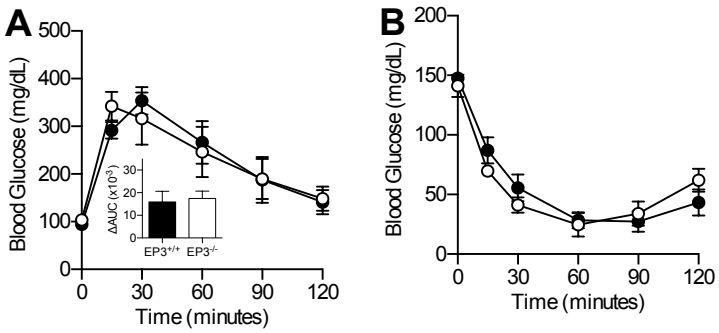

Figure 10. Chow fed EP3$^{-/-}$ female mice have no overt metabolic phenotype
A. Glucose tolerance was not different between 40 week old EP3$^{+/+}$ and EP3$^{-/-}$ female mice (P = 0.788). N = 5 each group. **B.** Insulin tolerance was not different between EP3$^{+/+}$ and EP3$^{-/-}$ mice at 40 weeks of age. N = 3 EP3$^{+/+}$ and 5 EP3$^{-/-}$.

observed differences among these studies may represent species differences between rat, mouse and human, off-target effects of high antagonist concentrations, or the physiologic status of the individuals at the time of islet harvest.

Consistent with EP3 gene deletion or blockade having no effect on GSIS *ex vivo*, we also found no change in GSIS *in vivo*. We did note a small improvement in glucose homeostasis in 40 week old male $EP3^{-/-}$ mice, but we could not attribute this to either improved GSIS or insulin sensitivity. Despite a previous study that reported that $EP3^{-/-}$ mice are obese (102), we found that both male and female mice maintain similar body and tissue weights. Results from the present studies are consistent with the first studies reporting the generation of $EP3^{-/-}$ mice, which also found no apparent morphological abnormalities (310,555). It is possible that $EP3^{-/-}$ mice do not develop obesity when fed a standard chow diet, which contains 13.5% calories from fat as compared to the 29% calories from fat found in breeder chow diet (102). If dietary fat significantly modulates the phenotype of the $EP3^{-/-}$ mouse, it would be of interest to examine the physiology of $EP3^{-/-}$ mice when fed matched, defined diets with varying fat content.

CHAPTER III

THE PGE_2 EP3 RECEPTOR REGULATES DIET-INDUCED ADIPOSITY IN 20 WEEK OLD MALE MICE

Introduction

Obesity and ectopic lipid accumulation are associated with insulin resistance, and contribute to the pathology of a number of diseases, notably type 2 diabetes. Obesity has been recognized as a disease of low-grade chronic inflammation, and circulating inflammatory cytokines increase in obesity and type 2 diabetes (reviewed in (26,320,388,561,562)). PGs are important mediators of inflammation that have been recognized to play a significant role in metabolic diseases (reviewed in (41,44,152,198)). These oxidative metabolites of arachidonic acid, are produced by cyclooxygenases (COX1 and COX2), and act locally in an autocrine or paracrine manner (reviewed in (43)). PGE_2 is a major COX metabolite, which mediates its effects by activation of four GPCRs, designated E-Prostanoid (EP)1 through EP4 (43). Analysis of GPCR expression across a panel of mouse tissues revealed that the EP3 receptor was most highly expressed in the pancreas, kidney and white adipose tissue, an expression pattern consistent with regulation of metabolic homeostasis (235).

PGs and other inflammatory mediators play an important role in adipose tissue physiology (320,388,390). EP3 has the highest expression of the four EP receptors in mouse epididymal fat pads (338). Pharmacological studies suggest that PGE_2 inhibits lipolysis and reduces intracellular cAMP in adipocytes via the EP3 receptor (101,284). cAMP-protein kinase A (PKA) signaling is a central regulator of lipolysis, being important for activating both hormone sensitive lipase (HSL) and adipose triglyceride lipase (ATGL) (401,403-405). Loss of PG production in adipose tissue by deletion of adipocyte phospholipase, AdPLA, increases lipolysis causing lipids to be stored in ectopic tissues (101). These $AdPLA^{-/-}$ mice are resistant to

obesity but are insulin resistant due to the ectopic triglyceride storage (101). Taken together these data suggest that the EP3 receptor plays a role in facilitating adipose tissue lipid accumulation by inhibiting lipolysis. Thus, a loss of EP3 signaling may limit adipose tissue lipid deposition and facilitate ectopic lipid distribution, which could exacerbate diet induced insulin resistance.

Contrary to what would be expected in a model of increased adipocyte lipolysis, mice with a global gene disruption of the EP3 receptor have increased body weight and fat pad mass when fed breeder chow (102). This report contrasts with a previous report that $EP3^{-/-}$ mice have normal growth rates (310) and our data from $EP3^{-/-}$ mice fed a standard chow diet (Chapter II). (310). To more completely characterize the interaction of the EP3 receptor with diet and its role in metabolism, $EP3^{-/-}$ mice were challenged with a high fat diet (HFD). We show that $EP3^{-/-}$ mice have no difference in body weight on a control or chow diet. However, when fed a HFD, $EP3^{-/-}$ mice gained more weight than did $EP3^{+/+}$ fed the same diet, similar to what was previously found when the $EP3^{-/-}$ mice were fed breeder chow (102). As with $EP3^{-/-}$ mice fed breeder chow, we noted insulin resistance and elevated blood glucose in $EP3^{-/-}$ mice fed HFD. We found that the insulin resistance in $EP3^{-/-}$ mice fed a HFD is accompanied by lipid redistribution from the adipose tissue to ectopic, insulin sensitive tissues such as liver and skeletal muscle. Fat pads in $EP3^{-/-}$ HFD fed mice were relatively smaller, had increased necrosis, increased inflammatory cytokine expression and failed to suppress lipolysis in response to PGE_2. Although $EP3^{-/-}$ mice were not hyperphagic, they were less active, became obese, had increased ectopic lipid accumulation and were insulin resistant.

Materials and Methods

Animal procedures & high fat diet feeding

Mice utilized for these experiments were maintained as previously described (Chapter II). Beginning at age 4 weeks, male C57BL/6 $EP3^{+/+}$ or $EP3^{-/-}$ mice were fed a control diet (10% calories from fat; 4.3% fat by weight, D12450Bi, Research Diets, New Brunswick, NJ) or high fat diet (HFD) (45% calories from fat; 24% fat by weight, D12451i, Research Diets) for 16 weeks. All procedures were approved by the Institutional Animal Care and Use Committee at Vanderbilt University.

Energy balance

A separate cohort of mice utilized for energy balance studies were fed HFD beginning at 7.5 weeks of age for 10.5 weeks until ~18 weeks of age. Energy balance studies were performed in a Promethion system (Sable Systems International, North Las Vegas, NV) for five days by the Vanderbilt Mouse Metabolic Phenotyping Center.

Plasma chemistry

Plasma was collected from blood obtained by terminal cardiac puncture. Plasma triglyceride quantification was performed by the Vanderbilt Translational Pathology Shared Resource. Plasma FFA quantification was performed by the Mouse Metabolic Phenotyping Center Lipid Lab.

Intraperitoneal glucose tolerance tests

IP-GTT was performed on male C57BL/6 $EP3^{+/+}$ or $EP3^{-/-}$ mice as previously described (Chapter II).

Intraperitoneal insulin tolerance tests

Male $EP3^{+/+}$ or $EP3^{-/-}$ mice were fasted for 6 hours during the light cycle and fasting blood glucose level were measured with the Accu-Check Aviva blood glucose meter using blood obtained from the tail. Following intraperitoneal injection of 0.75 U/kg insulin (human recombinant insulin, Novolin R, Novo Nordisk, Princeton, NJ) in 0.9% normal saline, blood glucose levels were measured at 15, 30, 60, 90, and 120 minutes post-injection.

Mouse static incubation insulin secretion

Pancreatic islets were isolated from 10.5 week old C57BL/6 mice, purchased from The Jackson Laboratory (Bar Harbor, ME), which had been fed control (D12450Bi) or HFD (D12451i) since 3.5 weeks of age. Briefly, isolated islets were cultured overnight in RPMI with 5.6 mM glucose. The following day islets were incubated in DMEM media for one hour in 5.6 mM glucose ± DG-041. Following the one-hour culture, islets were then incubated in DMEM media with the indicated glucose and drug concentrations and 100 μM IBMX for one hour. 200 μl of acid ethanol was used to disrupt islets for total insulin content. Islet isolation and culture and insulin and glucagon assays were performed at the Vanderbilt Islet Procurement & Analysis Core as previously described (558).

Prostanoid quantification

PG content of islet secretion media and epididymal fat pads were measured by the Vanderbilt Eicosanoid Core Laboratory as previously described (563).

Plasma Chemistry

At the end of the control and HFD feeding study, 20 weeks of age, plasma was collected from blood obtained by terminal cardiac puncture post-mortally from three to four *ad libitum* fed mice per group. Leptin and adiponectin were measured with a Luminex 100 system (Luminex

Corporation, Austin, TX) by the Vanderbilt University Hormone Assay & Analytical Services Core.

Skeletal muscle capillary density

Combined gastrocnemius and soleus skeletal muscle were fixed by freezing in OCT medium and sectioned by the Vanderbilt Translational Pathology Shared Resource. Frozen slides were allowed to equilibrate to room temperature and excess OCT was removed from slides prior to the beginning of staining. Slides were fixed in HPLC grade acetone for 10 minutes at room temperature then allowed to air dry for 10 minutes. Slides were washed in PBS three times for 3.3 minutes each. Slides were blocked for one-hour in a humidified chamber at room temperature in 3% BSA in PBS. Following blocking, slides were washed one time in PBS for 5 minutes. Slides were incubated with 1:200 rat anti-mouse CD31 antibodies (BD Pharmingen, San Diego, CA, Cat. No. 550274) in PBS with 0.1% Triton X-100 and 1% BSA overnight at 4° C in a humidified chamber. The next morning, slides were washed in PBS three times for five minutes each. Slides were incubated with 1:250 donkey anti-rat-rhodamine red (Jackson ImmunoResearch Laboratories, West Grove, PA, Cat. No. 712-259-150) and 1:10,000 DAPI in PBS with 0.1% Triton X-100 and 1% BSA for 1.5 hours at room temperature in a humidified chamber. Slides were washed in PBS three times for five minutes each and subsequently mounted with Vectashield (Vector Laboratories, Burlingame, CA, Cat. No. H-100). Slides were imaged with an Olympus BX51 microscope (Olympus America, Melville, NY) using a 20× objective with an exposure of 1.5 ms for DAPI and 50 ms for CD31. Three tissue sections from three mice from each diet×genotype group were analyzed with ImageJ 1.43u (National Institutes of Health, USA). Statistics were performed on the average staining from each mouse, which was an average of all three sections, which in turn was an average of at least 10 images.

Histology

Liver and epididymal fat pads from at least three individual mice per group were fixed in 10% formaldehyde overnight at 4°C and subsequently stored in 70% ethanol at 4°C prior then processed routinely, paraffin embedded, sectioned at 4 μm, and stained with hematoxylin and eosin (H&E) or immunohistochemistry. Liver samples from three individual mice per group were fixed by freezing in OCT medium for Oil Red O (ORO) staining. Histology was performed by the Vanderbilt Translational Pathology Shared Resource. All slides were imaged at 20× with a Leica SCN400 Slide Scanner (Leica Microsystems, Wetzlar, Germany) by the Vanderbilt Digital Histology Shared Resource. Whole slides were imaged at 20X magnification to a resolution of 0.5 μm/pixel. Adipocyte cell sizes were measured from 10 images per mouse with ImageJ using Adipocytes Tools (564). Epididymal fat pads were examined by an experienced veterinary pathologist (Kelli L. Boyd). Fat pad necrosis and inflammation (steatitis) were scored on a scale of zero to four, with zero being no steatitis or necrosis, one being minimal steatitis and necrosis not present, two being mild steatitis with necrosis of individual adipocytes, three being moderate steatitis with extensive areas of adipocyte necrosis, and four being severe steatitis with diffuse necrosis of the fat pad. The numbers of positive (brown) and negative (blue) nuclei were determined by analysis of 10 images per mouse in the Ariol® software (Leica Microsystems) at the Vanderbilt Digital Histology Shared Resource.

Mouse adipocyte lipolysis assay

Adipocytes were isolated from epididymal fat pads of ten week old male $EP3^{+/+}$ and $EP3^{-/-}$ mice that were maintained on a standard chow diet. Lipolysis was assessed as described (565). Each assay was performed in duplicate for each mouse. Briefly, fat pads were placed in an Adipocyte Incubation Solution (AIS) containing 1.8 g/L glucose, 0.1 g/L Magnesium Chloride

hexahydrate, 0.34 g/L Potassium Chloride, 7.0 g/L Sodium Chloride, 0.1 g/L Sodium Phosphate Dibasic, 0.18 g/L Sodium Phosphate Monobasic, 0.84 g/L Sodium Bicarbonate, 30 mM HEPES, and 3% (w/v) fatty acid free bovine albumin fraction V (MP Biomedical, Solon, OH) at pH 7.4. Fat pads were minced and digested in AIS with 500 nM adenosine (Sigma A4036) and 3 mg/ml type 1 collagenase (Worthington Biochemical Corporation, Lakewood, NJ) for one hour at 37°C while shaking at 200 rpm. Digested fat pads were filtered through 250 μm Pierce® Tissue Strainers (Thermo Scientific, Rockford, IL) and washed three times in AIS with adenosine. Adipocytes were resuspended in AIS and counted with Scepter™ Handheld Automated Cell Counter (Millipore Corporation, Billerica, MA). Lipolysis assays were performed on 6,000 to 9,000 adipocytes in 650 μl in 15 ml conicals at 37°C. At the start of the assay, adipocytes were incubated in the presence or absence of DG-041 or human recombinant insulin (Sigma I9288). PGE_2 (Cayman Chemical, Ann Arbor, MI) was added after 15 minutes to account for the slow binding of DG-041 (566,567). After 30 minutes a 50 μl sample was collected from each sample to establish baseline and isoproterenol (Sigma I6504) was added. Isoproterenol stimulated lipolysis was assessed one hour after the addition of isoproterenol. Glycerol was measured with a Glycerol Assay Kit (Sigma MAK117-1KT).

Tissue fatty acid composition

Lipids were extracted from ~100 mg flash frozen liver or combined gastrocnemius and soleus skeletal muscle tissue (568). The extracts were filtered, and lipids recovered in the chloroform phase. Individual lipid classes were separated by thin layer chromatography using Silica Gel 60 A plates developed in petroleum ether, ethyl ether, acetic acid (80:20:1) and visualized by rhodamine 6G. Phospholipids, diglycerides, triglycerides and cholesteryl esters were scraped from the plates and methylated using BF3/methanol (569). The methylated fatty

acids were extracted and analyzed by gas chromatography. Gas chromatographic analyses were carried out on an Agilent 7890A gas chromatograph equipped with flame ionization detectors, a capillary column (SP2380, Supelco, Bellefonte, PA). Helium was used as a carrier gas. Fatty acid methyl esters were identified by comparing the retention times to those of known standards. Triglycerides were quantified by the Mouse Metabolic Phenotyping Center Lipid Lab.

Quantitative real-time RT-PCR (qPCR)

Total RNA was isolated from approximately 50-100 mg frozen liver or 100-250 mg frozen epididymal fat pad using TRIzol Reagent (Invitrogen, Carlsbad, CA). Liver RNA was precipitated with isopropanol and ethanol from the aqueous phase of the TRIzol extraction then dissolved in RNase-free water and subsequently purified with RNeasy Mini Kit (Qiagen, Valencia, CA). Epididymal fat pad RNA was immediately purified from the aqueous phase of the TRIzol extraction with RNeasy Mini Kit. One μg RNA per mouse was reverse transcribed at a concentration of 50 ng/μl using High Capacity cDNA Reverse Transcription Kit (Applied Biosystems, Foster City, CA). Approximately 6.25 ng cDNA was utilized per 20 μl quantitative PCR reaction. Quantitative real-time RT-PCR was performed using TaqMan Gene Expression Assays (Applied Biosystems) for *Adipoq* (Mm00456425_m1), *Apob* (Mm01545156_m1), *Cebpb* (Mm00843434_s1), *Ccl2* (Mm00441242_m1), *Cpt1a* (Mm01231183_m1), *Emr1* (Mm00802529_m1), *Fasn* (Mm00662319_m1), *Gapdh* (Mm99999915_g1), *Il6* (Mm00446190_m1), *Lep* (Mm00434759_m1), *Mttp* (Mm00435015_m1), *Pecam1* (Mm01242584_m1), *Ptger3* (Mm01316856_m1), *Ptgs2* (Mm00478374_m1), *Tnf* (Mm00443258_m1), *Ucp1* (Mm01244861_m1), and *Vegfa* (Mm01281449_m1). All assays were run on a 7900HT Fast Real-Time PCR System (Applied Biosystems) at the Vanderbilt Technologies for Advanced Genomics. Gene expression data were collected from three

replicates of each sample and four replicates of each standard curve point. Replicate samples were averaged and analyzed using the Pfaffl method (570). Gene expression was normalized to *Gapdh* and the individual with the lowest relative gene expression was considered to have a fold change of 1.0.

Measurement of Systolic Blood Pressure

Systolic BP was determined in conscious mice by using tail-cuff plethysmography (Visitech systems BP-2000 Blood Pressure Analysis System, Apex NC). Mice were trained for three days to minimize stress. Each measurement is the average of at least 10 consecutive readings after stabilization on the last day.

Statistical analysis and calculations

Data are means ± SEM, using GraphPad Prism version 6.0e for Mac OS X (GraphPad Software, La Jolla, CA). All analyses were performed with a 2-way ANOVA comparing EP3 genotype and dietary treatment unless otherwise stated. Multiple comparison tests were performed with the Bonferroni correction for EP3 genotype only and are indicated on figures by asterisks corresponding to *P < 0.05, **P < 0.01, ***P < 0.001. For analyses of plasma insulin, fat mass, and lean mass over time, 2-way ANOVA with repeated measures was performed comparing the factors EP3 genotype and time keeping the dietary treatment consistent. HOMA-IR was calculated as the fasting insulin level (μU/mL) × blood glucose level (mg/dL) / 405. For all studies, $P < 0.05$ was considered statistically significant.

Results

$EP3^{-/-}$ mice are obese when fed a HFD

$EP3^{+/+}$ or $EP3^{-/-}$ male mice were fed either HFD (45% calories from fat) or a micronutrient matched control diet (10% calories from fat). Body weight increased in each of the

four groups over the course of the study (Figure 11A). Body weight in both $EP3^{+/+}$ and $EP3^{-/-}$ HFD fed mice increased at a greater rate than in animals fed control diet, with a divergence in body weight becoming apparent after eight weeks of age. Moreover, by 14 weeks of age the $EP3^{-/-}$ mice fed HFD were heavier than HFD-fed $EP3^{+/+}$ animals. $EP3^{-/-}$ mice continued to gain weight throughout the remainder of the study leading to a greater difference in body weight at 20 weeks of age ($P < 0.0001$).

$EP3^{-/-}$ mice are have increased adiposity and epididymal fat pad mass

Body composition analyses over the course of the study revealed that HFD fed $EP3^{-/-}$ mice had no difference in lean mass (Figure 11B) but had increased fat mass as compared to HFD fed $EP3^{+/+}$ (Figure 12A). A small but statistically significant increase in body fat was also observed at 20 weeks of age in $EP3^{-/-}$ mice vs. $EP3^{+/+}$ fed control diet. Post-mortem analysis of epididymal fat pads confirmed that, when fed a HFD, fat pads from $EP3^{-/-}$ mice were heavier than those from $EP3^{+/+}$ (Figure 12B).

When total fat mass determined from body composition analysis at 20 weeks of age was plotted as a function of body weight for HFD fed animals, the expected linear relationship was observed (Figure 12C); and although $EP3^{-/-}$ mice fed HFD were heavier, they had the same overall linear relationship of total fat mass to body weight ($P = 0.88$, Figure 12C). In both genotypes, heavier mice had more fat mass than did the lighter mice, as determined by the body composition scanner. However, when epididymal fat pad weight was plotted as a function of body weight, a striking difference was observed between genotypes (Figure 12D). The heaviest $EP3^{-/-}$ HFD-fed mice had smaller epididymal fat pads than did the lightest $EP3^{-/-}$ HFD-fed mice. In control diet fed animals, genotype did not affect the relationship between body weight and

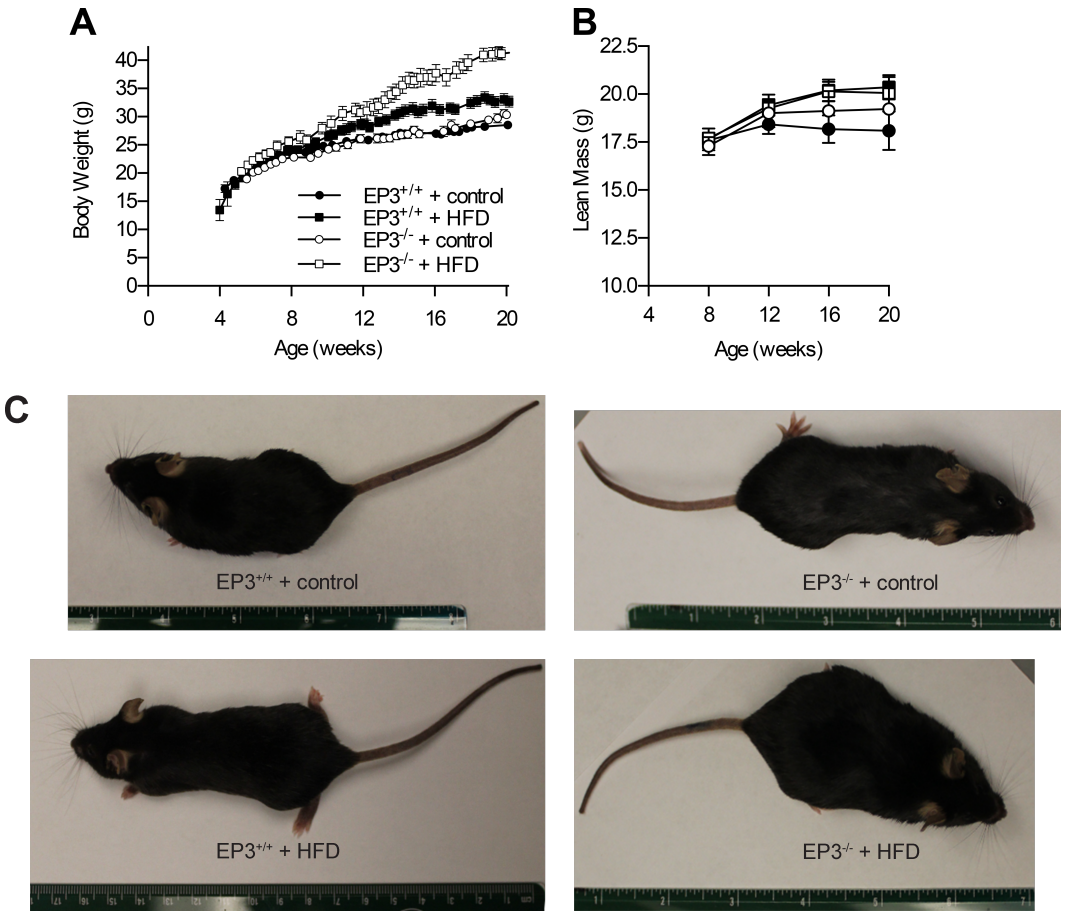

Figure 11. EP3$^{-/-}$ mice are obese when fed a HFD

A. Male EP3$^{+/+}$ and EP3$^{-/-}$ mice fed control diet or HFD were weighed between 4 weeks of age and 20 weeks of age. No difference in body weight was observed between genotypes in the control diet fed animals. EP3$^{-/-}$ mice fed HFD were significantly heavier than EP3$^{+/+}$ animals beginning around 14 weeks of age ($P = 0.0041$) and continuing until the end of the experiment at 20 weeks of age ($P < 0.0001$). **B.** Body composition of lean mass was assessed by pulsed NMR. **C.** Representative images of EP3$^{+/+}$ and EP3$^{-/-}$ mice fed control or HFD at 20 weeks of age. For all figures N = 9 EP3$^{+/+}$ control, 10 EP3$^{-/-}$ control, 7 EP3$^{+/+}$ HFD, 9 EP3$^{-/-}$ HFD. Values are expressed as mean ± SEM.

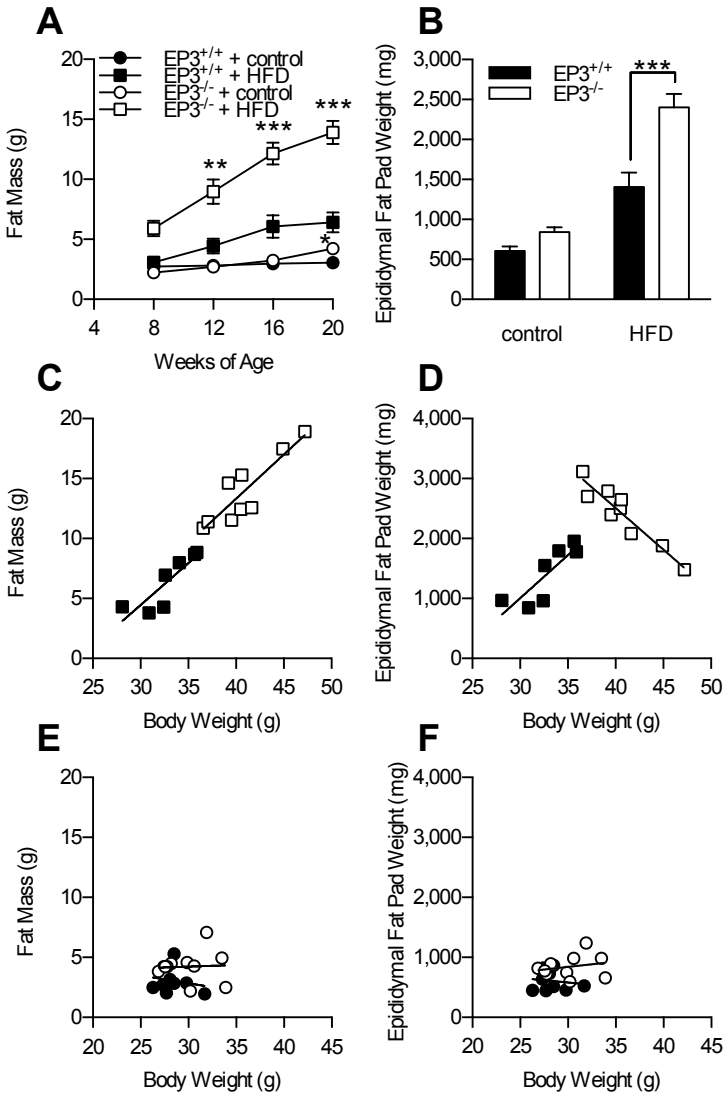

Figure 12. EP3$^{-/-}$ mice proportionately increase adiposity but not epididymal fat pad mass
A. Body composition of fat was assessed at four week intervals by pulsed NMR. EP3$^{-/-}$ mice had increased fat mass when fed HFD ($P = 0.0004$). **B.** Epididymal fat pads were weighed post mortem at the conclusion of the study. Epididymal fat pads mice were heavier from EP3$^{-/-}$ HFD fed mice ($P = 0.0038$). **C.** Mice fed HFD showed no difference in the total body fat to body weight ratio between genotypes ($P = 0.875$). **D.** The relationship between epididymal fat pad weight and body weight differ between EP3$^{-/-}$ and EP3$^{+/+}$ mice ($P < 0.0001$). **E.** Total fat mass determined by NMR plotted showed no correlation to body weight in EP3$^{+/+}$ and EP3$^{-/-}$ mice fed control diet ($R^2 < 0.04$ for both). **F.** Epididymal fat pad weight showed no correlation to body weight in EP3$^{+/+}$ and EP3$^{-/-}$ mice fed control diet ($R^2 < 0.06$ for both). For all figures N = 9 EP3$^{+/+}$ control, 10 EP3$^{-/-}$ control, 7 EP3$^{+/+}$ HFD, 9 EP3$^{-/-}$ HFD. Values are expressed as mean ± SEM.

either fat mass or epididymal fat pad weight (Figure 12E,F). These data are consistent with abnormal lipid accumulation in fat depots in EP3$^{-/-}$ mice when challenged with HFD feeding.

EP3$^{-/-}$ mice have changes in energy balance

A separate cohort of mice was fed HFD, beginning at 7.5 weeks of age, for energy balance studies (Figure 13A). Energy balance studies demonstrate that EP3$^{-/-}$ mice do not have changes in food consumption (Figure 13B). EP3$^{-/-}$ mice were found to have a significant decrease in movement during the dark cycle of the day (Figure 13C). This was accompanied by more time spent inactive (Figure 13D).

Changes in energy expenditure were also measured. EP3$^{-/-}$ mice were not found to have significant changes in energy expenditure (Figure 14A). Oxygen consumption was unchanged in these mice (Figure 14B); however, carbon dioxide production was increased in EP3$^{-/-}$ mice (Figure 14C). Because an increase in respiration contrasts with the decrease in ambulatory activity, expression of a gene involved in oxidative metabolism was measured. UCP1 is a protein found in the mitochondria of adipose tissue that uncouples respiration from ATP synthesis resulting in a loss of energy (318). Expression of *Ucp1* was increased in the epididymal fat pads of EP3$^{-/-}$ mice when fed a HFD (Figure 14D).

EP3$^{-/-}$ mice have increased adipocyte hypertrophy

Adipocytes from mouse epididymal fat pads were visualized by H&E staining (Figure 15A). Both HFD feeding and EP3$^{-/-}$ genotype were associated with an increase in average adipocyte cell size (Figure 15B). When adipocyte cell size was plotted as a function of body weight, cell size to body weight ratios for EP3$^{-/-}$ HFD fed mice were significantly different than those observed for EP3$^{+/+}$ HFD fed mice (Figure 15C). The size distribution showed that EP3$^{-/-}$ mice have a greater number of large adipocytes regardless of which diet they were fed (Figure

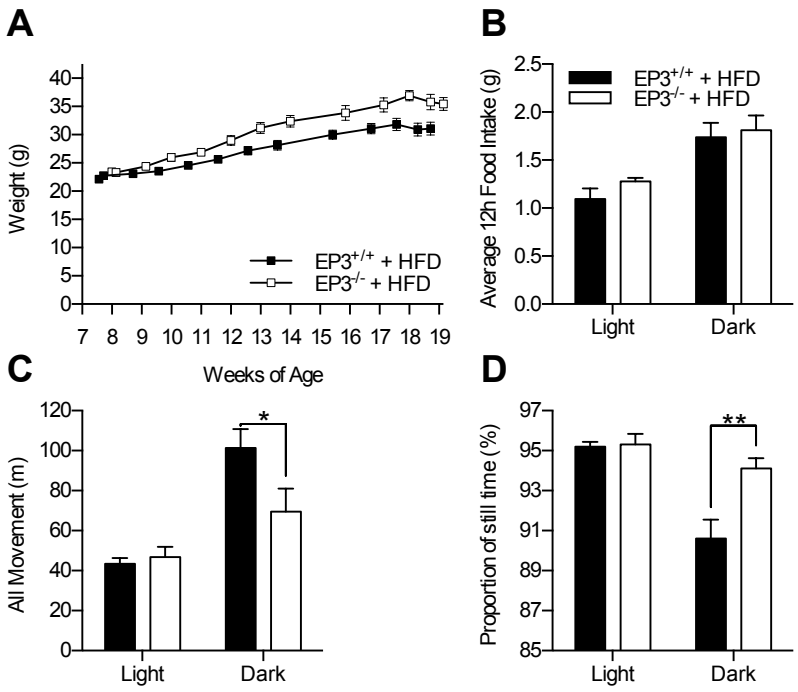

Figure 13. EP3$^{-/-}$ mice have decreased movement when fed a HFD
A. Male EP3$^{+/+}$ and EP3$^{-/-}$ mice were fed HFD between 7.5 weeks of age and 19 weeks of age. EP3$^{-/-}$ mice fed HFD were heavier than EP3$^{+/+}$ animals (P = 0.029). **B.** Total food intake was measured in male mice that had been fed HFD for 10.5 weeks. Mice consumed more food during the dark cycle (P = 0.0026), but no significant difference between EP3 genotypes (P = 0.35) or interaction between light cycle and genotype (P = 0.67) were observed. **C.** Total movement was measured in the same mice. EP3$^{-/-}$ mice were found to move significantly less than EP3$^{+/+}$ mice during the dark cycle. **D.** Mice were still for a greater amount of their time in the light cycle (P = 0.0053). EP3$^{-/-}$ mice spend a greater proportion of their time inactive (P = 0.014). For all figures N = 6 EP3$^{+/+}$ HFD, 4 EP3$^{-/-}$ HFD. All values are expressed as mean ± SEM.

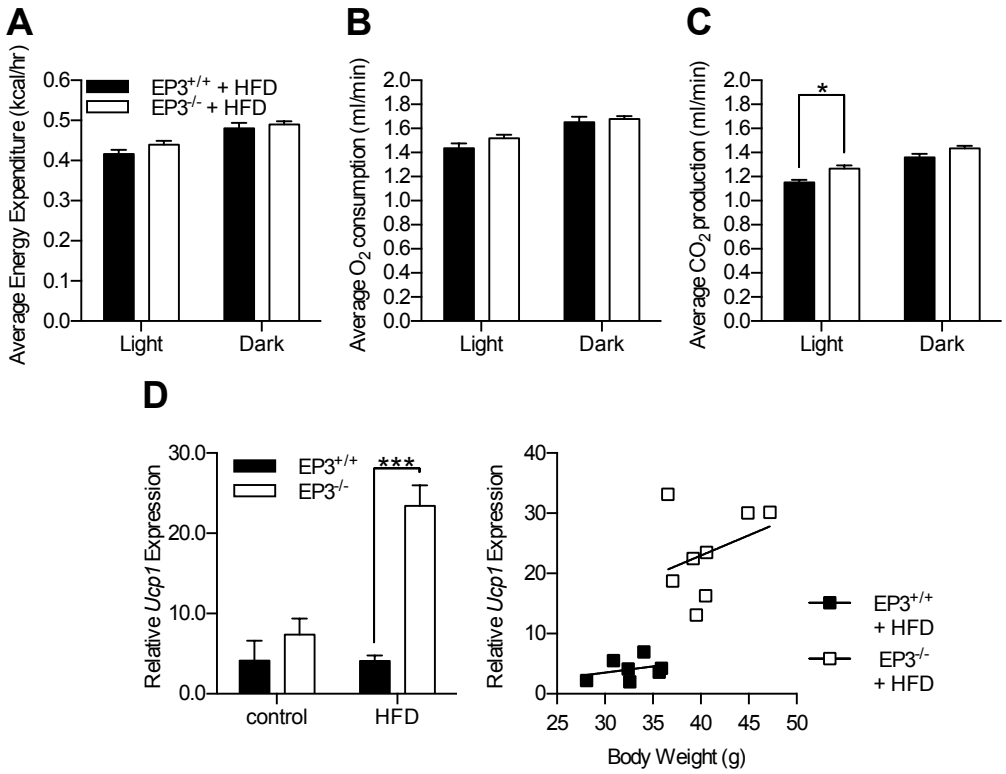

Figure 14. EP3$^{-/-}$ HFD fed mice have increased CO_2 production and uncoupling protein gene expression

A. Total energy expenditure was measured in male mice that had been fed HFD for 10.5 weeks. Mice had greater energy expenditure during the dark cycle ($P < 0.0001$), but no significant differences between EP3 genotype ($P = 0.315$) or interaction between light cycle and genotype ($P = 0.242$) were observed. **B.** Average oxygen consumption was measured in the same mice. Mice had greater oxygen during the dark cycle ($P < 0.0001$), but no significant differences between EP3 genotype ($P = 0.349$) or interaction between light cycle and genotype ($P = 0.142$) were observed. **C.** Average CO_2 production was also measured in these mice. Mice had greater CO_2 production during the dark cycle ($P < 0.0001$). EP3$^{-/-}$ mice demonstrated increased CO_2 production ($P = 0.0252$), but a significant interaction between genotype and light cycle was not observed ($P = 0.325$). For A-C, N = 6 EP3$^{+/+}$ HFD, 4 EP3$^{-/-}$ HFD. **D.** Gene expression of uncoupling protein 1 (*Ucp1*) in epididymal fat pads was measured in a separate cohort of 20 week old mice that had been fed control or HFD for 16 weeks. *Ucp1* expression was increased in EP3$^{-/-}$ mice ($P < 0.0001$). HFD feeding increased *Ucp1* expression ($P = 0.0008$) and interacted synergistically with EP3 genotype ($P = 0.0007$). *Ucp1* gene expression was plotted as a function of body weight. The relationships between *Ucp1* gene expression and body weight are not different in HFD fed mice ($P = 0.650$). N = 7 EP3$^{+/+}$ control, 9 EP3$^{-/-}$ control, 7 EP3$^{+/+}$ HFD, 8 EP3$^{-/-}$ HFD. For all figures values are expressed as mean ± SEM.

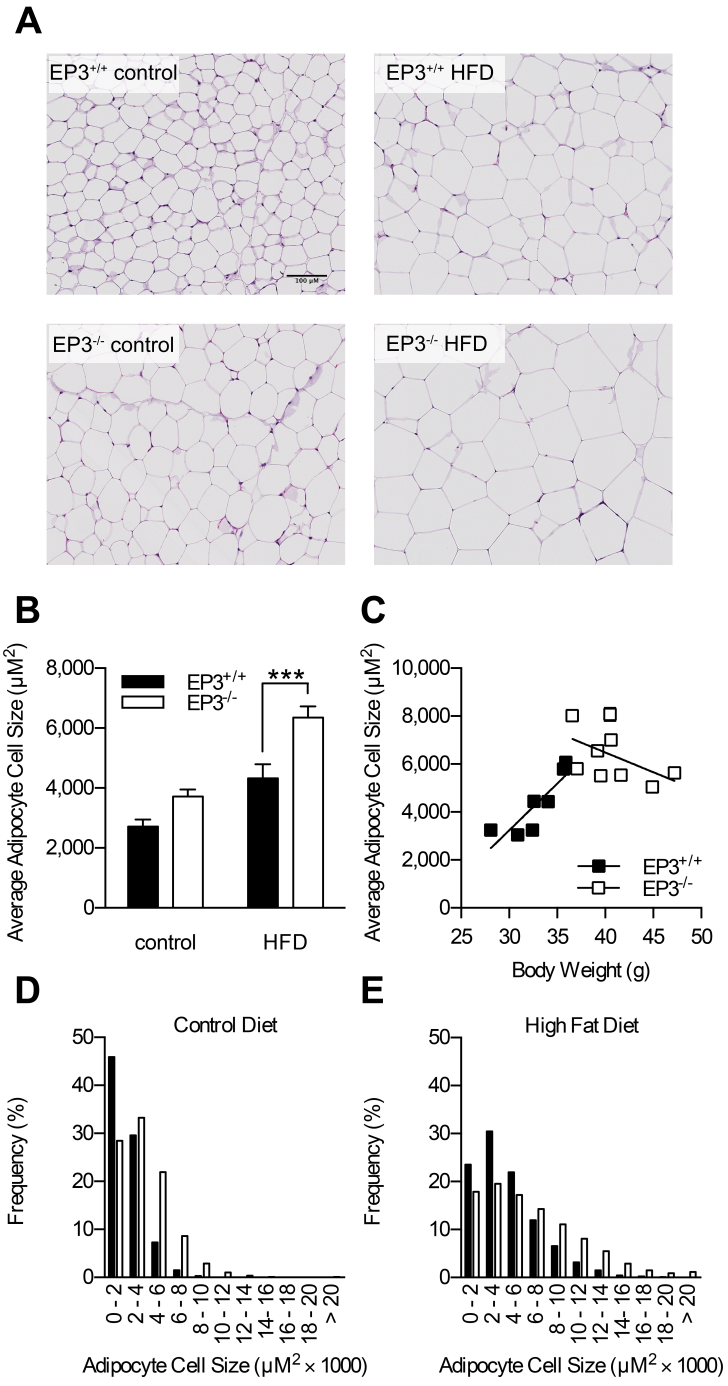
A
EP3+/+ control
EP3+/+ HFD
EP3-/- control
EP3-/- HFD
B
Average Adipocyte Cell Size (μM2)
8,000
6,000
4,000
2,000
0
EP3+/+
EP3-/-
***
control
HFD
C
Average Adipocyte Cell Size (μM2)
10,000
8,000
6,000
4,000
2,000
0
25
30
35
40
45
50
Body Weight (g)
EP3+/+
EP3-/-
D
Control Diet
Frequency (%)
50
40
30
20
10
0
0 - 2
2 - 4
4 - 6
6 - 8
8 - 10
10 - 12
12 - 14
14 - 16
16 - 18
18 - 20
> 20
Adipocyte Cell Size (μM2 × 1000)
E
High Fat Diet
Frequency (%)
50
40
30
20
10
0
0 - 2
2 - 4
4 - 6
6 - 8
8 - 10
10 - 12
12 - 14
14 - 16
16 - 18
18 - 20
> 20
Adipocyte Cell Size (μM2 × 1000)

Figure 15. EP3$^{-/-}$ mice have increased epididymal fat pad adipocyte cell size
A. H&E staining of epididymal fat pads. **B.** Average epididymal fat pad adipocyte cell sizes were calculated from measurements of adipocytes made using ImageJ software. EP3$^{-/-}$ mice were found to have larger adipocytes (P = 0.0002). **C.** Average adipocyte cell size from HFD fed mice was plotted as a function of body weight. The relationship between epididymal fat pad adipocyte cell size and body weight are significantly different (P = 0.0055). **D.** Distribution of adipocyte size from mice fed control diet. **E.** Distribution of adipocyte size from mice fed HFD. For all figures N = 8 EP3$^{+/+}$ control, 7 EP3$^{-/-}$ control, 7 EP3$^{+/+}$ HFD, 9 EP3$^{-/-}$ HFD. Images are a representative sample of those used to calculate adipocyte cell size. For B & C, values are expressed as mean ± SEM; for D & E, values are expressed as mean only.

15D,E). These data suggest that the altered correlation between epididymal fat pad mass and body weight observed in EP3$^{-/-}$ HFD fed animals is due to an inability to proportionally increase adipocyte size in heavier animals.

Adipose tissue from EP3$^{-/-}$ mice does not have changes in gene expression related to prostaglandin biosynthesis but does have changes in genes associated with increased adipogenesis

Gene expression was measured in the epididymal fat pads of EP3$^{-/-}$ mice. As expected, the EP3 gene (*Ptger3*) was not expressed in EP3$^{-/-}$ tissue (Figure 16A). Dietary fat did not have an effect on EP3 gene expression. Expression of the inducible COX2 gene (*Ptgs2*) was also measured and was found to be unaffected by dietary fat or EP3 genotype (Figure 16B). The expression of CCAAT/enhancer-binding protein β (*Cebpb*) was measured because it plays an important role promoting both adipogenesis (349,350) and COX2 transcription (346-348). The expression of *Cebpb* was increased in the adipose tissue of EP3$^{-/-}$ HFD fed mice (Figure 16C).

EP3$^{-/-}$ mice have increased adipocyte necrosis when fed HFD

H&E stained epididymal fat pads from HFD fed EP3$^{+/+}$ and EP3$^{-/-}$ mice were scored for necrosis on a scale of 0 to 4. EP3$^{-/-}$ mice showed areas of increased necrosis in the epididymal fat pads, which was largely absent in EP3$^{+/+}$ mice (Figure 17A). EP3$^{-/-}$ HFD fed mice showed areas of increased necrosis in the epididymal fat pads (Figure 17B). Necrosis was increased with increasing body weight in both genotypes of mice (Figure 17C). Thus, in the EP3$^{-/-}$ HFD cohort, the heaviest mice have the smallest epididymal fat pads (Figure 12D) and these were the most necrotic. Signaling through EP3 is known to promote the production of vascular endothelial growth factor (VEGF) and angiogenesis (571-573). EP3$^{-/-}$ might have decreased vascularization leading to ischemia and necrosis in the epididymal fat pads. Expression of *Vegfa* and platelet

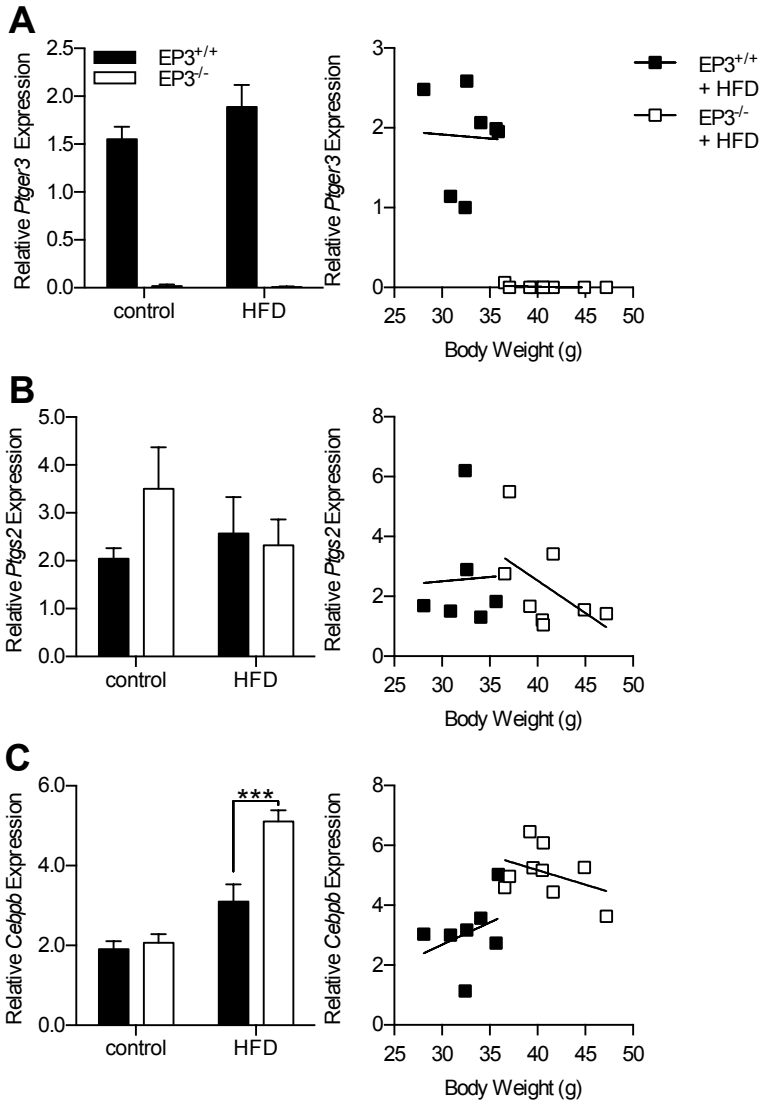

Figure 16. Adipose tissue from EP3$^{-/-}$ mice fed HFD expresses genes associated with adipocytes

Quantitative real-time RT-PCR analysis of EP3 RNA levels from epididymal fat pads from 20 week old EP3$^{+/+}$ and EP3$^{-/-}$ mice fed control or HFD. **A.** Diet did not have a significant effect on *Ptger3* expression in adipose (P = 0.160). **B.** COX-2 gene (*Ptgs2*) expression was not affected by dietary fat (P = 0.640) or EP3 genotype (P = 0.386). An interaction between diet and genotype also did not affect *Ptgs2* gene expression (P = 0.226). The relationships between *Ptgs2* gene expression and body weight are not different in HFD fed mice (P = 0.488). **C.** CCAAT/enhancer-binding protein β (*Cebpb*) gene expression was increased in EP3$^{-/-}$ mice (P = 0.0007). HFD feeding increased *Cebpb* expression (P < 0.0001) and interacted synergistically with EP3 genotype (P = 0.0027). *Cebpb* gene expression was plotted as a function of body weight. The relationships between *Cebpb* gene expression and body weight are not different in HFD fed mice (P = 0.195). N = 8 EP3$^{+/+}$ control, 10 EP3$^{-/-}$ control, 7 EP3$^{+/+}$ HFD, 9 EP3$^{-/-}$ HFD. For all figures values are expressed as mean ± SEM.

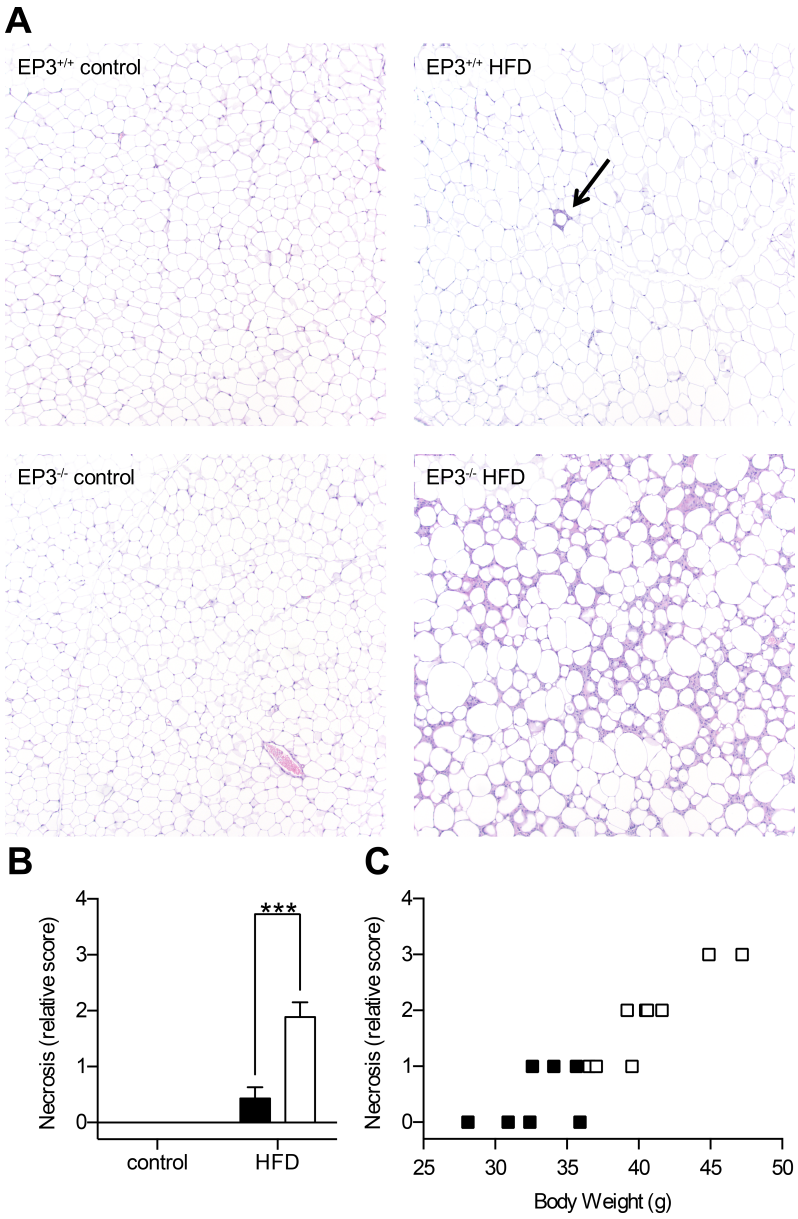

Figure 17. Epididymal fat pads from EP3$^{-/-}$ HFD fed mice have increased necrosis
A. Representative necrotic sections of H&E stained epididymal fat pads. **B.** For mice fed a HFD, Epididymal fat pads from EP3$^{-/-}$ mice had more necrosis than EP3$^{+/+}$ ($P < 0.0001$). No necrosis was observed in epididymal fat pads from control diet fed mice. **C.** The necrosis score of HFD fed mice was plotted as a function of body weight. A similar correlation between body weight and necrosis score was observed between the EP3$^{+/+}$ and EP3$^{-/-}$ genotypes ($P = 0.1$). For all figures N = 9 EP3$^{+/+}$ control, 10 EP3$^{-/-}$ control, 7 EP3$^{+/+}$ HFD, 9 EP3$^{-/-}$ HFD.

endothelial cell adhesion molecule-1 (*Pecam1*), markers of angiogenesis, were measured by qPCR (Figure 18A,B). Neither *Vegfa* nor *Pecam1* were significantly altered by either EP3 genotype or dietary fat demonstrating that lack of adequate vascularization does not correlate with the observed necrosis.

Necrosis is associated with macrophage accumulation (574). Macrophage infiltration of epididymal fat pads was assessed by qPCR for F4/80 gene expression (*Emr1,* EGF-like module-containing mucin-like hormone receptor-like 1). F4/80 gene expression demonstrated increased expression in the adipose tissue of $EP3^{-/-}$ mice when fed HFD (Figure 19A). In parallel with necrosis, macrophage infiltration of epididymal fat pads increased with increasing body weight. The slope of F4/80 gene expression versus body weight was increased in $EP3^{-/-}$ HFD fed mice compared to HFD fed $EP3^{+/+}$ mice and the smallest epididymal fat pads from the heaviest $EP3^{-/-}$ HFD fed mice had the greatest amount of both necrosis and F4/80 gene expression. In the obese state, secretion of adipokines is disrupted with increased secretion of pro-inflammatory, insulin resistance promoting cytokines and decreased secretion of anti-inflammatory, insulin-sensitizing cytokines (575). Increased expression of inflammation-associated adipokine genes was found in these epididymal fat pads; expression of TNF-α, Monocyte Chemoattractant Protein-1 (MCP-1), and IL-6 increased in $EP3^{-/-}$ mice when fed HFD (Figure 19B-D). Gene expression of leptin, which is normally increased during obesity, was also increased in epididymal fat pads from $EP3^{-/-}$ mice (Figure 19E). The higher gene expression combined with increased fat mass, were associated with elevated plasma leptin in $EP3^{-/-}$ HFD fed mice (Table 4). Gene expression of adiponectin, which is an insulin-sensitizing cytokine, was not altered in HFD fed $EP3^{+/+}$ mice (Figure 19F), consistent with what is seen in HFD fed C57BL/6 mice (576-578). In HFD fed $EP3^{-/-}$ mice, which have increased adiposity and inflammation in adipose tissue, gene expression

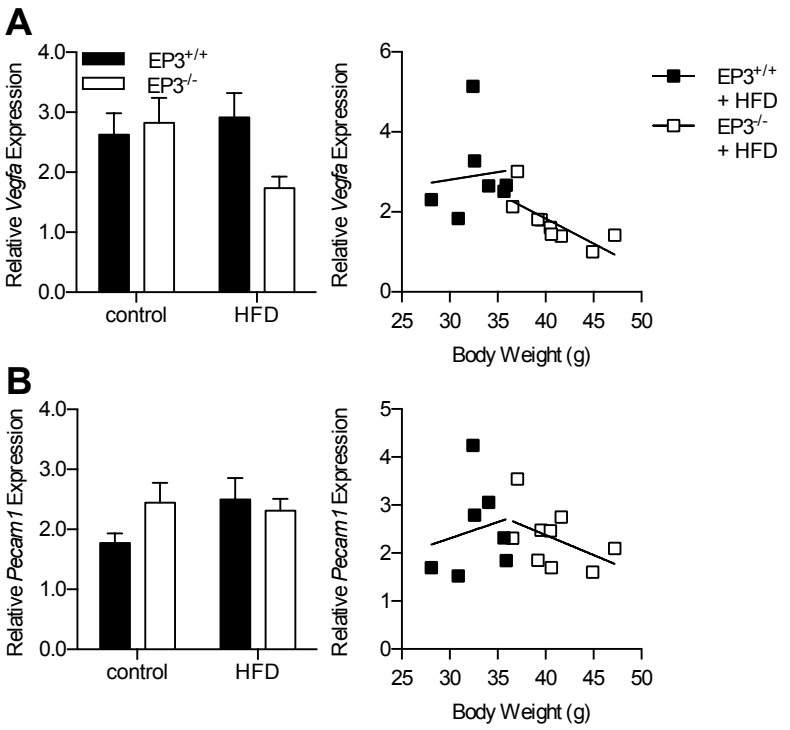

Figure 18. Vascularization markers are not changed in EP3$^{-/-}$ epididymal fat pads
Quantitative real-time RT-PCR analysis of epiddiymal fat pad gene expression from 20 week old EP3$^{+/+}$ and EP3$^{-/-}$ mice fed control or HFD. **A.** Vascular endothelial growth factor A (*Vegfa*) gene expression was not affected by HFD feeding (P = 0.277) or EP3 genotype (P = 0.184). No significant effect of interaction between dietary fat and EP3 on *Vegfa* was found (P = 0.0668). *Vegfa* gene expression was plotted as a function of body weight. The relationships between *Vegfa* gene expression and body weight are not different in HFD fed mice (P = 0.290). **B.** Gene expression of the endothelial cell marker, CD31, platelet endothelial cell adhesion molecule-1 (*Pecam1*), was not affected by HFD feeding (P = 0.302) or EP3 genotype (P = 0.389). *Pecam1* gene expression was plotted as a function of body weight. The relationships between *Pecam1* gene expression and body weight are not different in HFD fed mice (P = 0.311). N = 8 EP3$^{+/+}$ control, 10 EP3$^{-/-}$ control, 7 EP3$^{+/+}$ HFD, 9 EP3$^{-/-}$ HFD. For all figures values are expressed as mean ± SEM.

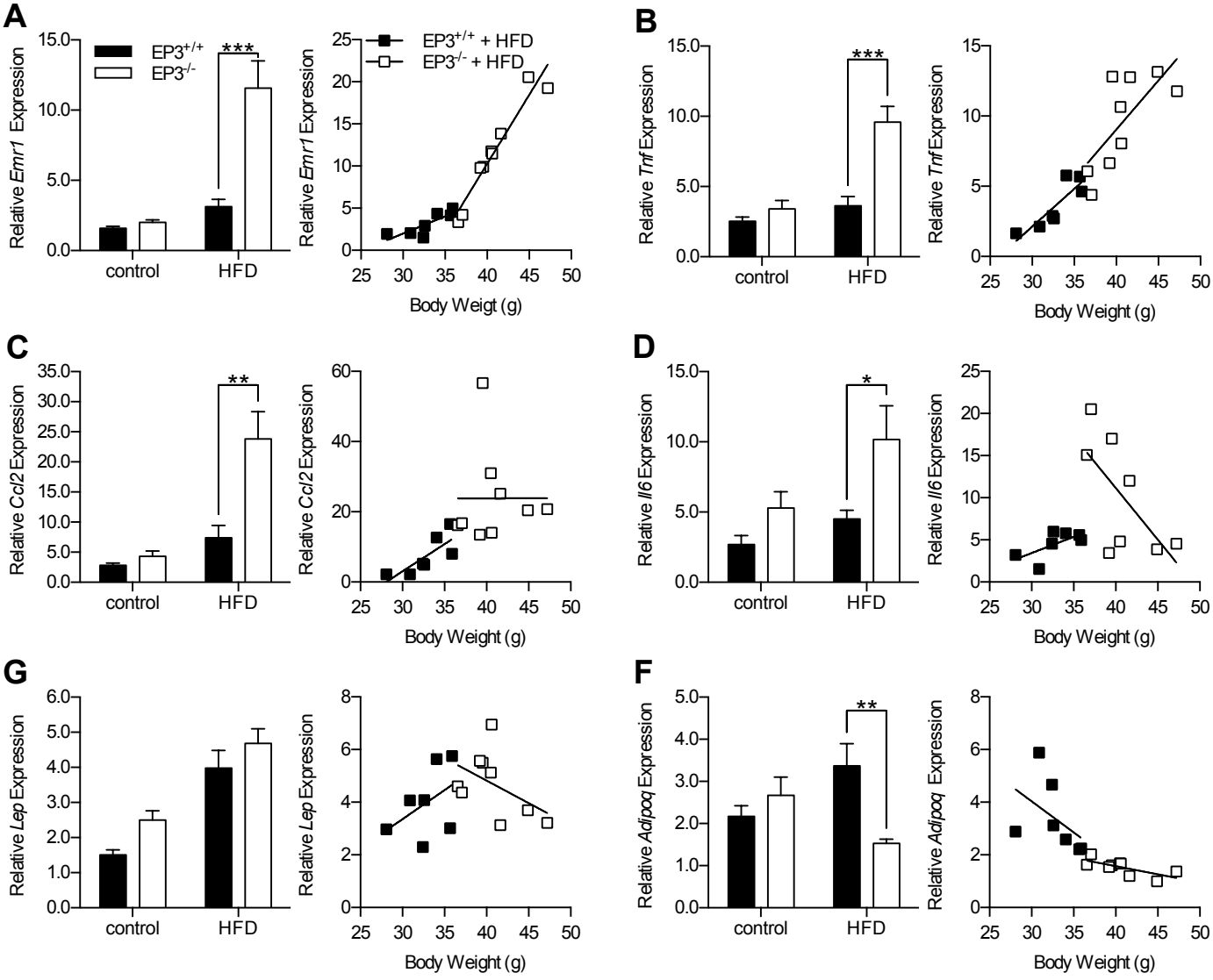
A
Relative Emr1 Expression
EP3+/+
EP3-/-
***
control
HFD
EP3+/+ + HFD
EP3-/- + HFD
Body Weigt (g)
B
Relative Tnf Expression
Body Weight (g)
C
Relative Ccl2 Expression
**
Body Weight (g)
D
Relative Il6 Expression
*
Body Weight (g)
G
Relative Lep Expression
Body Weight (g)
F
Relative Adipoq Expression
**
Body Weight (g)

Figure 19. EP3$^{-/-}$ HFD fed mice have increased expression of inflammation associated adipokines

hormone receptor-like 1, *Emr1*), was assessed by qPCR. HFD feeding increased F4/80 expression ($P < 0.0001$). F4/80 gene expression was increased in EP3$^{-/-}$ mice ($P = 0.0003$). An interaction between dietary fat and EP3 genotype increased F4/80 gene expression ($P = 0.0008$). F4/80 gene expression was plotted as a function of body weight. The relationship between F4/80 gene expression and body weight are significantly different in EP3$^{-/-}$ mice ($P = 0.0003$). **B.** Tumor necrosis factor α (*Tnf*) gene expression was increased in EP3$^{-/-}$ mice ($P < 0.0001$). HFD feeding increased *Tnf* expression ($P < 0.0001$) and interacted synergistically with EP3 genotype ($P = 0.0023$). *Tnf* gene expression was plotted as a function of body weight. The relationships between *Tnf* gene expression and body weight are not different in HFD fed mice ($P = 0.664$). **C.** Monocyte chemotactic protein 1 (MCP-1) gene (*Ccl2*) expression was measured by qPCR. HFD feeding increased MCP-1 expression ($P < 0.0001$). F4/80 gene expression was increased in EP3$^{-/-}$ mice ($P = 0.0019$). An interaction between dietary fat and EP3 genotype increased MCP-1 gene expression ($P = 0.0077$). MCP-1 gene expression was plotted as a function of body weight. The relationships between MCP-1 gene expression and body weight are not different in HFD fed mice ($P = 0.464$). **D.** Interleukin 6 (*Il6*) gene expression was increased in EP3$^{-/-}$ mice ($P = 0.0095$). HFD feeding increased *Il6* expression ($P = 0.0312$). EP3 genotype and dietary fat were not fount to interact synergistically to affect *Il6* expression ($P = 0.312$). *Il6* gene expression was plotted as a function of body weight. The relationship between Il6 gene expression and body weight was not significantly different between EP3$^{+/+}$ and EP3$^{-/-}$ HFD fed mice ($P = 0.0559$). **E.** Leptin (*Lep*) gene expression was increased in EP3$^{-/-}$ mice ($P = 0.0212$) and by HFD feeding ($P < 0.0001$). EP3 genotype and dietary fat did not interact synergistically to affect *Lep* expression ($P = 0.688$). *Lep* gene expression was plotted as a function of body weight. The relationships between *Lep* gene expression and body weight are not different in HFD fed mice ($P = 0.103$). **F.** Adiponectin gene (*Adipoq*) expression was not significantly affected by EP3 genotype ($P = 0.0703$) or by HFD feeding ($P = 0.932$). However, an interaction between dietary fat and EP3 genotype decreased *Adipoq* expression ($P = 0.0027$). *Adipoq* gene expression was plotted as a function of body weight. The relationships between *Adipoq* gene expression and body weight are not different in HFD fed mice ($P = 0.294$). N = 8 EP3$^{+/+}$ control, 10 EP3$^{-/-}$ control, 7 EP3$^{+/+}$ HFD, 9 EP3$^{-/-}$ HFD. For all figures values are expressed as mean ± SEM.

of adiponectin was blunted (Figure 19F). $EP3^{-/-}$ HFD fed mice have greater amounts of adipose tissue (Figure 12B,D), which in conjunction with the decreased adiponectin gene expression, was manifest by similar plasma levels of adiponectin in the HFD fed $EP3^{+/+}$ and $EP3^{-/-}$ mice (Table 4).

$EP3^{-/-}$ adipocytes have increased lipolysis

PGs play an important role in lipolysis (390,401,446), which may also affect adipocyte cell size and epididymal fat pad mass. Adipocytes were isolated from $EP3^{+/+}$ and $EP3^{-/-}$ mice and isoproterenol stimulated lipolysis was assessed (Figure 20). Isoproterenol stimulated lipolysis regardless of genotype. PGE_2 inhibited lipolysis in adipocytes isolated from $EP3^{+/+}$ mice but failed to inhibit lipolysis in adipocytes isolated from $EP3^{-/-}$ mice or treated with the EP3 antagonist, DG-041. Insulin inhibited lipolysis in both $EP3^{+/+}$ and $EP3^{-/-}$ adipocytes indicating that a loss of EP3 does not affect insulin signaling and regulation of lipolysis. We also quantified the PGs in the adipose tissue. We found no significant effect of EP3 genotype or dietary fat on the levels of any of the PGs examined, suggesting that changes in EP3 ligand concentration were not responsible for the observed phenotype (Table 3). Consistent with these data, the expression of the inducible COX-2 gene, *Ptgs2*, was also unaffected by dietary fat or EP3 genotype (Figure 16B). EP3 receptor expression was also unchanged as the expression of *Ptger3* in epididymal fat pads was not affected by HFD feeding (Figure 16A). Taken together, these data are consistent with defects in lipolysis regulation by PGE_2 and lipid storage in $EP3^{-/-}$ adipocytes by loss of the receptor despite the presence of the cognate ligand.

Because a defect in lipolysis regulation is expected to alter the lipids in the circulatory system, plasma lipids were measured (Table 4). HFD feeding increased plasma triglycerides of

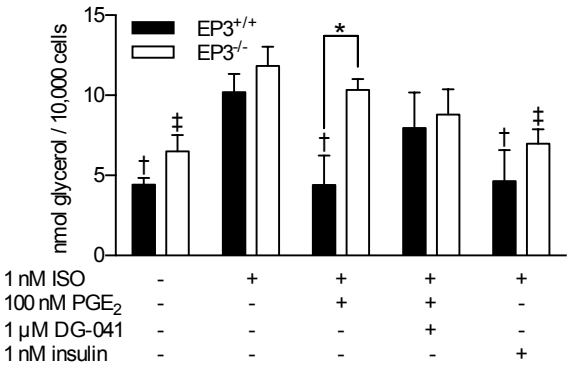

Figure 20. PGE_2 inhibits adipocyte lipolysis through the EP3 receptor
Isoproterenol (ISO) stimulated lipolysis in $EP3^{+/+}$ and $EP3^{-/-}$ adipocytes. PGE_2 inhibited lipolysis in $EP3^{+/+}$ adipocytes but had no effect in $EP3^{-/-}$ adipocytes. In $EP3^{+/+}$ adipocytes treated with the EP3 antagonist, DG-041, PGE_2 was unable to inhibit lipolysis. Insulin inhibited lipolysis in both $EP3^{+/+}$ and $EP3^{-/-}$ adipocytes. All statistics are from unpaired t-tests. † = $P < 0.05$ vs. $EP3^{+/+}$ + ISO, ‡ = $P < 0.05$ vs. $EP3^{-/-}$ + ISO. For each group N=3-4. Values are expressed as mean ± SEM.

Parameter	Wild Type - control		Wild Type - HFD		$EP3^{-/-}$ - control		$EP3^{-/-}$ -HFD		ANOVA p-value		
(*ng/g*)	mean	SEM	mean	SEM	mean	SEM	mean	SEM	Genotype	Diet	Interaction
Number	9		7		10		8				
PGE_2	1.74	0.39	3.84	2.23	2.75	1.12	3.78	1.85	0.747	0.288	0.713
PGD_2	0.60	0.14	1.09	0.37	0.87	0.20	1.72	0.89	0.355	0.177	0.715
$PGF_{2\alpha}$	3.20	0.70	2.08	0.57	3.05	0.70	2.63	0.90	0.792	0.309	0.638
6-Keto$PGF_{1\alpha}$	1.69	0.56	1.73	0.37	2.53	0.64	2.92	0.66	0.101	0.720	0.768
TxB_2	0.89	0.20	0.65	0.19	1.02	0.23	0.62	0.18	0.799	0.124	0.685

Table 3. Prostanoids in epididymal fat pads
Neither dietary fat nor EP3 genotype affected prostaglandin content of epididymal fat pads.

Parameter	Wild Type + control			Wild Type + HFD			EP3$^{-/-}$ + control			EP3$^{-/-}$ + HFD			ANOVA p-value		
	mean	SEM	N	mean	SEM	N	mean	SEM	N	mean	SEM	N	Genotype	Diet	Interaction
Glucose (*mg/dl*)	154.0	6.2	9	181.1*	17.0	7	156.9	8.8	10	143.6*	7.5	9	0.089	0.491	0.049
Insulin (*ng/ml*)	1.50	0.42	9	2.20***	0.24	7	1.44	0.36	10	7.56***	1.33	9	0.002	< 0.0001	0.001
C-peptide (*ng/ml*)	1.39	0.38	3	1.68	0.34	3	1.47	0.21	3	2.32	0.29	3	0.284	0.103	0.391
Leptin (*ng/ml*)	2.09	0.84	3	17.21**	0.90	3	6.74	3.41	3	37.26**	4.39	3	0.003	< 0.0001	0.027
Adiponectin (*µg/ml*)	10.59	0.73	4	14.04	1.49	4	9.70	0.60	4	14.21	1.20	4	0.742	0.003	0.626
ALT (*U/L*)	24.7	3.4	3	110.3	35.5	4	20.5	9.1	4	91.0	51.5	4	0.740	0.044	0.830
Glycerol (*µM*)	52.7	8.1	7	84.4	20.8	6	72.7	15.7	6	86.8	14.3	6	0.465	0.142	0.565
FFA (*mM*)	0.703	0.111	9	0.778	0.170	5	0.767	0.088	6	1.340	0.309	6	0.101	0.090	0.186
Triglyceride (*mg/dl*)	75.2	6.8	9	104.9	21.0	7	72.4	12.0	10	164.6	31.4	9	0.163	0.005	0.126

* Bonferroni post-hoc comparison to * in same row P<0.05
** Bonferroni post-hoc comparison to ** in same row P<0.01
*** Bonferroni post-hoc comparison to *** in same row P<0.001
Statistically significant values are highlighted

Table 4. Plasma profiles of EP3$^{-/-}$ mice during *ad libitum* feeding

Blood glucose and plasma insulin were obtained from mice via saphenous vein blood draw. C-peptide, leptin, adiponectin, glycerol, alanine aminotransferase (ALT), free fatty acid (FFA), and triglyceride were measured in plasma obtained via cardiac puncture post mortem.

both genotypes when measured during an *ad libitum* fed state. $EP3^{-/-}$ mice fed HFD displayed a trend toward increased plasma triglycerides and FFA when compared to $EP3^{+/+}$ mice fed HFD, though neither achieved statistical significance. Plasma free glycerol was unchanged by either dietary fat or EP3 genotype.

$EP3^{-/-}$ mice have increased ectopic lipid accumulation

We hypothesized that increased lipolysis and resulting defects in fat pad storage in $EP3^{-/-}$ mice fed HFD, would result in ectopic lipid storage in peripheral tissues. Liver weight was increased in $EP3^{-/-}$ mice when fed HFD, but not control diet (Figure 21A). The increased slope of liver weight versus body weight observed for $EP3^{-/-}$ mice fed HFD as compared to $EP3^{+/+}$ mice fed HFD (Figure 21B) is consistent with increased ectopic lipid accumulation in HFD fed $EP3^{-/-}$. Hepatic triglyceride levels were increased in $EP3^{-/-}$ mice fed HFD as compared to $EP3^{+/+}$ mice fed HFD, with no observed difference between genotypes when fed control diet (Figure 21C). Similarly an increased accumulation of triglycerides was observed in skeletal muscle from $EP3^{-/-}$ mice fed HFD compared to $EP3^{+/+}$ mice with no difference observed between genotypes fed control diet (Figure 21D). Dietary lipid and EP3 genotype affected the fatty acid composition of hepatic and muscle triglycerides (Tables 5 and 6 respectively). HFD fed $EP3^{-/-}$ mice with smaller epididymal fat pads demonstrated increased hepatic triglycerides indicative of lipid redistribution (Figure 21E). This effect was not seen in $EP3^{+/+}$ mice. Triglycerides in skeletal muscle did not vary with respect to epididymal fat pad mass in either genotype (Figure 21F).

We expected that lipid redistribution to the liver and subsequent hepatic lipidosis would cause liver damage. We examined the livers histologically using H&E (Figure 21G), and Oil red O (ORO) staining (Figure 21H). Livers from $EP3^{-/-}$ mice fed HFD showed markedly increased levels of steatosis and ORO staining. Steatosis in $EP3^{+/+}$ mice fed HFD was present but not as

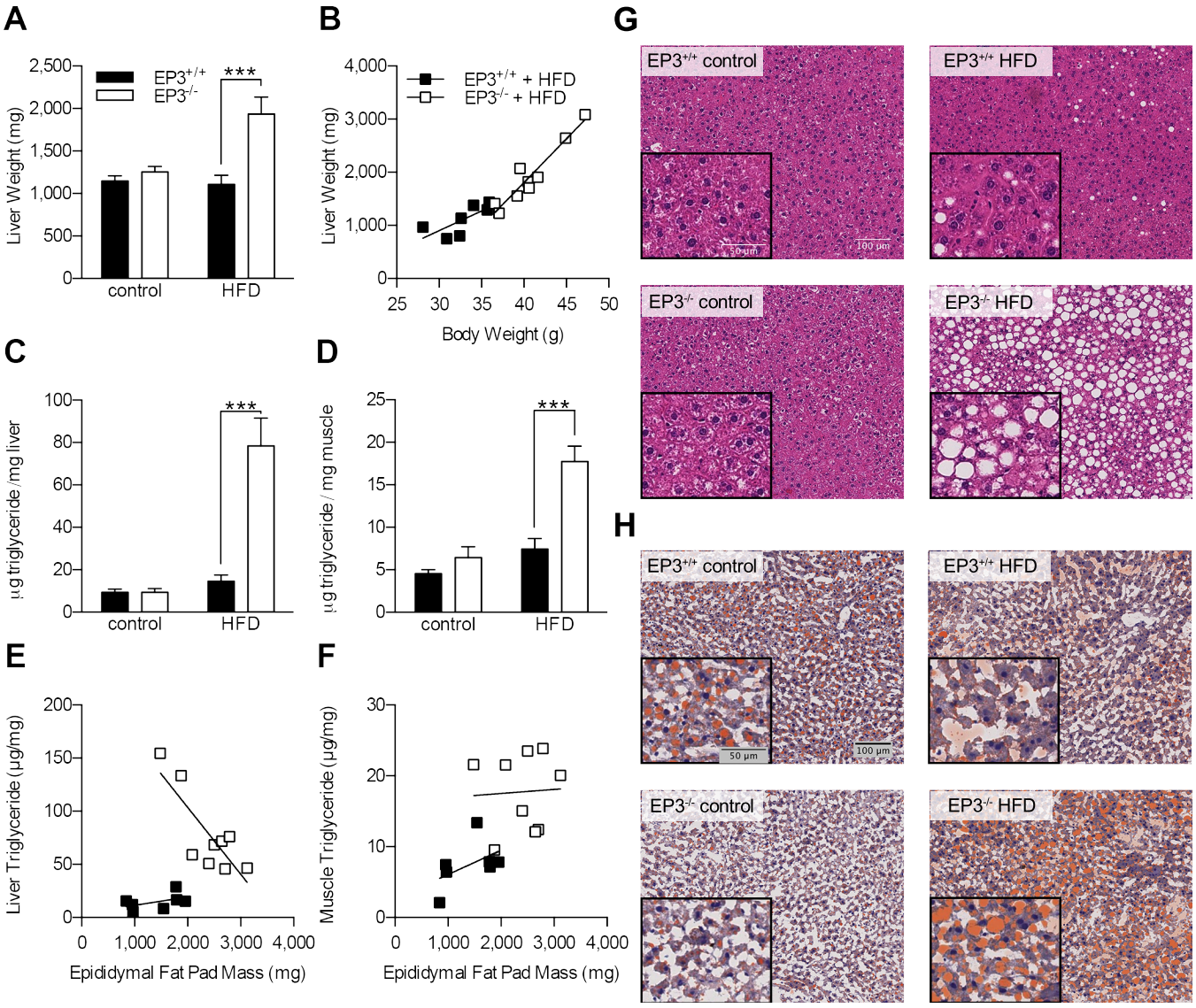
A
Liver Weight (mg)
2,500
2,000
1,500
1,000
500
0
EP3+/+
EP3-/-
***
control
HFD
B
Liver Weight (mg)
4,000
3,000
2,000
1,000
0
EP3+/+ + HFD
EP3-/- + HFD
25 30 35 40 45 50
Body Weight (g)
C
µg triglyceride /mg liver
100
80
60
40
20
0
***
control
HFD
D
µg triglyceride / mg muscle
25
20
15
10
5
0
***
control
HFD
E
Liver Triglyceride (µg/mg)
200
150
100
50
0
0 1,000 2,000 3,000 4,000
Epididymal Fat Pad Mass (mg)
F
Muscle Triglyceride (µg/mg)
30
20
10
0
0 1,000 2,000 3,000 4,000
Epididymal Fat Pad Mass (mg)
G
EP3+/+ control
EP3+/+ HFD
EP3-/- control
EP3-/- HFD
50 µm
100 µm
H
EP3+/+ control
EP3+/+ HFD
EP3-/- control
EP3-/- HFD
50 µm
100 µm

Figure 21. $EP3^{-/-}$ mice on HFD develop ectopic lipid accumulation
A. $EP3^{-/-}$ mice on HFD had increased liver weight (P = 0.0056). **B.** Liver weight to body weight ratio was higher in $EP3^{-/-}$ mice than $EP3^{+/+}$ (P = 0.0257). **C.** $EP3^{-/-}$ mice on HFD had a higher triglyceride to hepatic tissue ratio, which resulted in increased hepatic triglycerides (P < 0.0001). **D.** $EP3^{-/-}$ mice on HFD had a higher triglyceride to skeletal muscle tissue ratio, which resulted in increased muscle triglycerides (P = 0.0035). **E.** The relationship between hepatic triglyceride concentration to epididymal fat pad mass differs between $EP3^{+/+}$ and $EP3^{-/-}$ mice when fed HFD (P = 0.0059). **F.** The slope of skeletal muscle triglyceride concentration to epididymal fat pad mass is not different between $EP3^{+/+}$ and $EP3^{-/-}$ mice fed HFD (P = 0.612); however, the Y-intercept is changed (P = 0.0297). For A-F, N = 9 $EP3^{+/+}$ control, 10 $EP3^{-/-}$ control, 7 $EP3^{+/+}$ HFD, 9 $EP3^{-/-}$ HFD. Values are expressed as mean ± SEM. **G.** H&E staining of livers showed that $EP3^{-/-}$ mice fed HFD had increased steatosis. **H.** Oil Red O staining showed increased lipid staining in livers of $EP3^{-/-}$ mice fed HFD. All panels have the same magnification as upper left panel. Images are a representative sample from 3 mice per genotype × diet group, 2 sections per mouse.

Parameter	Wild Type - control		Wild Type - HFD		EP3$^{-/-}$ - control		EP3$^{-/-}$ - HFD		ANOVA p-value		
	mean	SEM	mean	SEM	mean	SEM	mean	SEM	Genotype	Diet	Interaction
g/100 g fatty acids											
14:0	0.76	0.11	0.37	0.13	0.78	0.13	0.68	0.02	0.145	0.032	0.203
16:0	26.00	1.18	26.09*	1.18	27.06	0.46	29.47*	0.41	0.013	0.147	0.179
16:1	6.16	0.37	1.99***	0.43	5.90	0.15	3.86***	0.12	0.007	< 0.001	0.001
17:0	0.00	0.00	0.00	0.00	0.00	0.00	0.00	0.00	NA	NA	NA
18:0	2.45	0.27	2.77**	0.26	2.58	0.27	1.71**	0.05	0.056	0.241	0.016
18:1ω9	44.74	1.08	35.48***	0.59	46.46	0.71	41.18***	0.86	< 0.001	< 0.001	0.027
18:1ω7	7.58	0.66	2.03	0.16	6.92	0.39	3.11	0.19	0.621	< 0.001	0.051
18:2	9.90	1.21	22.57***	1.24	8.68	0.62	14.53***	0.73	< 0.001	< 0.001	0.001
18:3ω6	0.00	0.00	0.36	0.13	0.02	0.02	0.37	0.03	0.785	< 0.001	0.991
18:3ω3	0.21	0.09	0.40	0.14	0.13	0.06	0.44	0.03	0.788	0.005	0.465
20:3ω6	0.34	0.14	1.12	0.22	0.16	0.07	0.88	0.04	0.098	< 0.001	0.783
20:4	0.96	0.29	2.81**	0.21	0.87	0.27	1.58**	0.13	0.010	< 0.001	0.025
20:5	0.00	0.00	0.00***	0.00	0.00	0.00	0.12***	0.03	0.002	0.002	0.002
22:4ω6	0.08	0.06	0.72	0.22	0.03	0.03	0.54	0.03	0.218	< 0.001	0.520
22:5ω6	0.13	0.08	0.66*	0.29	0.00	0.00	0.18*	0.04	0.020	0.007	0.158
22:5ω3	0.00	0.00	0.30	0.11	0.00	0.00	0.35	0.03	0.562	< 0.001	0.562
22:6	0.69	0.25	2.34***	0.29	0.40	0.14	0.99***	0.11	< 0.001	< 0.001	0.013
Ratio											
16:0/16:1	4.29	0.25	11.96***	1.12	4.60	0.09	7.67***	0.21	< 0.001	< 0.001	< 0.001
18:0/18:1	0.05	0.01	0.07***	0.01	0.05	0.01	0.04***	0.00	0.004	0.170	0.003
Saturated / Unsaturated†	0.42	0.02	0.42	0.02	0.44	0.01	0.47	0.01	0.031	0.378	0.362

†(14:0+16:0+17:0+18:0) / (16:1+18:1ω9+18:1ω7+18:2+18:3ω6+18:3ω3+20:3ω6+20:4+20:5+22:4ω6+22:5ω6+22:5ω3+22:6)
* Bonferroni post-hoc comparison to * in same row P<0.05
** Bonferroni post-hoc comparison to ** in same row P<0.01
*** Bonferroni post-hoc comparison to *** in same row P<0.001
Statistically significant values are highlighted

Table 5. Fatty acid composition of hepatic triglycerides

Fatty acid composition of hepatic triglycerides from male EP3$^{+/+}$ and EP3$^{-/-}$ mice, fed either HFD or control diet. N = 9 EP3$^{+/+}$ control, 10 EP3$^{-/-}$ control, 7 EP3$^{+/+}$ HFD, 9 EP3$^{-/-}$ HFD.

Parameter	Wild Type - control		Wild Type - HFD		EP3$^{-/-}$ - control		EP3$^{-/-}$ - HFD		ANOVA p-value		
	mean	SEM	mean	SEM	mean	SEM	mean	SEM	Genotype	Diet	Interaction
g/100 g fatty acids											
14:0	1.82	0.12	1.16	0.06	2.04	0.13	1.14	0.03	0.334	< 0.001	0.283
16:0	20.71	0.72	17.50*	0.52	21.55	0.91	20.08*	0.23	0.019	0.002	0.214
16:1	16.64	0.62	7.74	0.45	17.63	0.38	7.67	0.34	0.332	< 0.001	0.262
17:0	0.00	0.00	0.00	0.00	0.00	0.00	0.00	0.00	NA	NA	NA
18:0	1.64	0.14	2.35*	0.14	1.61	0.17	2.89*	0.13	0.101	< 0.001	0.071
18:1ω9	40.72	0.52	45.61**	0.50	39.55	0.50	42.92**	0.35	< 0.001	< 0.001	0.124
18:1ω7	3.97*	0.14	2.22	0.08	3.59*	0.13	1.93	0.06	0.006	< 0.001	0.720
18:2	13.58	0.41	22.04	0.41	12.98	0.51	21.37	0.34	0.158	< 0.001	0.934
18:3ω6	0.00	0.00	0.00	0.00	0.00	0.00	0.00	0.00	NA	NA	NA
18:3ω3	0.62	0.08	0.84	0.01	0.73	0.04	0.95	0.02	0.025	< 0.001	0.957
20:3ω6	0.00	0.00	0.06***	0.04	0.00	0.00	0.22***	0.01	< 0.001	< 0.001	< 0.001
20:4	0.30	0.08	0.40	0.07	0.28	0.08	0.54	0.01	0.411	0.009	0.245
20:5	0.00	0.00	0.00	0.00	0.00	0.00	0.00	0.00	NA	NA	NA
22:4ω6	0.00	0.00	0.02*	0.02	0.00	0.00	0.07*	0.02	0.051	0.003	0.051
22:5ω6	0.00	0.00	0.00	0.00	0.00	0.00	0.00	0.00	NA	NA	NA
22:5ω3	0.00	0.00	0.00	0.00	0.00	0.00	0.01	0.01	0.343	0.343	0.343
22:6	0.00	0.00	0.06***	0.04	0.04	0.03	0.20***	0.01	< 0.001	< 0.001	0.027
Ratio											
16:0/16:1	1.27	0.08	2.30	0.15	1.23	0.07	2.67	0.15	0.148	< 0.001	0.084
18:0/18:1	0.04	0.00	0.05*	0.00	0.04	0.00	0.06*	0.00	0.035	< 0.001	0.064
Saturated / Unsaturated†	0.32	0.02	0.27	0.01	0.34	0.02	0.32	0.01	0.033	0.024	0.321

†(14:0+16:0+17:0+18:0) / (16:1+18:1ω9+18:1ω7+18:2+18:3ω6+18:3ω3+20:3ω6+20:4+20:5+22:4ω6+22:5ω6+22:5ω3+22:6)
* Bonferroni post-hoc comparison to * in same row P<0.05
** Bonferroni post-hoc comparison to ** in same row P<0.01
*** Bonferroni post-hoc comparison to *** in same row P<0.001
Statistically significant values are highlighted

Table 6. Fatty acid composition of skeletal muscle triglycerides
Fatty acid composition of skeletal muscle triglycerides from male EP3$^{+/+}$ and EP3$^{-/-}$ mice, fed either HFD or control diet. N = 9 EP3$^{+/+}$ control, 10 EP3$^{-/-}$ control, 7 EP3$^{+/+}$ HFD, 9 EP3$^{-/-}$ HFD.

pronounced as in the $EP3^{-/-}$ counterparts. When fed control diet, neither genotype displayed hepatic steatosis. Macrophage infiltration of livers was assessed by counting F4/80 positive nuclei (Figure 22A,B) and by qPCR for F4/80 gene expression (Figure 22C). Macrophage infiltration of hepatic tissue was not altered by EP3 genotype or dietary fat. Though $EP3^{-/-}$ HFD fed livers appear markedly worse than $EP3^{+/+}$ HFD fed livers, mice from both genotypes showed elevated plasma alanine aminotransferase (Table 4), an enzymatic biomarker of hepatocyte membrane damage, indicating that HFD caused hepatocyte membrane damage in both genotypes though we did not observe fibrosis in the H&E stained sections in either genotype.

Livers from $EP3^{-/-}$ mice have modest changes in gene expression

Hepatosteatosis might also be precipitated by an increase in *de novo* lipid synthesis, decreased lipid secretion in the form of very-low-density lipoproteins (VLDL), and/or reduced β-oxidation of fatty acids. Genes affecting each of these processes were analyzed by qPCR. We found that $EP3^{-/-}$ mice have reduced carnitine palmitoyltransferase 1A (liver) (*Cpt1a*) expression regardless of diet, suggesting that a potential, small decrease in β-oxidation (Figure 23A). Fatty acid synthase (*Fasn*) was also not significantly affected by EP3 genotype (Figure 23B). Expression of genes involved in biosynthesis of VLDL was also investigated. Apolipoprotein B (*Apob*) was reduced in $EP3^{-/-}$ mice but microsomal triglyceride transfer protein (*Mttp*) was not significantly affected by EP3 genotype (Figures 23C,D).

$EP3^{-/-}$ mice are insulin resistant when fed a HFD

$EP3^{+/+}$ or $EP3^{-/-}$ mice had no differences in basal glucose, insulin levels or insulin resistance when fed a control diet (Table 4, Figure 24). When fed a HFD, fasted $EP3^{-/-}$ mice were hyperglycemic and had glucose levels comparable to what would be expected for $EP3^{+/+}$ mice of a similar body weight (Figure 24A). However, during the *ad libitum* fed state HFD fed $EP3^{-/-}$

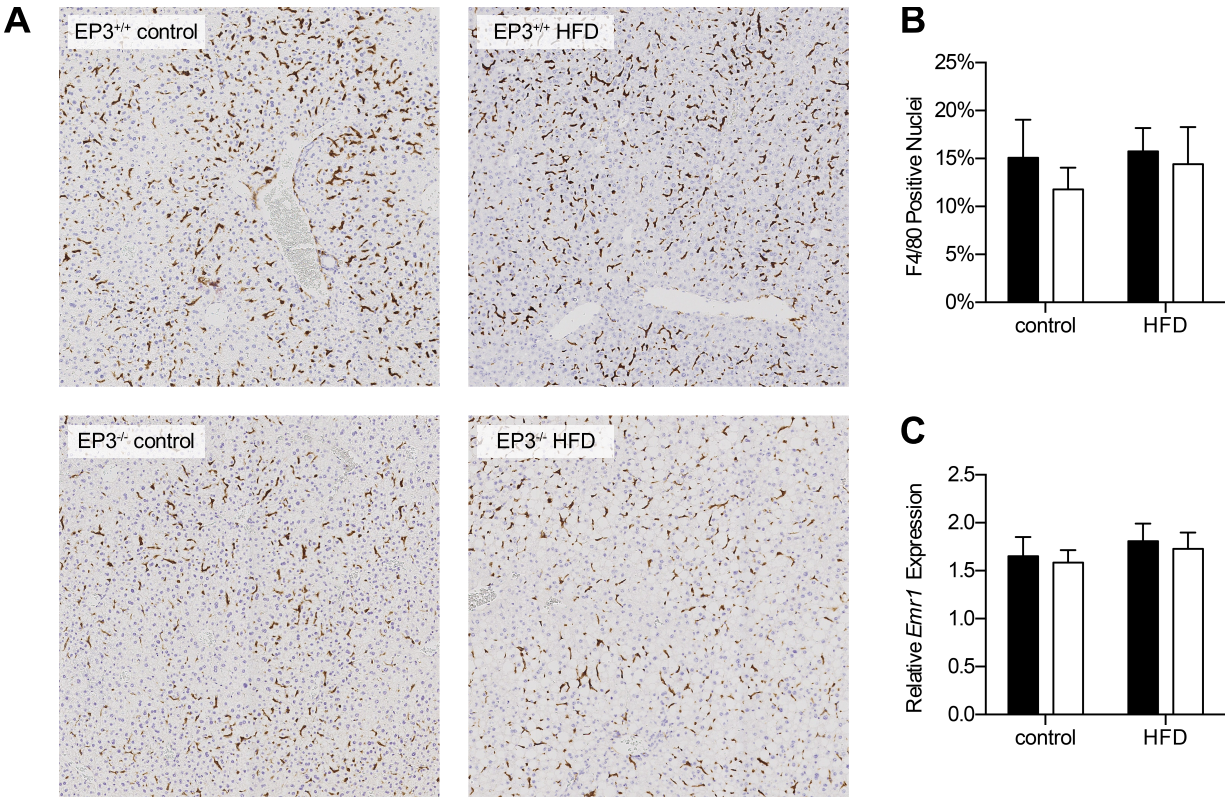

Figure 22. Macrophage infiltration is not changed in the liver of EP3$^{-/-}$ mice
Macrophage infiltration of tissues was assessed by immunohistochemical staining for the macrophage marker F4/80 and by quantitative real-time RT-PCR of its gene EGF-like module-containing mucin-like hormone receptor-like 1 (*Emr1*). **A.** Representative images of F4/80 staining in liver tissue. **B.** Neither HFD feeding nor EP3 genotype affected the percentage of F4/80 positive cells in liver tissue. **C.** *Emr1* gene expression in liver tissue was not affected by either EP3 genotype (P = 0.675) or HFD feeding (P = 0.381). Images are a representative sample from 3 mice per genotype × diet group. Values are expressed as mean ± SEM.

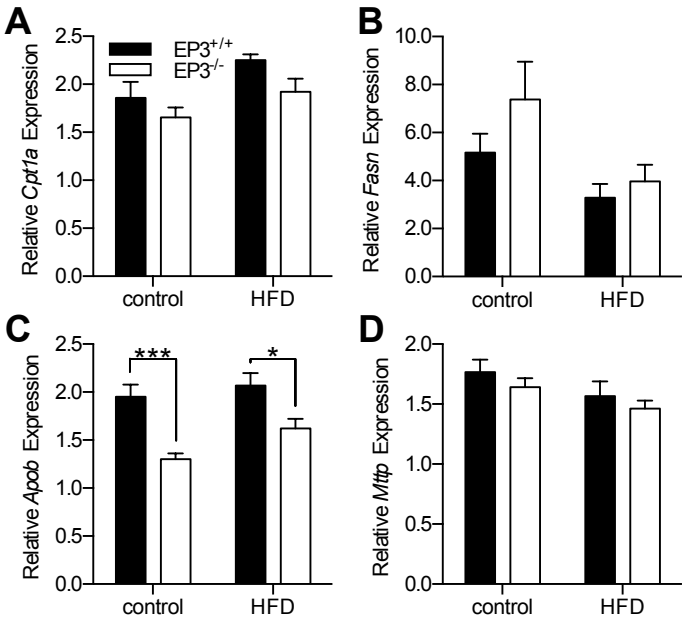

Figure 23. Decreased *Cpt1a* and *Apob* mRNA expression in EP3$^{-/-}$ liver
Quantitative real-time RT-PCR analysis of liver gene expression from 20 week old EP3$^{+/+}$ and EP3$^{-/-}$ mice fed control or HFD. **A.** Carnitine palmitoyltransferase 1A (liver) (*Cpt1a*) gene expression was reduced in EP3$^{-/-}$ mice (P = 0.0470). HFD feeding increased *Cpt1a* expression (P = 0.0154) but did not interact synergistically with EP3 genotype (P = 0.633). **B.** Fatty Acid Synthase (*Fasn*) gene expression was reduced by HFD feeding (P = 0.0209). EP3 genotype did not have a significant effect on *Fasn* expression (P = 0.195). **C.** Apolipoprotein B (*Apob*) gene expression was reduced in EP3$^{-/-}$ mice (P < 0.0001). HFD feeding increased *Apob* expression (P = 0.0475) but did not interact synergistically with EP3 genotype (P = 0.351). **D.** Microsomal triglyceride transfer protein (*Mttp*) gene expression was reduced by HFD feeding (P = 0.0446). EP3 genotype did not have a significant effect on *Mttp* expression (P = 0.216). For all figures N = 9 EP3$^{+/+}$ control, 10 EP3$^{-/-}$ control, 7 EP3$^{+/+}$ HFD, 9 EP3$^{-/-}$ HFD. Values are expressed as mean ± SEM.

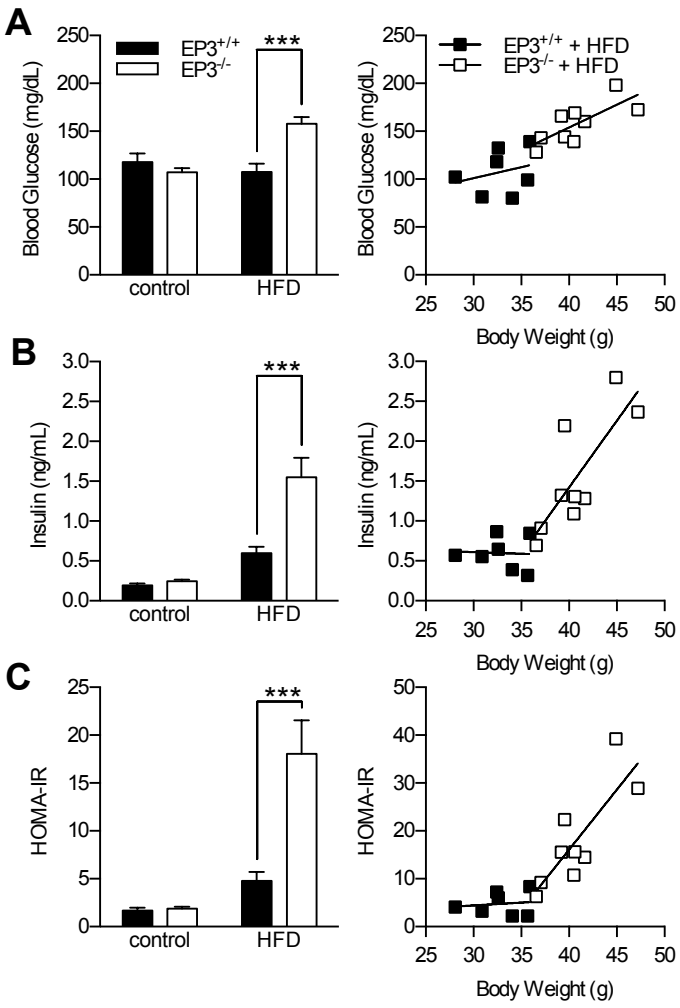

Figure 24. EP3$^{-/-}$ mice are hyperglycemic, hyperinsulinemic, and insulin resistant when fed a HFD

The effects of HFD and EP3 genotype on insulin resistance were assessed in 20 week old mice. **A.** An interaction between dietary fat and EP3 genotype increased fasting blood glucose (P = 0.0002). A similar correlation between body weight and fasting blood glucose was observed between the EP3$^{+/+}$ and EP3$^{-/-}$ genotypes for mice fed HFD (P = 0.497). **B.** HFD feeding increased 16-hour fasted plasma insulin (P < 0.0001). Fasting plasma insulin was increased in EP3$^{-/-}$ mice (P = 0.0005). An interaction between dietary fat and EP3 genotype increased fasting plasma insulin (P = 0.0016). The fasting plasma insulin to body weight ratio was greater in EP3$^{-/-}$ mice than EP3$^{+/+}$ (P = 0.0296). **C.** The homeostatic model assessment of insulin resistance (HOMA-IR), a function of fasting blood glucose and plasma insulin, was used to assess insulin resistance. HFD feeding increased the HOMA-IR (P < 0.0001). Insulin resistance was increased in EP3$^{-/-}$ mice (P = 0.0010). An interaction between dietary fat and EP3 genotype increased the HOMA-IR score (P = 0.0014). The HOMA-IR to body weight ratio was greater in EP3$^{-/-}$ mice than EP3$^{+/+}$ (P = 0.0464). For all figures N = 9 EP3$^{+/+}$ control, 10 EP3$^{-/-}$ control, 7 EP3$^{+/+}$ HFD, 9 EP3$^{-/-}$ HFD. Values are expressed as mean ± SEM.

mice had lower blood glucose (Table 4). $EP3^{-/-}$ HFD fed mice were hyperinsulinemic during both fed and fasted conditions (Table 4, Figure 24B); heavier $EP3^{-/-}$ mice had higher fasting insulin levels than would be expected of a $EP3^{+/+}$ mouse of a similar body weight, assuming a linear relationship between body weight and plasma insulin. Calculation of the homeostatic model assessment of insulin resistance (HOMA-IR) indicated that when fed a HFD, $EP3^{-/-}$ mice are more insulin resistant than $EP3^{+/+}$and that the heaviest $EP3^{-/-}$ mice were significantly more insulin resistant than would be expected of a $EP3^{+/+}$ mouse of a similar body weight, assuming a linear relationship between body weight and HOMA-IR (Figure 24C).

The intraperitoneal ITT is a standard measure of insulin resistance employed in rodents. ITT performed on $EP3^{-/-}$ HFD fed mice are consistent with insulin resistance in 20 week old animals (Figure 25B). However, these data are difficult to interpret for three reasons: 1) insulin has a half-life of 10 minutes while plasma glucose concentrations during the ITT were measured for 120 minutes 2) the dosing of insulin was based upon body weight, which is greater for $EP3^{-/-}$, instead of muscle mass, which was similar 3) fasting glucose concentrations were different in the $EP3^{-/-}$ HFD fed mice (579).

$EP3^{-/-}$ mice do not have capillary rarefaction

Capillary rarefaction, lessening of the density of capillaries, has been previously shown to cause insulin resistance in mice containing a muscle-specific deletion of the vascular endothelial growth factor (VEGF) (580). EP3 is known to be a positive regulator of VEGF and angiogenesis (571-573,581). Skeletal muscle capillary density was measured to determine if capillary rarefaction was present in $EP3^{-/-}$ mice potentially contributing to the insulin resistant phenotype of these mice when fed HFD (Figure 26). $EP3^{-/-}$ mice exhibited no differences in skeletal muscle capillary density regardless of dietary treatment.

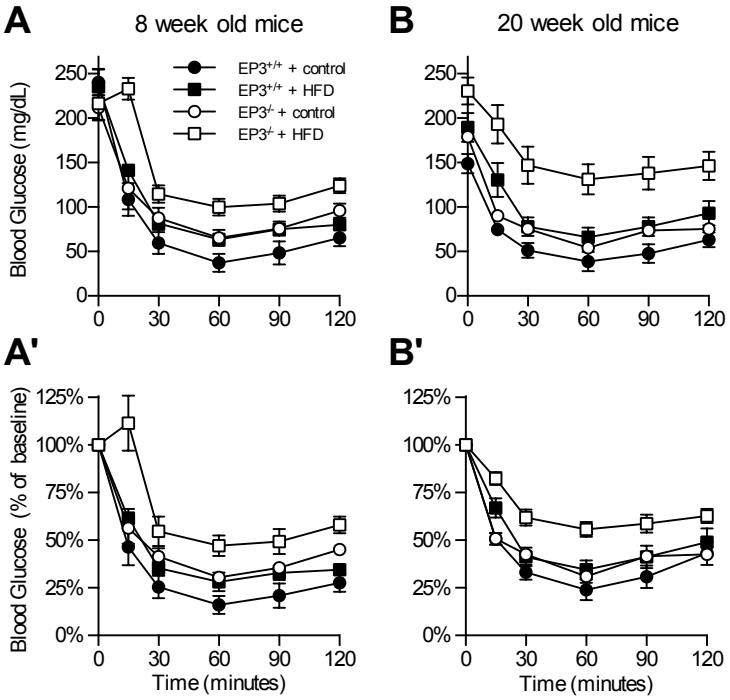

Figure 25. Insulin tolerance test of EP3$^{-/-}$ mice
Insulin tolerance was determined in male EP3$^{+/+}$ and EP3$^{-/-}$ mice, fed either HFD or control diet, **A.** at 8 weeks of age (N = 4 EP3$^{+/+}$ control, 5 EP3$^{-/-}$ control, 4 EP3$^{+/+}$ HFD, 4 EP3$^{-/-}$ HFD) and **B.** 20 weeks of age (N = 8 EP3$^{+/+}$ control, 10 EP3$^{-/-}$ control, 7 EP3$^{+/+}$ HFD, 9 EP3$^{-/-}$ HFD). Values are expressed as mean ± SEM.

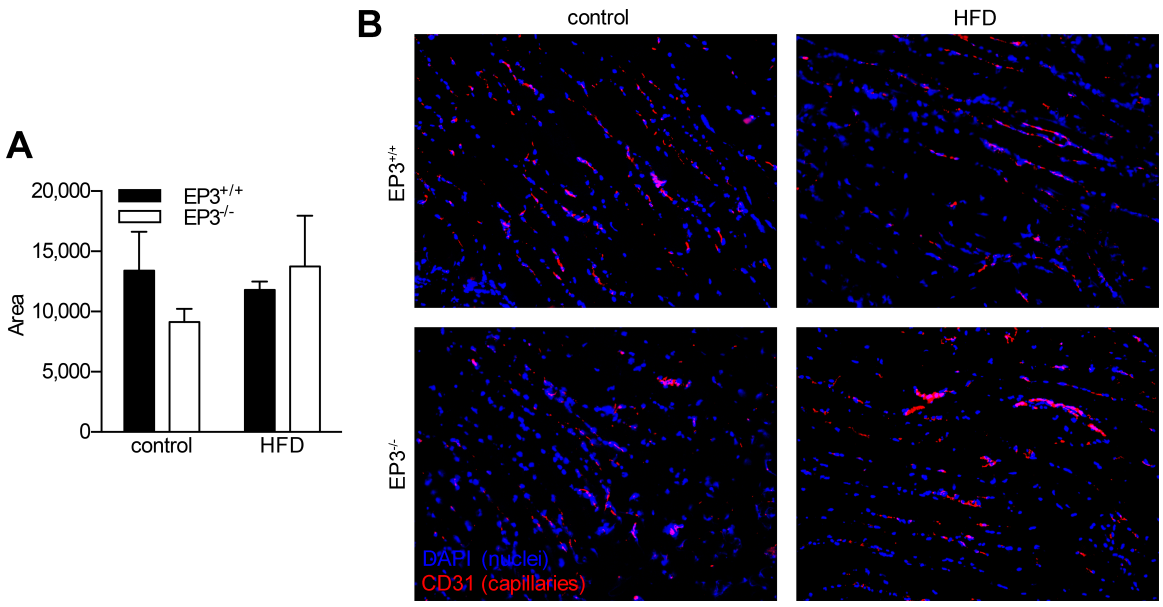

Figure 26. EP3$^{-/-}$ mice do not have differences in skeletal muscle capillary density
A. Capillary density in skeletal muscle was assessed by CD31 (PECAM) staining. Neither EP3 genotype (P = 0.675) nor HFD feeding (P = 0.598) affected capillary density. N = 3 mice per group. Values are expressed as mean ± SEM. **B.** Representative images of CD31 staining for each group.

EP3$^{-/-}$ mice are not glucose intolerant and do not have increased insulin secretion

An IP-GTT was used to assess glucose handling and *in vivo* insulin secretion. At eight weeks of age, having been on the control or HFD for four weeks, no difference in IP-GTT was observed between any of the groups (Figure 27A). When assessed at 20 weeks of age, HFD impaired glucose handling, although no effect of EP3 genotype was observed (Figure 27B). All groups of mice exhibited increased plasma insulin in response to glucose challenge during the IP-GTT (Figure 27C). When fed HFD, EP3$^{-/-}$ mice had elevated insulin levels compared to EP3$^{+/+}$. In contrast when fed a control diet, plasma insulin levels were unaffected by genotype. For mice fed HFD, the average peak insulin levels were found at 15 minutes post-glucose injection and were significantly higher for the EP3$^{-/-}$ (0.96±0.29 ng/mL, EP3$^{+/+}$ vs. 2.61±0.34 ng/mL, EP3$^{-/-}$). The change between peak and baseline fasting insulin was not significantly different between any groups. C-peptide levels were also not significantly changed in EP3$^{-/-}$ HFD fed mice when measured during *ad libitum* feeding (Table 4).

EP3 blockade reduces glucose stimulated insulin secretion in isles from HFD fed mice

Previous studies have shown that EP3 blockade improves insulin secretion in islets isolated from diabetic mice and humans (74). The effect of EP3 antagonist on GSIS in a separate cohort of EP3$^{+/+}$ mice fed control or HFD for seven weeks was investigated. At 9.5 weeks of age, mice fed HFD were heavier than mice fed control diet (Figure 28A). Fasted HFD fed mice were both hyperglycemic and hyperinsulinemic (Figure 28B,C). Calculation of the HOMA-IR indicated that mice from both genotypes are more insulin resistant after 7 weeks of HFD feeding (Figure 28D). Pancreatic islets isolated from these mice were assessed for alterations in GSIS by a static incubation insulin secretion assay. EP3 antagonist, DG-041, decreased GSIS in islets

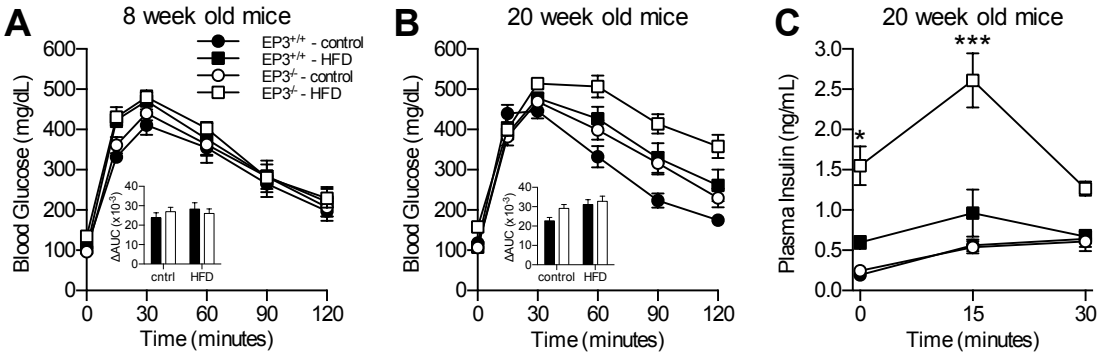

Figure 27. EP3$^{-/-}$ HFD fed mice have increased plasma insulin in response to glucose challenge

Glucose tolerance was assessed by an intraperitoneal glucose tolerance test (GTT) in male EP3$^{+/+}$ and EP3$^{-/-}$ mice, fed either HFD or control diet, **A.** at 8 weeks of age (N = 10 EP3$^{+/+}$ control, 11 EP3$^{-/-}$ control, 7 EP3$^{+/+}$ HFD, 9 EP3$^{-/-}$ HFD) and **B.** 20 weeks of age (N = 9 EP3$^{+/+}$ control, 10 EP3$^{-/-}$ control, 7 EP3$^{+/+}$ HFD, 9 EP3$^{-/-}$ HFD). HFD feeding worsened glucose homeostasis in 20 week old mice (P = 0.0112), but the effect of EP3 genotype was not significant (P = 0.0778). **C.** Insulin secretion during the GTT in 20 week old mice revealed that EP3$^{-/-}$ HFD fed mice have elevated plasma insulin in response to glucose challenge (P = 0.0002). The EP3 genotype had no effect on plasma insulin levels in mice fed control diets (P = 0.991). Data from B and C at time 0 are the same data that are show in 2A and 2B, respectively. For all figures N = 9 EP3$^{+/+}$ control, 10 EP3$^{-/-}$ control, 7 EP3$^{+/+}$ HFD, 9 EP3$^{-/-}$ HFD. Values are expressed as mean ± SEM.

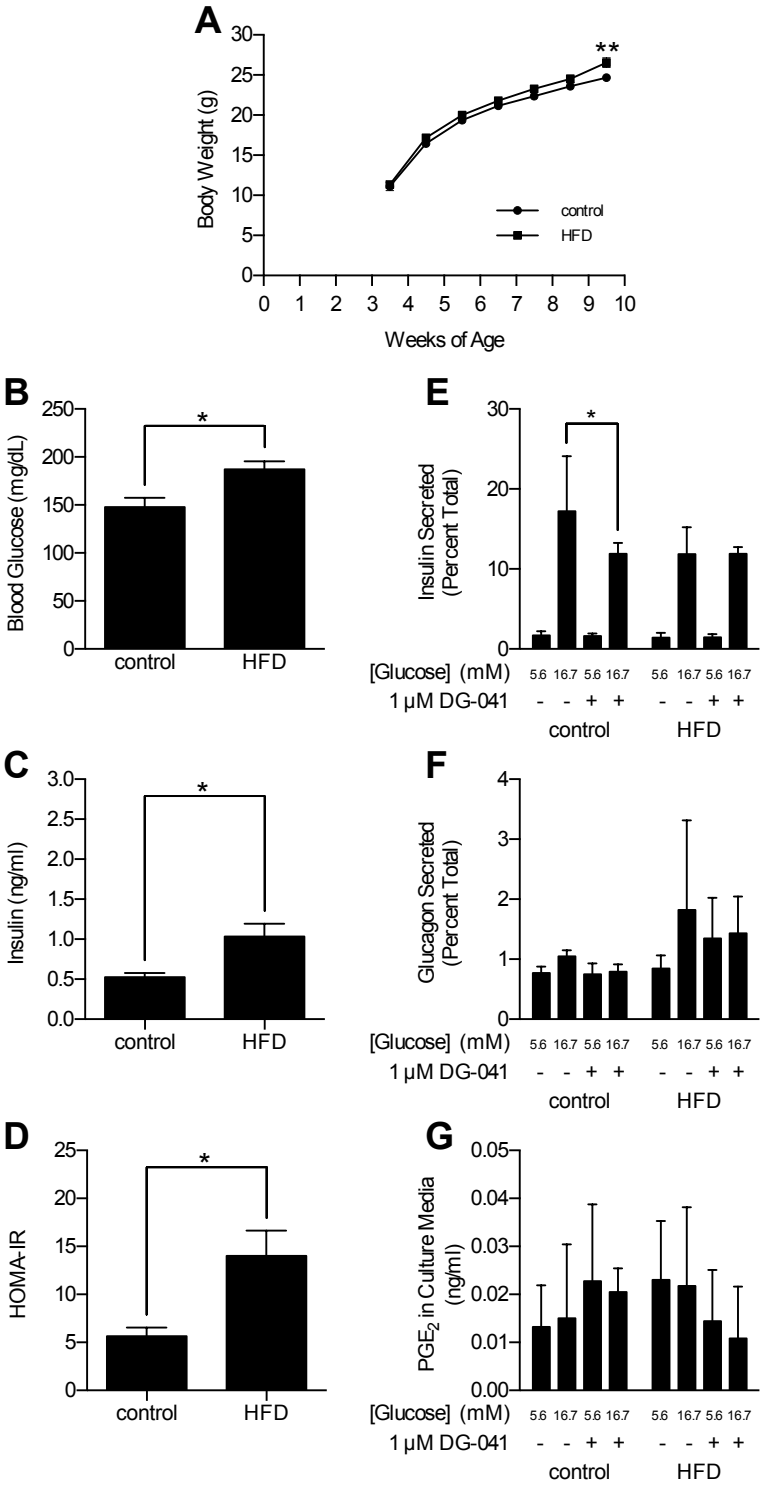
A
Body Weight (g)
Weeks of Age
control
HFD
**
B
Blood Glucose (mg/dL)
control
HFD
*
C
Insulin (ng/ml)
control
HFD
*
D
HOMA-IR
control
HFD
*
E
Insulin Secreted (Percent Total)
[Glucose] (mM)
5.6 16.7 5.6 16.7 5.6 16.7 5.6 16.7
1 μM DG-041
- - + + - - + +
control
HFD
*
F
Glucagon Secreted (Percent Total)
[Glucose] (mM)
5.6 16.7 5.6 16.7 5.6 16.7 5.6 16.7
1 μM DG-041
- - + + - - + +
control
HFD
G
PGE2 in Culture Media (ng/ml)
[Glucose] (mM)
5.6 16.7 5.6 16.7 5.6 16.7 5.6 16.7
1 μM DG-041
- - + + - - + +
control
HFD

Figure 28. EP3 antagonist reduces glucose stimulated insulin secretion in mice fed control diet

A separate cohort of $EP3^{+/+}$ mice was fed control or HFD from 3.5 to 10.5 weeks of age. **A.** Mice fed HFD showed a trend toward increased body weight throughout the study ($P = 0.056$) and were significantly heavier at 9.5 weeks of age ($P = 0.0053$). N = 6 each group. At 10 weeks of age, 6-hour fasting **B.** blood glucose and **C.** plasma insulin were found to be elevated in mice fed HFD ($P = 0.0118$ and $P = 0.0141$, respectively). **D.** The HOMA-IR showed that mice fed HFD were insulin resistant ($P = 0.0133$). For A-C, statistical significance was determined by an unpaired t-test. **E.** Static incubation insulin secretion from islets from these mice revealed that EP3 antagonist DG-041 reduced GSIS in islets from mice fed control diet ($P < 0.05$). **F.** HFD feeding increased glucagon secretion from these islets ($P = 0.0182$). **G.** PGE_2 measured in the culture media following the static incubation assay was not found to be different with respect to diet or genotype. For E-G, statistical significance was determined by a series of 2-way ANOVAs comparing diet and [glucose] keeping drug constant or comparing diet and drug keeping [glucose] constant. For B-G, N = 5 mice for each diet. Values are expressed as mean ± SEM.

isolated from control diet fed mice but had no effect on islets isolated from mice fed HFD (Figure 28E). The islets from control diet fed mice without DG-041 treatment demonstrated more GSIS than islets from HFD fed mice. Because these results are in direct contrast with prior studies (74), glucagon and PGE_2 release from these islets was measured. Glucose concentrations and DG-041 treatment did not affect glucagon secretion; however, islets from HFD fed mice had higher glucagon release (Figure 28F). The amount of PGE_2 in the media at the end of the experiment was unaffected by the animals' diet, glucose concentration, or DG-041 treatment (Figure 28G).

$EP3^{-/-}$ mice have lower blood pressure

Blood pressure in $EP3^{-/-}$ mice fed control and HFD was measured because it is a component of metabolic syndrome (582). $EP3^{-/-}$ mice were found to have lower systolic blood pressure regardless of dietary treatment (Figure 29).

Discussion

In the present studies, we found that $EP3^{-/-}$ mice when faced with a nutritional challenge are prone to obesity and dysregulation of adipocyte function. These findings show a novel interaction between EP3 genotype and dietary fat content. The effects of EP3 gene deletion are pleiotropic with changes observed in activity, body mass, inflammation and adipocyte function. We demonstrate here that the obesity phenotype is not penetrant when $EP3^{-/-}$ mice are maintained on either normal chow diet or on control diet; however, $EP3^{-/-}$ mice fed a HFD become more obese. These findings are consistent with previous studies that $EP3^{-/-}$ mice are obese, hyperleptinemic, insulin resistant and have impaired glucose homeostasis when fed breeder chow (102). $EP3^{-/-}$ mice were not hyperphagic but did show a significant reduction in activity, which may contribute to the increased body mass of these mice. This is significantly

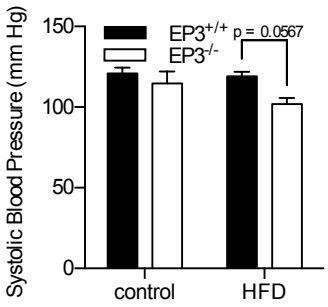

Figure 29. Decreased blood pressure in EP3$^{-/-}$ mice
Blood pressure was measured in 20 week old mice after 16 weeks of control or HFD feeding. EP3$^{-/-}$ mice had lower blood pressure (effect of genotype: P = 0.0400). N = 3 EP3$^{+/+}$ control, 4 EP3$^{-/-}$ control, 4 EP3$^{+/+}$ HFD, 4 EP3$^{-/-}$ HFD. Values are expressed as mean ± SEM.

different from previous studies, which showed a very modest increase in food intake and an increase in activity (102). Moreover those studies showed an increase in activity in the light cycle, whereas we observed no changes in activity in the light cycle, but a decrease in activity in the dark cycle. These observed differences may be due to differences in experimental conditions such as the diet (breeder chow vs. HFD) or the methodology used to collect the activity data (surgical radiotelemetry implantation vs. non-invasive "beambreak"). In any event, we do not observe an increase in food consumption to account for the obesity, and we do observe decreases in activity consistent with the obesity phenotype observed.

The $EP3^{-/-}$ mice demonstrate ectopic lipid accumulation and insulin resistance similar to the phenotype of $AdPLA^{-/-}$ mice, which lack PGE_2 – EP3 signaling in adipose tissue (101). Importantly, the phenotype of $EP3^{-/-}$ mice differs from that of $AdPLA^{-/-}$ mice in that $EP3^{-/-}$ mice are obese and have more adipose tissue whereas $AdPLA^{-/-}$ mice are lean. This suggests that the increased obesity and overall adiposity in $EP3^{-/-}$ HFD fed mice are due to a lack of EP3 signaling in non-adipose sites of action (e.g. central nervous system), in contrast to $AdPLA^{-/-}$ mice, which presumably have reduced EP3 signaling only in adipose tissue. It is our hypothesis that deletion of the EP3 receptor in a number of tissues contributes to the overall increased obesity, fat mass, and adipocyte size; changes in the adipose tissue of $EP3^{-/-}$ mice, including increased inflammation, cell death, and lipolysis, contribute to the proportional decrease of epididymal fat pad mass and adipocyte size and the increased ectopic lipid accumulation. PGs have been shown to play an important role in adipocyte function (390). Norepinephrine signaling in adipose tissue increases intracellular cAMP and thereby activates PKA, which phosphorylates and activates HSL, the rate-limiting step in lipolysis (401,403-405). PGE_2 inhibits norepinephrine-stimulated lipolysis (92,393,411,412,417-419). Adipocytes from $EP3^{-/-}$ mice had a loss of PGE_2-evoked

inhibition of lipolysis similar to that observed in AdPLA$^{-/-}$ mice. Insulin is also a potent suppressor of lipolysis in adipose tissue. We did not observe a statistically significant difference in either plasma triglyceride or free fatty acid levels, even though HFD fed EP3$^{-/-}$ mice had elevated plasma insulin. The failure of the elevated insulin to suppress free fatty acid levels indicates that the adipose tissue from in HFD fed EP3$^{-/-}$ mice is insulin resistant. In addition, significant accumulation of triglycerides in liver and skeletal muscle were observed in these mice and are further indications of persistent, chronic dyslipidemia and adipocyte dysfunction. It is of interest that while we observed an increase in macrophage infiltration and inflammatory cytokine levels in adipose tissue of the EP3$^{-/-}$ mice, these changes were not observed in the fat pads of AdPLA$^{-/-}$ mice (101), suggesting that unrestrained lipolysis alone is sufficient to contribute to ectopic lipid accumulation.

Increased necrosis was observed in parallel with increased macrophage infiltration in epididymal fat pads of EP3$^{-/-}$ HFD fed mice. Adipocyte cell death and macrophage infiltration may also result in the release of lipids from adipocytes and may exacerbate ectopic triglyceride accumulation (583-585). Previous studies demonstrated that when wild type C57BL/6 mice are fed a 60% HFD adipocyte death in epididymal fat pads results in decreased adipocyte size, lighter epididymal fat pads, increased macrophage infiltration, increased liver mass and steatosis, and insulin resistance (584). This study noted a similar correlation to what we have observed; epididymal fat pad weight negatively correlated with body weight in the heaviest mice in the group. In addition, Strissel, et al. found that the mice with the lightest epididymal fat pads had increased liver weight suggesting lipid redistribution from the epididymal fat pads to ectopic tissues, which likely contributed to insulin resistance (584). Data presented here are consistent with this phenotype and suggest that the deletion of the EP3 receptor may exacerbate or

accelerate this adipose tissue remodeling and resultant ectopic lipid accumulation. Thus increased lipolysis coupled with increased adipocyte cell death in the heaviest mice, as evidenced by the disproportionately increased macrophage infiltration, accounts for the reduced epididymal fat pad mass and the severe increase in hepatic triglycerides in the heaviest $EP3^{-/-}$ mice.

Although we saw an increase in circulating insulin levels in the obese, insulin resistant $EP3^{-/-}$ mice, we did not observe a corresponding increase in GSIS in isolated pancreatic islets. This difference may be partly attributed to normalization of the GSIS to insulin content in perifusion studies, implying loss of EP3 did not alter intrinsic islet function. Because basal insulin and glucose levels were increased in obese $EP3^{-/-}$ mice the hyperglycemia combined with other factors such as increased β-cell mass and/or altered autonomic tone to the islet may have sustained insulin secretion. Alternatively, increased insulin resistance results in increased plasma insulin due to reduced insulin clearance by the liver. Obese $EP3^{-/-}$ mice were not glucose intolerant, thus the underlying hyperinsulinemia was critical in maintaining normal glucose tolerance despite concomitant insulin resistance.

It has long been appreciated that PGE_2 modulates GSIS and has been suggested that blockade of the EP3 receptor would improve insulin secretion (197). Studies have indicated that pharmacological blockade of the EP3 receptor in pancreatic islets improves GSIS (74,233). In our studies we found no evidence suggesting improved GSIS in either chow fed (Chapter II) or control and HFD fed animals. It should be noted that previous studies showing GSIS differences in human islets only observed differences in EP3 mediated GSIS in islets isolated from diabetic individuals; no differences in GSIS were observed upon antagonist treatment of islets from non-diabetic individuals (74).

In summary, the $EP3^{-/-}$ mice are sensitive to caloric overload and display increased obesity, lipolysis, and adipocyte cell death, which is accompanied by reallocation of lipid storage from fat to ectopic tissues, leading to hepatic lipidosis and insulin resistance. These phenotypes are not penetrant when mice are fed control or chow diets, which contain less dietary fat. These studies demonstrate that EP3 is an important player in adipose tissue physiology.

CHAPTER IV

THE PGE_2 EP3 RECEPTOR REGULATES DIET-INDUCED ADIPOSITY IN 36 WEEK OLD MALE MICE

Introduction

The prevalence of diabetes increases significantly with age and affects approximately 18-30% of the elderly population in the United States (586-590). Type 2 diabetes is the most prevalent form of diabetes and has the highest economic burden of $159.5 billion per year (9). Type 2 diabetes results from a reduction in both insulin sensitivity and β-cell function. Aging populations are characterized by both declining β-cell function and insulin sensitivity (591,592). This includes a decreased responsiveness of β-cells to changes in glucose concentrations (592). Understanding the mechanisms of insulin secretion by β-cells will provide therapeutic targets to pharmacologically regulate these, improving β-cell function and ameliorating Type 2 diabetes.

Treating diabetes in the elderly is challenging for a number of reasons. Oftentimes elderly patients suffer multiple conditions, hence polypharmacy is common (593). In addition, elderly patients frequently suffer from cognitive or physical disorders that limit the ability to manage their disease (594,595). Furthermore, clinical presentation and symptoms of diabetes can be altered by age making it difficult to diagnose diabetes in the elderly (594). Drugs which boost a patient's own glucose stimulated insulin secretion (GSIS), such as exendin-4, a glucagon like peptide-1 (GLP-1) receptor agonist, are particularly useful because they augment a patient's insulin secretion in response to blood glucose removing the need to tightly regulate meals and injections (594). Drugs with similar mechanisms of action would also benefit elderly diabetic patients, especially if they can be taken orally.

Many nonsteroidal anti-inflammatory drugs (NSAIDS), such as aspirin, have long been known to increase GSIS (50,57,58,105,106). Therapeutically beneficial concentrations cause

adverse side effects and investigations into these drugs as therapies for diabetes were abandoned (80). NSAIDS act by inhibiting cyclooxygenase (COX) enzymes. COX converts arachadonic acid to PGH_2, which is converted into five primary bioactive prostanoids: PGE_2, $PGF_{2\alpha}$, PGD_2, PGI_2 (prostacyclin), and TXA_2 (thromboxane). The local action of PGs depends on activation of a family of specific GPCRs designated EP for E-prostanoid receptors, FP, DP, IP and TP receptors, for the other PGs, respectively (43,107). PGD_2, PGE_2, and $PGF_{2\alpha}$ are produced in pancreatic islets in response to glucose and may function as a way to fine-tune GSIS (74,169,172,174,175,177,178,181). PGD_2 and $PGF_{2\alpha}$ are typically associated with increasing insulin release, while PGE_2 has been published to inhibit insulin release (71,74,177,183-197). COX inhibition is hypothesized to increase GSIS by reducing PGE_2 levels (50,105,172). Expression of EP receptors has been observed in the mouse (181,235) and human pancreas (236), human pancreatic stellate cells (237), in human (221), mouse (74,181), rat (196,197,238), and guinea pig islets (71), mouse β-cells (239), in HIT and Min6 β-cell lines (71,74,227,240), 832/13 rat insulinoma cell line (238), and in the α-cell line, αTC1 (74). These aforementioned gene expression studies suggest that EP3, the $G\alpha_i$ coupled receptor, has the highest expression of the four EP receptors in islets. Expression of all three EP3 splice variants and PGE_2 production from islets are increased in diabetes (74). EP3, the $G\alpha_i$ coupled EP receptor, has been hypothesized to be responsible for mediating PGE_2's inhibition of GSIS as prior studies have shown that EP3 agonists decrease GSIS which can be ameliorated by an EP3 antagonist (71,74,194,197,233). However, EP3 blockade and gene knockout were not found to affect GSIS in my hands (Chapter II, Chapter III). PGE_2 is also an important inflammatory mediatory with the EP3 receptor evoked response mediating interleukin-1β (IL-1β), and lipopolysaccharide (LPS) induced febrile response (310). Inflammatory cytokines increase with age and a low level

state of inflammation is associated with diabetes (24,25). Blockade of PGE_2-EP3 signaling would be anti-inflammatory and may have salutary effects on diabetes further augmenting GSIS by lessening the auto-inhibitory response of islet-derived PGs in response to glucose.

I hypothesized that $EP3^{-/-}$ mice have enhanced GSIS that led to the improvement in glucose homeostasis. I have shown that $EP3^{-/-}$ mice have improved glucose homeostasis at 40 weeks of age when they are fed a standard chow diet (Chapter II). This effect is not seen at 20 weeks of age when both genotypes show a similar response to an IP-GTT. Only the 40 week old $EP3^{-/-}$ mice manifested an improvement in glucose homeostasis because improvements in β-cell function may not significantly affect glucose homeostasis in younger animals that already have proper glycemic control. I hypothesized that in a setting of diet induced type 2 diabetes, that aged $EP3^{-/-}$ mice would similarly show an improvement in glycemic control.

Young $EP3^{-/-}$ mice become obese and insulin resistant when fed a HFD but maintained similar body weights as compared to $EP3^{+/+}$ when fed a lower fat control diet (Chapter III). $EP3^{-/-}$ mice on HFD began to diverge from $EP3^{+/+}$ at approximately 12 weeks of age when they were shown to have an increased percentage of body fat as measured by NMR. The body weight of these HFD fed mice began to diverge soon after. In order to assess the effects of HFD in older mice, $EP3^{+/+}$ and $EP3^{-/-}$ were fed the same control (10% calories from fat) and HFD (45% calories from fat) for 16 weeks diets beginning at 20 weeks of age.

Methods

Animal procedures & high fat diet feeding

Mice utilized for these experiments were maintained as previously described (Chapter II). Beginning at age 20 weeks, male C57BL/6 $EP3^{+/+}$ or $EP3^{-/-}$ mice were fed a control diet (10% calories from fat; 4.3% fat by weight, D12450Bi, Research Diets, New Brunswick, NJ) or high

fat diet (HFD) (45% calories from fat; 24% fat by weight, D12451i, Research Diets) for 16 weeks. All procedures were approved by the Institutional Animal Care and Use Committee at Vanderbilt University.

Energy balance

A separate cohort of mice utilized for energy balance studies were fed HFD beginning at ~17 weeks of age for 10.5 weeks until ~28 weeks of age. Energy balance studies were performed in a Promethion system (Sable Systems International, North Las Vegas, NV) for five days by the Vanderbilt Mouse Metabolic Phenotyping Center.

Tissue fatty acid composition

Triglycerides were extracted from ~100 mg flash frozen liver by the Mouse Metabolic Phenotyping Center Lipid Lab as previously described (Chapter III).

Histology

Livers from 3 mice per genotype × diet treatment were fixed in 10% formaldehyde overnight at 4°C and subsequently stored in 70% ethanol at 4°C prior to paraffin embedding and hematoxylin and eosin (H&E) staining. Liver samples from 3 mice per genotype × diet treatment for were fixed by freezing in OCT for Oil Red O (ORO) staining. All slides were imaged with a 20× objective using an Olympus BX51 microscope. Histology was performed by the Vanderbilt Translational Pathology Shared Resource.

Intraperitoneal glucose tolerance tests

IP-GTT was performed on male C57BL/6 $EP3^{+/+}$ or $EP3^{-/-}$ mice as previously described (Chapter II).

Intraperitoneal insulin tolerance tests

Male $EP3^{+/+}$ or $EP3^{-/-}$ mice were fasted for 6 hours during the light cycle and fasting blood glucose level were measured with the Accu-Check Aviva blood glucose meter using blood obtained from the tail. Following intraperitoneal injection of 34.1 μg/kg insulin (human recombinant insulin, Sigma-I9278), for 24 week old mice, or 0.75 U/kg insulin (human recombinant insulin, Novolin R, Novo Nordisk, Princeton, NJ), for 36 week old mice, in 0.9% normal saline, blood glucose levels were measured at 15, 30, 60, 90, and 120 minutes post-injection.

Mouse islet perifusion

Pancreatic islets were isolated from male C57BL/6 $EP3^{+/+}$ or $EP3^{-/-}$ mice and perifusion assays were performed on fresh islets at the Vanderbilt Islet Procurement & Analysis Core as previously described (Chapter II). Mice utilized for islet perifusion experiment were 37 to 39.5 weeks old and had been fed HFD beginning around 17 weeks of age for 20.5 to 21.5 weeks.

Total Pancreatic Insulin

Insulin was extracted from whole pancreata. Excised pancreata were placed in 5 ml of acid-ethanol (1.8% 10N HCl in 70% ethanol) and frozen overnight at -20°C. Tissues were homogenized with a Tissue Master 240 (OMNI International, Kennesaw, GA) and frozen overnight at -20°C. Samples were centrifuged for 30 minutes at 2000 RPM in an Allegra 21 (Beckman Coulter, Brea, CA) and supernatant was transferred to a new tube. Supernatant was frozen overnight at -20°C and homogenization and centrifugation were repeated. Supernatants were normalized to 15 ml per sample with acid-ethanol. Insulin content was analyzed in duplicate by radioimmunoassay by Vanderbilt University Hormone Assay & Analytical Services Core.

Statistics

Statistics were performed as previously described (Chapter III).

Results

Body composition and energy balance of EP3$^{-/-}$ mice

To test the hypothesis that glucose handling in EP3$^{-/-}$ mice is more sensitive to diet than observed for EP3$^{+/+}$ mice, EP3$^{+/+}$ or EP3$^{-/-}$ males were fed either HFD (45% calories from fat) or a micronutrient matched control diet (10% calories from fat). Body weight in both EP3$^{+/+}$ and EP3$^{-/-}$ HFD fed mice increased at a greater rate than in animals fed control diet, with a divergence in body weight becoming apparent by 4 weeks of matched diet feeding ($P = 0.0007$; Figure 30A). Moreover, by 8 weeks after beginning the HFD, EP3$^{-/-}$ mice were heavier than EP3$^{+/+}$ animals ($P = 0.0296$; adjusted P-value Bonferonni post hoc test). Body composition analyses throughout the experimental time period revealed that lean body mass was affected by the EP3 genotype and age when fed a HFD ($P = 0.0487$, effect of interaction between genotype and age for HFD fed mice only; Figure 30B). Increased weight gain in EP3$^{-/-}$ mice on HFD coincided with increased fat mass, though this was not statistically significant (2-way ANOVA $P = 0.0904$; Figure 30C). Post-mortem analysis of epididymal fat pads confirmed that HFD feeding increased fat mass ($P = 0.0008$) but was not significantly altered by EP3 genotype ($P = 0.746$; Figure 30D). This test was underpowered and therefore unable to detect an effect of EP3 genotype on epididymal fat pad mass (power ≈ 0.05). Energy balance studies of HFD fed mice showed that EP3$^{-/-}$ mice do not have differences in food consumption (Figure 31B). EP3$^{-/-}$ mice did not have a significant change in movement (Figure 31C), but spent significantly more time inactive during the dark cycle (Figure 31D).

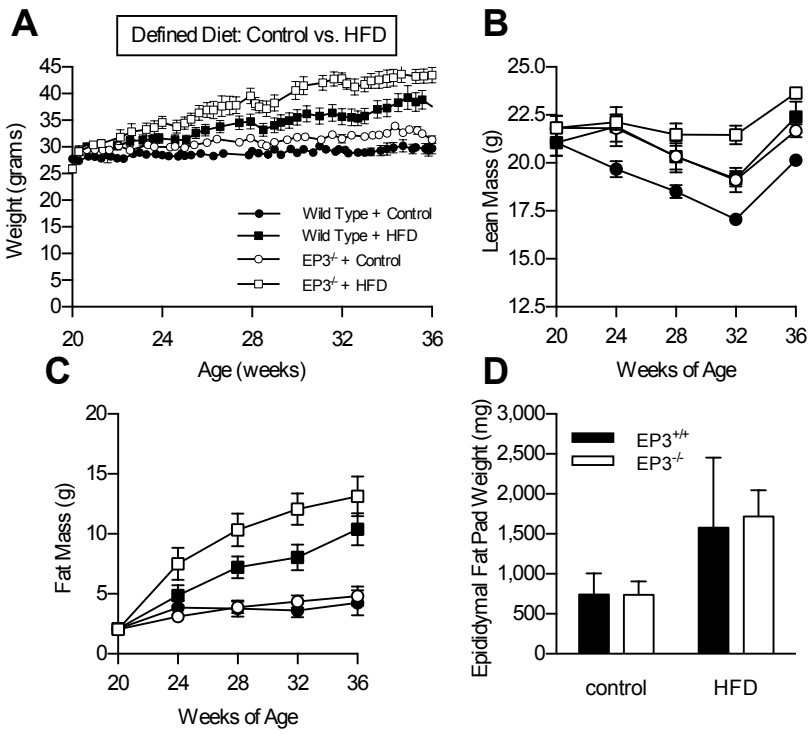

Figure 30. EP3$^{-/-}$ mice are obese when fed a HFD

A. Male EP3$^{+/+}$ and EP3$^{-/-}$ mice fed control diet or HFD were weighed weekly from age 20 weeks to age 36 weeks. No difference in body weight was observed between genotypes in the control fed animals. EP3$^{-/-}$ mice fed HFD were significantly heavier than EP3$^{+/+}$ animals beginning at 28 weeks of age. Body composition of **B.** lean and **C.** fat were assessed at four week intervals by pulsed NMR. For A-C N = 3 EP3$^{+/+}$ control, 9 EP3$^{-/-}$ control, 7 EP3$^{+/+}$ HFD, 7 EP3$^{-/-}$ HFD, values are expressed as mean ± SEM. **D.** Epididymal fat pads were weighed post mortem at the conclusion of the study. N = 3 EP3$^{+/+}$ control, 4 EP3$^{-/-}$ control, 2 EP3$^{+/+}$ HFD, 7 EP3$^{-/-}$ HFD. Values are expressed as mean ± StDev.

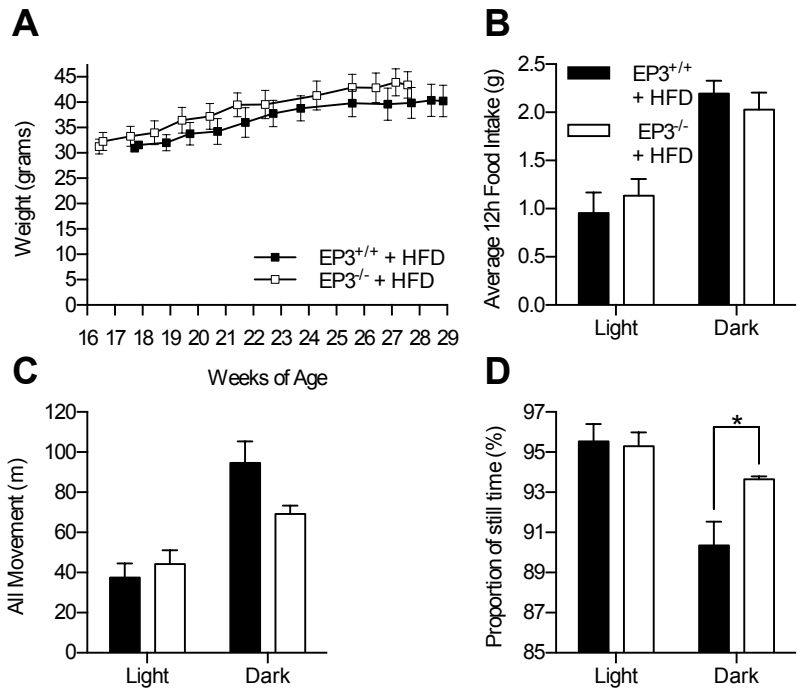

Figure 31. EP3$^{-/-}$ mice spend more time still during the dark cycle
A. Male EP3$^{+/+}$ and EP3$^{-/-}$ mice were fed HFD for 10.5 weeks between the ages of 16.5 weeks of age and 29 weeks of age. **B.** Total food intake was measured in these mice. Mice consumed more food during the dark cycle (P = 0.0055), but no significant difference between EP3 genotypes (P = 0.952) or interaction between light cycle and genotype (P = 0.426) were observed. **C.** Total movement was measured in the same mice. All mice were found to move more during the dark cycle (P = 0.0029). **D.** Mice were still for a greater amount of their time in the light cycle (P = 0.0223). EP3$^{-/-}$ mice were found to have a greater proportion of still time than EP3$^{+/+}$ mice during the dark cycle. For all figures N = 3 EP3$^{+/+}$ HFD, 3 EP3$^{-/-}$ HFD. All values are expressed as mean ± SEM.

Hepatic lipidosis in EP3$^{-/-}$ mice

Liver weight was increased in EP3$^{-/-}$ mice (P = 0.0145, effect of genotype) and by HFD feeding (P = 0.0164, effect of diet; Figure 32A). Hepatic triglyceride levels were also increased by HFD feeding (P = 0.0344, effect of diet) with hepatic triglycerides in EP3$^{-/-}$ mice increased when fed HFD (P = 0.0497, effect of interaction; Figure 32B). Dietary lipid and EP3 genotype affected the fatty acid composition of the hepatic triglycerides (Table 7). We observed steatosis in the livers histologically using H&E (Figure 32C), and Oil red O (ORO) staining (Figure 32D). Livers from EP3$^{-/-}$ mice fed HFD showed markedly increased levels of steatosis and ORO staining. Steatosis in EP3$^{+/+}$ mice fed HFD was present but not as pronounced as in the EP3$^{-/-}$ counterparts. When fed control diet, neither genotype displayed significant hepatic steatosis.

Glycemic control in EP3$^{-/-}$ mice

Glucose handling was assessed by IP-GTT. At 24 weeks of age, having been on the control or HFD for four weeks, no difference in IP-GTT was observed between any of the groups (Figure 33A). When assessed at 36 weeks of age, animals fed HFD demonstrated impaired glucose handling (Figure 33B, P = 0.0171), although an effect on genotype was not observed (P = 0.0706). EP3$^{-/-}$ HFD fed mice had elevated blood glucose at the start of the IP-GTT (P = 0.0228) that reduced the ability to detect changes in AUC. ITT performed on animals fed HFD showed that they were insulin resistant at 36 weeks of age independent of genotype. EP3$^{-/-}$ mice appear to have decreased insulin sensitivity (Figure 33D), although these data are difficult to interpret due to the short half-life of insulin injected (10 minutes) compared to the long time period analyzed for the ITT (579). Interpretation of the response of EP3$^{-/-}$ mice to exogenous insulin administration is further complicated because EP3$^{-/-}$ HFD fed mice showed elevated 6-hour fasting insulin (P < 0.0001). Exogenous insulin administration to EP3$^{-/-}$ HFD fed mice

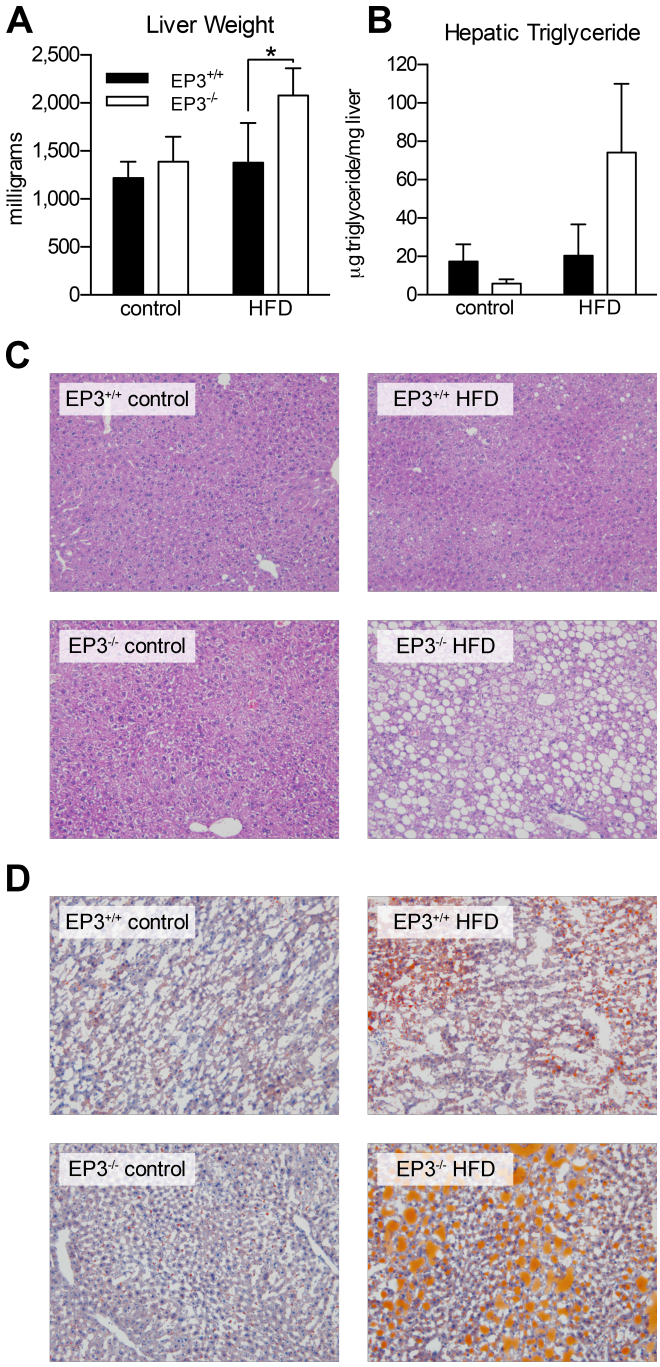

Figure 32. EP3$^{-/-}$ mice fed HFD develop hepatic steatosis
A. EP3$^{-/-}$ mice on HFD had increased liver weight. **B.** EP3$^{-/-}$ mice on HFD had in increased hepatic triglycerides. **C.** H&E staining of livers showed that EP3$^{-/-}$ mice fed HFD had increased steatosis. **D.** Oil Red O staining showed increased lipid staining in livers of EP3$^{-/-}$ mice fed HFD. 2-3 mice per genotype × diet group, 2 sections per mouse. For all figures N = 3 EP3$^{+/+}$ control, 4 EP3$^{-/-}$ control, 2 EP3$^{+/+}$ HFD, 7 EP3$^{-/-}$ HFD. All values are expressed as mean ± StDev.

Parameter	Wild Type - control		Wild Type - HFD		$EP3^{-/-}$ - control		$EP3^{-/-}$ - HFD		ANOVA p-value		
	mean	SEM	mean	SEM	mean	SEM	mean	SEM	Genotype	Diet	Interaction
g/100 g fatty acids											
14:0	0.63	0.57	0.31	0.44	0.18	0.37	0.62	0.04	0.711	0.746	0.056
16:0	29.03	1.70	28.34	0.49	29.39	2.00	29.68	0.68	0.263	0.788	0.514
16:1	5.23	1.21	1.54	2.17	3.45	2.33	3.38	0.34	0.969	0.036	0.041
17:0	0.00	0.00	0.00	0.00	0.00	0.00	0.00	0.00	NA	NA	NA
18:0	3.35	1.28	3.39	1.98	4.12	1.45	1.88	0.24	0.547	0.089	0.079
18:1ω9	45.13	3.21	36.61	3.98	43.54	2.48	39.51	1.37	0.621	<0.001	0.110
18:1ω7	6.86	1.58	1.41	1.99	5.38	1.23	2.78	0.38	0.924	<0.001	0.036
18:2	9.41	1.52	21.87*	6.33	13.11	2.79	15.89*	1.09	0.427	<0.001	0.004
18:3ω6	0.00	0.00	0.19	0.27	0.00	0.00	0.34	0.17	0.348	0.005	0.348
18:3ω3	0.09	0.16	0.25	0.35	0.00	0.00	0.36	0.17	0.907	0.018	0.309
20:3ω6	0.00	0.00	0.48**	0.67	0.00	0.00	1.05**	0.11	0.029	<0.001	0.029
20:4	0.14	0.24	2.94	1.70	0.37	0.74	1.87	0.23	0.260	<0.001	0.092
20:5	0.00	0.00	0.00	0.00	0.00	0.00	0.13	0.09	0.091	0.091	0.091
22:4ω6	0.00	0.00	1.78	1.66	0.22	0.43	0.71	0.09	0.172	0.002	0.049
22:5ω6	0.00	0.00	0.13	0.18	0.00	0.00	0.16	0.11	0.805	0.016	0.805
22:5ω3	0.00	0.00	0.22	0.30	0.00	0.00	0.39	0.18	0.337	0.004	0.337
22:6	0.14	0.24	0.58	0.81	0.25	0.50	1.25	0.27	0.108	0.008	0.236
Ratio											
16:0/16:1	5.77	1.49	NA	NA	6.25	0.73	8.86	0.96	NA	NA	NA
18:0/18:1	0.07	0.03	0.09	0.07	0.09	0.03	0.04	0.01	0.358	0.709	0.053
Saturated / Unsaturated†	0.49	0.06	0.47	0.02	0.51	0.08	0.47	0.02	0.722	0.297	0.812

†(14:0+16:0+17:0+18:0) / (16:1+18:1ω9+18:1ω7+18:2+18:3ω6+18:3ω3+20:3ω6+20:4+20:5+22:4ω6+22:5ω6+22:5ω3+22:6)
* Bonferroni post-hoc comparison to * in same row P<0.05
** Bonferroni post-hoc comparison to ** in same row P<0.01
*** Bonferroni post-hoc comparison to *** in same row P<0.001
Statistically significant values are highlighted

Table 7. Fatty acid composition of hepatic triglycerides
Fatty acid composition of hepatic triglycerides from male $EP3^{+/+}$ and $EP3^{-/-}$ mice, fed either HFD or control diet. N = 3 $EP3^{+/+}$ control, 4 $EP3^{-/-}$ control, 2 $EP3^{+/+}$ HFD, 7 $EP3^{-/-}$ HFD.

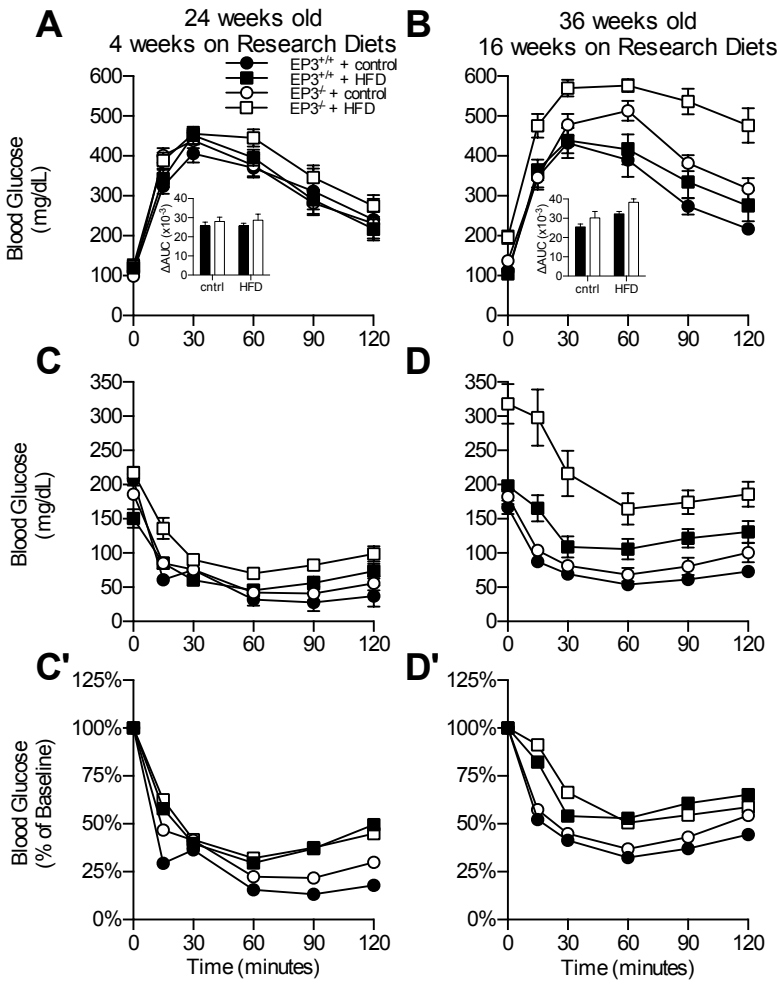

Figure 33. EP3$^{-/-}$ mice have elevated blood glucose

Glucose tolerance was determined in male EP3$^{+/+}$ and EP3$^{-/-}$ mice, fed either HFD or control diet. **A.** At 24 weeks of age neither HFD (P = 0.904) nor EP3 genotype (P = 0.342) affected glucose homeostasis. **B.** At 36 weeks of age HFD impaired the response to glucose challenge (P = 0.0171). Neither EP3 genotype (P = 0.0706) nor an interaction between EP3 genotype and dietary fat (P = 0.8148) affected response to glucose challenge. Insulin tolerance was determined in male EP3$^{+/+}$ and EP3$^{-/-}$ mice, fed either HFD or control diet, **C.** (**C'.**) at 24 weeks of age and **D.** (**D'.**) 36 weeks of age. At both ages EP3$^{-/-}$ HFD fed mice had elevated blood glucose, as compared to EP3$^{+/+}$, after a 6-hour fast at the beginning of the ITT (P = 0.0031 and 0.0001, respectively). For all figures N = 3 EP3$^{+/+}$ control, 9 EP3$^{-/-}$ control, 7 EP3$^{+/+}$ HFD, 7 EP3$^{-/-}$ HFD. All values are expressed as mean ± SEM.

caused a 102 mg/dl drop in blood glucose in the first 30 minutes which is similar to the response observed in $EP3^{+/+}$ and control diet fed mice. Elevated fasting glucose is an indication of insulin resistance and was found in $EP3^{-/-}$ HFD fed mice after both the 16- and 6-hour fasts.

Pancreatic islet insulin secretion and content in $EP3^{-/-}$ mice

EP3 blockade has been reported to improve GSIS in islets from diabetic mice (74). Pancreatic islets isolated from $EP3^{+/+}$ and $EP3^{-/-}$ mice fed HFD were assessed for alterations in GSIS by islet perifusion. $EP3^{-/-}$ islets showed impaired GSIS but were unaffected by PGE_2 (Figure 34A).

One physiologic response to increasing insulin resistance is an increase in pancreatic β-cell proliferation (596). Moreover, $G\alpha_z$ inhibits β-cell proliferation, possibly through interactions with EP3 (134), thus we examined islet and total pancreatic insulin as an indicator of β-cell mass. Insulin content of islets used for the perifusion experiment was not significantly different (Figure 34B). In addition, no statistically significant effect of EP3 genotype ($P = 0.541$) or HFD feeding ($P = 0.346$) on total pancreatic insulin content was found in 36 week old mice (Figure 34C). These tests were underpowered and therefore unable to detect differences in total pancreatic insulin (power ≈ 0.05).

Discussion

Blockade of PGE_2 action at the inhibitory EP3 receptor has been hypothesized to be a therapeutic target to improve GSIS, which would be beneficial for the treatment of diabetes. I have previously shown that 40 week old $EP3^{-/-}$ mice have improved glucose homeostasis when fed a standard chow diet (Chapter II). Here, I investigated the effect of HFD feeding in older mice. $EP3^{-/-}$ mice are more prone to developing obesity when fed HFD regardless of whether HFD feeding begins in young (4 weeks) or older (20 weeks) mice. The effects of HFD feeding

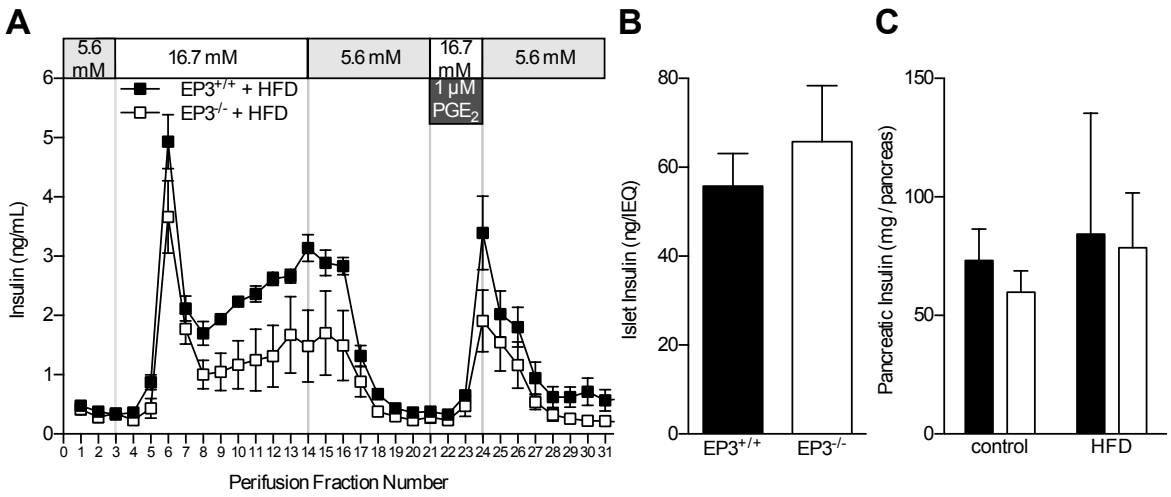

Figure 34. Islets from EP3$^{-/-}$ HFD fed mice have reduced GSIS
A. Perifusion of islets from HFD fed EP3$^{+/+}$ and EP3$^{-/-}$ mice showed reduced GSIS in EP3$^{-/-}$ HFD fed islets (P = 0.0337). GSIS was unaffected by PGE_2 (P = 0.295). **B.** Insulin content of islets used for perifusion was not different (P = 0.302). For A&B, N = 3 EP3$^{+/+}$ HFD, 3 EP3$^{-/-}$ HFD. Values are expressed as ± SEM. **C.** Measurement of total pancreatic insulin content reveals no differences with respect to either dietary fat or EP3 genotype. For C, N = 2 EP3$^{+/+}$ control, 3 EP3$^{-/-}$ control, 2 EP3$^{+/+}$ HFD, 7 EP3$^{-/-}$ HFD. Values are expressed as mean ± StDev.

were apparent more readily after transition to the HFD in older animals. This may be due to the animals being at a mature body weight when the diet treatment began. Dietary fat did not significantly affect body weight in younger mice until approximately 8 weeks of age, when they were near their mature body weight. $EP3^{-/-}$ mice become more obese than $EP3^{+/+}$ only when fed a HFD and then only after they have reached mature body weight.

$EP3^{-/-}$ mice appear to be more insulin resistant than $EP3^{+/+}$ mice when fed HFD. $EP3^{-/-}$ HFD fed mice had elevated glucose throughout the ITT due to an elevated baseline 6-hour fasting glucose. We previously reported that $EP3^{-/-}$ mice become insulin resistant when fed a HFD due to lipid redistribution to ectopic tissues (Chapter III). We observed a similar increase in liver weight and hepatic triglycerides in $EP3^{-/-}$ mice only when fed HFD.

We were not able to detect significant changes in glucose tolerance in part because $EP3^{-/-}$ HFD fed mice had elevated fasting glucose and the Accu-Check Aviva blood glucose meter has a maximum reading of 600 mg/dl, hence higher values were not able to be measured. It is not surprising that HFD fed $EP3^{-/-}$ mice have high glucose during an IP-GTT given that we found decreased GSIS in islets isolated from HFD fed $EP3^{-/-}$ mice. Decreased GSIS from $EP3^{-/-}$ islets is in contrast to a prior report that has shown that EP3 antagonist, L-798,106, raises GSIS in diabetic islets (74). We previously reported that EP3 antagonist, DG-041, lowers GSIS in islets from control diet fed animals (Chapter III). However, our previous study found no effect of DG-041 on GSIS in islets from HFD fed mice (Chapter III). It is possible that off target effects of the EP3 antagonists have lead to some of these discrepancies.

Our results are consistent with an earlier report which showed that $EP3^{-/-}$ mice fed a breeder chow become more glucose intolerant and insulin resistant as they age (102). These results are also consistent with our previous report of glucose handling in younger $EP3^{-/-}$ HFD

fed mice (Chapter III). In both studies, diet affected glucose homeostasis, but the effect of the EP3 genotype was not statistically significant.

These data show that obesity and related phenotypes become worse with age in $EP3^{-/-}$ mice when fed a HFD. The phenotypes are remarkably similar to what we have reported in younger mice of the same genotypes fed the same diets (Chapter III). Older $EP3^{-/-}$ mice fed HFD tended to have more obesity, worse insulin sensitivity, and poorer glucose homeostasis. Furthermore, we observed no improvement in glucose homeostasis in control diet fed animals which is in contrast to our prior report of improved glucose homeostasis in $EP3^{-/-}$ mice fed a standard chow diet.

CHAPTER V

THE EFFECT OF THE EP3 ANTAGONIST DG-041 ON MALE MICE WITH DIET-INDUCED OBESITY

Introduction

$EP3^{-/-}$ mice have been shown to be more susceptible to diet induced obesity (Chapter III, IV). The increased obesity in $EP3^{-/-}$ mice is the result of an interaction between the EP3 genotype and dietary fat, with $EP3^{-/-}$ mice becoming obese only on a HFD but having normal body weights and phenotypes on control or chow diets. In addition to becoming more obese, $EP3^{-/-}$ mice have increased lipolysis and adipocyte necrosis causing a redistribution of lipid to ectopic tissues resulting in insulin resistance (Chapter III).

These effects of EP3 on the metabolic phenotype were noted in a model of chronic EP3 disruption, utilizing mice that had a global EP3 gene disruption since birth. EP3 is expressed during gestation (597); hence, it is possible that some of the observed phenotypes may be in part due to the lack of EP3 during gestation and the early stages of growth. Maternal obesity and over-nutrition predispose offspring to obesity (598); hence, it is possible that EP3 loss in dams may contribute to the predisposition of obesity observed in their pups. Furthermore, PGE_2 is known to play an inhibitory role in adipocyte development inhibiting adipogenesis through the EP4 receptor (324,335,352,364).

In order to examine the effects of acute inhibition of EP3 on metabolic phenotype, EP3 antagonist DG-041 (556) was administered to wild-type mice for one week and changes in body weight, insulin sensitivity, and ectopic lipid distribution were assessed. DG-041 administration caused a reduction in skeletal muscle triglyceride content while showing a trend toward increased hepatic triglycerides which is constant with inhibition of hepatic lipolysis.

Materials & Methods

Mice

All mice were obtained from Jackson Labs. For pharmacokinetics studies, approximately 16 week old, 28 gram male C57BL/6 were utilized. Mice utilized for diet induced obesity studies were male F1 progeny of male C57BL/6 crossed with female Balb/c mice (Jackson Labs #100007). For diet studies mice were housed at Vanderbilt for three days on a standard chow diet (Laboratory Rodent Diet 5001, LabDiet) after which time they were fed either control (D12450Bi, Research Diets), HFD (D12451i, Research Diets), or very high fat diet (VHFD) (60% calories from fat; 34.9% fat by weight, D12492i, Research Diets). After 17 weeks of defined diet feeding, mice were injected with 20 mg/kg DG-041 or vehicle twice daily for one week. Mice were weighed weekly and body composition was assessed every four weeks by pulsed NMR (Brunker Intraments, The Woodlands, TX) at the Vanderbilt Mouse Metabolic Phenotyping Center. At the termination of the experiment, mice were euthanized by isoflurane overdose and liver, epididymal fat pads, and skeletal muscle were dissected.

In vivo *pharmacokinetics*

DG-041 was dissolved in DMSO, and was then diluted to one part DMSO+DG-041, six parts PEG400, and 3 parts 0.9% saline. Vehicle made of one part DMSO, six parts PEG400, and 3 parts 0.9% saline was used as the control. 20 mg/kg DG-041 was administered by subcutaneous injection. Plasma was collected by sapheneous vein blood draw into EDTA coated tubes (Sarstedt, Nümbrecht, Germany) with the final blood draw being obtained by cardiac puncture in euthanized mice. Plasma was stored at -80 °C until DG-041 was measured by HPLC/MS/MS analysis as previously described (599).

Assessment of insulin resistance

Mice were fasted for 6 hours during the light cycle. EDTA plasma was collected by sapheneous vein blood draw and insulin was quantified by RIA at the Vanderbilt Hormone Assay Core. While collecting blood for plasma, blood glucose was measured in excess sapheneous vein blood with an Accu-Check Aviva glucometer and glucose test strips (Roche Diagnostics). HOMA-IR was calculated as the fasting insulin level (μU/mL) × blood glucose level (mg/dL) / 405.

Histology

Livers from all mice were fixed, sectioned, and imaged as previously described (Chapter IV).

Tissue fatty acid composition

Triglycerides were extracted from ~100 mg flash frozen liver by the Mouse Metabolic Phenotyping Center Lipid Lab as previously described (Chapter III).

Plasma chemistry

Plasma triglycerides and FFAs were quantified from EDTA plasma as previously described (Chapter III).

Results

In vivo *pharmacokinetics of DG-041*

DG-041 achieved a maximum plasma concentration of 1385 nM (± 716) at 1 hours following subcutaneous administration and displayed an average AUC of 331.4 nM·h over the 26 hours (Figure 35). DG-041 was also found in the brain indicating that it crosses the blood- brain barrier. DG-041 was administered subcutaneously at 20 mg/kg twice daily in subsequent

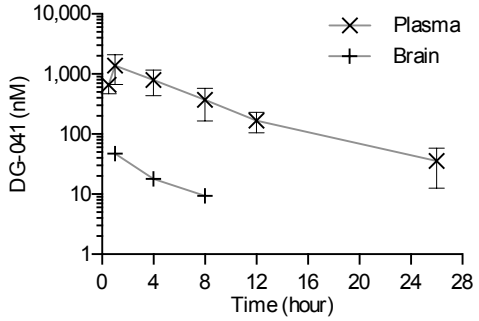

Figure 35. Plasma concentration-time profile of DG-041 following subcutaneous administration

20 mg/kg DG-041 was administered to mice by subcutaneous injection. Plasma DG-041 concentrations were measured from sapheneous vein blood at the indicated times. N = 4-6. Brain DG-041 concentrations were measured from mice euthanized at the indicated time. N = 1 each. Values are expressed as mean ± StDev.

experiments because DG-041 has an IC50 of 11 nM in [^{3}H]Ligand Displacent Binding Assay for the mouse EP3 receptor and the plasma concentrations of DG-041 at this dose will provide sufficient coverage antagonize endogeneous EP3 receptors (600).

C57BL/6×Balb/c mice are obese when fed a HFD

Wild-type C57BL/6×Balb/c male mice were fed either HFD (45% calories from fat), VHFD (60% calories from fat) or a micronutrient matched control diet (10% calories from fat). Body weight increased in each of the three groups over the course of the study (Figure 36A). Body weight in both HFD and VHFD fed mice increased at a greater rate than in animals fed control diet, with a divergence in body weight becoming apparent between six and eleven weeks of age. Body composition analyses over the course of the study revealed that fat mass also increased with age and dietary fat (Figure 36B). Lean mass was also increased by dietary fat (Figure 36C).

C57BL/6×Balb/c mice are insulin resistant when fed a HFD

Blood glucose and plasma insulin were measured in C57BL/6×Balb/c mice that had been fed control diet, HFD, or VHFD for 17 weeks. Regardless of dietary fat, mice in the fasted state had no differences in basal glucose levels (Figure 37A). Increasing dietary fat increased fasting insulin levels (Figure 37B). Calculation of the homeostatic model assessment of insulin resistance (HOMA-IR) indicated that increasing dietary fat increases insulin resistance (Figure 37C).

EP3 antagonist does not affect body composition

20 week old C57BL/6×Balb/c mice that had been fed control diet, HFD, or VHFD were administered EP3 antagonist, DG-041, or vehicle for one week by twice-daily subcutaneous injections. Body weight decreased in HFD and VHFD fed mice following administration of

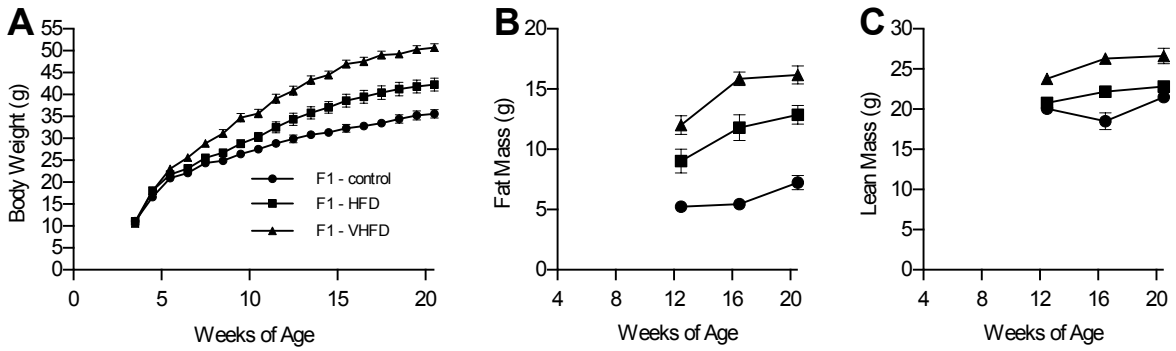

Figure 36. C57BL/6×Balb/c mice are obese when fed a HFD

A. Male mice fed control diet, HFD, or VHFD were weighed between 4 weeks of age and 20 weeks of age. At 3 weeks of VHFD feeding, mice were significantly heavier than mice fed control diet ($P = 0.0243$). At 4 weeks of VHFD feeding, mice were significantly heavier than mice fed HFD ($P = 0.0341$). At 8 weeks of HFD feeding, mice were significantly heavier than mice fed control diet ($P = 0.0219$). **B.** Body composition of fat was assessed by pulsed NMR. Fat mass in mice was increased by dietary fat and age ($P = < 0.0001$). **C.** Body composition of lean mass was assessed by pulsed NMR. Lean mass in mice was increased by dietary fat and age ($P = < 0.0001$). For all figures N = 8 control, 8 HFD, 9 VHFD. Values are expressed as mean ± SEM.

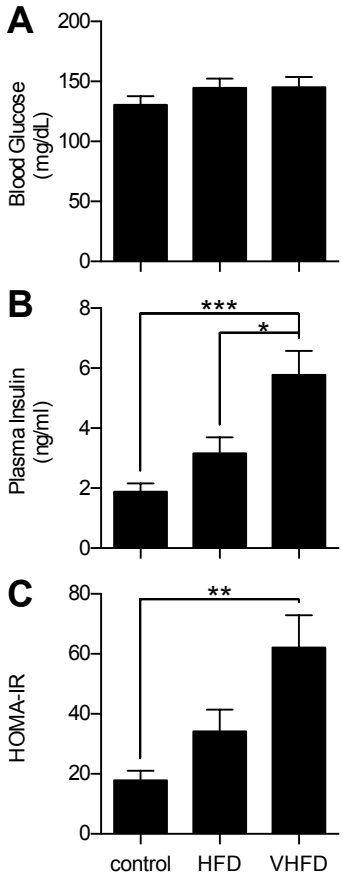

Figure 37. C57BL/6×Balb/c mice become hyperinsulinemic and insulin resistant when fed a HFD

The effects of dietary fat on insulin resistance was assessed in 20 week old C57BL/6×Balb/c mice. **A**. Dietary fat had no effect on blood glucose after a 6-hour fast (P = 0.365). **B.** Increasing dietary fat increased fasting plasma insulin (P = 0.0001). **C.** The homeostatic model assessment of insulin resistance (HOMA-IR), a function of fasting blood glucose and plasma insulin, revealed that increasing dietary fat increased insulin resistance (P = 0.0008). For all figures N = 8 control, 8 HFD, 9 VHFD. Values are expressed as mean ± SEM.

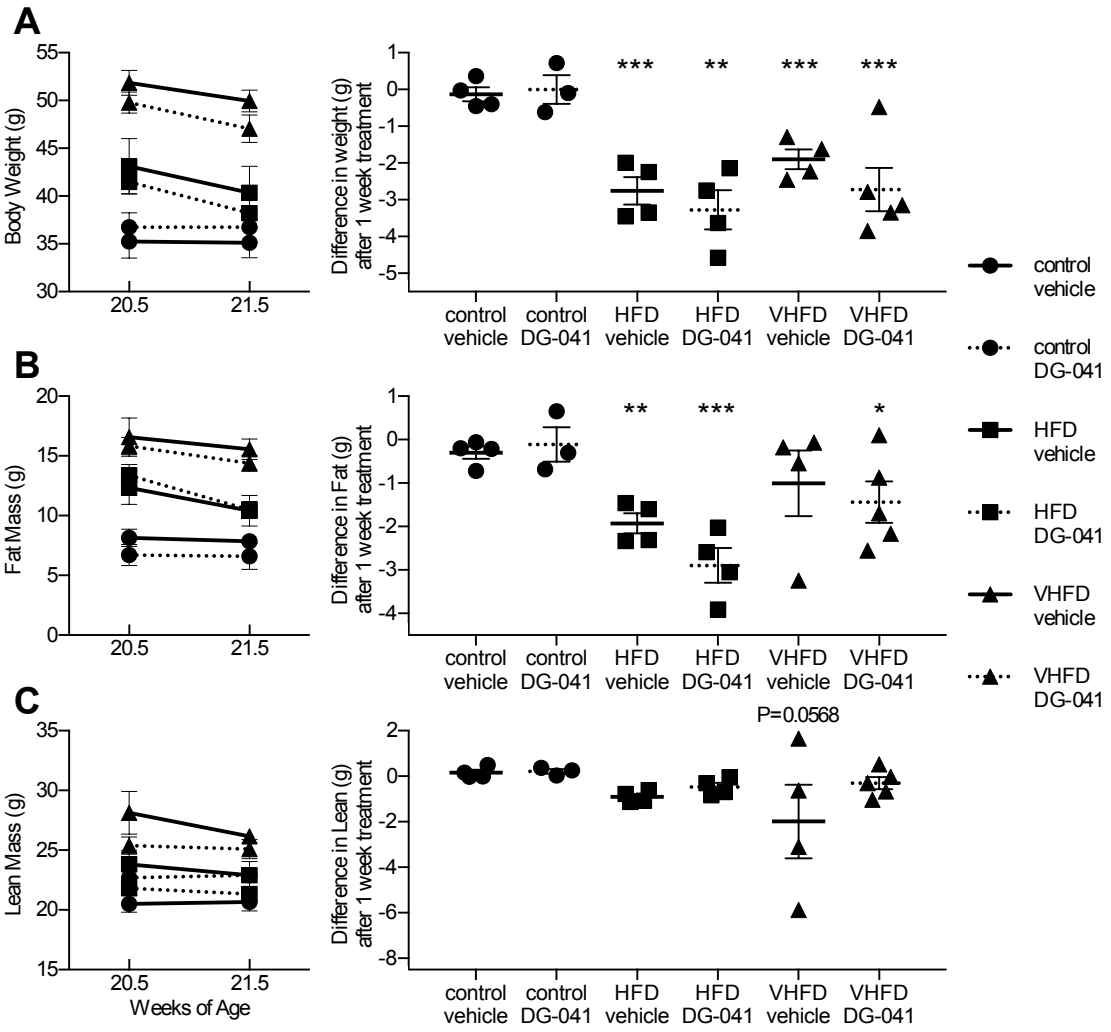

Figure 38. EP3 antagonist does not affect body composition

20 week old C57BL/6×Balb/c mice were administered DG-041 or vehicle by subcutaneous injection for one week (20.5 to 21.5 weeks of age). **A.** Administration of vehicle with or without DG-041 decreased body mass in mice fed HFD or VHFD. **B.** Body composition of fat was assessed by pulsed NMR. Injection of vehicle with or without DG-041 tended to decrease fat mass in mice fed HFD or VHFD. **C.** Body composition of lean mass was assessed by pulsed NMR. Lean mass was not significantly affected by DG-041 or vehicle. For all figures N = 4 control + vehicle (circle + solid line), 3 control + DG-041 (circle + DG-041), 4 HFD + vehicle (square + solid line), 4 HFD + DG-041 (square + dotted line), 4 VHFD + vehicle (triangle + solid line), 5 VHFD + DG-041 (triangle + dotted line). Differences between pre-DG-041 (week 20.5) and post-DG-041 (week 21.5) treatment were determined by Bonferroni post-hoc comparison and are indicated on figure. Values are expressed as mean ± SEM.

vehicle with or without DG-041 (Figure 38A). This indicates that the decreased body weight was due to the vehicle and/or the stress of twice-daily handlings and injections. A concomitant decrease in fat mass was also observed in these mice (Figure 38B). Lean mass was not significantly altered by DG-041 or vehicle (Figure 38C). Post-mortem analysis of liver weight and epididymal fat pad weight found that dietary fat increased liver and epididymal fat pad mass (Figure 39). In HFD and VHFD fed mice, DG-041 did not affect either liver or epididymal fat pad mass.

EP3 antagonist does not affect insulin sensitivity

Blood glucose and plasma insulin were measured in 6-hour fasted C57BL/6×Balb/c mice that had been fed control diet, HFD, or VHFD and were administered either vehicle or EP3 antagonist, DG-041, for one week by twice daily subcutaneous injections. Blood glucose and plasma insulin were not significantly affected by DG-041 treatment, though mice fed VHFD had reduced blood glucose when treated with vehicle but not DG-041 (Figure 40A,B). Consequently, HOMA-IR was also unaffected by DG-041 (Figure 40C). Treatment of the mice with vehicle improved insulin sensitivity; this may be due to the decreased body weight of HFD and VHFD fed mice.

Circulating plasma lipids are not affected by EP3 antagonist

Plasma FFAs and triglycerides were measured in *ad libitum* fed C57BL/6×Balb/c mice that had been fed control diet, HFD, or VHFD and were administered either vehicle or EP3 antagonist, DG-041, for one week by twice-daily subcutaneous injections (Figure 41). Dietary fat did not affect either plasma FFA or triglyceride concentrations. DG-041 also did not affect either plasma FFA or triglyceride concentrations.

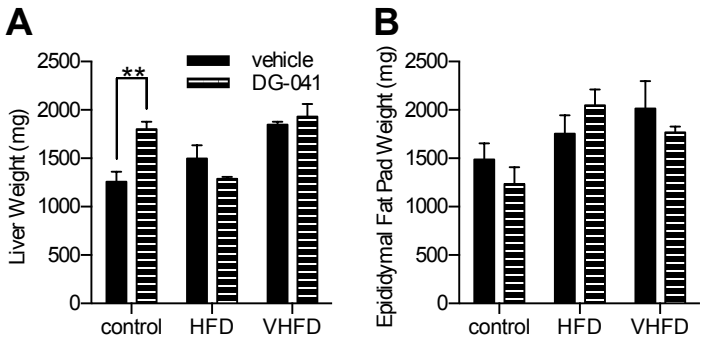

Figure 39. Liver and epdiddymal fat pad mass in mice treated with EP3 antagonist
The effect of EP3 antagonist, DG-041, on tissue weight was measured in 21 week old C57BL/6×Balb/c mice fed control, HFD, or VHFD. **A.** Increasing amounts of dietary fat increased liver mass in vehicle treated mice (One-way ANOVA test for linear trend, P = 0.0094). DG-041 did have a significant effect on the weight of the liver (Two-way ANOVA effect of drug, P = 0.0984), except in mice fed control diet. N = 4 control + vehicle, 3 control + DG-041, 4 HFD + vehicle, 4 HFD + DG-041, 4 VHFD + vehicle, 4 VHFD + DG-041. **B.** Dietary fat affected epididymal fat pad mass (Two-way ANOVA effect of diet, P = 0.0142). DG-041 did not significantly affect the weight of the epididymal fat pads (Two-way ANOVA effect of drug, P = 0.647). N = 4 control + vehicle, 3 control + DG-041, 4 HFD + vehicle, 4 HFD + DG-041, 4 VHFD + vehicle, 5 VHFD + DG-041. Values are expressed as mean ± SEM.

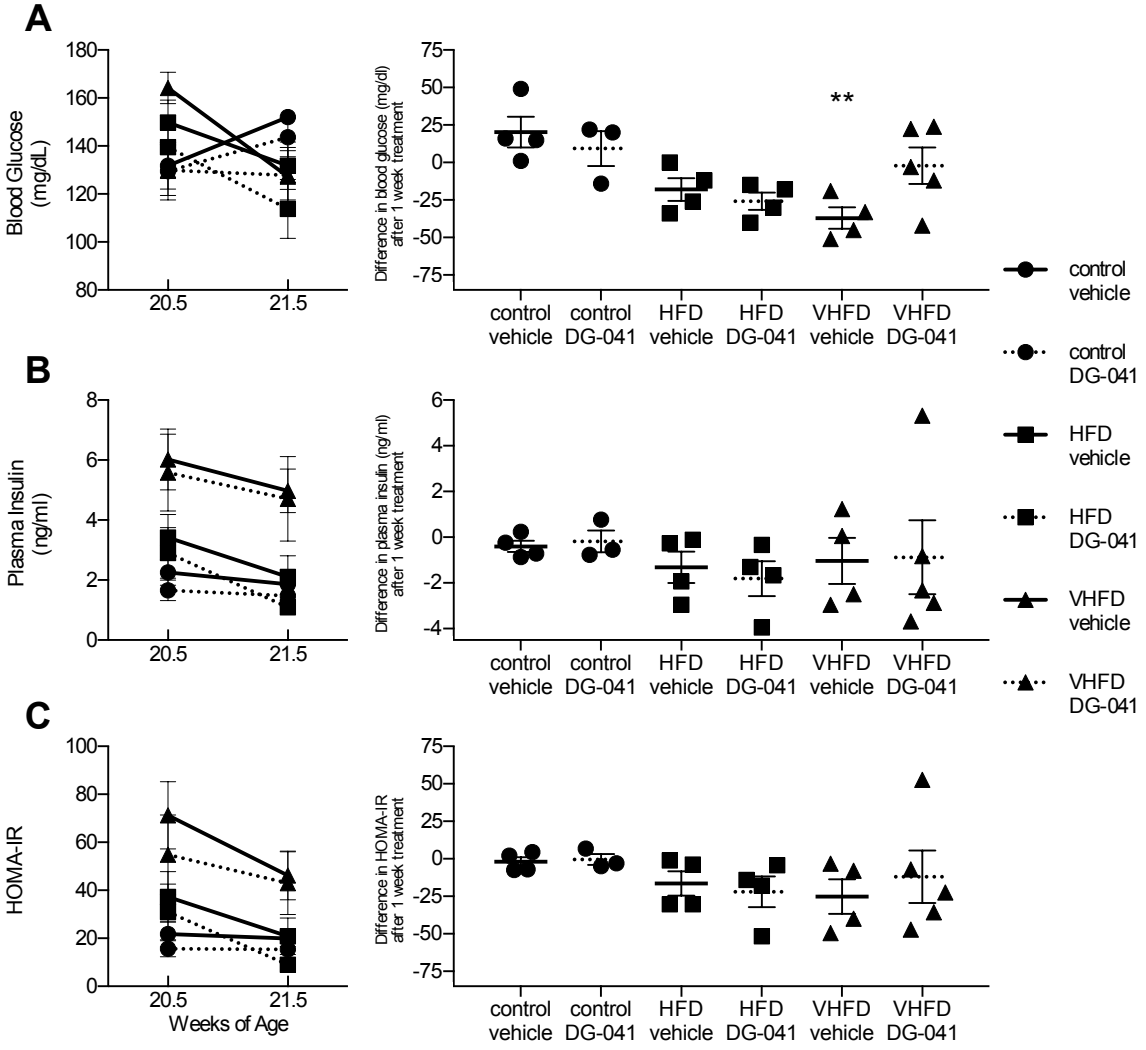
A
Blood Glucose (mg/dL)
180
160
140
120
100
80
20.5
21.5
Difference in blood glucose (mg/dl) after 1 week treatment
75
50
25
0
-25
-50
-75
**
control vehicle
control DG-041
HFD vehicle
HFD DG-041
VHFD vehicle
VHFD DG-041
B
Plasma Insulin (ng/ml)
8
6
4
2
0
Difference in plasma insulin (ng/ml) after 1 week treatment
6
4
2
0
-2
-4
C
HOMA-IR
100
80
60
40
20
0
Weeks of Age
Difference in HOMA-IR after 1 week treatment
control vehicle
control DG-041
HFD vehicle
HFD DG-041
VHFD vehicle
VHFD DG-041

Figure 40. EP3 antagonist does not affect insulin sensitivity
The effect of EP3 antagonist, DG-041, on insulin resistance was assessed in 20 week old C57BL/6×Balb/c mice fed control, HFD, or VHFD. **A**. Treatment of the mice with vehicle significantly reduced fasting blood glucose (Two-way ANOVA comparing vehicle and diet, effect of vehicle: $P = 0.0401$), though this trend was not observed in DG-041 treated mice (Two-way ANOVA comparing DG-041 and diet, effect of DG-041: $P = 0.358$). **B.** Treatment of the mice with vehicle or DG-041 did not have a significant effect on plasma insulin (Two-way ANOVA comparing vehicle/DG-041 and diet, effect of vehicle: $P = 0.0539$ and effect of DG-041: $P = 0.244$). **C.** The homeostatic model assessment of insulin resistance (HOMA-IR), a function of fasting blood glucose and plasma insulin, showed that treatment of the mice with vehicle significantly reduced HOMA-IR ((Two-way ANOVA comparing vehicle and diet, effect of vehicle: $P = 0.0235$), though this trend was not observed in DG-041 treated mice (Two-way ANOVA comparing DG-041 and diet, effect of DG-041: $P = 0.0701$). For all figures $N = 4$ control + vehicle, 3 control + DG-041, 4 HFD + vehicle, 4 HFD + DG-041, 4 VHFD + vehicle, 5 VHFD + DG-041. Differences between pre-DG-041 (week 20.5) and post-DG-041 (week 21.5) treatment were determined by Bonferroni post-hoc comparison and are indicated by asterisk on figure. Values are expressed as mean ± SEM.

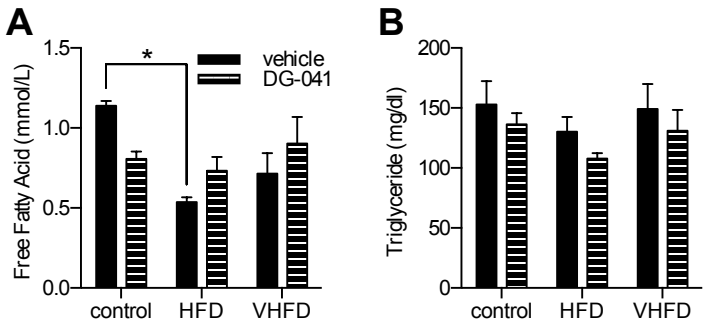

Figure 41. EP3 antagonist does not affect plasma lipids
The effect of EP3 antagonist, DG-041, on plasma lipids was measured in 21 week old *ad libitum* fed mice. **A.** Increasing amounts of dietary fat did not affect the amount of plasma free fatty acid (One-way ANOVA test for linear trend, P = 0.522). DG-041 also did not significantly affect the amount of plasma free fatty acids (Two-way ANOVA effect of drug, P = 0.839). **B.** Increasing amounts of dietary fat did not affect the amount of plasma triglycerides (One-way ANOVA test for linear trend, P = 0.176). DG-041 also did not significantly affect the amount of plasma triglycerides (Two-way ANOVA effect of drug, P = 0.164). For all figures N = 4 control + vehicle, 3 control + DG-041, 4 HFD + vehicle, 4 HFD + DG-041, 4 VHFD + vehicle, 5 VHFD + DG-041. Values are expressed as mean ± SEM.

Parameter	control + vehicle		control + DG-041		HFD + vehicle		HFD + DG-041		VHFD + vehicle		VHFD + DG-041		ANOVA p-value		
	mean	SEM	mean	SEM	mean	SEM	mean	SEM	mean	SEM	mean	SEM	DG-041	Diet	Interaction
g/100 g fatty acids															
14:0	0.90	0.06	0.85	0.06	0.09	0.08	0.00	0.00	0.13	0.08	0.22	0.06	0.772	< 0.001	0.335
16:0	25.14***	0.31	28.81***	0.77	24.35	0.64	23.68	0.29	26.10	0.28	26.15	0.42	0.015	< 0.001	0.001
16:1	5.83	0.48	6.26	0.22	1.65	0.26	1.50	0.09	1.12	0.01	1.24	0.10	0.506	< 0.001	0.523
17:0	0.00	0.00	0.00	0.00	0.00	0.00	0.00	0.00	0.00	0.00	0.00	0.00	NA	NA	NA
18:0	1.99	0.06	1.72	0.04	2.67	0.38	2.30	0.10	2.23	0.03	2.15	0.09	0.100	0.008	0.668
18:1ω9	43.14	1.05	44.96	1.58	35.74	1.62	36.74	0.18	32.68	0.35	35.23	0.53	0.038	< 0.001	0.717
18:1ω7	6.90	0.42	7.01	0.08	1.83	0.22	1.79	0.09	1.34	0.04	1.41	0.09	0.781	< 0.001	0.929
18:2	12.50**	0.72	7.88**	1.07	27.40	1.05	27.87	0.20	27.96*	0.24	25.37*	0.66	0.001	< 0.001	0.009
18:3ω6	0.00	0.00	0.00	0.00	0.54	0.18	0.33	0.19	0.73	0.02	0.67	0.03	0.339	< 0.001	0.633
18:3ω3	0.54	0.03	0.29	0.04	0.60	0.20	0.79	0.09	1.10	0.12	0.93	0.05	0.397	< 0.001	0.123
20:3ω6	0.50	0.02	0.43	0.09	0.64	0.22	0.61	0.21	0.85	0.03	1.05	0.03	0.526	0.004	0.765
20:4	1.39*	0.08	0.92*	0.18	1.87	0.11	1.89	0.12	1.99	0.05	1.98	0.09	0.094	< 0.001	0.060
20:5	0.00	0.00	0.00	0.00	0.00	0.00	0.00	0.00	0.06*	0.06	0.20*	0.05	0.154	0.002	0.123
22:4ω6	0.21	0.12	0.26	0.06	0.24	0.14	0.22	0.12	0.51	0.02	0.59	0.04	0.698	0.004	0.858
22:5ω6	0.19	0.11	0.10	0.10	0.16	0.09	0.00	0.00	0.15	0.09	0.16	0.07	0.287	0.592	0.573
22:5ω3	0.06	0.06	0.08	0.08	0.25	0.14	0.24	0.14	0.53	0.01	0.51	0.02	0.974	< 0.001	0.976
22:6	0.71	0.11	0.44	0.14	1.99	0.20	2.05	0.07	2.54	0.05	2.14	0.12	0.065	< 0.001	0.180
Ratio															
16:0/16:1	4.40***	0.36	4.60***	0.09	15.71	2.08	15.95	1.03	23.33	0.34	21.49	1.66	0.673	< 0.001	0.656
18:0/18:1	0.04	0.00	0.03	0.00	0.07	0.01	0.06	0.00	0.07	0.00	0.06	0.00	0.007	< 0.001	0.778
Saturated / Unsaturated†	0.39	0.00	0.46	0.02	0.37	0.01	0.35	0.01	0.40	0.00	0.40	0.01	0.034	< 0.001	< 0.001

†(14:0+16:0+17:0+18:0) / (16:1+18:1ω9+18:1ω7+18:2+18:3ω6+18:3ω3+20:3ω6+20:4+20:5+22:4ω6+22:5ω6+22:5ω3+22:6)
* Bonferroni post-hoc comparison to * in same row P<0.05
** Bonferroni post-hoc comparison to ** in same row P<0.01
*** Bonferroni post-hoc comparison to *** in same row P<0.001
Statistically significant values are highlighted

Table 8. Fatty acid composition of hepatic triglycerides
Fatty acid composition of hepatic triglycerides from male $EP3^{+/+}$ and $EP3^{-/-}$ mice, fed either HFD or control diet. N = 4 control + vehicle, 3 control + DG-041, 4 HFD + vehicle, 4 HFD + DG-041, 4 VHFD + vehicle, 5 VHFD + DG-041.

Parameter	control + vehicle		control + DG-041		HFD + vehicle		HFD + DG-041		VHFD + vehicle		VHFD + DG-041		ANOVA p-value		
	mean	SEM	mean	SEM	mean	SEM	mean	SEM	mean	SEM	mean	SEM	DG-041	Diet	Interaction
g/100 g fatty acids															
14:0	1.63	0.08	1.57	0.14	0.97	0.07	1.00	0.03	0.74	0.03	0.91	0.04	0.113	< 0.001	0.015
16:0	16.86	0.78	17.94	0.79	17.24	0.85	17.15	0.59	17.11	0.41	18.24	0.98	0.038	0.453	0.228
16:1	18.53	0.84	17.60	2.01	7.15	0.53	7.48	0.90	4.88	0.49	5.93	0.44	0.692	< 0.001	0.127
17:0	0.00	0.00	0.00	0.00	0.00	0.00	0.00	0.00	0.00	0.00	0.00	0.00	NA	NA	NA
18:0	1.18	0.23	1.27	0.24	2.58	0.23	2.62	0.36	3.24	0.10	3.02	0.18	0.737	< 0.001	0.382
18:1ω9	42.05	0.59	41.99	1.81	47.25	0.92	47.33	0.28	50.00	0.54	46.78	0.73	0.008	< 0.001	0.001
18:1ω7	4.42	0.26	4.44	0.18	1.88	0.22	2.12	0.21	1.46**	0.15	2.29**	0.33	0.002	< 0.001	0.010
18:2	14.34	0.49	14.00	1.40	21.41	0.59	20.55	0.46	21.63	0.34	21.55	0.31	0.116	< 0.001	0.455
18:3ω6	0.00	0.00	0.00	0.00	0.00	0.00	0.00	0.00	0.00	0.00	0.00	0.00	NA	NA	NA
18:3ω3	0.71	0.48	0.82	0.07	0.85	0.06	0.88	0.05	0.66	0.03	0.82	0.05	0.235	0.446	0.781
20:3ω6	0.00	0.00	0.00	0.00	0.13	0.09	0.19	0.01	0.11	0.01	0.03	0.08	0.720	< 0.001	0.062
20:4	0.28	0.32	0.37	0.32	0.41	0.10	0.48	0.05	0.18	0.03	0.39	0.06	0.110	0.206	0.695
20:5	0.00	0.00	0.00	0.00	0.00	0.00	0.00	0.00	0.00	0.00	0.00	0.00	NA	NA	NA
22:4ω6	0.00	0.00	0.00	0.00	0.03	0.05	0.03	0.06	0.00	0.00	0.00	0.00	0.948	0.166	0.948
22:5ω6	0.00	0.00	0.00	0.00	0.00	0.00	0.00	0.00	0.00	0.00	0.00	0.00	NA	NA	NA
22:5ω3	0.00	0.00	0.00	0.00	0.00	0.00	0.00	0.00	0.00	0.00	0.00	0.00	NA	NA	NA
22:6	0.00	0.00	0.00	0.00	0.13	0.09	0.19	0.02	0.02	0.03	0.03	0.06	0.240	< 0.001	0.458
Ratio															
16:0/16:1	0.91	0.08	1.03	0.08	2.43	0.24	2.33	0.38	3.54	0.49	3.10	0.39	0.310	< 0.001	0.255
18:0/18:1	0.03	0.00	0.03	0.00	0.05	0.01	0.05	0.01	0.06	0.00	0.06	0.00	0.908	< 0.001	0.822
Saturated / Unsaturated†	0.24	0.01	0.26	0.01	0.26	0.02	0.26	0.01	0.27	0.01	0.29	0.02	0.071	0.022	0.386

†(14:0+16:0+17:0+18:0) / (16:1+18:1ω9+18:1ω7+18:2+18:3ω6+18:3ω3+20:3ω6+20:4+20:5+22:4ω6+22:5ω6+22:5ω3+22:6)
* Bonferroni post-hoc comparison to * in same row P<0.05
** Bonferroni post-hoc comparison to ** in same row P<0.01
*** Bonferroni post-hoc comparison to *** in same row P<0.001
Statistically significant values are highlighted

Table 9. Fatty acid composition of skeletal muscle triglycerides
Fatty acid composition of skeletal muscle triglycerides from male $EP3^{+/+}$ and $EP3^{-/-}$ mice, fed either HFD or control diet. N = 4 control + vehicle, 3 control + DG-041, 4 HFD + vehicle, 4 HFD + DG-041, 4 VHFD + vehicle, 5 VHFD + DG-041.

EP3 antagonist decreases skeletal muscle triglcyerides

Because EP3$^{-/-}$ mice have been shown to have increased ectopic lipid accumulation when fed a HFD (Chapter III), ectopic lipid accumulation was measured in DG-041 treated mice that had been fed control diet, HFD, or VHFD. Triglycerides in both liver and skeletal muscle were increased with increasing dietary fat. DG-041 did not have a significant effect on liver triglcyerides (Figure 42A). Hepatic steatosis was observed in livers of mice fed HFD and VHFD, but did not appear to be affected by DG-041 (Figure 43). In skeletal muscle, DG-041 caused a marked reduction in the amount of triglyceride, especially in the mice fed VHFD (Figure 42B). Dietary fat and DG-041 treatment affected the fatty acid composition of hepatic and muscle triglycerides (Tables 1 and 2, respectively).

Discussion

Inbred strains of mice are known to have inherent genetic differences that affect their metabolic phenotype (601-609). C57BL/6×Balb/c F1 hybrid mice were investigated for their susceptibility to diet induced obesity and diabetes because C57BL/6 and Balb/c mice are known to differ in their susceptibility to HFD. C57BL/6 have been reported to be more prone to obesity than Balb/c mice (601), while Balb/c mice have more severe HFD-induced hepatic lipid accumulation (604-606). We chose to investigate C57BL/6×Balb/c F1 mice because they would have maximal heterozygosity while still being genetically and phenotypically uniform. These mice were found to be susceptible to diet induced obesity and insulin resistance. In fact, they consistently weighed more than C57BL/6 mice in previous studies (Chapter III). This is likely due to hybrid vigor of the C57BL/6×Balb/c F1 mice, although the differences due to maternal effects may also influence the phenotype of C57BL/6×Balb/c F1 mice (610-612).

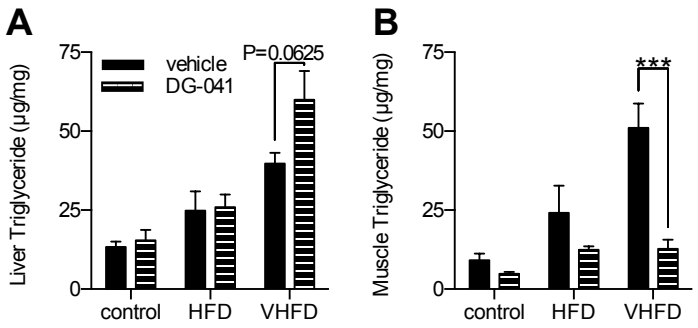

Figure 42. EP3 antagonist decreases skeletal muscle triglycerides

The effect of EP3 antagonist, DG-041, on triglyceride accumulation in ectopic tissues was measured in 21 week old C57BL/6×Balb/c mice fed control, HFD, or VHFD. **A.** Increasing amounts of dietary fat increased the amount of hepatic triglyceride (One-way ANOVA test for linear trend, P = 0.0234). DG-041 did not significantly affect the amount of triglycerides in the liver (Two-way ANOVA effect of drug, P = 0.132). **B.** Dietary fat affected the amount of triglycerides found in the skeletal muscle (One-way ANOVA test for linear trend, P = 0.0005). DG-041 significantly reduced the amount of triglycerides found in the skeletal muscle (Two-way ANOVA effect of drug, P = 0.0004). For all figures N = 4 control + vehicle, 3 control + DG-041, 4 HFD + vehicle, 4 HFD + DG-041, 4 VHFD + vehicle, 5 VHFD + DG-041. Values are expressed as mean ± SEM.

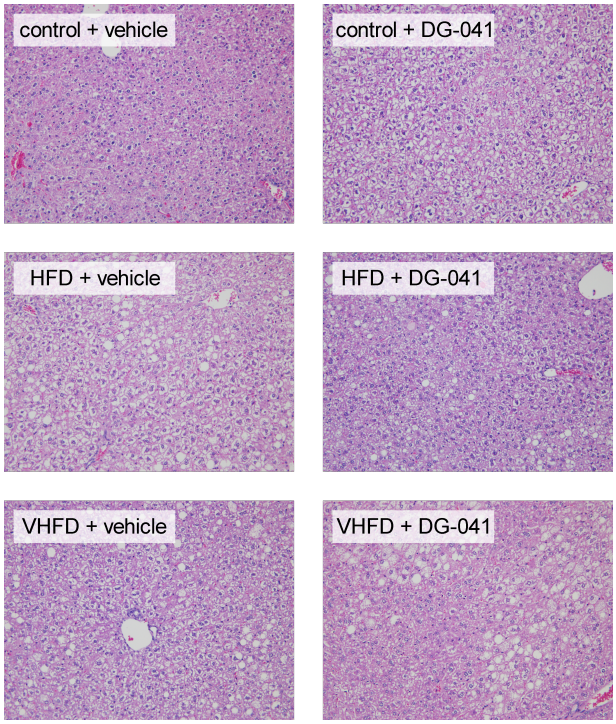

Figure 43. Hepatic steatosis in mice treated with EP3 antagonist
H&E staining of livers showed that dietary fat increased steatosis. No noticeable effect of DG-041 treatment on steatosis was observed. Images are a representative sample of sections from 4 control + vehicle, 3 control + DG-041, 3 HFD + vehicle, 4 HFD + DG-041, 4 VHFD + vehicle, 5 VHFD + DG-041.

In some studies, EP3 antagonists have been shown to increase GSIS in islets from diabetic individuals (74). Although my studies have not found an effect of DG-041 on isolated islets from HFD fed mice, $EP3^{-/-}$ mice fed HFD had increased plasma insulin suggesting decreased insulin clearance (Chapter III). The increased plasma insulin in $EP3^{-/-}$ mice fed HFD is associated with insulin resistance, which can be attributed to an increased ectopic lipid accumulation in these mice (Chapter III). In order to assess the effects of EP3 loss in a setting of diet induced obesity without the concomitant ectopic lipid accumulation and insulin insensitivity, EP3 antagonist, DG-041, was administered to C57BL/6×Balb/c mice fed control, HFD, or VHFD. Plasma insulin, blood glucose, and insulin sensitivity were not significantly affected by DG-041 treatment. These results may have been somewhat confounded by the administration of this drug, because treatment with the vehicle alone cause a reduction in body mass and fat mass in HFD and VHFD fed animals. This reduction in body mass and fat mass may have contributed toward a trend of improved insulin sensitivity in these mice.

Ectopic and plasma lipids were measured in these mice after treatment with EP3 antagonist, DG-041, for one week to determine if acute EP3 inhibition could affect lipid distribution. Mice treated with DG-041 were shown to have slightly increased hepatic triglycerides in VHFD fed animals, but surprisingly showed significantly decreased skeletal muscle triglycerides. These results are not consistent with increased lipolysis from adipocytes due to EP3 inhibition (101,284,Chapter III), which would result in increased triglycerides in both liver and skeletal muscle. These results are, however, consistent with decreased hepatic lipolysis. PGE_2 has been shown to decrease very-low-density lipoproteins (VLDL) secretion from hepatocytes (506,527). Decreased triglycerides during the rapid weight loss is not likely because both vehicle and DG-041 treated mice lost weight, but only DG-041 mice demonstrated

decreased skeletal muscle triglycerides. PGE_2 has also been shown to decrease the expression of genes involved in the packaging of lipoproteins: apolipoprotein B (ApoB) and microsomal triglyceride transfer protein (MTTP) (454,478). In $EP3^{-/-}$ mice *Apob* expression was decreased while the decrease in *Mttp* expression was not statistically significant (Chapter III). Decreased hepatic lipolysis is consistent with reduced triglyceride accumulation in most ectopic tissues, such as skeletal muscle, with increased hepatic triglycerides, a trend toward which was observed in mice fed VHFD and treated with DG-041. This effect of EP3 on hepatic lipolysis was likely not seen in $EP3^{-/-}$ mice fed HFD because the chronic EP3 inhibition and increased adipocyte lipolysis ultimately caused skeletal muscle triglyceride accumulation despite fewer triglycerides being released from the liver.

These studies suggest that EP3 may have a previously unrecognized role in metabolic physiology, being a regulator of hepatic lipolysis. Furthermore, they also establish that C57BL/6×Balb/c F1 mice are susceptible to diet induced obesity and insulin resistance.

CHAPTER VI

DISCUSSION AND FUTURE DIRECTIONS

The EP3 receptor affects obesity, insulin resistance, and glycemic control

The present studies highlight the importance of the EP3 receptor in obesity, insulin resistance, and glycemic control. Prior to beginning these studies, it was known that $EP3^{-/-}$ mice are obese, hyperglycemic, hyperinsulinemic, and insulin resistant when fed a breeder chow diet (102). There was also good evidence suggesting that PGE_2 signals through the EP3 receptor to inhibit GSIS (74,198-200,233). In addition, there was also ample evidence showing that PGE_2 inhibits lipolysis in adipocytes, also occurring in an EP3 dependent manner (101,284,390). In order to further elucidate the role of EP3 in metabolism, physiological studies were performed on global $EP3^{-/-}$ mice. These studies show that EP3 is a key regulator of multiple tissues and organs that are central to metabolic physiology.

Body Weight

These studies demonstrate that $EP3^{-/-}$ mice become obese only when they are fed a HFD. $EP3^{-/-}$ mice begin to become more obese than $EP3^{+/+}$ on a HFD after 14 weeks of age. When placed on a HFD after 14 weeks of age, $EP3^{-/-}$ mouse weights begin to diverge immediately suggesting that this phenotype is only observed in mature mice that have finished growing. An earlier study has shown that $EP3^{-/-}$ mice are obese (102). However, that study was the first report of obesity in $EP3^{-/-}$ mice, despite being published nine years after the first description of $EP3^{-/-}$ mice (310,555). The present studies show that there is a diet × genotype interaction with the EP3 genotype; $EP3^{-/-}$ mice only become obese on a HFD. The first report of obesity in $EP3^{-/-}$ mice utilized a breeder chow diet for all mice, which has a higher fat content than most standard chow

diets (102). It is possible that the obesity phenotype in $EP3^{-/-}$ mice was not observed for so long because most researchers maintained their mice on standard chow diets.

$EP3^{-/-}$ mice fed breeder chow were reported to be more obese due to increased food consumption (102). They also reported that $EP3^{-/-}$ mice were more active during the light cycle and that these mice spent their extra time awake eating. This increase in motor activity and food intake was not found throughout the day, but rather at a limited number of specific time points. These data are in contrast to what we have observed. We found that $EP3^{-/-}$ mice fed HFD have no differences in food consumption, but rather had decreased movement in the dark cycle. We hypothesize that the decreased activity is contributing to the observed increase in obesity in $EP3^{-/-}$ HFD fed mice.

Pancreas and islets

PGE_2 is typically thought to inhibit GSIS through the EP3 receptor (74,198-200,233). The current studies did not find that PGE_2-EP3 signaling inhibited GSIS. In fact, EP3 inhibition more frequently reduced GSIS contrary to our expected results. These results are in contrast to two prior studies which demonstrated that the EP3 antagonist L-798,106 improved GSIS (74,233). It should be noted that these studies found no effect of L-798,106 on islets at concentrations below 10 μM, while L-798,106 has an K_i for the human EP3 receptor of 300 pM (613). In Ins-1 (832/3) cells, L-798,106 only began to block the actions of 50 nM PGE_2 and 10 nM sulprostone at 100 nM and did not fully restore GSIS until 10 μM (74). Given that 100 nM is ~300 fold greater than K_i, more than a marginal response of L-798,106 is expected. The lack of effect of L-798,106 on GSIS at low concentrations is consistent with off target effects causing the observed responses at concentrations greater than 10 μM; especially off target effects at the EP4 receptor for which L-798,106 has a Ki of 916 nM (613).

IP-GTT studies also did not show an improvement in plasma insulin or glucose clearance in $EP3^{-/-}$ mice. Despite islets from $EP3^{-/-}$ mice not having improved GSIS, HFD fed $EP3^{-/-}$ mice were consistently hyperinsulinemic. These $EP3^{-/-}$ mice still exhibited increased plasma insulin in response to glucose challenge indicating that they maintained functional β-cells.

The elevated plasma insulin and glucose levels in $EP3^{-/-}$ HFD fed mice demonstrate that these mice are insulin resistant. Because insulin secretion does not appear to be increased by EP3 gene knockout, it is possible that the higher plasma insulin concentrations are due to reduced insulin clearance. $EP3^{-/-}$ HFD fed mice had lower blood glucose than did $EP3^{+/+}$ HFD fed mice when measured during *ad libitum* feeding. This indicates that these mice may be able to secrete enough insulin to overcome the insulin resistance and maintain normal glucose levels.

Adipose Tissue

PGE_2 has long been known to play an important role in obesity, having a role in both adipogenesis and adipocyte function, specifically lipolysis (390). C/EBPβ is transiently expressed during the early stages of adipogenesis and is critical for inducing the expression of PPARγ and C/EBPα, which are necessary for the final stages of adipogenesis (349,350). *Cebpb* was expressed at significantly higher levels in $EP3^{-/-}$ HFD fed mice indicating that adipogenesis might be increased. C/EBPβ is also a transcription factor for COX2 (346-348). Despite *Cebpb* up regulation, *Ptgs2* and PG levels were not different in the epididymal fat pads.

Numerous studies have shown that PGE_2 inhibits lipolysis in adipocytes (90-92,101,296,297,321,392-398,400). The main pathway leading to lipolysis from GPCRs is through the PKA pathway. Norepinephrine signaling in adipose tissue increases intracellular cAMP and thereby activates PKA, which phosphorylates and activates HSL, the rate-limiting step in lipolysis (401,403-405). PGE_2 inhibits norepinephrine stimulated lipolysis (92,393,417-

419). Several studies using EP receptor selective agonists suggest that PGE_2 inhibits lipolysis through the EP3 receptor (396,421,427). Recently two studies confirmed these results using EP3 selective antagonists, showing that their EP3 antagonists block PGE_2 mediated inhibition of cAMP accumulation (284) and FFA release (101). The present studies also confirm these prior results showing that a different EP3 antagonist and EP3 gene knockout block PGE_2 mediated inhibition of glycerol release. These three different mechanisms of measuring PGE_2 mediated inhibition of lipolysis each tell us something different. Measuring cAMP shows that canonical drivers of lipolysis are affected by EP3 (284). Glycerol is only released during the breakdown of triglycerides confirming that lipolysis is occurring. FFAs are the main lipids that are released into the circulatory system during lipolysis (101).

The cAMP-PKA signaling pathway that regulates lipolysis in adipocytes also regulates *Ucp1* expression (319). PGE_2 has been shown to increase *Ucp1* expression through the EP4 receptor, which classically opposes the actions of EP3 (282,286,324). In addition, increased *Ucp1* expression was found in the epdidymal fat pads of $AdPLA^{-/-}$ mice (101). *Ucp1* expression was greatly increased in the epididymal fat pads of HFD fed $EP3^{-/-}$ mice, which is consistent with increased lipolysis in these tissues. Increased *Ucp1* expression is expected to increase energy expenditure. Consistent with this, $EP3^{-/-}$ HFD fed mice were found to have increased CO_2 production.

We found that $EP3^{-/-}$ mice fed a HFD had a relative decrease in epididymal fat pad mass and adipocyte cell size in the heaviest $EP3^{-/-}$ HFD fed mice. In addition to having a loss of PGE_2-evoked inhibition of lipolysis, necrosis was increased in these same fat pads, both of which are likely to contribute to the loss of mass in the epididymal fat pads of the $EP3^{-/-}$ HFD fed mice.

The *in vivo* consequences of these defects were to cause a reallocation of lipid from adipose tissue to ectopic tissues in $EP3^{-/-}$ HFD fed mice.

Necrosis and macrophage infiltration were increased in the epididymal fat pads of $EP3^{-/-}$ HFD fed mice. Adipocyte cell death and macrophage infiltration also results in the release of lipids from adipocytes contributing to ectopic triglyceride accumulation (583-585). When C57BL/6 mice are fed a 60% very HFD adipocyte death in epididymal fat pads peaks at 16 weeks of very HFD feeding resulting in decreased adipocyte size, lighter epididymal fat pads, increased macrophage infiltration, increased liver mass and steatosis, and insulin resistance (584). This study noted a similar correlation to what we have observed; epididymal fat pad weight is positively correlated with body weight until ~35 grams but negatively correlated in mice ~40 grams and greater (584). In addition, they found that the mice with the lightest epididymal fat pads had increased liver weight suggesting lipid redistribution from the epididymal fat pads to ectopic tissues, which likely contributed to insulin resistance (584). We were not able to find a significant correlation between epididymal fat pad PGE_2 content or *Ptger3* gene expression with either body weight or epididymal fat pad mass, suggesting that lipolysis alone does not account for the striking relationship between body weight and epididymal fat pad mass found in $EP3^{-/-}$ mice. We hypothesize that increased adipocyte cell death in the heaviest mice, as evidenced by the disproportionately increased macrophage infiltration, accounts for the reduced epididymal fat pad mass and the severe increase in hepatic triglycerides in the heaviest $EP3^{-/-}$ mice.

An earlier study has shown that loss of PGE_2-EP3 mediated inhibition of lipolysis in $AdPLA^{-/-}$ mice causes ectopic lipid accumulation and insulin resistance due to FFAs leaving adipocytes and then being stored in ectopic tissues (101). My results provide confirmation of this

phenotype, with EP3$^{-/-}$ mice having both ectopic lipid accumulation and insulin resistance when fed a HFD. However, the phenotype of EP3$^{-/-}$ mice differs from that of AdPLA$^{-/-}$ mice in that EP3$^{-/-}$ mice are obese and have more adipose tissue whereas AdPLA$^{-/-}$ mice are lean. In addition, adipose tissue from EP3$^{-/-}$ HFD fed mice had increased expression of inflammatory genes, F4/80, TNF-α, IL-6, and MCP-1, which were unchanged in AdPLA$^{-/-}$ mice. This suggests that the lipolysis phenotype alone is sufficient to cause the increased ectopic lipid accumulation and insulin resistance. We hypothesize that the increased obesity and adiposity in EP3$^{-/-}$ HFD fed mice are due to decreased movement caused by a lack of EP3 signaling in the nervous system, while AdPLA$^{-/-}$ mice only have reduced EP3 signaling in adipose tissue and therefore do not have changes in behavior. It is also possible that the presence/lack of EP3 in the immune system contributes to the divergent phenotypes of EP3$^{-/-}$ and AdPLA$^{-/-}$ mice. It is our hypothesis that changes in the non-adipose tissues of EP3$^{-/-}$ mice contribute to the overall increased obesity, fat mass, and adipocyte size; whereas changes in the adipose tissue of EP3$^{-/-}$ mice, namely lipolysis and cell death, contribute to the proportional decrease of epididymal fat pad mass and adipocyte size and the increased ectopic lipid accumulation.

Immune cells and inflammation

PGE_2 is well known to be an important regulator of inflammation (41,44). Macrophage infiltration of epdidymal fat pads and liver tissue were measured. F4/80, a marker of macrophage, gene expression was elevated in the epididymal fat pads of EP3$^{-/-}$ HFD fed mice indicating increased macrophage infiltration. Gene expression of proinflammatory cytokines, TNF-α, MCP-1, and IL-6, were also increased in the epididymal fat pads of EP3$^{-/-}$ HFD fed mice. No change in macrophage infiltration was observed in the liver. This indicates that the inflammation observed in the adipose tissue is likely due to a local change in the adipocytes and

not due to a global change in the macrophage themselves. Necrosis and increased lipolysis were observed these epididymal fat pads, both of which could contribute to macrophage recruitment in this tissue (574,614).

Liver

Obesity and other models of liver damage increase hepatic PGE_2 production and expression of PGE_2 generating enzymes (454,458,465). The current studies show that the livers of $EP3^{-/-}$ mice develop steatosis and acquire excess triglycerides when the mice are fed a HFD. Increased liver weight was also observed in $EP3^{-/-}$ mice fed a breeder chow diet, though progression of fatty liver disease was not evaluated in that study (102). It is likely that the excess triglyceride accumulation in the livers of $EP3^{-/-}$ HFD fed mice is due to increased lipolysis from the adipose tissue, with the liver simply acting as a secondary storage site.

Though our hypothesis is that in our model the steatotic livers are due to defects in adipose tissue, PGE_2 has been reported to increase triglyceride content in hepatocytes by suppressing very low-density lipoprotein synthesis and triglyceride transport (454,506,527). In the current studies, mice treated with an EP3 antagonist have decreased muscle triglycerides, which is consistent with decreased VLDL transport out of the liver. In addition, $EP3^{-/-}$ mice have decreased *Apob* expression, but *Mttp* expression was unchanged. It should be noted that over 50% of ApoB protein is degraded and not used for VLDL synthesis, so the decrease in *Apob* expression itself does not indicate changes in hepatic lipolysis. Studies examining PGE_2 mediated inhibition of hepatic lipolysis suggests that PGE_2 mediates these effects via an EP2/4 mediated signaling pathway (465). Because the signaling pathway of EP3 classically opposes that of EP2/4, it is possible that EP3 plays a protective role in the liver mitigating EP2/4 induced hepatic lipid accumulation.

Future Directions

The present studies show a severe phenotype of metabolic dysfunction in mice with a global EP3 gene deletion in a setting of diet induced obesity that is likely due to the important functions of the EP3 receptor in multiple organ systems. In addition to characterizing the phenotypes of global $EP3^{-/-}$ mice, I have also investigated the effects of EP3 in isolated islets and adipocytes in an *ex vivo* setting. Further studies utilizing isolated tissues and cells from $EP3^{-/-}$ mice, as well as the use of temporal and tissue specific EP3 gene deletion models in a setting of diet induced obesity, will greatly aid in the understanding of how the EP3 receptor functions in the various tissues to affect metabolic physiology. In addition to PGE_2-EP3 signaling other PG receptors also play a role in these metabolically important tissues and the roles of many of these other receptors have not been well characterized in a setting of metabolic stress.

Further elucidation of the obesity and insulin resistance phenotypes

The present studies show a striking diet × genotype interaction where $EP3^{-/-}$ mice are obese when fed a HFD but not when they are fed a control or standard chow diet. One of the main unanswered questions is: why are $EP3^{-/-}$ mice are only more obese on the HFD, but maintain similar body weights on control and standard chow diet? The present studies suggest that $EP3^{-/-}$ HFD fed mice are less active than $EP3^{+/+}$, but do not investigate control diet fed mice. An earlier study has suggested that $EP3^{-/-}$ mice become more obese due to hyperphagia and night eating (102). If $EP3^{-/-}$ mice are consistently hyperphagic or less active, then why do they not also gain more weight when they are fed diets with a lower fat content? The observation that the $EP3^{-/-}$ mice only display the obesity phenotype on the HFD suggests that there is some mechanism that is causing them to either have increase food consumption or decreased activity only when they are faced with a HFD challenge. Measuring food consumption and energy

expenditure in mice fed both control and HFD will be necessary to determine if diet affects food consumption or activity in $EP3^{-/-}$ mice. It would also be bennefical if paired mice could be obtained from the same litter because maternal effects may influence behavior and obesity susceptibility.

Further studies characterizing insulin resistance in $EP3^{-/-}$ mice may be warranted. The HOMA-IR, used in the present studies, suggests that $EP3^{-/-}$ HFD fed mice are insulin insensitive, but this test has only been validated in humans. The ITTs performed here also suggest that these mice are insulin resistant, but they are confounded by the increased body weight of $EP3^{-/-}$ HFD fed mice, the higher fasting glucose levels fed mice, and the short half-live of insulin of $EP3^{-/-}$ HFD (579). The hyperinsulinemic-euglycemic clamp is the gold standard for determining insulin resistance. Furthermore, this test can be coupled with a radiolabeled glucose tracer to show which tissues are insulin resistant. From my studies, we can hypothesize that liver and skeletal muscle from $EP3^{-/-}$ HFD fed mice are insulin insensitive, but this has not been shown. It would also be interesting to determine if adipose tissue is insulin resistant *in vivo*, as I have only shown that the adipocytes from chow fed mice are insulin sensitive *ex vivo*. PGE_2 has been show to increase glucose metabolism in adipocytes (409), hence the effect of EP3 on adipocyte insulin sensitivity may be of interest. The use of hyperinsulinemic-euglycemic clamps would be especially interesting in pair fed mice, such a study would be useful in determining whether $EP3^{-/-}$ HFD mice are insulin resistant in the absence of hyperphagia.

It is possible that $EP3^{-/-}$ mice have a defect in their reward circuitry where they will become more easily "addicted" to the HFD and not to lower fat diets. If this were the case, then these mice would be expected to only consume more food when fed the HFD. In order to totally eliminate the overeating and/or eating at the wrong time component of these studies, the current

studies presented could be repeated in pair fed mice. If $EP3^{+/+}$ and $EP3^{-/-}$ mice were fed the same amount of control or HFD each morning and evening, then the effect of EP3 on glucose homeostasis and insulin sensitivity could be determined in the absence of an overeating/nighteating phenotype. Though caloric intake would be controlled, $EP3^{-/-}$ mice may still be more obese than $EP3^{+/+}$ due to decreased energy expenditure.

Characterizing the role of EP3 in energy expenditure and thermogenesis

It is possible that EP3 plays a role in thermogenesis and energy expenditure. EP3 is already well known to be necessary for pyrogen-induced fever (309-311). Hence, it is also possible that EP3 may play a role in normal thermogenesis. Through its role in fever, EP3 regulates sympathetic nervous signaling to adipocytes which increases lipolysis and uncoupled thermogenesis. In addition to potentially regulating norepinephrine signaling to adipose tissue, EP3 is also expressed on adipocytes and mediates PGE_2's inhibition of lipolysis which is linked to thermogenesis through similar signaling mechanisms.

$EP3^{-/-}$ HFD fed mice have increased *Ucp1* expression in epididymal fat pads, but it is not clear if this leads to a significant increased uncoupled thermogenesis, though we did find an increase in CO_2 production from $EP3^{-/-}$ HFD fed mice. In addition, epididymal adipose tissue is not the main site of adipocyte thermogenesis, so it would be interesting to determine if *Ucp1* expression is increased in other white adipose tissue in $EP3^{-/-}$ HFD fed mice. Thermogenic capacity could be tested in $EP3^{-/-}$ mice by examining oxygen consumption, cold tolerance, and changes in body temperature in response to a β_3 adrenergic receptor specific agonist. Furthermore, if global EP3 deletion is found to affect thermogenesis, it would be of interest to determine the contribution of EP3 in both adipocytes and the preoptic nucleus.

Further characterization of the role of EP3 in adipose tissue

The role of EP3 in these other adipose depots should also be examined because epididymal fat pads are not functionally representative of all fat depots in mice. $EP3^{-/-}$ mice are more obese than $EP3^{+/+}$ mice when fed HFD; but in the largest $EP3^{-/-}$ mice, the epididymal fat pads were smaller. We attributed this to decreased adipocyte size due to necrosis and lipolysis, but this does not explain where the extra weight is being stored. Some extra weight is being stored in the liver and other ectopic tissues, but it is has not been determined whether other fat depots have altered lipid storage in $EP3^{-/-}$ mice.

$EP3^{-/-}$ mice tended to have larger epididymal fat pads than $EP3^{+/+}$ when fed a HFD. Adipocyte size was increased in $EP3^{-/-}$ mice accounting for some of the increased mass. It is also possible that adipogenesis was increased in $EP3^{-/-}$ HFD fed mice and that a relative decrease in adipogenesis in the heaviest $EP3^{-/-}$ HFD fed mice could account for some of the relatively decreased fat pad mass. Expression of *Cebpb* was increased in $EP3^{-/-}$ HFD fed epididymal fat pads possibly indicating increased adipogenesis. Further studies examining the expression of C/EBPβ target genes and late stage adipogenesis transcription factors, *Pparg* and *Cebpa*, will be useful for determining whether adipogenesis is altered in $EP3^{-/-}$ mice. PGC-1α is a cofactor that modulates PPARγ's activity. Transcription of the gene encoding *Pgc1a* can be induced by p38α MAPK phosphorylation of the ATF-2 transcription factor (319). p38α MAPK activation in adipocytes can be mediated by the same cAMP-PKA signaling that also activates lipolysis. Because of this, we can predict that future studies will find *Pgc1a* expression increased in the epididymal fat pads of $EP3^{-/-}$ HFD fed mice which may play a role in adipocyte proliferation and differentiation in these tissues. In addition to measuring the expression of adipogenic genes, future studies examining the role of EP3 in adipogenesis should also examine more direct

measurements of proliferation. Proliferation and differentiation of $EP3^{-/-}$ mouse embryonic fibroblasts may be examined to determine the EP3's role in adipogenesis *in vitro*.

Studies examining the phenotype of an adipocyte specific EP3 knockout mouse would be of interest to determine which of the phenotypes I have observed in the global $EP3^{-/-}$ model are caused by the lack of EP3 in adipose tissue. I have hypothesized that the lipid redistribution and insulin resistance phenotypes are due to increased adipocyte lipolysis and cell death. However, it is not certain that all of these phenotypes are completely due to defects in the adipocytes.

Further characterization of the role of EP3 in liver tissue

I have hypothesized that the lipid redistribution to liver and insulin resistance phenotypes observed in $EP3^{-/-}$ mice are due to changes in the adipose tissue. It is possible that the lack of EP3 in the liver itself contributes to the increased hepatic lipid accumulation in global $EP3^{-/-}$ HFD fed mice. I have already shown that $EP3^{-/-}$ livers have decreased *Cpt1a* expression, which is consistent with reduced β-oxidation. Further experiments, such as measuring hepatocyte cellular metabolism, are needed to determine if hepatic β-oxidation is reduced in $EP3^{-/-}$ mice. Also, $EP3^{-/-}$ mice may also have reduced hepatic lipolysis. Again further experiments are needed to determine if this occurs. Measuring plasma triglyceride levels following the administration of a VLDL uptake inhibitor could be used to assess hepatic lipolysis *in vivo*.

PGE_2 has also been implicated in hepatic gluconeogenesis (75,76,482,494,505-516). The lack of EP3 in the liver may be contributing to the elevated glucose levels in $EP3^{-/-}$ HFD fed mice. Glycogen content from the livers can be measured to determine if there are defects in glycogen storage and more direct measurements of gluconeogenesis may be obtained utilizing cultured hepatocytes.

Further characterization of the role of EP3 in the pancreas and islets

The current studies have shown that EP3 inhibition, by either gene knockout or receptor blockade, does not improve GSIS in isolated islets or *in vivo*. Assessment of glucose homeostasis by IP-GTT showed no significant difference between $EP3^{+/+}$ and $EP3^{-/-}$ regardless of diet. Future studies should investigate the effect of global EP3 gene knockout on insulin secretion and glucose homeostasis in an oral glucose tolerance test (O-GTT). The lack of EP3 in islets may be beneficial in an O-GTT because incretins, which are secreted by the intestines, are expected to raise β-cell cAMP above baseline levels. Increasing intracellular cAMP above basal levels has been postulated to be necessary to observe the effects of PGE_2 in islets.

I did not find a significant change in the amount of total pancreatic insulin. However, our collaborators, Maureen Gannon and her lab, have found that the mice utilized for these studies have increased β-cell replication, with replication occurring after 16 weeks of HFD feeding. This is consistent with prior studies that have shown that PGE_2 inhibits β-cell proliferation (188,195) and that $G\alpha_z$ knockout mice have increase β-cell replication and mass (134). Further investigation into the mechanism behind EP3 inhibition of β-cell proliferation is warranted. Though EP3 antagonists may not be useful for treating diabetes, blockade of similar receptors may be useful for improving β-cell proliferation and mass.

In addition to affecting insulin secretion, EP3 may also play a role in other cell types in the pancreas. Several studies have suggested that PGE_2 increases glucagon secretion *in vivo* (183,189,208-210,217,218,234). When glucagon secretion was measured from islets treated with an EP3 antagonist in our studies, no clear result was obtained. Examining glucagon secretion from $EP3^{-/-}$ islets will be useful to determine the role of EP3 in α-cells. Furthermore, *in vivo* glucagon levels should also be measured as circulating glucagon plays a major role in glucose

homeostasis. In addition to having an effect on α-cells, my ligand binding studies suggest that EP3 is also be expressed in the exocrine tissue of the pancreas. Exocrine tissue in the pancreas secretes digestives enzymes and hence EP3 deletion from these tissues may affect digestion. This could lead to changes in food absorption that could affect energy intake, obesity, and diabetes.

Further characterization of the role of EP3 in immune cells

PGE_2 and EP3 are important regulators of immune function (41,44). Inflammation has been shown to be an important contributor to the pathogenesis of obesity and insulin resistance (23-25). The current studies show increased inflammation in the epididymal fat pads but not the liver of $EP3^{-/-}$ HFD fed mice. This suggests that these changes in inflammation are due to localized changes in these tissues and not a change in immune cell function. However, it has yet to be established whether EP3 genotype in the immune cells affects inflammation or the adiposity phenotype. This could be investigated by utilizing models of bone marrow and/or T cell transplant in $EP3^{+/+}$ and $EP3^{-/-}$ mice.

The role of prostaglandins in diabetic complications

Aside from the aforementioned tissues and organ systems, PGs play an important role in many other physiological systems. The involvement of PGs in these other physiological processes may implicate PGs in other diabetic complications such as nephropathy, retinopathy, peripheral neuropathy, and vascular complications (615). EP3 is also involved in adrenocorticotropic hormone release in response to endotoxin implicating EP3 in regulation of the hypothalamic-pituitary-adrenal (HPA) axis (616). By regulating the HPA axis, EP3 may also exert some of its effects on obesity and glucose homeostasis.

Summary

In closing, the present studies have answered several important questions about the role of the EP3 receptor in metabolic physiology. Studies by Sanchez-Alavez, *et al.* have shown obesity in $EP3^{-/-}$ mice, which was in disagreement with prior studies that found no differences in body weight (102,310,555). My studies have reconciled these opposing results by showing that $EP3^{-/-}$ mice are only obese when fed a diet containing high dietary fat. In addition, the studies by Sanchez-Alavez, *et al.* reported that $EP3^{-/-}$ mice are insulin resistant (102). My studies have demonstrated that $EP3^{-/-}$ mice are likely insulin resistant due to increased ectopic lipid accumulation. Furthermore, my studies are the first studies, to my knowledge, to utilize islets and adipocytes isolated from $EP3^{-/-}$ animals to investigate the effects of EP3 on GSIS and lipolysis, respectively. Despite my extensive phenotypic characterization of $EP3^{-/-}$ mice during HFD feeding, the present studies have only served to create more questions. Further studies will provide tissue specific information about the role of the EP3 receptor in diet induced obesity and diabetes.

REFERENCES

1. Stein CJ, Colditz GA. The epidemic of obesity. *J Clin Endocrinol Metab.* 2004;89(6):2522-2525.

2. Yang L, Colditz GA. Prevalence of Overweight and Obesity in the United States, 2007-2012. *JAMA internal medicine.* 2015;175(8):1412-1413.

3. Parikh NI, Pencina MJ, Wang TJ, Lanier KJ, Fox CS, D'Agostino RB, Vasan RS. Increasing trends in incidence of overweight and obesity over 5 decades. *Am J Med.* 2007;120(3):242-250.

4. Flegal KM, Graubard BI, Williamson DF, Gail MH. Cause-specific excess deaths associated with underweight, overweight, and obesity. *JAMA.* 2007;298(17):2028-2037.

5. Zamosky L. The obesity epidemic. While America swallows $147 billion in obesity-related healthcare costs, physicians called on to confront the crisis. *Medical economics.* 2013;90(4):14-17.

6. Bays HE, Chapman RH, Grandy S, Shield Investigators' Group. The relationship of body mass index to diabetes mellitus, hypertension and dyslipidaemia: comparison of data from two national surveys. *Int J Clin Pract.* 2007;61(5):737-747.

7. Hartz AJ, Rupley DC, Jr., Kalkhoff RD, Rimm AA. Relationship of obesity to diabetes: influence of obesity level and body fat distribution. *Preventive medicine.* 1983;12(2):351-357.

8. Koh-Banerjee P, Wang Y, Hu FB, Spiegelman D, Willett WC, Rimm EB. Changes in body weight and body fat distribution as risk factors for clinical diabetes in US men. *Am J Epidemiol.* 2004;159(12):1150-1159.

9. Dall TM, Mann SE, Zhang YD, Quick WW, Seifert RF, Martin J, Huang EA, Zhang SP. Distinguishing the Economic Costs Associated with Type 1 and Type 2 Diabetes. *Population Health Management.* 2009;12(2):103-110.

10. Centers for Disease Control and Prevention. National diabetes fact sheet: national estimates and general information on diabetes and prediabetes in the United States, 2011. In: U.S. Department of Health and Human Services - Centers for Disease Control and Prevention, ed. Atlanta, GA2011.

11. Prentki M, Nolan CJ. Islet β cell failure in type 2 diabetes. *J Clin Invest.* 2006;116(7):1802-1812.

12. Mudaliar S. Choice of early treatment regimen and impact on beta-cell preservation in type 2 diabetes. *Int J Clin Pract.* 2013;67(9):876-887.

13. Banting FG, Best CH, Collip JB, Campbell WR, Fletcher AA. Pancreatic Extracts in the Treatment of Diabetes Mellitus. *Canadian Medical Association journal.* 1922;12(3):141-146.

14. Henquin JC. The fiftieth anniversary of hypoglycaemic sulphonamides. How did the mother compound work? *Diabetologia.* 1992;35(10):907-912.

15. Malhotra R, Singh L, Eng J, Raufman JP. Exendin-4, a new peptide from *Heloderma suspectum* venom, potentiates cholecystokinin-induced amylase release from rat pancreatic acini. *Regul Pept.* 1992;41(2):149-156.

16. Bailey CJ, Turner RC. Drug therapy - Metformin. *New Engl J Med.* 1996;334(9):574-579.

17. Lucis OJ. The status of metformin in Canada. *Canadian Medical Association journal.* 1983;128(1):24-26.

18. American Diabetes Association. Standards of medical care in diabetes--2014. *Diabetes Care.* 2014;37 Suppl 1:S14-80.
19. Spiegelman BM. PPAR-γ: adipogenic regulator and thiazolidinedione receptor. *Diabetes.* 1998;47(4):507-514.
20. Sears DD, Hsiao G, Hsiao A, Yu JG, Courtney CH, Ofrecio JM, Chapman J, Subramaniam S. Mechanisms of human insulin resistance and thiazolidinedione-mediated insulin sensitization. *Proc Natl Acad Sci U S A.* 2009;106(44):18745-18750.
21. Deans KA, Sattar N. "Anti-inflammatory" drugs and their effects on type 2 diabetes. *Diabetes technology & therapeutics.* 2006;8(1):18-27.
22. Menkin V. Diabetes and Inflammation. *Science.* 1941;93(2419):456-458.
23. Donath MY, Shoelson SE. Type 2 diabetes as an inflammatory disease. *Nature reviews Immunology.* 2011;11(2):98-107.
24. Pickup JC. Inflammation and activated innate immunity in the pathogenesis of type 2 diabetes. *Diabetes Care.* 2004;27(3):813-823.
25. Wellen KE, Hotamisligil GS. Inflammation, stress, and diabetes. *J Clin Invest.* 2005;115(5):1111-1119.
26. Bourlier V, Bouloumie A. Role of macrophage tissue infiltration in obesity and insulin resistance. *Diabetes Metab.* 2009;35(4):251-260.
27. Ehses JA, Perren A, Eppler E, Ribaux P, Pospisilik JA, Maor-Cahn R, Gueripel X, Ellingsgaard H, Schneider MK, Biollaz G, Fontana A, Reinecke M, Homo-Delarche F, Donath MY. Increased number of islet-associated macrophages in type 2 diabetes. *Diabetes.* 2007;56(9):2356-2370.
28. Olefsky JM, Glass CK. Macrophages, inflammation, and insulin resistance. *Annu Rev Physiol.* 2010;72:219-246.
29. Pillon NJ, Bilan PJ, Fink LN, Klip A. Cross-talk between skeletal muscle and immune cells: muscle-derived mediators and metabolic implications. *Am J Physiol Endocrinol Metab.* 2013;304(5):E453-465.
30. Weisberg SP, McCann D, Desai M, Rosenbaum M, Leibel RL, Ferrante AW, Jr. Obesity is associated with macrophage accumulation in adipose tissue. *J Clin Invest.* 2003;112(12):1796-1808.
31. Xu H, Barnes GT, Yang Q, Tan G, Yang D, Chou CJ, Sole J, Nichols A, Ross JS, Tartaglia LA, Chen H. Chronic inflammation in fat plays a crucial role in the development of obesity-related insulin resistance. *J Clin Invest.* 2003;112(12):1821-1830.
32. Bunout D, Muñoz C, López M, de la Maza MP, Schlesinger L, Hirsch S, Pettermann M. Interleukin 1 and tumor necrosis factor in obese alcoholics compared with normal-weight patients. *Am J Clin Nutr.* 1996;63(3):373-376.
33. Pradhan AD, Manson JE, Rifai N, Buring JE, Ridker PM. C-reactive protein, interleukin 6, and risk of developing type 2 diabetes mellitus. *JAMA.* 2001;286(3):327-334.
34. Visser M, Bouter LM, McQuillan GM, Wener MH, Harris TB. Elevated C-reactive protein levels in overweight and obese adults. *JAMA.* 1999;282(22):2131-2135.
35. Samuel VT, Shulman GI. Mechanisms for insulin resistance: common threads and missing links. *Cell.* 2012;148(5):852-871.
36. Cai D, Yuan M, Frantz DF, Melendez PA, Hansen L, Lee J, Shoelson SE. Local and systemic insulin resistance resulting from hepatic activation of IKK-β and NF-κB. *Nat Med.* 2005;11(2):183-190.

37. Arkan MC, Hevener AL, Greten FR, Maeda S, Li Z-W, Long JM, Wynshaw-Boris A, Poli G, Olefsky J, Karin M. IKK-β links inflammation to obesity-induced insulin resistance. *Nat Med.* 2005;11(2):191-198.
38. Gao Z, Hwang D, Bataille F, Lefevre M, York D, Quon MJ, Ye J. Serine phosphorylation of insulin receptor substrate 1 by inhibitor κB kinase complex. *J Biol Chem.* 2002;277(50):48115-48121.
39. McDaniel ML, Kwon G, Hill JR, Marshall CA, Corbett JA. Cytokines and nitric oxide in islet inflammation and diabetes. *P Soc Exp Biol Med.* 1996;211(1):24-32.
40. Osborn O, Gram H, Zorrilla EP, Conti B, Bartfai T. Insights into the roles of the inflammatory mediators IL-1, IL-18 and PGE2 in obesity and insulin resistance. *Swiss Med Wkly.* 2008;138(45-46):665-673.
41. Aoki T, Narumiya S. Prostaglandins and chronic inflammation. *Trends Pharmacol Sci.* 2012;33(6):304-311.
42. Harris SG, Padilla J, Koumas L, Ray D, Phipps RP. Prostaglandins as modulators of immunity. *Trends in Immunology.* 2002;23(3):144-150.
43. Hata AN, Breyer RM. Pharmacology and signaling of prostaglandin receptors: multiple roles in inflammation and immune modulation. *Pharmacol Ther.* 2004;103(2):147-166.
44. Kawahara K, Hohjoh H, Inazumi T, Tsuchiya S, Sugimoto Y. Prostaglandin E-induced inflammation: Relevance of prostaglandin E receptors. *Biochim Biophys Acta.* 2015;1851(4):414-421.
45. Narumiya S. Prostanoids and inflammation: a new concept arising from receptor knockout mice. *J Mol Med.* 2009;87(10):1015-1022.
46. Hayashino Y, Hennekens CH, Kurth T. Aspirin use and risk of type 2 diabetes in apparently healthy men. *Am J Med.* 2009;122(4):374-379.
47. Vane JR. Inhibition of prostaglandin synthesis as a mechanism of action for aspirin-like drugs. *Nature: New biology.* 1971;231(25):232-235.
48. Kopp E, Ghosh S. Inhibition of NF-κB by sodium salicylate and aspirin. *Science.* 1994;265(5174):956-959.
49. Goldfine AB, Fonseca V, Shoelson SE. Therapeutic approaches to target inflammation in type 2 diabetes. *Clin Chem.* 2011;57(2):162-167.
50. Rumore MM, Kim KS. Potential role of salicylates in type 2 diabetes. *Ann Pharmacother.* 2010;44(7-8):1207-1221.
51. Piria M. Sur de nouveaux produits extraits de la salicine. *Comptes rendus.* 1838;6:620-624.
52. Buchner A. Ueber das Rigatellische Fiebermittel und über eine in der Weidenrinde entdeckte alcaloidische Substanz. *Repertorium für die Pharmacie.* 1828;29:405-420.
53. Jack DB. One hundred years of aspirin. *Lancet.* 1997;350(9075):437-439.
54. Stone E. An Account of the Success of the Bark of the Willow in the Cure of Agues. In a Letter to the Right Honourable George Earl of Macclesfield, President of R. S. from the Rev. Mr. Edmund Stone, of Chipping-Norton in Oxfordshire. *Philosophical Transactions.* 1763;53:195-200.
55. Ebstein W. Zur Therapie des Diabetes mellitus, insbesondere über die Anwendung des salicylsauren Natron bei demselben. *Berliner Klinische Wochenschrift.* 1876;13:337–340.
56. Williamson RT. On the Treatment of Glycosuria and Diabetes Mellitus with Sodium Salicylate. *Br Med J.* 1901;1(2100):760-762.

57. Reid J, Macdougall AI, Andrews MM. Aspirin and diabetes mellitus. *Br Med J.* 1957;2(5053):1071-1074.
58. Reid J, Lightbody TD. The insulin equivalence of salicylate. *Br Med J.* 1959;1(5126):897-900.
59. Field JB, Boyle C, Remer A. Effect of salicylate infusion on plasma-insulin and glucose tolerance in healthy persons and mild diabetics. *Lancet.* 1967;1(7501):1191-1194.
60. Kurzrok R, Lieb CC. Biochemical Studies of Human Semen. II. The Action of Semen on the Human Uterus. *Proc Soc Exp Biol Med.* 1930;28:268-272.
61. von Euler US. Über die Spezifische Blutdrucksenkende Substanz des Menschlichen Prostata- und Samenblasensekretes. *Klin Wochenschr.* 1935;14(33):1182-1183.
62. Bergström S, Sjövall J. The Isolation of Prostaglandin. *Acta Chem Scan.* 1957;11(6):1086.
63. Bergström S, Sjövall J. The isolation of prostaglandin E from sheep prostate glands. *Acta Chem Scand.* 1960;14:1701-1705.
64. Bergström S, Duner H, von Euler US, Pernow B, Sjövall J. Observations on the effects of infusion of prostaglandin E in man. *Acta Physiol Scand.* 1959;45:145-151.
65. Bergström S, Sjövall J. The Isolation of Prostaglandin F from Sheep Prostate Glands. *Acta Chem Scand.* 1960;14:1693-1700.
66. Hamberg M, Svensson J, Samuelsson B. Thromboxanes: a new group of biologically active compounds derived from prostaglandin endoperoxides. *Proc Natl Acad Sci U S A.* 1975;72(8):2994-2998.
67. Nugteren DH, Hazelhof E. Isolation and properties of intermediates in prostaglandin biosynthesis. *Biochim Biophys Acta.* 1973;326(3):448-461.
68. Whittaker N, Bunting S, Salmon J, Moncada S, Vane JR, Johnson RA, Morton DR, Kinner JH, Gorman RR, McGuire JC, Sun FF. The chemical structure of prostaglandin X (prostacyclin). *Prostaglandins.* 1976;12(6):915-928.
69. Luo C, Kallajoki M, Gross R, Mulari M, Teros T, Ylinen L, Mäkinen M, Laine J, Simell O. Cellular distribution and contribution of cyclooxygenase COX-2 to diabetogenesis in NOD mouse. *Cell Tissue Res.* 2002;310(2):169-175.
70. Robertson RP, Gavareski DJ, Porte D, Bierman EL. Inhibition of in vivo insulin secretion by prostaglandin E_1. *J Clin Invest.* 1974;54(2):310-315.
71. Robertson RP, Tsai P, Little SA, Zhang HJ, Walseth TF. Receptor-mediated adenylate cyclase-coupled mechanism for PGE_2 inhibition of insulin secretion in HIT cells. *Diabetes.* 1987;36(9):1047-1053.
72. Sugimoto Y, Negishi M, Hayashi Y, Namba T, Honda A, Watabe A, Hirata M, Narumiya S, Ichikawa A. Two isoforms of the EP_3 receptor with different carboxyl-terminal domains. Identical ligand binding properties and different coupling properties with G_i proteins. *J Biol Chem.* 1993;268(4):2712-2718.
73. Chissoe S, Inventor; 20080200568 , assignee. Genes associated with type ll diabetes mellitus. 2008.
74. Kimple ME, Keller MP, Rabaglia MR, Pasker RL, Neuman JC, Truchan NA, Brar HK, Attie AD. Prostaglandin E_2 Receptor, EP3, Is Induced in Diabetic Islets and Negatively Regulates Glucose- and Hormone-Stimulated Insulin Secretion. *Diabetes.* 2013;62(6):1904-1912.

75. DeRubertis FR, Zenser TV, Curnow RT. Inhibition of glucagon-mediated increases in hepatic cyclic adenosine 3', 5'-monophosphate by prostaglandin E_1 and E_2. *Endocrinology.* 1974;95(1):93-101.
76. Levine RA, Schwartzel EH, Jr. Prostaglandin E_2 inhibition of glucagon-induced hepatic gluconeogenesis and cyclic adenosine 3',5'-monophosphate accumulation. *Biochem Pharmacol.* 1980;29(5):681-684.
77. Yin M-J, Yamamoto Y, Gaynor RB. The anti-inflammatory agents aspirin and salicylate inhibit the activity of IκB kinase-β. *Nature.* 1998;396(6706):77-80.
78. Kim JK, Kim Y-J, Fillmore JJ, Chen Y, Moore I, Lee J, Yuan M, Li ZW, Karin M, Perret P, Shoelson SE, Shulman GI. Prevention of fat-induced insulin resistance by salicylate. *J Clin Invest.* 2001;108(3):437-446.
79. Yuan M, Konstantopoulos N, Lee J, Hansen L, Li Z-W, Karin M, Shoelson SE. Reversal of obesity- and diet-induced insulin resistance with salicylates or targeted disruption of Ikkβ. *Science.* 2001;293(5535):1673-1677.
80. Mork NL, Robertson RP. Effects of nonsteroidal antiinflammatory drugs in conventional dosage on glucose homeostasis in patients with diabetes. *West J Med.* 1983;139(1):46-49.
81. Faghihimani E, Aminorroaya A, Rezvanian H, Adibi P, Ismail-Beigi F, Amini M. Reduction of insulin resistance and plasma glucose level by salsalate treatment in persons with prediabetes. *Endocr Pract.* 2012;18(6):826-833.
82. Fleischman A, Shoelson SE, Bernier R, Goldfine AB. Salsalate improves glycemia and inflammatory parameters in obese young adults. *Diabetes Care.* 2008;31(2):289-294.
83. Goldfine AB, Silver R, Aldhahi W, Cai D, Tatro E, Lee J, Shoelson SE. Use of salsalate to target inflammation in the treatment of insulin resistance and type 2 diabetes. *Clinical and translational science.* 2008;1(1):36-43.
84. Goldfine AB, Fonseca V, Jablonski KA, Pyle L, Staten MA, Shoelson SE. The effects of salsalate on glycemic control in patients with type 2 diabetes: a randomized trial. *Ann Intern Med.* 2010;152(6):346-357.
85. Goldfine AB, Conlin PR, Halperin F, Koska J, Permana P, Schwenke D, Shoelson SE, Reaven PD. A randomised trial of salsalate for insulin resistance and cardiovascular risk factors in persons with abnormal glucose tolerance. *Diabetologia.* 2013;56(4):714-723.
86. Goldfine AB, Fonseca V, Jablonski KA, Chen Y-DI, Tipton L, Staten MA, Shoelson SE. Salicylate (salsalate) in patients with type 2 diabetes: a randomized trial. *Ann Intern Med.* 2013;159(1):1-12.
87. Koska J, Ortega E, Bunt JC, Gasser A, Impson J, Hanson RL, Forbes J, de Courten B, Krakoff J. The effect of salsalate on insulin action and glucose tolerance in obese non-diabetic patients: results of a randomised double-blind placebo-controlled study. *Diabetologia.* 2009;52(3):385-393.
88. Carlson LA, Östman J. Effect of salicylates on plasma free fatty acid in normal and diabetic subjects. *Metabolism.* 1961;10:781-787.
89. Gilgore SG, Drew WL, Rupp JJ. The effect of salicylate on plasma nonesterified fatty acids. *Am J Med Sci.* 1963;245:456-458.
90. Fredholm BB, Hedqvist P. Role of pre- and postjunctional inhibition by prostaglandin E_2 of lipolysis induced by sympathetic nerve stimulation in dog subcutaneous adipose tissue *in situ*. *Br J Pharmacol.* 1973;47(4):711-718.

91. Steinberg D, Vaughan M, Nestel PJ, Bergström S. Effects of prostaglandin E opposing those of catecholamines on blood pressure and on triglyceride breakdown in adipose tissue. *Biochem Pharmacol.* 1963;12:764-766.
92. Steinberg D, Vaughan M, Nestel PJ, Strand O, Bergström S. Effects of the Prostaglandins on Hormone-Induced Mobilization of Free Fatty Acids. *J Clin Invest.* 1964;43:1533-1540.
93. Butcher RW, Sutherland EW. The effects of the catecholamines, adrenergic blocking agents, prostaglandin E_1, and insulin on cyclic AMP levels in the rat epididymal fat pad in vitro. *Ann N Y Acad Sci.* 1967;139(3):849-859.
94. Butcher RW, Baird CE. Effects of prostaglandins on adenosine 3',5'-monophosphate levels in fat and other tissues. *J Biol Chem.* 1968;243(8):1713-1717.
95. Shaw JE, Ramwell PW. Release of prostaglandin from rat epididymal fat pad on nervous and hormonal stimulation. *J Biol Chem.* 1968;243(7):1498-1503.
96. Curtis-Prior PB. Prostaglandins and obesity. *Lancet.* 1975;1(7912):897-899.
97. Breddin K, Überla K, Walter E. German-Austrian Multicenter 2 Years Prospective-Study on Prevention of Secondary Myocardial-Infarction by Asa in Comparison to Phenprocoumon and Placebo. *Thromb Haemostasis.* 1977;38(1):168-168.
98. Fain JN, Ballou LR, Bahouth SW. Obesity is induced in mice heterozygous for cyclooxygenase-2. *Prostaglandins Other Lipid Mediat.* 2001;65(4):199-209.
99. Ghoshal S, Trivedi DB, Graf GA, Loftin CD. Cyclooxygenase-2 deficiency attenuates adipose tissue differentiation and inflammation in mice. *J Biol Chem.* 2011;286(1):889-898.
100. Fjære E, Aune UL, Røen K, Keenan AH, Ma T, Borokowsky K, Kristensen DM, Novotny GW, Mandrup-Poulsen T, Hudson BD, Milligan G, Xi Y, Newman JW, Haj FG, Liaset B, Kristiansen K, Madsen L. Indomethacin treatment prevents high-fat diet-induced obesity and insulin resistance, but not glucose intolerance in C57BL/6J mice. *J Biol Chem.* 2014;289(23):16032-16045.
101. Jaworski K, Ahmadian M, Duncan RE, Sarkadi-Nagy E, Varady KA, Hellerstein MK, Lee H-Y, Samuel VT, Shulman GI, Kim K-H, de Val S, Kang C, Sul HS. AdPLA ablation increases lipolysis and prevents obesity induced by high-fat feeding or leptin deficiency. *Nat Med.* 2009;15(2):159-168.
102. Sanchez-Alavez M, Klein I, Brownell SE, Tabarean IV, Davis CN, Conti B, Bartfai T. Night eating and obesity in the EP3R-deficient mouse. *Proc Natl Acad Sci U S A.* 2007;104(8):3009-3014.
103. Anderson K, Wherle L, Park M, Nelson K, Nguyen L. Salsalate, an old, inexpensive drug with potential new indications: a review of the evidence from 3 recent studies. *American health & drug benefits.* 2014;7(4):231-235.
104. Desouza CV. An overview of salsalate as a potential antidiabetic therapy. *Drugs Today (Barc).* 2010;46(11):847-853.
105. Robertson RP. Hypothesis. PGE, carbohydrate homeostasis, and insulin secretion. A suggested resolution of the controversy. *Diabetes.* 1983;32(3):231-234.
106. Chen M, Robertson RP. Effects of prostaglandin synthesis inhibitors on human insulin secretion and carbohydrates tolerance. *Prostaglandins.* 1979;18(4):557-567.
107. Breyer RM, Bagdassarian CK, Myers SA, Breyer MD. Prostanoid receptors: subtypes and signaling. *Annu Rev Pharmacol Toxicol.* 2001;41:661-690.

108. Robertson RP. Prostaglandins, Thromboxanes, and Leukotrienes. In: Becker KL, ed. *Principles and Practice of Endocrinology and Metabolism*. 3 ed: Lippincott Williams & Wilkins; 2001:1581-1588.
109. Sugimoto Y, Narumiya S. Prostaglandin E receptors. *J Biol Chem.* 2007;282(16):11613-11617.
110. Gronich JH, Bonventre JV, Nemenoff RA. Identification and characterization of a hormonally regulated form of phospholipase A_2 in rat renal mesangial cells. *J Biol Chem.* 1988;263(32):16645-16651.
111. Lin L-L, Lin AY, Knopf JL. Cytosolic phospholipase A_2 is coupled to hormonally regulated release of arachidonic acid. *Proc Natl Acad Sci U S A.* 1992;89(13):6147-6151.
112. Dennis EA, Cao J, Hsu Y-H, Magrioti V, Kokotos G. Phospholipase A_2 enzymes: physical structure, biological function, disease implication, chemical inhibition, and therapeutic intervention. *Chem Rev.* 2011;111(10):6130-6185.
113. Leslie CC. Cytosolic phospholipase A_2: Physiological function and role in disease. *J Lipid Res.* 2015.
114. Murakami M, Taketomi Y, Girard C, Yamamoto K, Lambeau G. Emerging roles of secreted phospholipase A_2 enzymes: Lessons from transgenic and knockout mice. *Biochimie.* 2010;92(6):561-582.
115. Murakami M, Taketomi Y, Miki Y, Sato H, Hirabayashi T, Yamamoto K. Recent progress in phospholipase A_2 research: from cells to animals to humans. *Progress in lipid research.* 2011;50(2):152-192.
116. Murakami M, Sato H, Miki Y, Yamamoto K, Taketomi Y. A New Era of Secreted Phospholipase A_2 ($sPLA_2$). *J Lipid Res.* 2015.
117. Simonsson E, Ahrén B. Phospholipase A_2 and its potential regulation of islet function. *International journal of pancreatology : official journal of the International Association of Pancreatology.* 2000;27(1):1-11.
118. Hartley P. On the nature of the fat contained in the liver, kidney, and heart. *J Physiol.* 1907;36(1):17-26.
119. Needleman P, Turk J, Jakschik BA, Morrison AR, Lefkowith JB. Arachidonic acid metabolism. *Annu Rev Biochem.* 1986;55:69-102.
120. Shimizu T, Wolfe LS. Arachidonic acid cascade and signal transduction. *J Neurochem.* 1990;55(1):1-15.
121. Dubois RN, Abramson SB, Crofford L, Gupta RA, Simon LS, Van De Putte LB, Lipsky PE. Cyclooxygenase in biology and disease. *FASEB J.* 1998;12(12):1063-1073.
122. Simmons DL, Botting RM, Hla T. Cyclooxygenase isozymes: the biology of prostaglandin synthesis and inhibition. *Pharmacol Rev.* 2004;56(3):387-437.
123. Patrignani P, Patrono C. Cyclooxygenase inhibitors: From pharmacology to clinical read-outs. *Biochim Biophys Acta.* 2015;1851(4):422-432.
124. Samuelsson B, Morgenstern R, Jakobsson P-J. Membrane prostaglandin E synthase-1: a novel therapeutic target. *Pharmacol Rev.* 2007;59(3):207-224.
125. Ullrich V, Brugger R. Prostacyclin and Thromboxane Synthase - New Aspects of Hemethiolate Catalysis. *Angew Chem Int Edit.* 1994;33(19):1911-1919.
126. Urade Y, Watanabe K, Hayaishi O. Prostaglandin D, E, and F synthases. *Journal of lipid mediators and cell signalling.* 1995;12(2-3):257-273.

127. Urade Y, Hayaishi O. Biochemical, structural, genetic, physiological, and pathophysiological features of lipocalin-type prostaglandin D synthase. *Biochim Biophys Acta.* 2000;1482(1-2):259-271.
128. Watanabe K. Prostaglandin F synthase. *Prostag Oth Lipid M.* 2002;68–69(0):401-407.
129. Wu KK, Liou JY. Cellular and molecular biology of prostacyclin synthase. *Biochem Biophys Res Commun.* 2005;338(1):45-52.
130. Kotelevets L, Foudi N, Louedec L, Couvelard A, Chastre E, Norel X. A new mRNA splice variant coding for the human $EP_{3\text{-}I}$ receptor isoform. *Prostaglandins Leukot Essent Fatty Acids.* 2007;77(3-4):195-201.
131. Hasegawa H, Katoh H, Yamaguchi Y, Nakamura K, Futakawa S, Negishi M. Different membrane targeting of prostaglandin EP3 receptor isoforms dependent on their carboxy-terminal tail structures. *FEBS Lett.* 2000;473(1):76-80.
132. Namba T, Sugimoto Y, Negishi M, Irie A, Ushikubi F, Kakizuka A, Ito S, Ichikawa A, Narumiya S. Alternative splicing of C-terminal tail of prostaglandin E receptor subtype EP3 determines G-protein specificity. *Nature.* 1993;365(6442):166-170.
133. Kimple ME, Nixon AB, Kelly P, Bailey CL, Young KH, Fields TA, Casey PJ. A role for G_z in pancreatic islet β-cell biology. *J Biol Chem.* 2005;280(36):31708-31713.
134. Kimple ME, Moss JB, Brar HK, Rosa TC, Truchan NA, Pasker RL, Newgard CB, Casey PJ. Deletion of $G\alpha_z$ protein protects against diet-induced glucose intolerance via expansion of β-cell mass. *J Biol Chem.* 2012;287(24):20344-20355.
135. Chun K-S, Lao H-C, Trempus CS, Okada M, Langenbach R. The prostaglandin receptor EP2 activates multiple signaling pathways and β-arrestin1 complex formation during mouse skin papilloma development. *Carcinogenesis.* 2009;30(9):1620-1627.
136. Chun K-S, Lao H-C, Langenbach R. The prostaglandin E_2 receptor, EP2, stimulates keratinocyte proliferation in mouse skin by G protein-dependent and β-arrestin1-dependent signaling pathways. *J Biol Chem.* 2010;285(51):39672-39681.
137. Bilson HA, Mitchell DL, Ashby B. Human prostaglandin EP3 receptor isoforms show different agonist-induced internalization patterns. *FEBS Lett.* 2004;572(1-3):271-275.
138. Neuschäfer-Rube F, Oppermann M, Möller U, Böer U, Püschel GP. Agonist-induced phosphorylation by G protein-coupled receptor kinases of the EP4 receptor carboxyl-terminal domain in an EP3/EP4 prostaglandin E_2 receptor hybrid. *Mol Pharmacol.* 1999;56(2):419-428.
139. Leduc M, Breton B, Galés C, Le Gouill C, Bouvier M, Chemtob S, Heveker N. Functional selectivity of natural and synthetic prostaglandin EP_4 receptor ligands. *J Pharmacol Exp Ther.* 2009;331(1):297-307.
140. Buchanan FG, Gorden DL, Matta P, Shi Q, Matrisian LM, DuBois RN. Role of β-arrestin 1 in the metastatic progression of colorectal cancer. *Proc Natl Acad Sci U S A.* 2006;103(5):1492-1497.
141. Kim JI, Lakshmikanthan V, Frilot N, Daaka Y. Prostaglandin E_2 promotes lung cancer cell migration via EP4-βArrestin1-c-Src signalsome. *Mol Cancer Res.* 2010;8(4):569-577.
142. Goupil E, Wisehart V, Khoury E, Zimmerman B, Jaffal S, Hébert TE, Laporte SA. Biasing the prostaglandin F2α receptor responses toward EGFR-dependent transactivation of MAPK. *Mol Endocrinol.* 2012;26(7):1189-1202.

143. Yue L, Haroun S, Parent J-L, de Brum-Fernandes AJ. Prostaglandin D_2 induces apoptosis of human osteoclasts through ERK1/2 and Akt signaling pathways. *Bone.* 2014;60:112-121.
144. O'Keeffe MB, Reid HM, Kinsella BT. Agonist-dependent internalization and trafficking of the human prostacyclin receptor: a direct role for Rab5a GTPase. *Biochim Biophys Acta.* 2008;1783(10):1914-1928.
145. Smyth EM, Austin SC, Reilly MP, FitzGerald GA. Internalization and sequestration of the human prostacyclin receptor. *J Biol Chem.* 2000;275(41):32037-32045.
146. Habib A, Vezza R, Créminon C, Maclouf J, FitzGerald GA. Rapid, agonist-dependent phosphorylation *in vivo* of human thromboxane receptor isoforms. Minimal involvement of protein kinase C. *J Biol Chem.* 1997;272(11):7191-7200.
147. Parent J-L, Labrecque P, Orsini MJ, Benovic JL. Internalization of the TXA_2 receptor α and β isoforms. Role of the differentially spliced COOH terminus in agonist-promoted receptor internalization. *J Biol Chem.* 1999;274(13):8941-8948.
148. Walsh M-T, Foley JF, Kinsella BT. The α, but not the β, isoform of the human thromboxane A_2 receptor is a target for prostacyclin-mediated desensitization. *J Biol Chem.* 2000;275(27):20412-20423.
149. Midgett C, Stitham J, Martin K, Hwa J. Prostacyclin receptor regulation--from transcription to trafficking. *Current molecular medicine.* 2011;11(7):517-528.
150. Regan JW. EP_2 and EP_4 prostanoid receptor signaling. *Life Sci.* 2003;74(2-3):143-153.
151. Yokoyama U, Iwatsubo K, Umemura M, Fujita T, Ishikawa Y. The prostanoid EP4 receptor and its signaling pathway. *Pharmacol Rev.* 2013;65(3):1010-1052.
152. Hardwick JP, Eckman K, Lee YK, Abdelmegeed MA, Esterle A, Chilian WM, Chiang JY, Song B-J. Eicosanoids in metabolic syndrome. *Advances in pharmacology.* 2013;66:157-266.
153. In't Veld P, Marichal M. Microscopic anatomy of the human islet of Langerhans. In: Islam S, ed. *The Islets of Langerhans*2010:1-19.
154. Gauthier BR, Wollheim CB. Synaptotagmins bind calcium to release insulin. *Am J Physiol Endocrinol Metab.* 2008;295(6):E1279-1286.
155. Pang ZP, Südhof TC. Cell biology of Ca^{2+}-triggered exocytosis. *Curr Opin Cell Biol.* 2010;22(4):496-505.
156. Broniowska KA, Oleson BJ, Corbett JA. β-Cell Responses to Nitric Oxide. In: Litwack G, ed. *Pancreatic Beta Cell.* Vol 95. United States: New York, Academic Press.; 2014:299-322.
157. Tiano JP, Mauvais-Jarvis F. Importance of oestrogen receptors to preserve functional β-cell mass in diabetes. *Nat Rev Endocrinol.* 2012;8(6):342-351.
158. Bartolome A, Guillén C. Role of the mammalian target of rapamycin (mTOR) complexes in pancreatic β-cell mass regulation. In: Litwack G, ed. *Pancreatic Beta Cell.* Vol 95. United States: New York, Academic Press.; 2014:425-469.
159. Ahrén B. Islet G protein-coupled receptors as potential targets for treatment of type 2 diabetes. *Nat Rev Drug Discov.* 2009;8(5):369-385.
160. Winzell MS, Ahrén B. G-protein-coupled receptors and islet function-implications for treatment of type 2 diabetes. *Pharmacol Ther.* 2007;116(3):437-448.
161. Vikman J, Svensson H, Huang YC, Kang Y, Andersson SA, Gaisano HY, Eliasson L. Truncation of SNAP-25 reduces the stimulatory action of cAMP on rapid exocytosis in insulin-secreting cells. *Am J Physiol Endocrinol Metab.* 2009;297(2):E452-461.

162. Leech CA, Chepurny OG, Holz GG. Epac2-Dependent Rap1 Activation and the Control of Islet Insulin Secretion by Glucagon-Like Peptide-1. *Vitam Horm.* 2010;84:279-302.
163. Nagy G, Reim K, Matti U, Brose N, Binz T, Rettig J, Neher E, Sørensen JB. Regulation of releasable vesicle pool sizes by protein kinase A-dependent phosphorylation of SNAP-25. *Neuron.* 2004;41(3):417-429.
164. Ehses JA, Lee SST, Pederson RA, McIntosh CHS. A new pathway for glucose-dependent insulinotropic polypeptide (GIP) receptor signaling: evidence for the involvement of phospholipase A_2 in GIP-stimulated insulin secretion. *J Biol Chem.* 2001;276(26):23667-23673.
165. Schwetz TA, Ustione A, Piston DW. Neuropeptide Y and somatostatin inhibit insulin secretion through different mechanisms. *Am J Physiol Endocrinol Metab.* 2013;304(2):E211-221.
166. Zhang H, Yasrebi-Nejad H, Lang J. G-protein βγ-binding domains regulate insulin exocytosis in clonal pancreatic β-cells. *FEBS Lett.* 1998;424(3):202-206.
167. Zhao Y, Fang Q, Straub SG, Lindau M, Sharp GWG. Noradrenaline inhibits exocytosis via the G protein βγ subunit and refilling of the readily releasable granule pool via the $\alpha_{i1/2}$ subunit. *J Physiol.* 2010;588(Pt 18):3485-3498.
168. Dalle S, Ravier MA, Bertrand G. Emerging roles for β-arrestin-1 in the control of the pancreatic β-cell function and mass: new therapeutic strategies and consequences for drug screening. *Cell Signal.* 2011;23(3):522-528.
169. Wolf BA, Pasquale SM, Turk J. Free fatty acid accumulation in secretagogue-stimulated pancreatic islets and effects of arachidonate on depolarization-induced insulin secretion. *Biochemistry.* 1991;30(26):6372-6379.
170. Wolf BA, Turk J, Sherman WR, McDaniel ML. Intracellular Ca^{2+} mobilization by arachidonic acid. Comparison with *myo*-inositol 1,4,5-trisphosphate in isolated pancreatic islets. *J Biol Chem.* 1986;261(8):3501-3511.
171. Nowatzke W, Ramanadham S, Ma Z, Hsu F-F, Bohrer A, Turk J. Mass spectrometric evidence that agents that cause loss of Ca^{2+} from intracellular compartments induce hydrolysis of arachidonic acid from pancreatic islet membrane phospholipids by a mechanism that does not require a rise in cytosolic Ca^{2+} concentration. *Endocrinology.* 1998;139(10):4073-4085.
172. Fujita H, Kakei M, Fujishima H, Morii T, Yamada Y, Qi Z, Breyer MD. Effect of selective cyclooxygenase-2 (COX-2) inhibitor treatment on glucose-stimulated insulin secretion in C57BL/6 mice. *Biochem Biophys Res Commun.* 2007;363(1):37-43.
173. Dorrell C, Schug J, Lin CF, Canaday PS, Fox AJ, Smirnova O, Bonnah R, Streeter PR, Stoeckert CJ, Jr., Kaestner KH, Grompe M. Transcriptomes of the major human pancreatic cell types. *Diabetologia.* 2011;54(11):2832-2844.
174. Evans MH, Pace CS, Clements RS. Endogenous prostaglandin synthesis and glucose-induced insulin secretion from the adult rat pancreatic islet. *Diabetes.* 1983;32(6):509-515.
175. Horie H, Narumiya S, Matsuyama T, Nonaka K, Tarui S. Presence of prostaglandin D_2, E_2 and $F_{2\alpha}$ in rat pancreatic islets. *Prostaglandins Leukot Med.* 1984;16(1):39-44.
176. Kelly KL, Laychock SG. Activity of prostaglandin biosynthetic pathways in rat pancreatic islets. *Prostaglandins.* 1984;27(6):925-938.
177. Parazzoli S, Harmon JS, Vallerie SN, Zhang T, Zhou H, Robertson RP. Cyclooxygenase-2, Not Microsomal Prostaglandin E Synthase-1, Is the Mechanism for Interleukin-1β-

induced Prostaglandin E_2 Production and Inhibition of Insulin Secretion in Pancreatic Islets. *J Biol Chem.* 2012;287(38):32246-32253.

178. Ramanadham S, Gross RW, Han X, Turk J. Inhibition of arachidonate release by secretagogue-stimulated pancreatic islets suppresses both insulin secretion and the rise in β-cell cytosolic calcium ion concentration. *Biochemistry.* 1993;32(1):337-346.

179. Turk J, Colca JR, Kotagal N, McDaniel ML. Arachidonic acid metabolism in isolated pancreatic islets. I. Identification and quantitation of lipoxygenase and cyclooxygenase products. *Biochim Biophys Acta.* 1984;794(1):110-124.

180. Turk J, Mueller M, Bohrer A, Ramanadham S. Arachidonic acid metabolism in isolated pancreatic islets. VI. Carbohydrate insulin secretagogues must be metabolized to induce eicosanoid release. *Biochim Biophys Acta.* 1992;1125(3):280-291.

181. Vennemann A, Gerstner A, Kern N, Bouzas NF, Narumiya S, Maruyama T, Nüsing RM. PTGS-2-PTGER2/4 Signaling Pathway Partially Protects From Diabetogenic Toxicity of Streptozotocin in Mice. *Diabetes.* 2012;61(7):1879-1887.

182. Wogensen LD, Kolb-Bachofen V, Christensen P, Dinarello CA, Mandrup-Poulsen T, Martin S, Nerup J. Functional and morphological effects of interleukin-1β on the perfused rat pancreas. *Diabetologia.* 1990;33(1):15-23.

183. Akpan JO, Hurley MC, Pek S, Lands WEM. The effects of prostaglandins on secretion of glucagon and insulin by the perfused rat pancreas. *Can J Biochem.* 1979;57(6):540-547.

184. Cheng H, Straub SG, Sharp GWG. Protein acylation in the inhibition of insulin secretion by norepinephrine, somatostatin, galanin, and PGE_2. *Am J Physiol Endocrinol Metab.* 2003;285(2):E287-294.

185. Giugliano D, Di Pinto P, Torella R, Frascolla N, Saccomanno F, Passariello N, D'Onofrio F. A role for endogenous prostaglandin E in biphasic pattern of insulin release in humans. *Am J Physiol.* 1983;245(6):E591-597.

186. Horie H, Matsuyama T, Namba M, Nonaka K, Tarui S. Modulation by prostaglandin D_2 of glucagon and insulin secretion in the perfused rat pancreas. *Prostaglandins Leukot Med.* 1983;12(3):315-321.

187. Matsuyama T, Horie H, Namba M, Nonaka K, Tarui S. Glucose dependent stimulation by prostaglandin D_2 of glucagon and insulin in perfused rat pancreas. *Life Sci.* 1983;32(9):979-982.

188. Oshima H, Taketo MM, Oshima M. Destruction of pancreatic β-cells by transgenic induction of prostaglandin E_2 in the islets. *J Biol Chem.* 2006;281(39):29330-29336.

189. Pek S, Tai T-Y, Elster A. Stimulatory effects of prostaglandins E-1, E-2, and F-2-alpha on glucagon and insulin release in vitro. *Diabetes.* 1978;27(8):801-809.

190. Robertson RP. In vivo insulin secretion: prostaglandin and adrenergic interrelationships. *Prostaglandins.* 1974;6(6):501-508.

191. Robertson RP, Chen M. Role for Prostaglandin-E in Defective Insulin-Secretion and Carbohydrate Intolerance in Diabetes-Mellitus. *J Clin Invest.* 1977;60(3):747-753.

192. Robertson RP, Chen M. Modulation of insulin secretion in normal and diabetic humans by prostaglandin E and sodium salicylate. *Trans Assoc Am Physicians.* 1977;90:353-365.

193. Saccà L, Perez G, Rengo F, Pascucci I, Condorelli M. Reduction of circulating insulin levels during the infusion of different prostaglandins in the rat. *Acta Endocrinol.* 1975;79(2):266-274.

194. Seaquist ER, Walseth TF, Nelson DM, Robertson RP. Pertussis toxin-sensitive G protein mediation of PGE_2 inhibition of cAMP metabolism and phasic glucose-induced insulin secretion in HIT cells. *Diabetes.* 1989;38(11):1439-1445.

195. Sjöholm Å. Prostaglandins inhibit pancreatic β-cell replication and long-term insulin secretion by pertussis toxin-insensitive mechanisms but do not mediate the actions of interleukin-1β. *Biochim Biophys Acta.* 1996;1313(2):106-110.

196. Tran POT, Gleason CE, Poitout V, Robertson RP. Prostaglandin E_2 Mediates Inhibition of Insulin Secretion by Interleukin-1β. *J Biol Chem.* 1999;274(44):31245-31248.

197. Tran POT, Gleason CE, Robertson RP. Inhibition of interleukin-1β-induced COX-2 and EP3 gene expression by sodium salicylate enhances pancreatic islet β-cell function. *Diabetes.* 2002;51(6):1772-1778.

198. Luo P, Wang M-H. Eicosanoids, β-cell function, and diabetes. *Prostaglandins Other Lipid Mediat.* 2011;95(1-4):1-10.

199. Robertson RP. Eicosanoids as pluripotential modulators of pancreatic islet function. *Diabetes.* 1988;37(4):367-370.

200. Robertson RP. Molecular Regulation of Pancreatic Islet Prostaglandin Synthesis and Its Relevance to Diabetes Mellitus. In: Curtis-Prior P, ed. *The Eicosanoids*. Chichester, UK: John Wiley & Sons, Ltd; 2004:277-287.

201. Hamberg M, Samuelsson B. On the metabolism of prostaglandins E_1 and E_2 in man. *J Biol Chem.* 1971;246(22):6713-6721.

202. Piper PJ, Vane JR, Wyllie JH. Inactivation of prostaglandins by the lungs. *Nature.* 1970;225(5233):600-604.

203. Yatomi A, Iguchi A, Yanagisawa S, Matsunaga H, Niki I, Sakamoto N. Prostaglandins affect the central nervous system to produce hyperglycemia in rats. *Endocrinology.* 1987;121(1):36-41.

204. Bressler R, Vargas-Cord M, Lebovitz HE. Tranylcypromine: a potent insulin secretagogue and hypoglycemic agent. *Diabetes.* 1968;17(10):617-624.

205. Hertelendy F, Todd H, Ehrhart K, Blute R. Studies on growth hormone secretion. IV. In vivo effects of prostaglandin E_1. *Prostaglandins.* 1972;2(2):79-91.

206. Konturek SJ, Mikoś EM, Król R, Wierzbicki Z, Dobrzańska M. Effect of methylated prostaglandin E_2 analogue on insulin secretion in man. *Prostaglandins.* 1978;15(4):591-602.

207. McRae JR, Metz SA, Robertson RP. A Role for Endogenous Prostaglandins in Defective Glucose Potentiation of Non-Glucose Insulin Secretagogues in Diabetics. *Metabolism.* 1981;30(11):1065-1075.

208. Giugliano D, Torella R, Improta L, D'Onofrio F. Effects of prostaglandin E_1 and prostaglandin $F_{2\alpha}$ on insulin and glucagon plasma levels during the intravenous glucose tolerance test in man. *Diabete Metab.* 1978;4(3):187-191.

209. Giugliano D, Torella R, Sgambato S, D'Onofrio F. Prostaglandin E_1 increases basal glucagon in man. *Pharmacol Res Commun.* 1978;10(9):813-821.

210. Giugliano D, Torella R, Sgambato S, D'Onofrio F. Effects of α-and β-adrenergic inhibition and somatostatin on plasma glucose, free fatty acids, insulin glucagon and growth hormone responses to prostaglandin E_1 in man. *J Clin Endocrinol Metab.* 1979;48(2):302-308.

211. Giugliano D, Torella R, D'Onofrio F. Arguments for an inhibiting role of prostaglandin E_1 on insulin secretion in man. *Farmaco Sci.* 1979;34(2):157-164.

212. Giugliano D, Torella R. Prostaglandin E_1 inhibits glucose-induced insulin secretion in man. *Prostaglandins Med.* 1978;1(2):165-166.
213. D'Onofrio F, Torella R, Giugliano D, Improta L, Grazioli A. Effects of vaso-inactive doses of PGA_1 and PGE_1 on insulin secretion in the rat. *Pharmacol Res Commun.* 1977;9(5):427-436.
214. Lefebvre PJ, Luyckx AS. Stimulation of insulin secretion after prostaglandin PGE_1 in the anesthetized dog. *Biochem Pharmacol.* 1973;22(14):1773-1779.
215. Robertson RP, Guest RJ. Reversal by methysergide of inhibition of insulin secretion by prostaglandin E in the dog. *J Clin Invest.* 1978;62(5):1014-1019.
216. Robertson RP, Guest RJ. Effects of prostaglandin B_1 on basal and stimulated circulating levels of insulin, glucose and free fatty acids. *Prostaglandins.* 1974;8(3):231-240.
217. Pek S, Tai T-Y, Elster A, Fajans. Stimulation by prostaglandin E_2 of glucagon and insulin release from isolated rat pancreas. *Prostaglandins.* 1975;10(3):493-502.
218. Nishi S, Seino Y, Seino S, Tsuda K, Takemura J, Shimizu T, Hayashi O, Imura H. Different effects of prostaglandin E_1, E_2 and D_2 on pancreatic somatostatin release. *Horm Metab Res.* 1984;16 Suppl 1:114-118.
219. Landgraf R, Landgraf-Leurs MMC. The prostaglandins system and insulin release. Studies with the isolated perfused rat pancreas. *Prostaglandins.* 1979;17(4):599-613.
220. Dodi G, Santoro MG, Jaffe BM. Effect of a synthetic analogue of PGE_2 on exocrine and endocrine pancreatic function in the rat. *Surgery.* 1978;83(2):206-213.
221. Persaud SJ, Muller D, Belin VD, Kitsou-Mylona I, Asare-Anane H, Papadimitriou A, Burns CJ, Huang GC, Amiel SA, Jones PM. The role of arachidonic acid and its metabolites in insulin secretion from human islets of langerhans. *Diabetes.* 2007;56(1):197-203.
222. Zawalich WS, Zawalich KC, Yamazaki H. Divergent effects of epinephrine and prostaglandin E_2 on glucose-induced insulin secretion from perifused rat islets. *Metabolism.* 2007;56(1):12-18.
223. Hirano T, Fukuyama S, Nagano S, Takahashi T. The effect of exogenous arachidonic acid on insulin secretion in isolated perifused hamster islets. *Endocrinol Jpn.* 1984;31(5):549-555.
224. Burr IM, Sharp R. Effects of prostaglandin E_1 and of epinephrine on the dynamics of insulin release in vitro. *Endocrinology.* 1974;94(3):835-839.
225. Heitmeier MR, Kelly CB, Ensor NJ, Gibson KA, Mullis KG, Corbett JA, Maziasz TJ. Role of cyclooxygenase-2 in cytokine-induced β-cell dysfunction and damage by isolated rat and human islets. *J Biol Chem.* 2004;279(51):53145-53151.
226. Laychock SG, Bilgin S. Calcium mobilization, prostaglandin E_2 and α_2-adrenoceptor modulation of glucose utilization and insulin secretion in pancreatic islets. *Biochem Pharmacol.* 1989;38(15):2511-2520.
227. Meng ZX, Sun JX, Ling JJ, Lv JH, Zhu DY, Chen Q, Sun YJ, Han X. Prostaglandin E_2 regulates Foxo activity via the Akt pathway: implications for pancreatic islet beta cell dysfunction. *Diabetologia.* 2006;49(12):2959-2968.
228. Meng Z, Lv J, Luo Y, Lin Y, Zhu Y, Nie J, Yang T, Sun Y, Han X. Forkhead box O1/pancreatic and duodenal homeobox 1 intracellular translocation is regulated by c-Jun N-terminal kinase and involved in prostaglandin E_2-induced pancreatic β-cell dysfunction. *Endocrinology.* 2009;150(12):5284-5293.

229. Johnson DG, Fujimoto WY, Williams RH. Enhanced release of insulin by prostaglandins in isolated pancreatic islets. *Diabetes.* 1973;22(9):658-663.
230. Vance JE, Buchanan KD, Williams RH. Glucagon and insulin release. Influence of drugs affecting the autonomic nervous system. *Diabetes.* 1971;20(2):78-82.
231. Metz S, Fujimoto W, Robertson RP. Modulation of insulin secretion by cyclic AMP and prostaglandin E: the effects of theophylline, sodium salicylate and tolbutamide. *Metabolism.* 1982;31(10):1014-1022.
232. Metz SA, Robertson RP, Fujimoto WY. Inhibition of prostaglandin E synthesis augments glucose-induced insulin secretion is cultured pancreas. *Diabetes.* 1981;30(7):551-557.
233. Shridas P, Zahoor L, Forrest KJ, Layne JD, Webb NR. Group X Secretory Phospholipase A_2 Regulates Insulin Secretion Through a Cyclooxygenase-2-Dependent Mechanism. *J Biol Chem.* 2014;289(40):27410-27417.
234. Saccà L, Perez G. Influence of prostaglandins on plasma glucagon levels in the rat. *Metabolism.* 1976;25(2):127-130.
235. Regard JB, Sato IT, Coughlin SR. Anatomical profiling of G protein-coupled receptor expression. *Cell.* 2008;135(3):561-571.
236. Kotani M, Tanaka I, Ogawa Y, Usui T, Mori K, Ichikawa A, Narumiya S, Yoshimi T, Nakao K. Molecular cloning and expression of multiple isoforms of human prostaglandin E receptor EP_3 subtype generated by alternative messenger RNA splicing: multiple second messenger systems and tissue-specific distributions. *Mol Pharmacol.* 1995;48(5):869-879.
237. Charo C, Holla V, Arumugam T, Hwang R, Yang P, Dubois RN, Menter DG, Logsdon CD, Ramachandran V. Prostaglandin E_2 regulates pancreatic stellate cell activity via the EP4 receptor. *Pancreas.* 2013;42(3):467-474.
238. Burke SJ, Collier JJ. The gene encoding cyclooxygenase-2 is regulated by IL-1β and prostaglandins in 832/13 rat insulinoma cells. *Cell Immunol.* 2011;271(2):379-384.
239. Berger M, Scheel DW, Macias H, Miyatsuka T, Kim H, Hoang P, Ku GM, Honig G, Liou A, Tang Y, Regard JB, Sharifnia P, Yu L, Wang J, Coughlin SR, Conklin BR, Deneris ES, Tecott LH, German MS. $G\alpha_{i/o}$-coupled receptor signaling restricts pancreatic β-cell expansion. *Proc Natl Acad Sci U S A.* 2015;112(9):2888-2893.
240. Papadimitriou A, King AJF, Jones PM, Persaud SJ. Anti-apoptotic effects of arachidonic acid and prostaglandin E_2 in pancreatic β-cells. *Cell Physiol Biochem.* 2007;20(5):607-616.
241. Zeender E, Maedler K, Bosco D, Berney T, Donath MY, Halban PA. Pioglitazone and sodium salicylate protect human β-cells against apoptosis and impaired function induced by glucose and interleukin-1β. *J Clin Endocrinol Metab.* 2004;89(10):5059-5066.
242. Yasui M, Tamura Y, Minami M, Higuchi S, Fujikawa R, Ikedo T, Nagata M, Arai H, Murayama T, Yokode M. The Prostaglandin E2 Receptor EP4 Regulates Obesity-Related Inflammation and Insulin Sensitivity. *PLoS One.* 2015;10(8):e0136304.
243. Lindskog C, Korsgren O, Pontén F, Eriksson JW, Johansson L, Danielsson A. Novel pancreatic beta cell-specific proteins: antibody-based proteomics for identification of new biomarker candidates. *J Proteomics.* 2012;75(9):2611-2620.
244. Ragolia L, Palaia T, Hall CE, Maesaka JK, Eguchi N, Urade Y. Accelerated glucose intolerance, nephropathy, and atherosclerosis in prostaglandin D_2 synthase knock-out mice. *J Biol Chem.* 2005;280(33):29946-29955.

245. Virtue S, Feldmann H, Christian M, Tan CY, Masoodi M, Dale M, Lelliott C, Burling K, Campbell M, Eguchi N, Voshol P, Sethi JK, Parker M, Urade Y, Griffin JL, Cannon B, Vidal-Puig A. A new role for lipocalin prostaglandin D synthase in the regulation of brown adipose tissue substrate utilization. *Diabetes.* 2012;61(12):3139-3147.

246. Virtue S, Masoodi M, Velagapudi V, Tan CY, Dale M, Suorti T, Slawik M, Blount M, Burling K, Campbell M, Eguchi N, Medina-Gomez G, Sethi JK, Orešič M, Urade Y, Griffin JL, Vidal-Puig A. Lipocalin prostaglandin D synthase and PPARγ2 coordinate to regulate carbohydrate and lipid metabolism in vivo. *PLoS One.* 2012;7(7):e39512.

247. Tanaka R, Miwa Y, Mou K, Tomikawa M, Eguchi N, Urade Y, Takahashi-Yanaga F, Morimoto S, Wake N, Sasaguri T. Knockout of the *l-pgds* gene aggravates obesity and atherosclerosis in mice. *Biochem Biophys Res Commun.* 2009;378(4):851-856.

248. Ye C-l, Yuan Z-y, Shen B, Liu J-j, Lu C-x. Effects of $PGF_{2\alpha}$ on the glucose-stimulated insulin secretion in NIT-1β cells. *Zhongguo Yaolixue Tongbao.* 2006;22:579-582.

249. Gurgul-Convey E, Hanzelka K, Lenzen S. Mechanism of prostacyclin-induced potentiation of glucose-induced insulin secretion. *Endocrinology.* 2012;153(6):2612-2622.

250. Heaney TP, Larkins RG. The effect of prostacyclin and 6-keto-prostaglandin $F_{1\alpha}$ on insulin secretion and cyclic adenosine 3', 5'-monophosphate content in isolated rat islets. *Diabetes.* 1981;30(10):824-828.

251. Sieradzki J, Wolan H, Szczeklik A. Effects of prostacyclin and its stable analog, iloprost, upon insulin secretion in isolated pancreatic islets. *Prostaglandins.* 1984;28(3):289-296.

252. Yan S, Zhang Q, Zhong X, Tang J, Wang Y, Yu J, Zhou Y, Zhang J, Guo F, Liu Y, FitzGerald GA, Yu Y. I Prostanoid Receptor-Mediated Inflammatory Pathway Promotes Hepatic Gluconeogenesis Through Activation of PKA and Inhibition of AKT. *Diabetes.* 2014;63(9):2911-2923.

253. Inoue E, Ichiki T, Takeda K, Matsuura H, Hashimoto T, Ikeda J, Kamiharaguchi A, Sunagawa K. Beraprost sodium, a stable prostacyclin analogue, improves insulin resistance in high-fat diet-induced obese mice. *J Endocrinol.* 2012;213(3):285-291.

254. Sato N, Kaneko M, Tamura M, Kurumatani H. The prostacyclin analog Beraprost sodium ameliorates characteristics of metabolic syndrome in obese Zucker (fatty) rats. *Diabetes.* 2010;59(4):1092-1100.

255. Szczeklik A, Piętoń R, Sieradzki J, Niżankowski R. The effects of prostacyclin on glycemia and insulin release in man. *Prostaglandins.* 1980;19(6):959-968.

256. Patrono C, Pugliese F, Ciabattoni G, Di Blasi S, Pierucci A, Cinotti GA, Maseri A, Chierchia S. Prostacyclin does not affect insulin secretion in humans. *Prostaglandins.* 1981;21(3):379-385.

257. Dembińska-Kieć A, Kostka-Trąbka E, Grodzińska L, Żmuda A, Bieroń K, Kędzior A, Ochmański W, Żelazny T. Prostacyclin and blood glucose levels in humans and rabbits. *Prostaglandins.* 1981;21(1):113-121.

258. Arita S, Une S, Ohtsuka S, Kawahara T, Kasraie A, Smith CV, Mullen Y. Increased islet viability by addition of Beraprost sodium to collagenase solution. *Pancreas.* 2001;23(1):62-67.

259. Yeğen C, Aktan AÖ, Döşlüoğlu HH, Ercan S, Yalin R. The effect of Iloprost (ZK 36374) on isolated and transplanted pancreatic islet cells. *Prostaglandins Leukot Essent Fatty Acids.* 1994;51(4):257-262.

260. Utsunomiya K. Treatment strategy for type 2 diabetes from the perspective of systemic vascular protection and insulin resistance. *Vascular health and risk management.* 2012;8:429-436.
261. Baron SH. Salicylates as hypoglycemic agents. *Diabetes Care.* 1982;5(1):64-71.
262. Kimple ME, Neuman JC, Linnemann AK, Casey PJ. Inhibitory G proteins and their receptors: emerging therapeutic targets for obesity and diabetes. *Experimental & molecular medicine.* 2014;46:e102.
263. Metz SA, McRae JR, Robertson RP. Hypothesis: prostaglandins mediate defective glucose recognition in diabetes mellitus. *Prostaglandins Med.* 1980;4(4):247-254.
264. Metz SA, Fujimoto WY, Robertson RP. Oxygenation products of arachidonic acid: third messengers for insulin release. *J Allergy Clin Immunol.* 1984;74(3 Pt 2):391-402.
265. Neuman JC, Kimple ME. The EP3 Receptor: Exploring a New Target for Type 2 Diabetes Therapeutics. *J Endocrinol Diabetes Obes.* 2013;1(1):1002.
266. Persaud SJ, Muller D, Belin VD, Papadimitriou A, Huang GC, Amiel SA, Jones PM. Expression and function of cyclooxygenase and lipoxygenase enzymes in human islets of Langerhans. *Archives of physiology and biochemistry.* 2007;113(3):104-109.
267. Robertson RP. Prostaglandins as modulators of pancreatic islet function. *Diabetes.* 1979;28(10):943-948.
268. Robertson RP, Metz SA. Sounding board. Prostaglandins, the glucoreceptor, and diabetes. *N Engl J Med.* 1979;301(26):1446-1447.
269. Robertson RP. Prostaglandins, glucose homeostasis, and diabetes mellitus. *Med Clin North Am.* 1981;65(4):759-771.
270. Robertson RP. Prostaglandins, glucose homeostasis, and diabetes mellitus. *Annu Rev Med.* 1983;34:1-12.
271. Robertson RP. Arachidonic-Acid Metabolism, the Endocrine Pancreas, and Diabetes-Mellitus. *Pharmacol Therapeut.* 1984;24(1):91-106.
272. Robertson RP, Seaquist ER, Walseth TF. G proteins and modulation of insulin secretion. *Diabetes.* 1991;40(1):1-6.
273. Robertson RP. Molecular regulation of prostaglandin synthesis Implications for endocrine systems. *Trends Endocrinol Metab.* 1995;6(9-10):293-297.
274. Robertson RP. Dominance of cyclooxygenase-2 in the regulation of pancreatic islet prostaglandin synthesis. *Diabetes.* 1998;47(9):1379-1383.
275. Bassil MS, Gougeon R. Muscle protein anabolism in type 2 diabetes. *Curr Opin Clin Nutr Metab Care.* 2013;16(1):83-88.
276. Bennet WM, Rennie MJ. Protein anabolic actions of insulin in the human body. *Diabet Med.* 1991;8(3):199-207.
277. Shakur Y, Holst LS, Landstrom TR, Movsesian M, Degerman E, Manganiello V. Regulation and function of the cyclic nucleotide phosphodiesterase (PDE3) gene family. *Progress in nucleic acid research and molecular biology.* 2001;66:241-277.
278. Smith CJ, Vasta V, Degerman E, Belfrage P, Manganiello VC. Hormone-sensitive cyclic GMP-inhibited cyclic AMP phosphodiesterase in rat adipocytes. Regulation of insulin- and cAMP-dependent activation by phosphorylation. *J Biol Chem.* 1991;266(20):13385-13390.
279. Kahn SE, Hull RL, Utzschneider KM. Mechanisms linking obesity to insulin resistance and type 2 diabetes. *Nature.* 2006;444(7121):840-846.

280. Ii H, Hatakeyama S, Tsutsumi K, Sato T, Akiba S. Group IVA phospholipase A_2 is associated with the storage of lipids in adipose tissue and liver. *Prostaglandins Other Lipid Mediat.* 2008;86(1-4):12-17.
281. Ii H, Yokoyama N, Yoshida S, Tsutsumi K, Hatakeyama S, Sato T, Ishihara K, Akiba S. Alleviation of high-fat diet-induced fatty liver damage in group IVA phospholipase A_2-knockout mice. *PLoS One.* 2009;4(12):e8089.
282. Vegiopoulos A, Müller-Decker K, Strzoda D, Schmitt I, Chichelnitskiy E, Ostertag A, Berriel Diaz M, Rozman J, Hrabe de Angelis M, Nüsing RM, Meyer CW, Wahli W, Klingenspor M, Herzig S. Cyclooxygenase-2 controls energy homeostasis in mice by de novo recruitment of brown adipocytes. *Science.* 2010;328(5982):1158-1161.
283. Massiera F, Saint-Marc P, Seydoux J, Murata T, Kobayashi T, Narumiya S, Guesnet P, Amri E-Z, Negrel R, Ailhaud G. Arachidonic acid and prostacyclin signaling promote adipose tissue development: a human health concern? *J Lipid Res.* 2003;44(2):271-279.
284. Iyer A, Lim J, Poudyal H, Reid RC, Suen JY, Webster J, Prins JB, Whitehead JP, Fairlie DP, Brown L. An Inhibitor of Phospholipase A_2 Group IIA Modulates Adipocyte Signaling and Protects Against Diet-Induced Metabolic Syndrome in Rats. *Diabetes.* 2012;61(9):2320-2329.
285. Li X, Shridas P, Forrest K, Bailey W, Webb NR. Group X secretory phospholipase A_2 negatively regulates adipogenesis in murine models. *FASEB J.* 2010;24(11):4313-4324.
286. Madsen L, Pedersen LM, Lillefosse HH, Fjære E, Bronstad I, Hao Q, Petersen RK, Hallenborg P, Ma T, De Matteis R, Araujo P, Mercader J, Bonet ML, Hansen JB, Cannon B, Nedergaard J, Wang J, Cinti S, Voshol P, Døskeland SO, Kristiansen K. UCP1 induction during recruitment of brown adipocytes in white adipose tissue is dependent on cyclooxygenase activity. *PLoS One.* 2010;5(6):e11391.
287. Furuyashiki T, Narumiya S. Stress responses: the contribution of prostaglandin E_2 and its receptors. *Nat Rev Endocrinol.* 2011;7(3):163-175.
288. Baile CA, Simpson CW, Bean SM, McLaughlin CL, Jacobs HL. Prostaglandins and food intake of rats: a component of energy balance regulation? *Physiology & behavior.* 1973;10(6):1077-1085.
289. Doggett NS, Jawaharlal K. Some observations on the anorectic activity of prostaglandin $F_{2\alpha}$. *Br J Pharmacol.* 1977;60(3):409-415.
290. Levine AS, Morley JE. The effect of prostaglandins (PGE_2 and $PGF_{2\alpha}$) on food intake in rats. *Pharmacol Biochem Behav.* 1981;15(5):735-738.
291. Scaramuzzi OE, Baile CA, Mayer J. Prostaglandins and food intake of rats. *Experientia.* 1971;27(3):256-257.
292. Doggett NS, Jawaharlal K. Anorectic activity of prostaglandin precursors. *Br J Pharmacol.* 1977;60(3):417-423.
293. Lal J. Possible role of prostaglandins in the regulation of food intake in the newborn rat. *Archives internationales de pharmacodynamie et de therapie.* 1984;272(1):140-149.
294. Baile CA, Martin FH, Forbes JM, Webb RL, Kingsbury W. Intrahypothalamic injections of prostaglandins and prostaglandin antagonists and feeding in sheep. *J Dairy Sci.* 1974;57(1):81-88.
295. Ohinata K, Suetsugu K, Fujiwara Y, Yoshikawa M. Activation of prostaglandin E receptor EP_4 subtype suppresses food intake in mice. *Prostaglandins Other Lipid Mediat.* 2006;81(1-2):31-36.

296. Fain JN, Leffler CW, Bahouth SW. Eicosanoids as endogenous regulators of leptin release and lipolysis by mouse adipose tissue in primary culture. *J Lipid Res.* 2000;41(10):1689-1694.
297. Fain JN, Leffler CW, Bahouth SW, Rice AM, Rivkees SA. Regulation of leptin release and lipolysis by PGE_2 in rat adipose tissue. *Prostaglandins Other Lipid Mediat.* 2000;62(4):343-350.
298. Bastard J-P, Maachi M, Lagathu C, Kim MJ, Caron M, Vidal H, Capeau J, Feve B. Recent advances in the relationship between obesity, inflammation, and insulin resistance. *European cytokine network.* 2006;17(1):4-12.
299. Ohinata K, Takagi K, Biyajima K, Fujiwara Y, Fukumoto S, Eguchi N, Urade Y, Asakawa A, Fujimiya M, Inui A, Yoshikawa M. Central prostaglandin D_2 stimulates food intake via the neuropeptide Y system in mice. *FEBS Lett.* 2008;582(5):679-684.
300. Elias E, Benrick A, Behre CJ, Ekman R, Zetterberg H, Stenlöf K, Wallenius V. Central nervous system lipocalin-type prostaglandin D2-synthase is correlated with orexigenic neuropeptides, visceral adiposity and markers of the hypothalamic-pituitary-adrenal axis in obese humans. *J Neuroendocrinol.* 2011;23(6):501-507.
301. Hayaishi O. Humoral mechanisms of sleep–wake regulation: Historical review of prostaglandin D_2 and related substances. *Sleep and Biological Rhythms.* 2011;9:3-9.
302. Ueno R, Ishikawa Y, Nakayama T, Hayaishi O. Prostaglandin D_2 induces sleep when microinjected into the preoptic area of conscious rats. *Biochem Biophys Res Commun.* 1982;109(2):576-582.
303. Urade Y, Hayaishi O. Prostaglandin D2 and sleep/wake regulation. *Sleep medicine reviews.* 2011;15(6):411-418.
304. Matsumura H, Honda K, Goh Y, Ueno R, Sakai T, Inoué S, Hayaishi O. Awaking effect of prostaglandin E_2 in freely moving rats. *Brain Res.* 1989;481(2):242-249.
305. Matsumura H, Goh Y, Ueno R, Sakai T, Hayaishi O. Awaking effect of PGE_2 microinjected into the preoptic area of rats. *Brain Res.* 1988;444(2):265-272.
306. Matsumura H, Honda K, Choi WS, Inoué S, Sakai T, Hayaishi O. Evidence that brain prostaglandin E_2 is involved in physiological sleep-wake regulation in rats. *Proc Natl Acad Sci U S A.* 1989;86(14):5666-5669.
307. Onoe H, Watanabe Y, Ono K, Koyama Y, Hayaishi O. Prostaglandin E_2 exerts an awaking effect in the posterior hypothalamus at a site distinct from that mediating its febrile action in the anterior hypothalamus. *J Neurosci.* 1992;12(7):2715-2725.
308. Oishi Y, Yoshida K, Scammell TE, Urade Y, Lazarus M, Saper CB. The roles of prostaglandin E_2 and D_2 in lipopolysaccharide-mediated changes in sleep. *Brain Behav Immun.* 2015;47:172-177.
309. Milton AS, Wendlandt S. A possible role for prostaglandin E_1 as a modulator for temperature regulation in the central nervous system of the cat. *J Physiol.* 1970;207(2):76P-77P.
310. Ushikubi F, Segi E, Sugimoto Y, Murata T, Matsuoka T, Kobayashi T, Hizaki H, Tuboi K, Katsuyama M, Ichikawa A, Tanaka T, Yoshida N, Narumiya S. Impaired febrile response in mice lacking the prostaglandin E receptor subtype EP_3. *Nature.* 1998;395(6699):281-284.
311. Lazarus M, Yoshida K, Coppari R, Bass CE, Mochizuki T, Lowell BB, Saper CB. EP3 prostaglandin receptors in the median preoptic nucleus are critical for fever responses. *Nat Neurosci.* 2007;10(9):1131-1133.

312. Morrison SF, Madden CJ, Tupone D. Central neural regulation of brown adipose tissue thermogenesis and energy expenditure. *Cell Metab.* 2014;19(5):741-756.
313. Cammock S, Dascombe MJ, Milton AS. Prostaglandins in thermoregulation. *Adv Prostaglandin Thromboxane Res.* 1976;1:375-380.
314. Cranston WI, Hellon RF, Mitchell D. Is brain prostaglandin synthesis involved in responses to cold? *J Physiol.* 1975;249(2):425-434.
315. Nonogaki K, Iguchi A, Yatomi A, Uemura K, Miura H, Tamagawa T, Ishiguro T, Sakamoto N. Dissociation of hyperthermic and hyperglycemic effects of central prostaglandin F2α. *Prostaglandins.* 1991;41(5):451-462.
316. Förstermann U, Heldt R, Hertting G. Effects of intracerebroventricular administration of prostaglandin D_2 on behaviour, blood pressure and body temperature as compared to prostaglandins E_2 and $F_{2\alpha}$. *Psychopharmacology (Berl).* 1983;80(4):365-370.
317. Ueno R, Narumiya S, Ogorochi T, Nakayama T, Ishikawa Y, Hayaishi O. Role of prostaglandin D2 in the hypothermia of rats caused by bacterial lipopolysaccharide. *Proc Natl Acad Sci U S A.* 1982;79(19):6093-6097.
318. Cannon B, Nedergaard J. Brown adipose tissue: function and physiological significance. *Physiological reviews.* 2004;84(1):277-359.
319. Collins S, Yehuda-Shnaidman E, Wang H. Positive and negative control of *Ucp1* gene transcription and the role of β-adrenergic signaling networks. *Int J Obes (Lond).* 2010;34 Suppl 1:S28-33.
320. Masoodi M, Kuda O, Rossmeisl M, Flachs P, Kopecky J. Lipid signaling in adipose tissue: Connecting inflammation & metabolism. *Biochim Biophys Acta.* 2015;1851(4):503-518.
321. Chu X, Nishimura K, Jisaka M, Nagaya T, Shono F, Yokota K. Up-regulation of adipogenesis in adipocytes expressing stably cyclooxygenase-2 in the antisense direction. *Prostaglandins Other Lipid Mediat.* 2010;91(1-2):1-9.
322. Fain JN, Kanu A, Bahouth SW, Cowan GSM, Hiler ML, Leffler CW. Comparison of PGE_2, prostacyclin and leptin release by human adipocytes versus explants of adipose tissue in primary culture. *Prostaglandins Leukot Essent Fatty Acids.* 2002;67(6):467-473.
323. Fajas L, Miard S, Briggs MR, Auwerx J. Selective cyclo-oxygenase-2 inhibitors impair adipocyte differentiation through inhibition of the clonal expansion phase. *J Lipid Res.* 2003;44(9):1652-1659.
324. García-Alonso V, López-Vicario C, Titos E, Morán-Salvador E, González-Périz A, Rius B, Párrizas M, Werz O, Arroyo V, Clària J. Coordinate functional regulation between microsomal prostaglandin E synthase-1 (mPGES-1) and peroxisome proliferator-activated receptor γ (PPARγ) in the conversion of white-to-brown adipocytes. *J Biol Chem.* 2013;288(39):28230-28242.
325. Hadad N, Burgazliev O, Elgazar-Carmon V, Solomonov Y, Wueest S, Item F, Konrad D, Rudich A, Levy R. Induction of cytosolic phospholipase $A_2\alpha$ is required for adipose neutrophil infiltration and hepatic insulin resistance early in the course of high-fat feeding. *Diabetes.* 2013;62(9):3053-3063.
326. Mazid MA, Chowdhury AA, Nagao K, Nishimura K, Jisaka M, Nagaya T, Yokota K. Endogenous 15-deoxy-$\Delta^{12,14}$-prostaglandin J_2 synthesized by adipocytes during maturation phase contributes to upregulation of fat storage. *FEBS Lett.* 2006;580(30):6885-6890.

327. Michaud A, Lacroix-Pépin N, Pelletier M, Daris M, Biertho L, Fortier MA, Tchernof A. Expression of genes related to prostaglandin synthesis or signaling in human subcutaneous and omental adipose tissue: depot differences and modulation by adipogenesis. *Mediators of inflammation.* 2014;2014:451620.

328. Michaud A, Lacroix-Pépin N, Pelletier M, Veilleux A, Noël S, Bouchard C, Marceau P, Fortier MA, Tchernof A. Prostaglandin (PG) F2 alpha synthesis in human subcutaneous and omental adipose tissue: modulation by inflammatory cytokines and role of the human aldose reductase AKR1B1. *PLoS One.* 2014;9(3):e90861.

329. Nishimura K, Setoyama T, Tsumagari H, Miyata N, Hatano Y, Xu L, Jisaka M, Nagaya T, Yokota K. Endogenous prostaglandins E_2 and $F_{2\alpha}$ serve as an anti-apoptotic factor against apoptosis induced by tumor necrosis factor-α in mouse 3T3-L1 preadipocytes. *Biosci Biotechnol Biochem.* 2006;70(9):2145-2153.

330. Pastel E, Pointud J-C, Loubeau G, Dani C, Slim K, Martin G, Volat F, Sahut-Barnola I, Val P, Martinez A, Lefrançois-Martinez A-M. Aldose Reductases Influence Prostaglandin $F_{2\alpha}$ Levels and Adipocyte Differentiation in Male Mouse and Human Species. *Endocrinology.* 2015;156(5):1671–1684.

331. Petersen RK, Jørgensen C, Rustan AC, Frøyland L, Muller-Decker K, Furstenberger G, Berge RK, Kristiansen K, Madsen L. Arachidonic acid-dependent inhibition of adipocyte differentiation requires PKA activity and is associated with sustained expression of cyclooxygenases. *J Lipid Res.* 2003;44(12):2320-2330.

332. Quinkler M, Bujalska IJ, Tomlinson JW, Smith DM, Stewart PM. Depot-specific prostaglandin synthesis in human adipose tissue: a novel possible mechanism of adipogenesis. *Gene.* 2006;380(2):137-143.

333. Rahman MS, Syeda PK, Khan F, Nishimura K, Jisaka M, Nagaya T, Shono F, Yokota K. Cultured preadipocytes undergoing stable transfection with cyclooxygenase-1 in the antisense direction accelerate adipogenesis during the maturation phase of adipocytes. *Applied biochemistry and biotechnology.* 2013;171(1):128-144.

334. Xie Y, Kang X, Ackerman WEt, Belury MA, Koster C, Rovin BH, Landon MB, Kniss DA. Differentiation-dependent regulation of the cyclooxygenase cascade during adipogenesis suggests a complex role for prostaglandins. *Diabetes Obes Metab.* 2006;8(1):83-93.

335. Xu L, Nishimura K, Jisaka M, Nagaya T, Yokota K. Gene expression of arachidonate cyclooxygenase pathway leading to the delayed synthesis of prostaglandins E_2 and $F_{2\alpha}$ in response to phorbol 12-myristate 13-acetate and action of these prostanoids during life cycle of adipocytes. *Biochim Biophys Acta.* 2006;1761(4):434-444.

336. Yan H, Kermouni A, Abdel-Hafez M, Lau DCW. Role of cyclooxygenases COX-1 and COX-2 in modulating adipogenesis in 3T3-L1 cells. *J Lipid Res.* 2003;44(2):424-429.

337. Hétu P-O, Riendeau D. Down-regulation of microsomal prostaglandin E_2 synthase-1 in adipose tissue by high-fat feeding. *Obesity (Silver Spring).* 2007;15(1):60-68.

338. Tang EHC, Cai Y, Wong CK, Rocha VZ, Sukhova GK, Shimizu K, Ge X, Vanhoutte PM, Libby P, Xu A. Activation of prostaglandin E_2-EP4 signaling reduces chemokine production in adipose tissue. *Journal of Lipid Research.* 2015;56(2):358-368.

339. Chowdhury AA, Hossain MS, Rahman MS, Nishimura K, Jisaka M, Nagaya T, Shono F, Yokota K. Sustained expression of lipocalin-type prostaglandin D synthase in the antisense direction positively regulates adipogenesis in cloned cultured preadipocytes. *Biochem Biophys Res Commun.* 2011;411(2):287-292.

340. Fujimori K, Aritake K, Urade Y. A novel pathway to enhance adipocyte differentiation of 3T3-L1 cells by up-regulation of lipocalin-type prostaglandin D synthase mediated by liver X receptor-activated sterol regulatory element-binding protein-1c. *J Biol Chem.* 2007;282(25):18458-18466.

341. Hossain MS, Chowdhury AA, Rahman MS, Nishimura K, Jisaka M, Nagaya T, Shono F, Yokota K. Stable expression of lipocalin-type prostaglandin D synthase in cultured preadipocytes impairs adipogenesis program independently of endogenous prostanoids. *Exp Cell Res.* 2012;318(4):408-415.

342. Jowsey IR, Murdock PR, Moore GBT, Murphy GJ, Smith SA, Hayes JD. Prostaglandin D_2 synthase enzymes and PPARγ are co-expressed in mouse 3T3-L1 adipocytes and human tissues. *Prostaglandins Other Lipid Mediat.* 2003;70(3-4):267-284.

343. Urbanet R, Cat AND, Feraco A, Venteclef N, Mogrhabi SE, Sierra-Ramos C, de la Rosa DA, Adler GK, Quilliot D, Rossignol P, Fallo F, Touyz RM, Jaisser F. Adipocyte Mineralocorticoid Receptor Activation Leads to Metabolic Syndrome and Induction of Prostaglandin D2 Synthase. *Hypertension.* 2015.

344. Fujimori K, Ueno T, Nagata N, Kashiwagi K, Aritake K, Amano F, Urade Y. Suppression of adipocyte differentiation by aldo-keto reductase 1B3 acting as prostaglandin $F_{2\alpha}$ synthase. *J Biol Chem.* 2010;285(12):8880-8886.

345. Volat FE, Pointud J-C, Pastel E, Morio B, Sion B, Hamard G, Guichardant M, Colas R, Lefrançois-Martinez A-M, Martinez A. Depressed levels of prostaglandin $F_{2\alpha}$ in mice lacking Akr1b7 increase Basal adiposity and predispose to diet-induced obesity. *Diabetes.* 2012;61(11):2796-2806.

346. Kim Y, Fischer SM. Transcriptional regulation of cyclooxygenase-2 in mouse skin carcinoma cells. Regulatory role of CCAAT/enhancer-binding proteins in the differential expression of cyclooxygenase-2 in normal and neoplastic tissues. *J Biol Chem.* 1998;273(42):27686-27694.

347. Reddy ST, Wadleigh DJ, Herschman HR. Transcriptional regulation of the cyclooxygenase-2 gene in activated mast cells. *J Biol Chem.* 2000;275(5):3107-3113.

348. Wadleigh DJ, Reddy ST, Kopp E, Ghosh S, Herschman HR. Transcriptional activation of the cyclooxygenase-2 gene in endotoxin-treated RAW 264.7 macrophages. *J Biol Chem.* 2000;275(9):6259-6266.

349. Rosen ED, Walkey CJ, Puigserver P, Spiegelman BM. Transcriptional regulation of adipogenesis. *Genes & development.* 2000;14(11):1293-1307.

350. Tang QQ, Lane MD. Adipogenesis: from stem cell to adipocyte. *Annu Rev Biochem.* 2012;81:715-736.

351. Serrero G, Lepak NM, Goodrich SP. Paracrine regulation of adipose differentiation by arachidonate metabolites: prostaglandin $F_{2\alpha}$ inhibits early and late markers of differentiation in the adipogenic cell line 1246. *Endocrinology.* 1992;131(6):2545-2551.

352. Inazumi T, Shirata N, Morimoto K, Takano H, Segi-Nishida E, Sugimoto Y. Prostaglandin E_2-EP4 signaling suppresses adipocyte differentiation in mouse embryonic fibroblasts via an autocrine mechanism. *J Lipid Res.* 2011;52(8):1500-1508.

353. Négrel R, Gaillard D, Ailhaud G. Prostacyclin as a potent effector of adipose-cell differentiation. *Biochem J.* 1989;257(2):399-405.

354. Saint-Marc P, Kozak LP, Ailhaud G, Darimont C, Negrel R. Angiotensin II as a trophic factor of white adipose tissue: stimulation of adipose cell formation. *Endocrinology.* 2001;142(1):487-492.

355. Cohen-Luria R, Danon A, Rimon G. Fatty acid binding protein (FABP) modulates prostaglandin E binding to rat epididymal adipocyte membrane similarly to albumin. *Biochim Biophys Acta.* 1990;1021(1):96-100.
356. Day RP, Little SA, Robertson RP. Characterization of prostaglandin E_2 binding to isolated human adipocytes. *Diabetes.* 1985;34(2):161-165.
357. Miller CW, Casimir DA, Ntambi JM. The mechanism of inhibition of 3T3-L1 preadipocyte differentiation by prostaglandin $F_{2\alpha}$. *Endocrinology.* 1996;137(12):5641-5650.
358. Børglum JD, Pedersen SB, Ailhaud G, Négrel R, Richelsen B. Differential expression of prostaglandin receptor mRNAs during adipose cell differentiation. *Prostaglandins Other Lipid Mediat.* 1999;57(5-6):305-317.
359. Rahman MS, Khan F, Syeda PK, Nishimura K, Jisaka M, Nagaya T, Shono F, Yokota K. Endogenous synthesis of prostacyclin was positively regulated during the maturation phase of cultured adipocytes. *Cytotechnology.* 2014;66(4):635-646.
360. Negrel R, Grimaldi P, Ailhaud G. Differentiation of ob 17 preadipocytes to adipocytes. Effects of prostaglandin $F_{2\alpha}$ and relationship to prostaglandin synthesis. *Biochim Biophys Acta.* 1981;666(1):15-24.
361. Serrero G, Lepak NM, Goodrich SP. Prostaglandin F2α inhibits the differentiation of adipocyte precursors in primary culture. *Biochem Biophys Res Commun.* 1992;183(2):438-442.
362. Williams IH, Polakis SE. Differentiation of 3T3-L1 fibroblasts to adipocytes. The effect of indomethacin, prostaglandin E_1 and cyclic AMP on the process of differentiation. *Biochem Biophys Res Commun.* 1977;77(1):175-186.
363. Russell TR, Ho R-J. Conversion of 3T3 fibroblasts into adipose cells: triggering of differentiation by prostaglandin $F_{2\alpha}$ and 1-methyl-3-isobutyl xanthine. *Proc Natl Acad Sci U S A.* 1976;73(12):4516-4520.
364. Tsuboi H, Sugimoto Y, Kainoh T, Ichikawa A. Prostanoid EP4 receptor is involved in suppression of 3T3-L1 adipocyte differentiation. *Biochem Biophys Res Commun.* 2004;322(3):1066-1072.
365. Sugimoto Y, Tsuboi H, Okuno Y, Tamba S, Tsuchiya S, Tsujimoto G, Ichikawa A. Microarray evaluation of EP4 receptor-mediated prostaglandin E_2 suppression of 3T3-L1 adipocyte differentiation. *Biochem Biophys Res Commun.* 2004;322(3):911-917.
366. Négrel R. Prostacyclin as a critical prostanoid in adipogenesis. *Prostaglandins Leukot Essent Fatty Acids.* 1999;60(5-6):383-386.
367. Aubert J, Ailhaud G, Negrel R. Evidence for a novel regulatory pathway activated by (carba)prostacyclin in preadipose and adipose cells. *FEBS Lett.* 1996;397(1):117-121.
368. Catalioto R-M, Gaillard D, Maclouf J, Ailhaud G, Negrel R. Autocrine control of adipose cell differentiation by prostacyclin and $PGF_{2\alpha}$. *Biochim Biophys Acta.* 1991;1091(3):364-369.
369. Darimont C, Vassaux G, Ailhaud G, Negrel R. Differentiation of preadipose cells: paracrine role of prostacyclin upon stimulation of adipose cells by angiotensin-II. *Endocrinology.* 1994;135(5):2030-2036.
370. Aubert J, Saint-Marc P, Belmonte N, Dani C, Négrel R, Ailhaud G. Prostacyclin IP receptor up-regulates the early expression of C/EBPβ and C/EBPδ in preadipose cells. *Mol Cell Endocrinol.* 2000;160(1-2):149-156.

371. Vassaux G, Gaillard D, Ailhaud G, Négrel R. Prostacyclin is a specific effector of adipose cell differentiation. Its dual role as a cAMP- and Ca^{2+}-elevating agent. *J Biol Chem.* 1992;267(16):11092-11097.

372. Vassaux G, Gaillard D, Darimont C, Ailhaud G, Negrel R. Differential response of preadipocytes and adipocytes to prostacyclin and prostaglandin E_2: physiological implications. *Endocrinology.* 1992;131(5):2393-2398.

373. Hopkins NK, Gorman RR. Regulation of 3T3-L1 fibroblast differentiation by prostacyclin (prostaglandin I_2). *Biochim Biophys Acta.* 1981;663(2):457-466.

374. Annamalai D, Clipstone NA. Prostaglandin F2α inhibits adipogenesis via an autocrine-mediated interleukin-11/glycoprotein 130/STAT1-dependent signaling cascade. *J Cell Biochem.* 2014;115(7):1308-1321.

375. Casimir DA, Miller CW, Ntambi JM. Preadipocyte differentiation blocked by prostaglandin stimulation of prostanoid FP^2 receptor in murine 3T3-L1 cells. *Differentiation; research in biological diversity.* 1996;60(4):203-210.

376. Draman MS, Grennan-Jones F, Zhang L, Taylor PN, Tun TK, McDermott J, Moriarty P, Morris D, Lane C, Sreenan S, Dayan C, Ludgate M. Effects of prostaglandin $F_{2\alpha}$ on adipocyte biology relevant to graves' orbitopathy. *Thyroid : official journal of the American Thyroid Association.* 2013;23(12):1600-1608.

377. Kamon J, Naitoh T, Kitahara M, Tsuruzoe N. Prostaglandin F_2alpha enhances glucose consumption through neither adipocyte differentiation nor GLUT1 expression in 3T3-L1 cells. *Cell Signal.* 2001;13(2):105-109.

378. Lepak NM, Serrero G. Inhibition of adipose differentiation by 9α, 11β-prostaglandin F2α. *Prostaglandins.* 1993;46(6):511-517.

379. Liu L, Clipstone NA. Prostaglandin F2α inhibits adipocyte differentiation via a Gαq-calcium-calcineurin-dependent signaling pathway. *J Cell Biochem.* 2007;100(1):161-173.

380. Reginato MJ, Krakow SL, Bailey ST, Lazar MA. Prostaglandins promote and block adipogenesis through opposing effects on peroxisome proliferator-activated receptor γ. *J Biol Chem.* 1998;273(4):1855-1858.

381. Taketani Y, Yamagishi R, Fujishiro T, Igarashi M, Sakata R, Aihara M. Activation of the prostanoid FP receptor inhibits adipogenesis leading to deepening of the upper eyelid sulcus in prostaglandin-associated periorbitopathy. *Invest Ophthalmol Vis Sci.* 2014;55(3):1269-1276.

382. Kim JW. Topical prostaglandin analogue drugs inhibit adipocyte differentiation. *Korean journal of ophthalmology : KJO.* 2014;28(3):257-264.

383. Serrero G, Lepak NM. Prostaglandin $F_{2\alpha}$ receptor (FP receptor) agonists are potent adipose differentiation inhibitors for primary culture of adipocyte precursors in defined medium. *Biochem Biophys Res Commun.* 1997;233(1):200-202.

384. Fujitani Y, Aritake K, Kanaoka Y, Goto T, Takahashi N, Fujimori K, Kawada T. Pronounced adipogenesis and increased insulin sensitivity caused by overproduction of prostaglandin D_2 *in vivo*. *FEBS J.* 2010;277(6):1410-1419.

385. Forman BM, Tontonoz P, Chen J, Brun RP, Spiegelman BM, Evans RM. 15-Deoxy-$\Delta^{12,14}$-prostaglandin J_2 is a ligand for the adipocyte determination factor PPARγ. *Cell.* 1995;83(5):803-812.

386. Kliewer SA, Lenhard JM, Willson TM, Patel I, Morris DC, Lehmann JM. A prostaglandin J_2 metabolite binds peroxisome proliferator-activated receptor γ and promotes adipocyte differentiation. *Cell.* 1995;83(5):813-819.

387. Yu K, Bayona W, Kallen CB, Harding HP, Ravera CP, McMahon G, Brown M, Lazar MA. Differential activation of peroxisome proliferator-activated receptors by eicosanoids. *J Biol Chem.* 1995;270(41):23975-23983.
388. Iyer A, Fairlie DP, Prins JB, Hammock BD, Brown L. Inflammatory lipid mediators in adipocyte function and obesity. *Nature Reviews Endocrinology.* 2010;6(2):71-82.
389. Fujimori K. Prostaglandins as PPARγ Modulators in Adipogenesis. *PPAR research.* 2012;2012:527607.
390. Richelsen B. Release and effects of prostaglandins in adipose tissue. *Prostaglandins Leukot Essent Fatty Acids.* 1992;47(3):171-182.
391. Hsieh P-S, Jin J-S, Chiang C-F, Chan P-C, Chen C-H, Shih K-C. COX-2-mediated inflammation in fat is crucial for obesity-linked insulin resistance and fatty liver. *Obesity.* 2009;17(6):1150-1157.
392. Chatzipanteli K, Rudolph S, Axelrod L. Coordinate control of lipolysis by prostaglandin E_2 and prostacyclin in rat adipose tissue. *Diabetes.* 1992;41(8):927-935.
393. Dalton C, Hope H, Martikes L. Prostaglandin inhibition of cyclic-AMP accumulation and rate of lipolysis in fat cells. *Prostaglandins.* 1974;7(4):319-326.
394. Illiano G, Cuatrecasas P. Endogenous prostaglandins modulate lipolytic processes in adipose tissue. *Nature: New biology.* 1971;234(46):72-74.
395. Kather H. Effects of prostaglandin E2 on adenylate cyclase activity and lipolysis in human adipose tissue. *Int J Obes.* 1981;5(6):659-663.
396. Kather H. Inhibition of hormone-stimulated human fat cell-lipolysis by prostaglandin E2 and its synthetic analogue sulprostrone. *Prostaglandins Leukot Med.* 1982;8(5):525-529.
397. Richelsen B, Beck-Nielsen H. Decrease of prostaglandin E_2 receptor binding is accompanied by reduced antilipolytic effects of prostaglandin E_2 in isolated rat adipocytes. *J Lipid Res.* 1985;26(1):127-134.
398. Richelsen B, Pedersen SB. Antilipolytic effect of prostaglandin E_2 in perifused rat adipocytes. *Endocrinology.* 1987;121(4):1221-1226.
399. Rosak C, Hittelman KJ. Characterization of lipolytic responses of isolated white adipocytes from hamsters. *Biochim Biophys Acta.* 1977;496(2):458-474.
400. Steinfelder HJ, Schramm S, Joost H-G. Prostaglandin E_2 differentiates between two forms of glucose transport inhibition by lipolytic agents. *Naunyn Schmiedebergs Arch Pharmacol.* 1987;336(1):105-110.
401. Chaves VE, Frasson D, Kawashita NH. Several agents and pathways regulate lipolysis in adipocytes. *Biochimie.* 2011;93(10):1631-1640.
402. Frühbeck G, Méndez-Giménez L, Fernández-Formoso JA, Fernández S, Rodríguez A. Regulation of adipocyte lipolysis. *Nutrition research reviews.* 2014;27(1):63-93.
403. Granneman JG, Moore H-PH. Location, location: protein trafficking and lipolysis in adipocytes. *Trends Endocrinol Metab.* 2008;19(1):3-9.
404. Holm C, Østerlund T, Laurell H, Contreras JA. Molecular mechanisms regulating hormone-sensitive lipase and lipolysis. *Annual review of nutrition.* 2000;20:365-393.
405. Lampidonis AD, Rogdakis E, Voutsinas GE, Stravopodis DJ. The resurgence of Hormone-Sensitive Lipase (HSL) in mammalian lipolysis. *Gene.* 2011;477(1-2):1-11.
406. Butcher RW, Sneyd JG, Park CR, Sutherland EW, Jr. Effect of insulin on adenosine 3',5'-monophosphate in the rat epididymal fat pad. *J Biol Chem.* 1966;241(7):1651-1653.
407. Docanto MM, Ham S, Corbould A, Brown KA. Obesity-Associated Inflammatory Cytokines and Prostaglandin E2 Stimulate Glucose Transporter mRNA Expression and

Glucose Uptake in Primary Human Adipose Stromal Cells. *Journal of interferon & cytokine research : the official journal of the International Society for Interferon and Cytokine Research.* 2015.

408. Kuroda M, Honnor RC, Cushman SW, Londos C, Simpson IA. Regulation of insulin-stimulated glucose transport in the isolated rat adipocyte. cAMP-independent effects of lipolytic and antilipolytic agents. *J Biol Chem.* 1987;262(1):245-253.

409. Richelsen B, Hjøllund E, Pedersen O, Sørensen NS. Effects of prostaglandin E_2, indomethacin and adenosine deaminase on basal and insulin-stimulated glucose metabolism in human adipocytes. *Biochim Biophys Acta.* 1985;844(3):359-366.

410. Bergström S, Carlson LA, Orö L. Effect of Prostaglandins on Catecholamine Induced Changes in the Free Fatty Acids of Plasma and in Blood Pressure in the Dog. Prostaglandin and Related Factors 22. *Acta Physiol Scand.* 1964;60:170-180.

411. Bergström S, Carlson LA. Inhibitory Action of Prostaglandin E_1 on the Mobilization of Free Fatty Acids and Glycerol from Human Adipose Tissue in Vitro Prostaglandin and related factors. *Acta Physiologica Scandinavica.* 1965;63(1-2):195-196.

412. Efendić S. Influence of prostaglandin E_1 on lipolysis induced by noradrenaline, isopropylnoradrenaline, theophylline, and dibutyryl cAMP in human omental adipose tissue in vitro. *Acta medica Scandinavica.* 1970;187(6):503-507.

413. Kather H, Simon B. Biphasic effects of prostaglandin E_2 on the human fat cell adenylate cyclase. *J Clin Invest.* 1979;64(2):609-612.

414. Kather H, Simon B. Inhibition of the stimulatory effect of adrenaline and prostaglandin E_1 on the human fat cell adenylate cyclase by adenosine. *Horm Metab Res.* 1980;12(4):169-172.

415. Kather H, Simon B. Stimulatory and inhibitory effects of catecholamines and of prostaglandin E_2 on human fat cell adenylate cyclase. *Advances in cyclic nucleotide research.* 1981;14:555-562.

416. Lambert B, Jacquemin C. Synergic effect of insulin and prostaglandin E_1 on stimulated lipolysis. *Prostaglandins Med.* 1980;5(5):375-382.

417. Moskowitz J, Fain JN. Hormonal regulation of lipolysis and phosphorylase activity in human fat cells. *J Clin Invest.* 1969;48(10):1802-1808.

418. Mühlbachova E, Sólyom A, Puglisi L. Investigations on the mechanism of the prostaglandin E_1 antagonism to norepinephrine and theophylline-induced lipolysis. *European Journal of Pharmacology.* 1967;1(4):321–325.

419. Stock K, Prilop M. Dissociation of catecholamine-induced formation of adenosine 3'5'-monophosphate and release of glycerol in fat cells by prostaglandin E_1, E_2 and N^6-phenylisopropyladenosine. *Naunyn Schmiedebergs Arch Pharmacol.* 1974;282(1):15-31.

420. Aktories K, Schultz G, Jakobs KH. Inhibition of hamster fat cell adenylate cyclase by prostaglandin E_1 and epinephrine: requirement for GTP and sodium ions. *FEBS Lett.* 1979;107(1):100-104.

421. Cohen-Luria R, Rimon G. Prostaglandin E_2 can bimodally inhibit and stimulate the epididymal adipocyte adenylyl cyclase activity. *Cell Signal.* 1992;4(3):331-335.

422. Fredholm BB, Hamberg M. Metabolism and effect of prostaglandin H_2 in adipose tissue. *Prostaglandins.* 1976;11(3):507-518.

423. Hittelman KJ, Butcher RW. Effects of antilipolytic agents and α-adrenergic antagonists on cyclic AMP metabolism in hamster white adipocytes. *Biochim Biophys Acta.* 1973;316(3):403-410.

424. Kather H. Sodium ions amplify prostaglandin E2-induced inhibition of human fat cell adenylate cyclase. *Horm Metab Res.* 1982;14(10):556.
425. Kather H. Sodium ions discriminate between stimulatory and inhibitory effects of prostaglandin E_2 on human fat cell adenylate cyclase. *Prostaglandins Leukot Med.* 1982;9(5):531-537.
426. Sólyom A, Puglisi L, Muhlbachova E. Effect *in vitro* of theophylline and prostaglandin E_1 on free fatty acid release and on triglyceride synthesis in rat adipose tissue. *Biochem Pharmacol.* 1967;16(3):521-525.
427. Strong P, Coleman RA, Humphrey PPA. Prostanoid-induced inhibition of lipolysis in rat isolated adipocytes: probable involvement of EP_3 receptors. *Prostaglandins.* 1992;43(6):559-566.
428. Kupiecki FP. Effects of prostaglandin E_1 on lipolysis and plasma free fatty acids in the fasted rat. *J Lipid Res.* 1967;8(6):577-580.
429. MacDermot J, Barnes PJ, Waddell KA, Dollery CT, Blair IA. Prostacyclin binding to guinea pig pulmonary receptors. *Eur J Pharmacol.* 1981;75(2-3):127-130.
430. Gericke MT, Kosacka J, Koch D, Nowicki M, Schroder T, Ricken AM, Nieber K, Spanel-Borowski K. Receptors for NPY and PACAP differ in expression and activity during adipogenesis in the murine 3T3-L1 fibroblast cell line. *Br J Pharmacol.* 2009;157(4):620-632.
431. Nakada MT, Stadel JM, Crooke ST. Mobilization of extracellular Ca^{2+} by prostaglandin $F_{2\alpha}$ can be modulated by fluoride in 3T3-L1 fibroblasts. *Biochem J.* 1990;272(1):167-174.
432. Nakao A, Watanabe T, Taniguchi S, Nakamura M, Honda Z, Shimizu T, Kurokawa K. Characterization of prostaglandin $F_{2\alpha}$ receptor of mouse 3T3 fibroblasts and its functional expression in *Xenopus laevis* oocytes. *J Cell Physiol.* 1993;155(2):257-264.
433. Vassaux G, Far DF, Gaillard D, Ailhaud G, Negrel R. Inhibition of prostacyclin-induced Ca^{2+} mobilization by phorbol esters in Ob1771 preadipocytes. *Prostaglandins.* 1993;46(5):441-451.
434. Chiou G-Y, Fong JC. Prostaglandin $F_{2\alpha}$ increases glucose transport in 3T3-L1 adipocytes through enhanced GLUT1 expression by a protein kinase C-dependent pathway. *Cell Signal.* 2004;16(4):415-421.
435. Chiou G-Y, Fong JC. Synergistic effect of prostaglandin F2α and cyclic AMP on glucose transport in 3T3-L1 adipocytes. *J Cell Biochem.* 2005;94(3):627-634.
436. Micossi P, Pontiroli AE, Baron SH, Tamayo RC, Lengel F, Bevilacqua M, Raggi U, Norbiato G, Foa PP. Aspirin stimulates insulin and glucagon secretion and increases glucose tolerance in normal and diabetic subjects. *Diabetes.* 1978;27(12):1196-1204.
437. Sun X, Han F, Yi J, Han L, Wang B. Effect of aspirin on the expression of hepatocyte NF-κB and serum TNF-α in streptozotocin-induced type 2 diabetic rats. *J Korean Med Sci.* 2011;26(6):765-770.
438. Bizzi A, Codegoni AM, Garattini S. Salicylate, a Powerful Inhibitor of Free Fatty Acid Release. *Nature.* 1964;204:1205.
439. Bizzi A, Garattini S, Veneroni E. The action of salicylate in reducing plasma free fatty acids and its pharmacological consequences. *British journal of pharmacology and chemotherapy.* 1965;25(1):187-196.

440. Carlson LA, Östman J. Inhibition of the Mobilization of Free Fatty Acids from Adipose Tissue in Diabetes. Ii. Effect of Nicotinic Acid and Acetylsalicylate on Blood Glucose in Human Diabetics. *Acta medica Scandinavica.* 1965;178:71-79.

441. Giugliano D, Luyckx AS, Lefebvre PJ. Effects of acetylsalicylic acid on blood glucose, plasma FFA, glycerol, 3-hydroxybutyrate, alanine, C-peptide, glucagon and growth hormone responses to arginine in insulin-dependent diabetics. *Diabete Metab.* 1980;6(1):39-46.

442. Koyuncuoğlu H, Öz H, Geng E, Sağduyu H, Aykaq G, Sivas A, Uysal M. The effects of sodium salicylate and flufenamic acid on the levels of some hormones and enzymes, and on the lipid metabolism in rabbits. *Pharmacol Res Commun.* 1976;8(3):267-278.

443. Vik-Mo H, Hove K, Mjøs OD. Effects of sodium salicylate on plasma insulin concentration and fatty acid turnover in dogs. *Acta Physiol Scand.* 1978;103(2):113-119.

444. Bellet S, Sandberg H, Maeda S, Yoshimine N. The effects of aspirin ingestion of blood fibrinolysis, glucose, and immunoreactive insulin levels in man. *Angiology.* 1972;23(7):445-451.

445. Cavagnini F, Di Landro A, Invitti C, Raggi U, Alessandrini P, Pinto M, Girotti G, Vigo P. Effects of acetylsalicylic acid and indomethacin on growth hormone secretion in man. *Metabolism.* 1977;26(2):193-200.

446. Ahmadian M, Wang Y, Sul HS. Lipolysis in adipocytes. *Int J Biochem Cell Biol.* 2010;42(5):555-559.

447. Nordlie RC, Foster JD, Lange AJ. Regulation of glucose production by the liver. *Annual review of nutrition.* 1999;19:379-406.

448. Bechmann LP, Hannivoort RA, Gerken G, Hotamisligil GS, Trauner M, Canbay A. The interaction of hepatic lipid and glucose metabolism in liver diseases. *J Hepatol.* 2012;56(4):952-964.

449. Ashwell MS, Ceddia RP, House RL, Cassady JP, Eisen EJ, Eling TE, Collins JB, Grissom SF, Odle J. *Trans*-10, *cis*-12-conjugated linoleic acid alters hepatic gene expression in a polygenic obese line of mice displaying hepatic lipidosis. *J Nutr Biochem.* 2010;21(9):848-855.

450. Anderson N, Borlak J. Molecular mechanisms and therapeutic targets in steatosis and steatohepatitis. *Pharmacol Rev.* 2008;60(3):311-357.

451. Püschel GP, Jungermann K. Integration of function in the hepatic acinus: intercellular communication in neural and humoral control of liver metabolism. *Progress in liver diseases.* 1994;12:19-46.

452. Püschel GP. Control of hepatocyte metabolism by sympathetic and parasympathetic hepatic nerves. *The anatomical record Part A, Discoveries in molecular, cellular, and evolutionary biology.* 2004;280(1):854-867.

453. Giannitrapani L, Ingrao S, Soresi M, Florena AM, La Spada E, Sandonato L, D'Alessandro N, Cervello M, Montalto G. Cyclooxygenase-2 expression in chronic liver diseases and hepatocellular carcinoma: an immunohistochemical study. *Ann N Y Acad Sci.* 2009;1155:293-299.

454. Henkel J, Frede K, Schanze N, Vogel H, Schürmann A, Spruss A, Bergheim I, Püschel GP. Stimulation of fat accumulation in hepatocytes by PGE_2-dependent repression of hepatic lipolysis, β-oxidation and VLDL-synthesis. *Lab Invest.* 2012;92(11):1597-1606.

455. Mater MK, Thelen AP, Jump DB. Arachidonic acid and PGE_2 regulation of hepatic lipogenic gene expression. *J Lipid Res.* 1999;40(6):1045-1052.

456. Nanji AA, Miao L, Thomas P, Rahemtulla A, Khwaja S, Zhao S, Peters D, Tahan SR, Dannenberg AJ. Enhanced cyclooxygenase-2 gene expression in alcoholic liver disease in the rat. *Gastroenterology.* 1997;112(3):943-951.

457. Sorli CH, Zhang HJ, Armstrong MB, Rajotte RV, Maclouf J, Robertson RP. Basal expression of cyclooxygenase-2 and nuclear factor-interleukin 6 are dominant and coordinately regulated by interleukin 1 in the pancreatic islet. *Proc Natl Acad Sci U S A.* 1998;95(4):1788-1793.

458. Sun Y, Jia Z, Yang G, Kakizoe Y, Liu M, Yang K, Liu Y, Yang B, Yang T. mPGES-2 Deletion Remarkably Enhances Liver Injury in Streptozotocin-Treated Mouse via Induction of GLUT2. *J Hepatol.* 2014;61(6):1328–1336.

459. Yu J, Ip E, Dela Peña A, Hou JY, Sesha J, Pera N, Hall P, Kirsch R, Leclercq I, Farrell GC. COX-2 induction in mice with experimental nutritional steatohepatitis: Role as pro-inflammatory mediator. *Hepatology.* 2006;43(4):826-836.

460. Wójcik M, Ramadori P, Blaschke M, Sultan S, Khan S, Malik IA, Naz N, Martius G, Ramadori G, Schultze FC. Immunodetection of cyclooxygenase-2 (COX-2) is restricted to tissue macrophages in normal rat liver and to recruited mononuclear phagocytes in liver injury and cholangiocarcinoma. *Histochem Cell Biol.* 2012;137(2):217-233.

461. Engström L, Ruud J, Eskilsson A, Larsson A, Mackerlova L, Kugelberg U, Qian H, Vasilache AM, Larsson P, Engblom D, Sigvardsson M, Jönsson J-I, Blomqvist A. Lipopolysaccharide-induced fever depends on prostaglandin E2 production specifically in brain endothelial cells. *Endocrinology.* 2012;153(10):4849-4861.

462. Connor AJ, Chen LC, Joseph LB, Laskin JD, Laskin DL. Distinct responses of lung and liver macrophages to acute endotoxemia: role of toll-like receptor 4. *Experimental and molecular pathology.* 2013;94(1):216-227.

463. Dieter P, Scheibe R, Jakobsson P-J, Watanabe K, Kolada A, Kamionka S. Functional coupling of cyclooxygenase 1 and 2 to discrete prostanoid synthases in liver macrophages. *Biochem Biophys Res Commun.* 2000;276(2):488-492.

464. Qu W, Zhong Z, Goto M, Thurman RG. Kupffer cell prostaglandin E_2 stimulates parenchymal cell O_2 consumption: alcohol and cell-cell communication. *Am J Physiol.* 1996;270(4 Pt 1):G574-580.

465. Enomoto N, Ikejima K, Yamashina S, Enomoto A, Nishiura T, Nishimura T, Brenner DA, Schemmer P, Bradford BU, Rivera CA, Zhong Z, Thurman RG. Kupffer cell-derived prostaglandin E_2 is involved in alcohol-induced fat accumulation in rat liver. *Am J Physiol-Gastr L.* 2000;279(1):G100-G106.

466. O'Brien AJ, Fullerton JN, Massey KA, Auld G, Sewell G, James S, Newson J, Karra E, Winstanley A, Alazawi W, Garcia-Martinez R, Cordoba J, Nicolaou A, Gilroy DW. Immunosuppression in acutely decompensated cirrhosis is mediated by prostaglandin E_2. *Nat Med.* 2014;20(5):518-523.

467. Hespeling U, Püschel GP, Jungermann K, Götze O, Zwirner J. Stimulation of glycogen phosphorylase in rat hepatocytes via prostanoid release from Kupffer cells by recombinant rat anaphylatoxin C5a but not by native human C5a in hepatocyte/Kupffer cell co-cultures. *FEBS Lett.* 1995;372(1):108-112.

468. Püschel GP, Hespeling U, Oppermann M, Dieter P. Increase in prostanoid formation in rat liver macrophages (Kupffer cells) by human anaphylatoxin C3a. *Hepatology.* 1993;18(6):1516-1521.

469. Schieferdecker HL, Pestel S, Rothermel E, Püschel GP, Götze O, Jungermann K. Stimulation by anaphylatoxin C5a of glycogen phosphorylase in rat hepatocytes via prostanoid release from hepatic stellate cells but not sinusoidal endothelial cells. *FEBS Lett.* 1998;434(3):245-250.

470. Schieferdecker HL, Pestel S, Püschel GP, Götze O, Jungermann K. Increase by anaphylatoxin C5a of glucose output in perfused rat liver via prostanoids derived from nonparenchymal cells: direct action of prostaglandins and indirect action of thromboxane A_2 on hepatocytes. *Hepatology.* 1999;30(2):454-461.

471. Callery MP, Mangino MJ, Flye MW. Kupffer cell prostaglandin-E_2 production is amplified during hepatic regeneration. *Hepatology.* 1991;14(2):368-372.

472. Goss JA, Mangino MJ, Flye MW. Prostaglandin E_2 production during hepatic regeneration downregulates Kupffer cell IL-6 production. *Ann Surg.* 1992;215(6):553-559; discussion 559-560.

473. Goss JA, Mangino MJ, Callery MP, Flye MW. Prostaglandin E_2 downregulates Kupffer cell production of IL-1 and IL-6 during hepatic regeneration. *Am J Physiol.* 1993;264(4 Pt 1):G601-608.

474. Kuiper J, Zijlstra FJ, Kamps JAAM, van Berkel TJC. Identification of prostaglandin D_2 as the major eicosanoid from liver endothelial and Kupffer cells. *Biochim Biophys Acta.* 1988;959(2):143-152.

475. Mion F, Jasuja R, Johnston DE. The contribution of hepatocytes to prostaglandin synthesis in rat liver. *Prostaglandins Leukot Essent Fatty Acids.* 1995;53(2):109-115.

476. Rodriguez de Turco EB, Spitzer JA. Eicosanoid production in nonparenchymal liver cells isolated from rats infused with *E. coli* endotoxin. *J Leukoc Biol.* 1990;48(6):488-494.

477. Ujihara M, Urade Y, Eguchi N, Hayashi H, Ikai K, Hayaishi O. Prostaglandin D_2 formation and characterization of its synthetases in various tissues of adult rats. *Arch Biochem Biophys.* 1988;260(2):521-531.

478. Henkel J, Gärtner D, Dorn C, Hellerbrand C, Schanze N, Elz SR, Püschel GP. Oncostatin M produced in Kupffer cells in response to PGE_2: possible contributor to hepatic insulin resistance and steatosis. *Lab Invest.* 2011;91(7):1107-1117.

479. Garrity MJ, Westcott KR, Eggerman TL, Andersen NH, Storm DR, Robertson RP. Interrelationships between PGE_2 and PGI_2 Binding and Stimulation of Adenylate-Cyclase. *Am J Physiol.* 1983;244(4):E367-E372.

480. Garrity MJ, Reed MM, Brass EP. Coupling of hepatic prostaglandin receptors to adenylate cyclase through a pertussis toxin sensitive guanine nucleotide regulatory protein. *J Pharmacol Exp Ther.* 1989;248(3):979-983.

481. Hashimoto N, Watanabe T, Ikeda Y, Toda G, Yamada H, Yoshikawa Y, Mitsui H, Kurokawa K. Down-regulation of prostaglandin E_2 receptors in regenerating rat liver and its physiological significance. *Biochem Biophys Res Commun.* 1991;176(1):226-232.

482. Hashimoto N, Watanabe T, Ikeda Y, Yamada H, Taniguchi S, Mitsui H, Kurokawa K. Prostaglandins induce proliferation of rat hepatocytes through a prostaglandin E_2 receptor EP_3 subtype. *Am J Physiol.* 1997;272(3 Pt 1):G597-604.

483. Kuiper J, Zijlstra FJ, Kamps JAAM, Van Berkel TJC. Cellular communication inside the liver. Binding, conversion and metabolic effect of prostaglandin D_2 on parenchymal liver cells. *Biochem J.* 1989;262(1):195-201.

484. Neuschäfer-Rube F, Püschel GP, Jungermann K. Characterization of prostaglandin-$F_{2\alpha}$-binding sites on rat hepatocyte plasma membranes. *Eur J Biochem.* 1993;211(1-2):163-169.

485. Püschel GP, Miura H, Neuschäfer-Rube F, Jungermann K. Inhibition by the protein kinase C activator 4β-phorbol 12-myristate 13-acetate of the prostaglandin $F_{2\alpha}$-mediated and noradrenaline-mediated but not glucagon-mediated activation of glycogenolysis in rat liver. *Eur J Biochem.* 1993;217(1):305-311.

486. Rice MG, McRae JR, Storm DR, Robertson RP. Up-regulation of hepatic prostaglandin E receptors in vivo induced by prostaglandin synthesis inhibitors. *Am J Physiol.* 1981;241(4):E291-297.

487. Robertson RP, Westcott KR, Storm DR, Rice MG. Down-regulation in vivo of PGE receptors and adenylate cyclase stimulation. *Am J Physiol.* 1980;239(1):E75-80.

488. Virgolini I, Peskar BA, Sinzinger H. Thiopental and ether anaesthesia decrease the prostaglandin receptor density of the rat liver. *Prostaglandins Leukot Essent Fatty Acids.* 1991;43(1):25-28.

489. Boie Y, Stocco R, Sawyer N, Slipetz DM, Ungrin MD, Neuschäfer-Rube F, Püschel GP, Metters KM, Abramovitz M. Molecular cloning and characterization of the four rat prostaglandin E_2 prostanoid receptor subtypes. *Eur J Pharmacol.* 1997;340(2-3):227-241.

490. Fennekohl A, Schieferdecker HL, Jungermann K, Püschel GP. Differential expression of prostanoid receptors in hepatocytes, Kupffer cells, sinusoidal endothelial cells and stellate cells of rat liver. *J Hepatol.* 1999;30(1):38-47.

491. Fennekohl A, Lucas M, Püschel GP. Induction by interleukin 6 of G_s-coupled prostaglandin E_2 receptors in rat hepatocytes mediating a prostaglandin E_2-dependent inhibition of the hepatocyte's acute phase response. *Hepatology.* 2000;31(5):1128-1134.

492. Kataoka K, Takikawa Y, Lin SD, Suzuki K. Prostaglandin E2 receptor EP4 agonist induces Bcl-xL and independently activates proliferation signals in mouse primary hepatocytes. *J Gastroenterol.* 2005;40(6):610-616.

493. Kuzumoto Y, Sho M, Ikeda N, Hamada K, Mizuno T, Akashi S, Tsurui Y, Kashizuka H, Nomi T, Kubo A, Kanehiro H, Nakajima Y. Significance and therapeutic potential of prostaglandin E_2 receptor in hepatic ischemia/reperfusion injury in mice. *Hepatology.* 2005;42(3):608-617.

494. Meisdalen K, Dajani OF, Christoffersen T, Sandnes D. Prostaglandins enhance epidermal growth factor-induced DNA synthesis in hepatocytes by stimulation of E prostanoid 3 and F prostanoid receptors. *J Pharmacol Exp Ther.* 2007;322(3):1044-1050.

495. Pérez S, Maldonado EN, Aspichueta P, Ochoa B, Chico Y. Differential modulation of prostaglandin receptor mRNA abundance by prostaglandins in primary cultured rat hepatocytes. *Mol Cell Biochem.* 2004;266(1-2):183-189.

496. Neuschäfer-Rube F, DeVries C, Hänecke K, Jungermann K, Püschel GP. Molecular cloning and expression of a prostaglandin E_2 receptor of the $EP_{3\beta}$ subtype from rat hepatocytes. *FEBS Lett.* 1994;351(1):119-122.

497. Neuschäfer-Rube F, Möller U, Püschel GP. Structure of the 5'-flanking region of the rat prostaglandin $F_{2\alpha}$ receptor gene and its transcriptional control functions in hepatocytes. *Biochem Biophys Res Commun.* 2000;278(2):278-285.

498. Fennekohl A, Sugimoto Y, Segi E, Maruyama T, Ichikawa A, Püschel GP. Contribution of the two Gs-coupled PGE_2-receptors EP2-receptor and EP4-receptor to the inhibition by PGE_2 of the LPS-induced TNFα-formation in Kupffer cells from EP2-or EP4-

receptor-deficient mice. Pivotal role for the EP4-receptor in wild type Kupffer cells. *J Hepatol.* 2002;36(3):328-334.

499. Habegger KM, Heppner KM, Geary N, Bartness TJ, DiMarchi R, Tschöp MH. The metabolic actions of glucagon revisited. *Nat Rev Endocrinol.* 2010;6(12):689-697.

500. Gall D, Baus E, Dupont G. Activation of the liver glycogen phosphorylase by Ca^{2+} oscillations: a theoretical study. *J Theor Biol.* 2000;207(4):445-454.

501. Heilmeyer LMG. Molecular basis of signal integration in phosphorylase kinase. *Biochim Biophys Acta.* 1991;1094(2):168-174.

502. Swulius MT, Waxham MN. Ca^{2+}/calmodulin-dependent protein kinases. *Cell Mol Life Sci.* 2008;65(17):2637-2657.

503. Wilde MW, Slonczewski JL, Carson M, Zigmond SH. Glycogen phosphorylase: a noninvasive indicator of cytoplasmic calcium. *Methods Enzymol.* 1987;141:18-25.

504. Wu D, Jia Y, Rozi A. Effects of inositol 1,4,5-trisphosphate receptor-mediated intracellular stochastic calcium oscillations on activation of glycogen phosphorylase. *Biophysical chemistry.* 2004;110(1-2):179-190.

505. Hespeling U, Jungermann K, Püschel GP. Feedback-inhibition of glucagon-stimulated glycogenolysis in hepatocyte/Kupffer cell cocultures by glucagon-elicited prostaglandin production in Kupffer cells. *Hepatology.* 1995;22(5):1577-1583.

506. Björnsson ÓG, Sparks JD, Sparks CE, Gibbons GF. Prostaglandins suppress VLDL secretion in primary rat hepatocyte cultures: relationships to hepatic calcium metabolism. *J Lipid Res.* 1992;33(7):1017-1027.

507. Brass EP, Garrity MJ. Effect of E-series prostaglandins on cyclic AMP-dependent and -independent hormone-stimulated glycogenolysis in hepatocytes. *Diabetes.* 1985;34(3):291-294.

508. Brass EP, Garrity MJ. Structural specificity for prostaglandin effects on hepatocyte glycogenolysis. *Biochem J.* 1990;267(1):59-62.

509. Brønstad GO, Christoffersen T. Inhibitory effect of prostaglandins on the stimulation by glucagon and adrenaline of formation of cyclic AMP in rat hepatocytes. *Eur J Biochem.* 1981;117(2):369-374.

510. Grinde B, Ichihara A. Effects of prostaglandins and divalent cations on cAMP production in isolated rat hepatocytes. *Exp Cell Res.* 1983;148(1):163-172.

511. Kanemaki T, Kitade H, Hiramatsu Y, Kamiyama Y, Okumura T. Stimulation of glycogen degradation by prostaglandin E_2 in primary cultured rat hepatocytes. *Prostaglandins.* 1993;45(5):459-474.

512. Okumura T, Sago T, Saito K. Effect of prostaglandins and their analogues on hormone-stimulated glycogenolysis in primary cultures of rat hepatocytes. *Biochim Biophys Acta.* 1988;958(2):179-187.

513. Püschel GP, Christ B. Inhibition by PGE_2 of glucagon-induced increase in phosphoenolpyruvate carboxykinase mRNA and acceleration of mRNA degradation in cultured rat hepatocytes. *FEBS Lett.* 1994;351(3):353-356.

514. Melien Ø, Winsnes R, Refsnes M, Gladhaug IP, Christoffersen T. Pertussis toxin abolishes the inhibitory effects of prostaglandins E_1, E_2, I_2 and $F_{2\alpha}$ on hormone-induced cAMP accumulation in cultured hepatocytes. *Eur J Biochem.* 1988;172(2):293-297.

515. Okumura T, Sago T, Saito K. Pertussis toxin blocks an inhibition of hormone-stimulated glycogenolysis by prostaglandin E_2 and its analogue in cultured hepatocytes. *Prostaglandins.* 1988;36(4):463-475.

516. Püschel GP, Kirchner C, Schröder A, Jungermann K. Glycogenolytic and antiglycogenolytic prostaglandin E_2 actions in rat hepatocytes are mediated via different signalling pathways. *Eur J Biochem.* 1993;218(3):1083-1089.

517. Altin JG, Bygrave FL. Prostaglandin $F_{2\alpha}$ and the thromboxane A_2 analogue ONO-11113 stimulate Ca^{2+} fluxes and other physiological responses in rat liver. Further evidence that prostanoids may be involved in the action of arachidonic acid and platelet-activating factor. *Biochem J.* 1988;249(3):677-685.

518. Buxton DB, Fisher RA, Briseno DL, Hanahan DJ, Olson MS. Glycogenolytic and haemodynamic responses to heat-aggregated immunoglobulin G and prostaglandin E_2 in the perfused rat liver. *Biochem J.* 1987;243(2):493-498.

519. Gómez-Foix AM, Rodriguez-Gil JE, Guinovart JJ, Bosch F. Prostaglandins E_2 and $F_{2\alpha}$ affect glycogen synthase and phosphorylase in isolated hepatocytes. *Biochem J.* 1989;261(1):93-97.

520. Häussinger D, Stehle T, Tran-Thi T-A, Decker K, Gerok W. Prostaglandin responses in isolated perfused rat liver: $Ca^{2\oplus}$ and $K^{\oplus}$ fluxes, hemodynamic and metabolic effects. *Biol Chem Hoppe Seyler.* 1987;368(11):1509-1513.

521. Iwai M, Gardemann A, Püschel G, Jungermann K. Potential role for prostaglandin $F_{2\alpha}$, D_2, E_2 and thromboxane A_2 in mediating the metabolic and hemodynamic actions of sympathetic nerves in perfused rat liver. *Eur J Biochem.* 1988;175(1):45-50.

522. Mine T, Kojima I, Ogata E. Mechanism of prostaglandin E_2-induced glucose production in rat hepatocytes. *Endocrinology.* 1990;126(6):2831-2836.

523. Deaciuc IV, D'Souza NB, Lang CH, Spitzer JJ. Effects of acute alcohol intoxication on gluconeogenesis and its hormonal responsiveness in isolated, perfused rat liver. *Biochem Pharmacol.* 1992;44(8):1617-1624.

524. Okumura T, Kanemaki T, Kitade H. Stimulation of glucose incorporation into glycogen by E-series prostaglandins in cultured rat hepatocytes. *Biochim Biophys Acta.* 1993;1176(1-2):137-142.

525. Casteleijn E, Kuiper J, Van Rooij HCJ, Kamps JAAM, Koster JF, Van Berkel TJC. Prostaglandin D_2 mediates the stimulation of glycogenolysis in the liver by phorbol ester. *Biochem J.* 1988;250(1):77-80.

526. Gibbons GF, Wiggins D, Brown A-M, Hebbachi A-M. Synthesis and function of hepatic very-low-density lipoprotein. *Biochemical Society transactions.* 2004;32(Pt 1):59-64.

527. Pérez S, Aspichueta P, Ochoa B, Chico Y. The 2-series prostaglandins suppress VLDL secretion in an inflammatory condition-dependent manner in primary rat hepatocytes. *Biochim Biophys Acta.* 2006;1761(2):160-171.

528. Lewis GF, Carpentier A, Adeli K, Giacca A. Disordered fat storage and mobilization in the pathogenesis of insulin resistance and type 2 diabetes. *Endocr Rev.* 2002;23(2):201-229.

529. Loria P, Lonardo A, Anania F. Liver and diabetes. A vicious circle. *Hepatol Res.* 2013;43(1):51-64.

530. Smith BW, Adams LA. Nonalcoholic fatty liver disease and diabetes mellitus: pathogenesis and treatment. *Nat Rev Endocrinol.* 2011;7(8):456-465.

531. Solís Herruzo JA, García Ruiz I, Pérez Carreras M, Muñoz Yagüe MT. Non-alcoholic fatty liver disease. From insulin resistance to mitochondrial dysfunction. *Rev Esp Enferm Dig.* 2006;98(11):844-874.

532. Ameer F, Scandiuzzi L, Hasnain S, Kalbacher H, Zaidi N. *De novo* lipogenesis in health and disease. *Metabolism.* 2014;63(7):895-902.
533. Choi SH, Ginsberg HN. Increased very low density lipoprotein (VLDL) secretion, hepatic steatosis, and insulin resistance. *Trends Endocrinol Metab.* 2011;22(9):353-363.
534. García-Ruiz C, Baulies A, Mari M, García-Rovés PM, Fernandez-Chace JC. Mitochondrial dysfunction in nonalcoholic fatty liver disease and insulin resistance: Cause or consequence? *Free Radic Res.* 2013.
535. Trauner M, Arrese M, Wagner M. Fatty liver and lipotoxicity. *Biochim Biophys Acta.* 2010;1801(3):299-310.
536. Bucher NLR. Liver regeneration: an overview. *J Gastroenterol Hepatol.* 1991;6(6):615-624.
537. Hossain MA, Wakabayashi H, Izuishi K, Okano K, Yachida S, Maeta H. The role of prostaglandins in liver ischemia-reperfusion injury. *Curr Pharm Des.* 2006;12(23):2935-2951.
538. Kalish BT, Kieran MW, Puder M, Panigrahy D. The growing role of eicosanoids in tissue regeneration, repair, and wound healing. *Prostaglandins Other Lipid Mediat.* 2013;104-105:130-138.
539. Peltekian KM, Makowka L, Williams R, Blendis LM, Levy GA. Prostaglandins in liver failure and transplantation: regeneration, immunomodulation, and cytoprotection. Prostaglandins in Liver Transplantation Research Group. *Liver transplantation and surgery : official publication of the American Association for the Study of Liver Diseases and the International Liver Transplantation Society.* 1996;2(3):171-184.
540. Quiroga J, Prieto J. Liver cytoprotection by prostaglandins. *Pharmacol Ther.* 1993;58(1):67-91.
541. Arai M, Peng X-X, Currin RT, Thurman RG, Lemasters JJ. Protection of sinusoidal endothelial cells against storage/reperfusion injury by prostaglandin E_2 derived from Kupffer cells. *Transplantation.* 1999;68(3):440-445.
542. Casado M, Mollá B, Roy R, Fernández-Martínez A, Cucarella C, Mayoral R, Boscá L, Martín-Sanz P. Protection against Fas-induced liver apoptosis in transgenic mice expressing cyclooxygenase 2 in hepatocytes. *Hepatology.* 2007;45(3):631-638.
543. Francés DE, Ingaramo PI, Mayoral R, Través P, Casado M, Valverde ÁM, Martín-Sanz P, Carnovale CE. Cyclooxygenase-2 over-expression inhibits liver apoptosis induced by hyperglycemia. *J Cell Biochem.* 2013;114(3):669-680.
544. Horrillo R, Planagumà A, González-Périz A, Ferré N, Titos E, Miquel R, López-Parra M, Masferrer JL, Arroyo V, Clària J. Comparative protection against liver inflammation and fibrosis by a selective cyclooxygenase-2 inhibitor and a nonredox-type 5-lipoxygenase inhibitor. *J Pharmacol Exp Ther.* 2007;323(3):778-786.
545. Abdel Salam OME, Sleem AA, Omara EA, Hassan NS. Hepatoprotective effects of misoprostol and silymarin on carbon tetrachloride-induced hepatic damage in rats. *Fundamental & clinical pharmacology.* 2009;23(2):179-188.
546. Kasai K, Sato S-i, Suzuki K. A novel prostaglandin E receptor subtype agonist, 0N0-4819, attenuates acute experimental liver injury in rats. *Hepatol Res.* 2001;21(3):252-260.
547. Kuzumoto Y, Sho M, Ikeda N, Mizuno T, Hamada K, Akashi S, Tsurui Y, Kashizuka H, Nomi T, Kanehiro H, Nakajima Y. Role of EP4 prostaglandin E_2 receptor in the ischemic liver. *Transplant Proc.* 2005;37(1):422-424.

548. Okamoto T, Saito T, Tabata Y, Uemoto S. Immunological tolerance in a mouse model of immune-mediated liver injury induced by 16,16 dimethyl PGE2 and PGE2-containing nanoscale hydrogels. *Biomaterials.* 2011;32(21):4925-4935.
549. Ushio A, Takikawa Y, Lin SD, Miyamoto Y, Suzuki K. Induction of Bcl-xL is a possible mechanism of anti-apoptotic effect by prostaglandin E2 EP4-receptor agonist in human hepatocellular carcinoma HepG2 cells. *Hepatol Res.* 2004;29(3):173-179.
550. Nagai H, Aoki M, Shimazawa T, Yakuo I, Koda A, Kasahara M. Effect of OKY-046 and ONO-3708 on liver injury in mice. *Jpn J Pharmacol.* 1989;51(2):191-197.
551. Xu Q, Sakai K, Suzuki Y, Tambo C, Sakai Y, Matsumoto K. Suppression of fibrogenic gene expression and liver fibrosis using a synthetic prostacyclin agonist. *Biomedical research.* 2013;34(5):241-250.
552. Nakatani Y, Kitazawa T, Fujimoto M, Tamura N, Uemura M, Yamao J, Fukui H. Effect of prostaglandin E receptor subtype EP4 selective agonist on the secretion of tumor necrosis factor-alpha by macrophages in acute ethanol-loaded rats. *Alcohol Clin Exp Res.* 2004;28(8 Suppl Proceedings):123S-128S.
553. Treffkorn L, Scheibe R, Maruyama T, Dieter P. PGE_2 exerts its effect on the LPS-induced release of TNF-α, ET-1, IL-1α, IL-6 and IL-10 via the EP2 and EP4 receptor in rat liver macrophages. *Prostaglandins Other Lipid Mediat.* 2004;74(1-4):113-123.
554. Kimple ME, Joseph JW, Bailey CL, Fueger PT, Hendry IA, Newgard CB, Casey PJ. $G\alpha_z$ negatively regulates insulin secretion and glucose clearance. *J Biol Chem.* 2008;283(8):4560-4567.
555. Fleming EF, Athirakul K, Oliverio MI, Key M, Goulet J, Koller BH, Coffman TM. Urinary concentrating function in mice lacking EP_3 receptors for prostaglandin E_2. *Am J Physiol.* 1998;275(6 Pt 2):F955-961.
556. Heptinstall S, Espinosa DI, Manolopoulos P, Glenn JR, White AE, Johnson A, Dovlatova N, Fox SC, May JA, Hermann D, Magnusson O, Stefansson K, Hartman D, Gurney M. DG-041 inhibits the EP3 prostanoid receptor--a new target for inhibition of platelet function in atherothrombotic disease. *Platelets.* 2008;19(8):605-613.
557. Eriksen EF, Richelsen B, Gesser BP, Jacobsen NO, Stengaard-Pedersen K. Prostaglandin-E_2 receptors in the rat kidney: biochemical characterization and localization. *Kidney Int.* 1987;32(2):181-186.
558. Dai C, Brissova M, Hang Y, Thompson C, Poffenberger G, Shostak A, Chen Z, Stein R, Powers AC. Islet-enriched gene expression and glucose-induced insulin secretion in human and mouse islets. *Diabetologia.* 2012;55(3):707-718.
559. Rahier J, Guiot Y, Goebbels RM, Sempoux C, Henquin JC. Pancreatic β-cell mass in European subjects with type 2 diabetes. *Diabetes Obes Metab.* 2008;10 Suppl 4:32-42.
560. Takano M, Nishimura H, Kimura Y, Washizu J, Mokuno Y, Nimura Y, Yoshikai Y. Prostaglandin E_2 protects against liver injury after *Escherichia coli* infection but hampers the resolution of the infection in mice. *J Immunol.* 1998;161(6):3019-3025.
561. Calabrò P, Golia E, Maddaloni V, Malvezzi M, Casillo B, Marotta C, Calabrò R, Golino P. Adipose tissue-mediated inflammation: the missing link between obesity and cardiovascular disease? *Intern Emerg Med.* 2009;4(1):25-34.
562. Ikeoka D, Mader JK, Pieber TR. Adipose tissue, inflammation and cardiovascular disease. *Rev Assoc Med Bras.* 2010;56(1):116-121.

563. Liu T, Laidlaw TM, Feng C, Xing W, Shen S, Milne GL, Boyce JA. Prostaglandin E_2 deficiency uncovers a dominant role for thromboxane A_2 in house dust mite-induced allergic pulmonary inflammation. *Proc Natl Acad Sci U S A.* 2012;109(31):12692-12697.
564. Baecker V. ImageJ Macro Tool Sets for Biological Image Analysis. Paper presented at: ImageJ User and Developer Conference 20122012; Luxembourg.
565. Viswanadha S, Londos C. Optimized conditions for measuring lipolysis in murine primary adipocytes. *J Lipid Res.* 2006;47(8):1859-1864.
566. Jones RL, Woodward DF, Wang JW, Clark RL. Roles of affinity and lipophilicity in the slow kinetics of prostanoid receptor antagonists on isolated smooth muscle preparations. *Br J Pharmacol.* 2011;162(4):863-879.
567. Singh J, Zeller W, Zhou N, Hategen G, Mishra R, Polozov A, Yu P, Onua E, Zhang J, Zembower D, Kiselyov A, Ramírez JL, Sigthorsson G, Bjornsson JM, Thorsteinsdottir M, Andresson T, Bjarnadottir M, Magnusson O, Fabre J-E, Stefansson K, Gurney ME. Antagonists of the EP_3 receptor for prostaglandin E_2 are novel antiplatelet agents that do not prolong bleeding. *ACS Chem Biol.* 2009;4(2):115-126.
568. Folch J, Lees M, Sloane Stanley GH. A simple method for the isolation and purification of total lipides from animal tissues. *J Biol Chem.* 1957;226(1):497-509.
569. Morrison WR, Smith LM. Preparation of Fatty Acid Methyl Esters and Dimethylacetals from Lipids with Boron Fluoride--Methanol. *J Lipid Res.* 1964;5:600-608.
570. Pfaffl MW. A new mathematical model for relative quantification in real-time RT-PCR. *Nucleic Acids Res.* 2001;29(9):e45.
571. Amano H, Hayashi I, Endo H, Kitasato H, Yamashina S, Maruyama T, Kobayashi M, Satoh K, Narita M, Sugimoto Y, Murata T, Yoshimura H, Narumiya S, Majima M. Host prostaglandin E_2-EP3 signaling regulates tumor-associated angiogenesis and tumor growth. *J Exp Med.* 2003;197(2):221-232.
572. Oba K, Hosono K, Amano H, Okizaki S-i, Ito Y, Shichiri M, Majima M. Downregulation of the proangiogenic prostaglandin E receptor EP3 and reduced angiogenesis in a mouse model of diabetes mellitus. *Biomed Pharmacother.* 2014;68(8):1125-1133.
573. Taniguchi T, Fujino H, Israel DD, Regan JW, Murayama T. Human $EP3_I$ prostanoid receptor induces VEGF and VEGF receptor-1 mRNA expression. *Biochem Biophys Res Commun.* 2008;377(4):1173-1178.
574. Cinti S, Mitchell G, Barbatelli G, Murano I, Ceresi E, Faloia E, Wang S, Fortier M, Greenberg AS, Obin MS. Adipocyte death defines macrophage localization and function in adipose tissue of obese mice and humans. *J Lipid Res.* 2005;46(11):2347-2355.
575. Jung UJ, Choi M-S. Obesity and its metabolic complications: the role of adipokines and the relationship between obesity, inflammation, insulin resistance, dyslipidemia and nonalcoholic fatty liver disease. *Int J Mol Sci.* 2014;15(4):6184-6223.
576. Anderson NJ, King MR, Delbruck L, Jolivalt CG. Role of insulin signaling impairment, adiponectin and dyslipidemia in peripheral and central neuropathy in mice. *Dis Model Mech.* 2014;7(6):625-633.
577. Barnea M, Shamay A, Stark AH, Madar Z. A high-fat diet has a tissue-specific effect on adiponectin and related enzyme expression. *Obesity (Silver Spring).* 2006;14(12):2145-2153.
578. Sumiyoshi M, Sakanaka M, Kimura Y. Chronic intake of high-fat and high-sucrose diets differentially affects glucose intolerance in mice. *J Nutr.* 2006;136(3):582-587.

579. McGuinness OP, Ayala JE, Laughlin MR, Wasserman DH. NIH experiment in centralized mouse phenotyping: the Vanderbilt experience and recommendations for evaluating glucose homeostasis in the mouse. *Am J Physiol Endocrinol Metab.* 2009;297(4):E849-855.

580. Bonner JS, Lantier L, Hasenour CM, James FD, Bracy DP, Wasserman DH. Muscle-specific vascular endothelial growth factor deletion induces muscle capillary rarefaction creating muscle insulin resistance. *Diabetes.* 2013;62(2):572-580.

581. Kamoshita E, Ikeda Y, Fujita M, Amano H, Oikawa A, Suzuki T, Ogawa Y, Yamashina S, Azuma S, Narumiya S, Unno N, Majima M. Recruitment of a prostaglandin E receptor subtype, EP3-expressing bone marrow cells is crucial in wound-induced angiogenesis. *Am J Pathol.* 2006;169(4):1458-1472.

582. Cornier M-A, Dabelea D, Hernandez TL, Lindstrom RC, Steig AJ, Stob NR, Van Pelt RE, Wang H, Eckel RH. The metabolic syndrome. *Endocr Rev.* 2008;29(7):777-822.

583. Alkhouri N, Gornicka A, Berk MP, Thapaliya S, Dixon LJ, Kashyap S, Schauer PR, Feldstein AE. Adipocyte apoptosis, a link between obesity, insulin resistance, and hepatic steatosis. *J Biol Chem.* 2010;285(5):3428-3438.

584. Strissel KJ, Stancheva Z, Miyoshi H, Perfield JW, DeFuria J, Jick Z, Greenberg AS, Obin MS. Adipocyte death, adipose tissue remodeling, and obesity complications. *Diabetes.* 2007;56(12):2910-2918.

585. Wueest S, Rapold RA, Schumann DM, Rytka JM, Schildknecht A, Nov O, Chervonsky AV, Rudich A, Schoenle EJ, Donath MY, Konrad D. Deletion of Fas in adipocytes relieves adipose tissue inflammation and hepatic manifestations of obesity in mice. *J Clin Invest.* 2010;120(1):191-202.

586. Cowie CC, Rust KF, Byrd-Holt DD, Eberhardt MS, Flegal KM, Engelgau MM, Saydah SH, Williams DE, Geiss LS, Gregg EW. Prevalence of diabetes and impaired fasting glucose in adults in the U.S. population: National Health And Nutrition Examination Survey 1999-2002. *Diabetes Care.* 2006;29(6):1263-1268.

587. Cowie CC, Rust KF, Ford ES, Eberhardt MS, Byrd-Holt DD, Li C, Williams DE, Gregg EW, Bainbridge KE, Saydah SH, Geiss LS. Full accounting of diabetes and pre-diabetes in the U.S. population in 1988-1994 and 2005-2006. *Diabetes Care.* 2009;32(2):287-294.

588. Iozzo P, Beck-Nielsen H, Laakso M, Smith U, Yki-Järvinen H, Ferrannini E. Independent influence of age on basal insulin secretion in nondiabetic humans. European Group for the Study of Insulin Resistance. *J Clin Endocrinol Metab.* 1999;84(3):863-868.

589. Kusnik-Joinville O, Weill A, Ricordeau P, Allemand H. Diabète traité en France en 2007: un taux de prévalence proche de 4 % et des disparités géographiques croissantes. *Bulletin épidémiologique hebdomadaire.* 2008;43:409-413.

590. Virally M, Laloi-Michelin M, Kevorkian J-P, Bitu J, Guillausseau P. Spécificités du diabète de type 2 chez le sujet âgé. *Sang Thromb Vaiss.* 2011;23(8):409-415.

591. Gunasekaran U, Gannon M. Type 2 Diabetes and the Aging Pancreatic Beta Cell. *Aging-Us.* 2011;3(6):565-575.

592. Scheen AJ. Diabetes mellitus in the elderly: insulin resistance and/or impaired insulin secretion? *Diabetes Metab.* 2005;31 Spec No 2:5S27-25S34.

593. Munger MA. Polypharmacy and combination therapy in the management of hypertension in elderly patients with co-morbid diabetes mellitus. *Drugs Aging.* 2010;27(11):871-883.

594. Abbatecola AM, Maggi S, Paolisso G. New approaches to treating type 2 diabetes mellitus in the elderly: role of incretin therapies. *Drugs Aging.* 2008;25(11):913-925.

595. Tanwani LK. Insulin therapy in the elderly patient with diabetes. *Am J Geriatr Pharmacother.* 2011;9(1):24-36.
596. Ackermann AM, Gannon M. Molecular regulation of pancreatic β-cell mass development, maintenance, and expansion. *J Mol Endocrinol.* 2007;38(1-2):193-206.
597. Arosh JA, Banu SK, Chapdelaine P, Fortier MA. Temporal and tissue-specific expression of prostaglandin receptors EP2, EP3, EP4, FP, and cyclooxygenases 1 and 2 in uterus and fetal membranes during bovine pregnancy. *Endocrinology.* 2004;145(1):407-417.
598. Rooney K, Ozanne SE. Maternal over-nutrition and offspring obesity predisposition: targets for preventative interventions. *Int J Obes (Lond).* 2011;35(7):883-890.
599. Downey JD, Saleh SA, Bridges TM, Morrison RD, Daniels JS, Lindsley CW, Breyer RM. Development of an in vivo active, dual EP1 and EP3 selective antagonist based on a novel acyl sulfonamide bioisostere. *Bioorg Med Chem Lett.* 2013;23(1):37-41.
600. Singh J, Zeller W, Zhou N, Hategan G, Mishra RK, Polozov A, Yu P, Onua E, Zhang J, Ramírez JL, Sigthorsson G, Thorsteinnsdottir M, Kiselyov AS, Zembower DE, Andrésson T, Gurney ME. Structure-activity relationship studies leading to the identification of (2*E*)-3-[l-[(2,4-dichlorophenyl)methyl]-5-fluoro-3-methyl-l*H*-indol-7-yl]-*N*-[(4,5-d ichloro-2-thienyl)sulfonyl]-2-propenamide (DG-041), a potent and selective prostanoid EP3 receptor antagonist, as a novel antiplatelet agent that does not prolong bleeding. *J Med Chem.* 2010;53(1):18-36.
601. Alexander J, Chang GQ, Dourmashkin JT, Leibowitz SF. Distinct phenotypes of obesity-prone AKR/J, DBA2J and C57BL/6J mice compared to control strains. *Int J Obes (Lond).* 2006;30(1):50-59.
602. Andrikopoulos S, Massa CM, Aston-Mourney K, Funkat A, Fam BC, Hull RL, Kahn SE, Proietto J. Differential effect of inbred mouse strain (C57BL/6, DBA/2, 129T2) on insulin secretory function in response to a high fat diet. *J Endocrinol.* 2005;187(1):45-53.
603. Funkat A, Massa CM, Jovanovska V, Proietto J, Andrikopoulos S. Metabolic adaptations of three inbred strains of mice (C57BL/6, DBA/2, and 129T2) in response to a high-fat diet. *J Nutr.* 2004;134(12):3264-3269.
604. Nishikawa S, Yasoshima A, Doi K, Nakayama H, Uetsuka K. Involvement of sex, strain and age factors in high fat diet-induced obesity in C57BL/6J and BALB/cA mice. *Experimental animals / Japanese Association for Laboratory Animal Science.* 2007;56(4):263-272.
605. Nishikawa S, Doi K, Nakayama H, Uetsuka K. The effect of fasting on hepatic lipid accumulation and transcriptional regulation of lipid metabolism differs between C57BL/6J and BALB/cA mice fed a high-fat diet. *Toxicologic pathology.* 2008;36(6):850-857.
606. Nishikawa S, Sugimoto J, Okada M, Sakairi T, Takagi S. Gene expression in livers of BALB/C and C57BL/6J mice fed a high-fat diet. *Toxicologic pathology.* 2012;40(1):71-82.
607. Pi J, Bai Y, Daniel KW, Liu D, Lyght O, Edelstein D, Brownlee M, Corkey BE, Collins S. Persistent oxidative stress due to absence of uncoupling protein 2 associated with impaired pancreatic beta-cell function. *Endocrinology.* 2009;150(7):3040-3048.
608. West DB, Boozer CN, Moody DL, Atkinson RL. Dietary obesity in nine inbred mouse strains. *Am J Physiol.* 1992;262(6 Pt 2):R1025-1032.
609. Zraika S, Aston-Mourney K, Laybutt DR, Kebede M, Dunlop ME, Proietto J, Andrikopoulos S. The influence of genetic background on the induction of oxidative

stress and impaired insulin secretion in mouse islets. *Diabetologia.* 2006;49(6):1254-1263.

610. Legates JE. The role of maternal effects in animal breeding. IV. Maternal effects in laboratory species. *J Anim Sci.* 1972;35(6):1294-1302.

611. Mikami H, Onishi A. 'Heterosis' in litter size of chimaeric mice. *Genetical research.* 1985;46(1):85-94.

612. Rülicke T, Guncz N, Wedekind C. Early maternal investment in mice: no evidence for compatible-genes sexual selection despite hybrid vigor. *Journal of evolutionary biology.* 2006;19(3):922-928.

613. Juteau H, Gareau Y, Labelle M, Sturino CF, Sawyer N, Tremblay N, Lamontagne S, Carrière M-C, Denis D, Metters KM. Structure-activity relationship of cinnamic acylsulfonamide analogues on the human EP_3 prostanoid receptor. *Bioorg Med Chem.* 2001;9(8):1977-1984.

614. Kosteli A, Sugaru E, Haemmerle G, Martin JF, Lei J, Zechner R, Ferrante AW, Jr. Weight loss and lipolysis promote a dynamic immune response in murine adipose tissue. *J Clin Invest.* 2010;120(10):3466-3479.

615. Tessaro FH, Ayala TS, Martins JO. Lipid Mediators Are Critical in Resolving Inflammation: A Review of the Emerging Roles of Eicosanoids in Diabetes Mellitus. *BioMed research international.* 2015;2015:568408.

616. Matsuoka Y, Furuyashiki T, Bito H, Ushikubi F, Tanaka Y, Kobayashi T, Muro S, Satoh N, Kayahara T, Higashi M, Mizoguchi A, Shichi H, Fukuda Y, Nakao K, Narumiya S. Impaired adrenocorticotropic hormone response to bacterial endotoxin in mice deficient in prostaglandin E receptor EP1 and EP3 subtypes. *Proc Natl Acad Sci U S A.* 2003;100(7):4132-4137.